The dynamic characteristics of a hydrostatic transmission system.

Worton-Griffiths, J. F.

Award date:
1973

Awarding institution:
University of Bath

The DYNAMIC CHARACTERISTICS Of A HYDROSTATIC TRANSMISSION SYSTEM

Submitted by: J.F. Worton Griffiths

For the Degree of Ph.D. of the University of Bath
1973

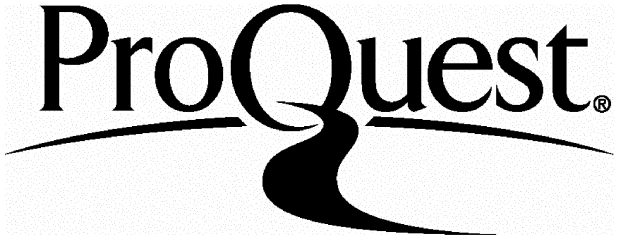

SUMMARY

The dynamic performance of a hydrostatic transmission with a variable delivery pump used for speed control is predicted using a simple mathematical model. A detailed analytical study and experimental determination of the performance of the pump and motor is carried out. The analysis of the transmission is then extended to take into account the pump and motor slip and torque losses, and the prime mover droop, by employing signal flow techniques. The results of theoretical predictions of dynamic performance made using this technique were compared with those from an extensive test programme employing electro-hydraulic test techniques carried out on a typical hydrostatic drive.

The signal flow analysis improved the prediction of the transmission dynamic performance over that of the simple mathematical model, but it was found that errors of up to 40 per cent were occurring as many of the loads employed could not be accurately represented by simple mathematical models. A vector approach was adopted using experimentally determined load loci that provided a correlation of within 5 per cent of the experimentally measured response by using the isentropic tangent bulk modulus of the oil obtained from the results of the most recent static tests carried out by the oil manufacturer. Mean return line pressure, restricted boost system, and flexible pipeline effects were evaluated by the vector locus technique and verified by an experimental programme.

The work was extended to investigate aeration effects by developing the test facility to enable the transmission to be supplied with oil with an artificially high quantity of gas dissolved in it. No significant effects upon the transmission steady state or dynamic performance could be determined.

ACKNOWLEDGEMENTS

The author wishes to express his sincere thanks to his supervisor, Dr. D.E. Bowns, for his invaluable help and guidance during the work on this thesis. Also the staff and technicians of the School of Engineering of the University of Bath for numerous consultations.

Acknowledgement is also given to the Staff of the Computer Unit of the University of Bath for processing much of the experimental data.

The typing of the text from the original manuscript was by Mrs. June O'Keefe, of Cessna Fluid Power Limited, and the author wishes to thank her for her skill and patience whilst undertaking this presentation.

The additional equipment for the aeration study was provided by the Mobil Oil Company, and the author wishes to thank them for their interest and participation in this work.

CONTENTS

	Page
TITLE	i
SUMMARY	ii
ACKNOWLEDGEMENTS	iii
CONTENTS	iv
NOTATION	
LIST of FIGURES	
INTRODUCTION /	

Page

1. INTRODUCTION

1.1 The Historical Evolution of Oil Hydrostatic Power Transmission 1

1.2 The Closed Circuit Hydrostatic Transmission 6

1.3 The Dynamic Performance of Hydrostatic Transmissions (8)

2. POSITIVE DISPLACEMENT PUMPS and MOTORS Used In HYDROSTATIC TRANSMISSION And Their PERFORMANCE CHARACTERISTICS 19

2.1 Positive Displacement Pumps and Motors 19

2.1.1 Vane Units 20

2.1.2 Gear Units 20

2.1.3 Piston Units 21

2.1.4 Variable Delivery 25

2.2 The Theoretical Discharge of a Swash Plate Pump 26

2.2.1 Theoretical Discharge with the Swash Plate Fixed 26

2.2.2 Theoretical Discharge with Swash Plate Oscillating about Zero Swash 29

2.2.3 Theoretical Discharge with Swash Plate Oscillating about a Mean Swash 30

2.3/

Page

2.3 The Steady State Performance of Positive Displacement Pumps and Motors 32

2.3.1 The Volumetric Efficiency of Positive Displacement Pumps and Motors 33

2.3.1.1 The Effect of Oil Compressibility on Volumetric Efficiency 36

2.3.2 The Mechanical Efficiency of Positive Displacement Pumps and Motors 40

2.3.3 The Mathematical Model for a Hydrostatic Transmission 43

3. The DYNAMIC ANALYSIS of a HYDROSTATIC TRANSMISSION 49

3.1 Basis of Model 49

3.2 Linearized Analysis of a Hydrostatic Transmission with Constant Speed Prime Mover 52

3.3 Signal Flow Analysis of a Hydrostatic Transmission Driven by a Prime Mover whose Speed will Fall with Torque 56

3.3.1 The Effect of a Change in System Parameters on the Natural Frequency and Damping Ratio 64

3.3.2 The Effect of Prime Mover Droop 65

3.4 /

Page

3.4 Vector Analysis to Determine the Dynamic Response of a Hydrostatic Transmission when the Load cannot be Represented by a Simple Mathematical Model 67

3.4.1 Vector Analysis Used to Determine the Effect of Return Line Pressure Variations 71

4. OIL COMPRESSIBILITY and its AFFECT UPON HYDRAULIC SYSTEM PERFORMANCE 82

4.1 Introduction 82

4.2 The Physical Determination of Oil Compressibility 84

4.2.1 Definitions and Relationships 84

4.2.2 Experimentally Determined Values of Bulk Modulus 90

4.3 The Use of Oil Bulk Modulus in the Determination of Hydraulic System Performance 92

4.4 Aeration of Hydraulic Fluids - The Effect Upon Hydraulic System Performance and Oil Compressibility 97

4.4.1 Mechanism of Aeration and Cavitation 97

4.4.1.1 Cavitation 98

4.4.1.2 Aeration 99

4.4.2 The Effects of Air Entrainment Upon Oil Compressibility and Hydraulic System Performance 101

		Page
5.	HYDROSTATIC TRANSMISSION TEST RIG and EXPERIMENTAL TECHNIQUES for MEASURING DYNAMIC RESPONSE	109
5.1	Elements of Hydrostatic Transmission Test Rig	109
5.2	Selection of Hydrostatic Pump and Motor	110
5.2.1	Hydrostatic Pump and Motor Swash Servos	112
5.3	Hydraulic Circuit of a Closed Loop Hydrostatic Transmission	113
5.3.1	Improved Boost System	116
5.3.2	System Filtration	118
5.4	The Prime Mover	119
5.4.1	Electro-Hydraulic Governing of Diesel Engine	120
5.4.2	Installation of Diesel Engine	121
5.5	Load Simulation	122
5.5.1	Coulomb Friction Plus Viscous Load Torque Simulation	124
5.5.2	Windage Load Simulation	125
5.5.3	Constant Horse Power Load	127
5.5.4	Experimental Determination of Simulated Load	128
5.6	Instrumentation and Measuring Equipment	129

		Page
6.	The EXPERIMENTAL DETERMINATION of the DYNAMIC RESPONSE of a HYDROSTATIC TRANSMISSION	157
6.1	Experimental Determination of Transmission System Parameters and Steady State Operating Conditions	157
6.1.1	System Physical Parameters	157
6.1.2	Loss Co-efficients for Pumps and Motors	159
6.1.3	The Steady State Conditions for Dynamic Testing	163
6.2	Dynamic Testing Procedures	165
6.2.1	Frequency Response Testing	165
6.2.2	Step Response Testing	167
6.3	Preliminary Dynamic Testing of Hydraulic Transmission (Tests 1 - 19)	167
6.3.1	Test Programme	167
6.3.2	Discussion of Preliminary Test Results	169
6.4	Test Programme (Tests 20 - 54) Using Modified Procedure to Investigate Scatter in Previous Tests	172
6.4.1	The Effect of Cycle Loading on Transmission Performance (Tests 20 - 24)	172
6.4.2	The Effects of Load Torque Speed Characteristics	174
6.4.2.1	A Typical Windage Load (Tests 25 - 28)	174
6.4.2.2	Variation of Load Damping Co-efficient f_L (Tests 29 - 32)	175
6.4.2.3	Effect of Amplitude on Input Signal (Tests 33 - 36)	175
6.4.2.4	Step Response Tests for a Variety of Load Damping Co-efficients (Tests 37 - 54)	176
6.4.2.5	The Dynamic Characteristics of the Load	177

Page

6.5 Correlation 179

6.5.1 Assessment of Methods Used to Determine Transmission Dynamic Performance 179

6.5.2 Bulk Modulus Evaluation 182

6.5.3 The Effect of Oscillating the Pump Swash Upon Its Performance 183

6.6 Further Investigation of the Effect of System Parameters Upon Hydraulic Transmission Dynamic Performance 184

6.6.1 The Effect of Load Inertia 185

6.6.2 Mean Return Line Pressure Effects 186

6.6.3 Effect of Boost System 187

6.6.4 Effect of Flexible Hose 189

6.6.5 Effect of Pressure Gauges 191

7. The DYNAMICS of HYDROSTATIC TRANSMISSION TEST RIG Used to INVESTIGATE AERATION EFFECTS 218

7.1 The Effects of Aeration Upon Hydrostatic Transmission Performance and the Proposed Experimental Investigation 218

7.2 Modifications to Hydraulic Transmission Test Rig 221

7.2.1 Test Set-Up for Atmospheric Tests 221

7.2.2 Test Set-Up to Pressurise Supply Oil with Gas 222

7.2.2.1 Design and Installation of Pressurised Oil Reservoir 223

7.2.2.2 Design and Installation of Atmospheric Overflow Reservoir 224

		Page
7.3	Test Programme	225
7.3.1	Dynamic Response Tests with Oil at Atmospheric Pressure	226
7.3.2	Dynamic Response Tests with the Oil in the Reservoir Pressurised with Air	227
7.3.3	Dynamic Response Tests with the Oil in the Reservoir Pressurised with Carbon Dioxide	229
7.4	Correlation of Test Results	230
7.4.1	The Effect of Low Mean Return Line Pressures with the Oil at Atmospheric Pressure	230
7.4.2	The Effect of Oil in the Reservoir being Pressurised with Air	231
7.4.3	The Effect of Oil in the Reservoir being Pressurised with Carbon Dioxide	232
7.5	Further Work	233
8.	CONCLUSIONS	256
8.1	The Positive Displacement Pump and Motor	256
8.2	Predicting Dynamic Response	259
8.3	Aeration Effects Upon Transmission Performance	263
REFERENCES		265

Page

APPENDICES

APPENDIX I

COMPUTER PROGRAMMES 273

A.1.1 The Flow from a Hydrostatic Pump with Swash Plate Oscillating about a Mean Non Zero Swash Angle

Programme 1 : 'DELIV' 274

A.1.2 The Evaluation of the Overall Transfer Function of a Hydrostatic Transmission Using Signal Flow Analysis

Programme 2 : 'TRDRES' 277

A.1.2.1 Main Programme 277

A.1.2.2 Subroutine 'RESP' 278

A.1.2.3 Subroutine 'SOLVE' 279

A.1.3 The Dynamic Analysis of a Hydrostatic Transmission Using Vectors

Programme 3 : 'VECTAN' 284

A.1.3.1 Main Programme Elements 285

A.1.3.2 Subroutine 'LOCI' 289

APPENDIX II /

Page

APPENDIX II

The DESIGN, DEVELOPMENT, and CONSTRUCTION Of the DOWNEL PUMP and MOTOR ELECTRO-HYDRAULIC SWASH SERVOS 301

A.2.1 General Description 301

A.2.2 Servo Development 302

APPENDIX III

DESIGN PROCEDURES 309

APPENDIX IV

The DYNAMIC CHARACTERISTICS of a HYDROSTATIC TRANSMISSION SYSTEM 318

Bowns, Dr. D.E., Worton-Griffiths, J.

Proc. Inst. Mech. E. Vol. 186 No. 55, 1972

NOTATION

A	Piston Area
A_S	Area of Fuel Pack Servo Jack
a	Amplitude of Sinusoidal Oscillation
B_o	Bulk Modulus of Oil
B_P	Bulk Modulus of Pipe
B_e	Effective Bulk Modulus of Oil in Pipe
B_T	Isothermal Tangent Bulk Modulus
B_S	Isentropic Tangent Bulk Modulus
$\overline{B_T}$	Isothermal Secant Bulk Modulus
$\overline{B_S}$	Isentropic Secant Bulk Modulus
C_D	Viscous Torque Co-efficient
C_F	Co-efficient of Pressure Dependent Torque Loss
	C_{FV} - Co-efficient Dependent on Static Pressure
	C_{FT} - Co-efficient Dependent on Dynamic Pressure
C_M	Co-efficient of m^{th} harmonic in Fourier Series
C_{RV}	Relief Valve Constant
C_S	Slip Co-efficient
	C_{SV} - Co-efficient of Viscous Slip Losses
	C_{St} - Co-efficient of Turbulent Slip Losses

d	Internal Diameter of Supply Line Pipe
D_M	Maximum Motor Displacement/Radian of Rotation
D_P	Maximum Pump Displacement/Radian of Rotation
D_2	Motor Displacement/Radian of Swash/Radian of Rotation
D_1	Pump Displacement/Radian of Swash/Radian of Rotation
e	Crank Eccentricity
E	Young's Modulus for Pipe Material
f_E	Engine Viscous Torque Co-efficient
f_M	Motor Viscous Torque Loss Co-efficient
f_P	Pump Viscous Torque Loss Co-efficient
f_L	Load Torque Variations with Speed Known as Load Damping Co-efficient
g	1st Co-efficient of Polynomial in Pressure for Secant Bulk Modulus
h	2nd Co-efficient of Polynomial in Pressure for Secant Bulk Modulus
J_E	Engine Inertia
J_P	Pump Inertia
$J_1 = J_E + J_P$	Driving Inertia
J_M	Motor Inertia
J_L	Load Inertia
$J_2 = J_M + J_L$	Driven Inertia
K	Output Speed/Pump Swash Steady State Gain
K_A	Fuel Rack Servo Amplifier Gain

K_E	Governed Engine Speed Droop with Load
K_P	Fuel Rack Servo Feedback Constant
K_{FM}	Motor Pressure Dependent Torque Loss Co-efficient
K_{FP}	Pump Pressure Dependent Torque Loss Co-efficient
K_G	Governor Speed Control Constant
K_M	Motor Slip Flow Loss Co-efficient
K_o	Constant Term of Polynomial in Pressure for Secant Bulk Modulus
K_P	Pump Slip Flow Loss Co-efficient
K_{RV}	Relief Valve Flow Dependent Pressure Co-efficient
K_T	Engine Governor Loop Feedback Constant
K_V	Fuel Rack Servo Valve Gain
l	Length of Piston Stroke
m	Harmonic No. in Fourier Series
n	Number of Pistons in Multi-Cylinder Pump
P	Pressure
P_H	Supply Line Pressure
P_L	Return Line Pressure
$P_D = P_H - P_L$	Pressure Difference Across Lines
P_o	Atmospheric Pressure
Q_A	Actual Flow
Q_P	Pump Output Flow
Q_M	Flow to Motor

Q_L	Flow Losses due to: Q_S - Slip Flow Losses Q_C - Compressible Flow Losses
Q_T	Theoretical Flow
R	Radius of Pistons in Cylinder Barrel from Shaft Axis
t	Supply Line Pipe Wall Thickness
T	Oil Temperature
T_A	Actual Torque
T_C	Constant Friction Torque
T_D	Viscous Torque Loss
T_E	Available Torque from Engine
T_F	Pressure Dependent Torque Loss
T_L	Load Torque
T_M	Torque Developed by Hydraulic Motor
T_P	Torque Available to Drive Pump
T_T	Theoretical Torque
T_2	Torque Required to Accelerate Motor and Load
v	Velocity of Pressure Wave through Fluid Medium
V	Volume of Oil in Supply Line including the Dead Volume of Pump and Motor exposed to Supply Line
V_1	Volume of Fluid in Cylinder at Moment of Switching from Low to High Pressure Port
V_A	Volume of Air at Atmospheric Pressure

V_C	Volume of Compressed Oil
V_D	Dead Volume
V_{Max}	Swept Volume at Maximum Swash
V_o	Fluid Volume at Atmospheric Pressure
V_P	Volume of Oil at Pressure P
X	Swash Plate Angle
X_M	Motor Swash Plate Angle
X_P	Pump Swash Plate Angle
Y	Engine Governor Setting
Z	Position of Piston from Datum
Ω	Rotational Speed
Ω_1	Input Speed to Transmission Engine and Pump Rotational Speed
Ω_2	Output Speed from Transmission Motor and Load Rotational Speed
ω_n	Transmission and Load Natural Frequency
ω	Frequency of Sinusoidal Swash Plate Variations
ξ	Damping Ratio
ρ	Oil Density
μ	Oil Absolute Viscosity
ν	Oil Dynamic Viscosity
$s = \frac{d}{dt}$	Differential Operator

τ_1 & τ_2	Time Constants	
Suffices	P	Pump
	M	Motor
	LP	Load Pump
	RV	Relief Valve
	NV	Needle Valve

Lower Case Letters throughout the text refers to small variations about a Steady State Operating Condition, unless otherwise stated.

Page

LIST of FIGURES

1.1	Historical Development of the Oil Hydraulics Industry	11
1.2	The Pittler Rotary Pump and Motor	12
1.3	The Manly Variable Speed Transmission	13
1.4	The Lenz Gear	13
1.5	The 40 H.P. Williams-Janney Hydraulic Variable Speed Gear - 1913	14
1.6	The Hele-Shaw Rotary Pump and Motor Unit	15
1.7	Motor Wagon fitted with Hele-Shaw Transmission	16
1.8	Open and Closed Loop Hydrostatic Transmission Circuits	17
1.9	The Four Basic Configurations of Pump and Motor in Hydrostatic Drives and their Characteristic Performance Curves	18
2.1	The Three Main Types of Positive Displacement Pump and Motor Units	44
2.2	Radial Piston Positive Displacement Pump and Motor Units	45
2.3	Axial Piston Positive Displacement Pump and Motor Units	46
2.4	Diagramatic Layout of Swash Plate Pump and Delivery of Single Cylinder	47
2.5	Illustration of Compressibility Effects during Piston Pump Cycle	48

		Page
3.1	Diagramatic Layout and Block Diagram of a Lossless Hydrostatic Transmission	74
3.2	Signal Flow Analysis	75
3.3	Transmission Signal Flow Diagram and Resultant Transfer Function	76
3.4	The Effect of System Volume on Transmission Natural Frequency and Damping Ratio	77
3.5	Effect of Load Inertia on System Natural Frequency and Damping Ratio	78
3.6	The Frequency Response of a Hydrostatic Transmission Driven by a Prime Mover of Significant Droop.	79
3.7	Vector Analysis for Determining Overall Transmission Response Using Measured Load Locus	80
3.8	Behaviour of Return Line During Frequency Response Tests	81
4.1	Isothermal and Isentropic Oil Compression Curves	104
4.2	Graphical Representation of Tangent and Secant Bulk Modulus	105
4.3	Isentropic Tangent Bulk Modulus against Temperature and Pressure for Shell Tellus Oil 27	106
4.4	Rate of Solution of Air Bubbles in Mineral Oil	107
4.5	Effect of Aeration on the Bulk Modulus of Hydraulic Oil	108

		Page
5.1	Dynamics of Hydrostatic Transmission Rig	138
5.2	Layout of Engine Driven Hydrostatic Transmission and Load Pump	139
5.3	Sectional View of Downel Variable Displacement Pump/Motor	140
5.4	Pump and Motor Swash Servos	141
5.5	Closed Loop Hydrostatic Transmission Circuit and Boost Circuit	142
5.6	Valve Block for Boost System	143
5.7	Pressure-Flow Characteristic of Boost Pressure Valve in Valve Block	144
5.8	Pressure-Flow Characteristic of Cross Line High Pressure Relief Valve in Valve Block	145
5.9	Closed Loop Hydrostatic Transmission Circuit with Simplified Large Capacity Boost System	146
5.10	Pilot Operated Unloader Valve	147
5.11	Pressure -Flow Characteristic of Relief Valve Used in High Capacity Boost System	148
5.12	Block Diagram of Diesel Engine with Electro-Hydraulic Speed Governor	149
5.13	Photograph, Block Diagram and Transfer Function of Fuel Rack Servo	150
5.14	Block Diagram and Transfer Function of Diesel Engine Electro-Hydraulic Speed Governor	151
5.15	Typical Speed-Load Characteristics of Diesel Engine with Variable Feedback Electro-Hydraulic Governor	152

		Page
5.16	Vickers Variable Delivery Pressure Compensated Axial Piston Load Pump	153
5.17	Pressure Flow Characteristics for Loading Valves	154
5.18	The Simulation of Variable Slope Load Torque and Motor Speed Windage Loads	155
5.19	Typical Experimentally Determined Load Simulations	156
6.1	Test Rig for Measuring Steady State Performance Characteristics of Downel Pump	199
6.2	Variation of Pump Flow with Pressure at Constant Speed	200
6.3	Pump Slip and Viscous Torque Loss Co-efficients	201
6.4	Variation of Pump Torque with Pressure Difference at Constant Speed	202
6.5	Variation of Pump Torque with Speed at Constant Pressure	203
6.6	Schematic Illustrating Technique for Frequency Response Testing	204
6.7	Experimentally Determined Frequency Response for Test 5 compared with Theoretically Computed Results	205
6.8	Overall Frequency Response of Transmission with Windage Load	206
6.9	Effect of Load Damping Co-efficient on Transmission Dynamic Response	207

		Page
6.10	The Effect of Load Damping Co-efficient on Overall Transmission Response using Smaller input Amplitude	208
6.11	Step Response Galvanometer Recording for Test 44	209
6.12	Variation of Transmission Apparent Natural Frequency with Load Damping Co-efficient f_L Measured by Step Response Technique	210
6.13	Variation of Transmission Damping Ratio with Load Damping Co-efficient Measured by Step Response Technique	211
6.14	The Locus of the Measured Hydrostatic Load	212
6.15	The Effect of an Increased Inertial Load on Overall Transmission Response	213
6.16	Galvanometer Readings of Swash Plate Angle, Output Speed, Return Line Pressure, for Restricted Boost Systems	214
6.17	The Effect of Restricted Boost Supply Upon Overall Transmission Response	215
6.18	The Effect of Using a Flexible Hose Supply Line on Overall Transmission Response	216
6.19	Static Test Determination of Effective Bulk Modulus of Oil in Flexible Hose Using Deadweight Tester	217
7.1/		

		Page
7.1	Modified Hydrostatic Transmission Circuit for Work on Aeration	250
7.2	Layout of 15 Gallon Pressurised Tank	251
7.3	Layout of 5 Gallon Atmospheric Tank	252
7.4	Logarithmic Plot for Test 86. Output from Programme 'VECTAN'	253
7.5	Loci for Test 86. Output from Programme 'VECTAN'	254
7.6	Pressure Speed and Swash Traces for System with Boost Pressure Maintained by Gas Pressure and Boost Pump	255
A.1.1.1	Flow Chart for 'DELIV'	275
A.1.1.2	Programme Listing for 'DELIV'	276
A.1.2.1	Flow Chart for 'TRDRES'	280
A.1.2.2	Flow Charts for Subroutines 'RESP' and 'SOLVE'	281
A.1.2.3	Programme Listing for 'TRDRES'	282
A.1.2.4	Programme Listing for Subroutines 'RESP' and 'SOLVE'	283
A.1.3.1	Flow Chart for 'VECTAN'	290
A.1.3.2	Programme Listing for 'VECTAN'	292

		Page
A.2.1	Elements of Swash Servos	306
A.2.2	Frequency Response Tests of Motor Swash Servo	307
A.2.3	Closed Loop Frequency Response Tests of Motor Swash Servo with Increased Forward Path Gain	308
A.3.1	Design Procedure Block Diagram	317

CHAPTER 1 : INTRODUCTION

1.1 The Historical Evolution of Oil Hydrostatic Power Transmission

The term hydrostatic power transmission is used to describe systems which transmit power through liquids by pressure and displacement of mechanical parts rather than by momentum transfer. It is particularly applied to drives incorporating rotary input and output elements and it is in this sense that the term is applied in this thesis.

At the end of the nineteenth century extensive use was being made of high pressure water for power transmission not only in stationary equipment such as hydraulic presses, but also as a means of distributing power from a control source. The culmination of this development was reached in the public hydraulic power supply systems in London, and at least eight other large cities (1). The London Hydraulic Power Company is well known and still supplies high pressure water for the machinery that operates the bascules of the Tower Bridge and several other installations.

The introduction of electrical power distribution networks led to a rapid decline in the installation of water pressure mains, the superiority of electric power distribution over any distance being readily appreciated.

Like much of the early slow reciprocating machinery, the water hydraulics machinery which remains is still in remarkably good condition and is being actively preserved.

Fig 1.1 reproduced from (2) shows the development of the oil hydraulics industry. After 1900 the accent was on the transmission and modulation of power between prime movers and loads leading to the development of self contained hydraulic drives which were able to recirculate the working fluid. It became common practice to use oil instead of water, and the change to oil was the most significant step in the development of hydraulics and led to many improvements in design.

The pioneering period in the Oil Hydraulics Industry described by Beacham (2), was initiated by Hall (3) whose differential gear drive comprised a pump and motor each with three radial cylinders. The pump with a rotating fixed throw crank delivered through piston valves to a motor with a stationary variable throw crank.

In 1907 Pittler in Germany developed a transmission whose pumps and motors were of the vane type (4). By linking two pumps of different capacities to a motor with valve control it was possible to achieve three forward and reverse speeds. A significant feature was that the motion of the vanes was in the axial direction, Fig. 1.2.

There were four other well known transmissions of this period. The American Manly Gear (5) had a pump with five radial cylinders driven by a single crank, Fig. 1.3, and incorporated two eccentrics rotating relative to one another for adjusting the crank throw. Each pump cylinder was of variable displacement and delivered to one or more fixed displacement motors.

The Lenz Gear, Fig. 1.4, used fixed capacity vane type pumps with valve control arranged so as to give a number of different gear ratios (6). The first of the more familiar rotary cylinder swashplate type drives was the Williams and Janney transmission Fig. 1.5, (7), and the first transmission with an outward thrusting radial cylinder pump and motor was the Hele-Shaw transmission, Fig. 1.6, (8).

The developers of these early transmissions were quick to apply their work. The Pittler, Hall gear, Williams and Janney Transmission and Hele-Shaw Transmission, were all fitted to different types of trucks and buses, and drives were supplied for conveyors, printing presses, machine tools, and railway swing bridges (7). Fig. 1.7 shows a motor wagon constructed by Messrs. Compayne Limited of London in 1912. It incorporated the Hele-Shaw transmission, and it is interesting to note that many of the features incorporated are now common practice. These include such items as the 'boost' pump, wheel motor, and servo operated stroke control of the pump. Pipe connections in a unit of this complexity must have been a great problem with no flexible pipes available.

The development of the traction application was shortlived; the improved design of mechanical transmissions led to a decline in the use of hydrostatic drives that was to last for nearly half a century. Between the two world wars the diversification of hydraulic power transmission application spread through the marine industrial and machine tool fields. The development of hydraulic equipment continued with Thoma, Constantinesco, Dowty, and the Towler Brothers, making significant contributions, Fig. 1.1.

Thoma's design of tilting head axial piston pump proved very successful and has provided the basis for many designs of pump and motor units. The Towler Brothers introduced a range of high pressure piston pumps for application to heavy industrial machinery such as hydraulic pressures steadily increasing the speed and pressure capability of their units. Some of these units are currently applied to hydrostatic drives.

Constantinesco and Dowty became known for their applications of hydraulic equipment as ancillaries for aircraft and marine use, but Constantinesco's early theoretical work on transient pipe flow won him world renown even though it was many years before it was recognised.

A major advance came with the development of synthetic rubber sealing and its associated technology which enabled spillage and internal leakage to be reduced.

Other notable developments were improved filtration to prolong system life; high pressure flexible hose; special hydraulic fluids including fire resistant fluids; and the rubber sac hydraulic accumulator assisting the storage of hydraulic power.

The early hydrostatic transmissions already described provided a foundation for the steady growth in this field, and the reawakening of interest in the traction field added extra momentum. As developments took place in pump and motor design these were incorporated into the transmissions of the day.

The tilting head Thoma pump, the variable stroke slipper type swashplate pump, the slow radial cylinder motor, the ball type pump and motor, and the high speed motor, were all incorporated for different types of application. System pressures have increased in an effort to increase the power to weight ratio of the drives, and considerable design effort has been expended to minimise losses and increase life of units by hydrostatically and hydrodynamically balancing bearing loads.

1.2 The Closed Circuit Hydrostatic Transmission /

1.2 The Closed Circuit Hydrostatic Transmission

The hydrostatic transmission for producing a controlled and variable speed or position may be one of two basic types; open circuit or closed circuit. The former, shown in Fig. 1.8(a), comprises a pump drawing fluid from a reservoir. Directional control is achieved by means of a self centreing valve. There are two limitations upon the open loop type of transmission. Complex valve circuits are required if a breaking torque is to be incorporated, and because of the low pressures that may occur at the pump inlet, the risk of cavitation is high especially at high pump speeds.

This has led to the use of closed loop transmissions of which a typical circuit is shown in Fig. 1.8(b). An additional pump capable of making up for any leakage in the pump and motor units has been incorporated with a relief valve preset to maintain a 'boost pressure' in the return line, and relief valves between the supply and return lines to prevent overloads. The drive is fully reversible. The basic configurations described are for single power outlet systems, but multi-outlet systems are commonplace. The case of two and four independent wheel drives is an obvious example. The valve gear necessary to control multi-outlet systems has a strong influence on system performance.

There are four basic combinations of fixed and variable displacement pumps and motor units. These are shown in Fig. 1.9 along with the relevant characteristics. The fixed displacement pump and motor (a) gives a fixed drive and acts rather like a flexible mechanical drive shaft. The constant output pump driving a variable displacement motor (b) gives an increase in motor speed as the motor displacement is reduced, byt this is accompanied by a fall off in torque capability. It can give constant power over a large speed range. The variable output pump and fixed displacement motor (c) is the commonest drive and has constant torque capability. It will act as a disengaged clutch when the pump displacement is reduced to zero. The fourth case where both pump and motor are of variable displacement (d) permits the best efficiency to be obtained over a very wide speed and torque range, and it makes it suitable for traction or other applications where this is required (9).

The work of matching transmission performance to load characteristics has led to the development of more complex split torque and split speed differential arrangements. For vehicle propulsion applications these units have been built up into special systems capable of single lever control and housed in their own reservoir. As a proportion of the power is transmitted mechanically at some points in the operating range they are more efficient than a pure hydraulic drive.

The overall efficiency of pump and motor units varies from about 80% for gear units up to a value of 95% for some high performance axial piston units. When pump and motor units are combined together to form a hydrostatic transmission the peak efficiency that can be expected is of the order of 85%. It should be stressed however that this is a peak value and far lower efficiencies may be expected unless careful consideration is given to the selection of the pump and motor units and their configurations (9).

This is a very simplified description of hydrostatic transmissions; the range of possible applications make the number of possible circuit designs very extensive. It is this versatility of the hydrostatic drive that makes it so appealing to user industries. However, the majority of the work carried out in this investigation considers a very typical closed circuit loop transmission of the type shown in Fig 1.8 (b) using axial piston type pump and motor units.

1.3 The Dynamic Performance of Hydrostatic Transmissions

The original work carried out to evaluate the dynamic performance of hydrostatic speed control transmissions stemmed from its application as the power element of servomechanisms. Typical servo applications were those of gun positioning apparatus and ship steering gear.

It is desirable when designing servo systems to be able to represent each element of the system by a differential equation or transfer function relating output to input, enabling overall performance evaluation and optimisation to be carried out. In addition it may be necessary to evaluate transient conditions such as those that occur when loads are suddenly applied or removed both intentionally or due to system failure. These transient conditions may be extreme and a conception of the factors affecting their nature is essential if they are to be limited to acceptable values.

One of the earliest attempts at dynamic analysis of hydrostatic transmissions was carried out in 1947 by Newton (10), who backed up his analysis with some experimental work. This early work was of considerable significance and has since been referred to in several texts, but appreciable errors were recorded between theoretical predictions and experimental results. Mention was made of several possible sources of error, but since that time there have been very few reported attempts to verify this analysis and its assumptions.

The general method of approach is to consider the pump and motor as continuous linear elements driving a viscous and inertial load, the pump and motor being connected by a compressible oil column. A transfer function relating any two variables such as changes in motor output speed with pump swash plate angular position changes or load torque is then evaluated.

Well known authors who have outlined this simple analysis include Shearer (11), Lewis and Stern (12), Thoma (13), and Gille (14). None of them recorded any experimental work carried out to investigate the dynamic performance of hydrostatic transmissions. More recent work has turned toward the valve controlled hydrostatic servo and much discussion has centred upon the valve characteristics and the inherent non-linearities present in the system.

This thesis describes a theoretical analysis of a hydrostatic transmission with consideration given to extreme cases where the transmission departs from its assumed linear behaviour.

The availability of sophisticated dynamic measuring equipment in recent years has considerably simplified the task of dynamic testing. It was therefore possible to carry out an extensive test programme which hitherto would have been impossible. The experiments employed electro-hydraulic test techniques both for the control of the load and for providing the necessary inputs to the transmission.

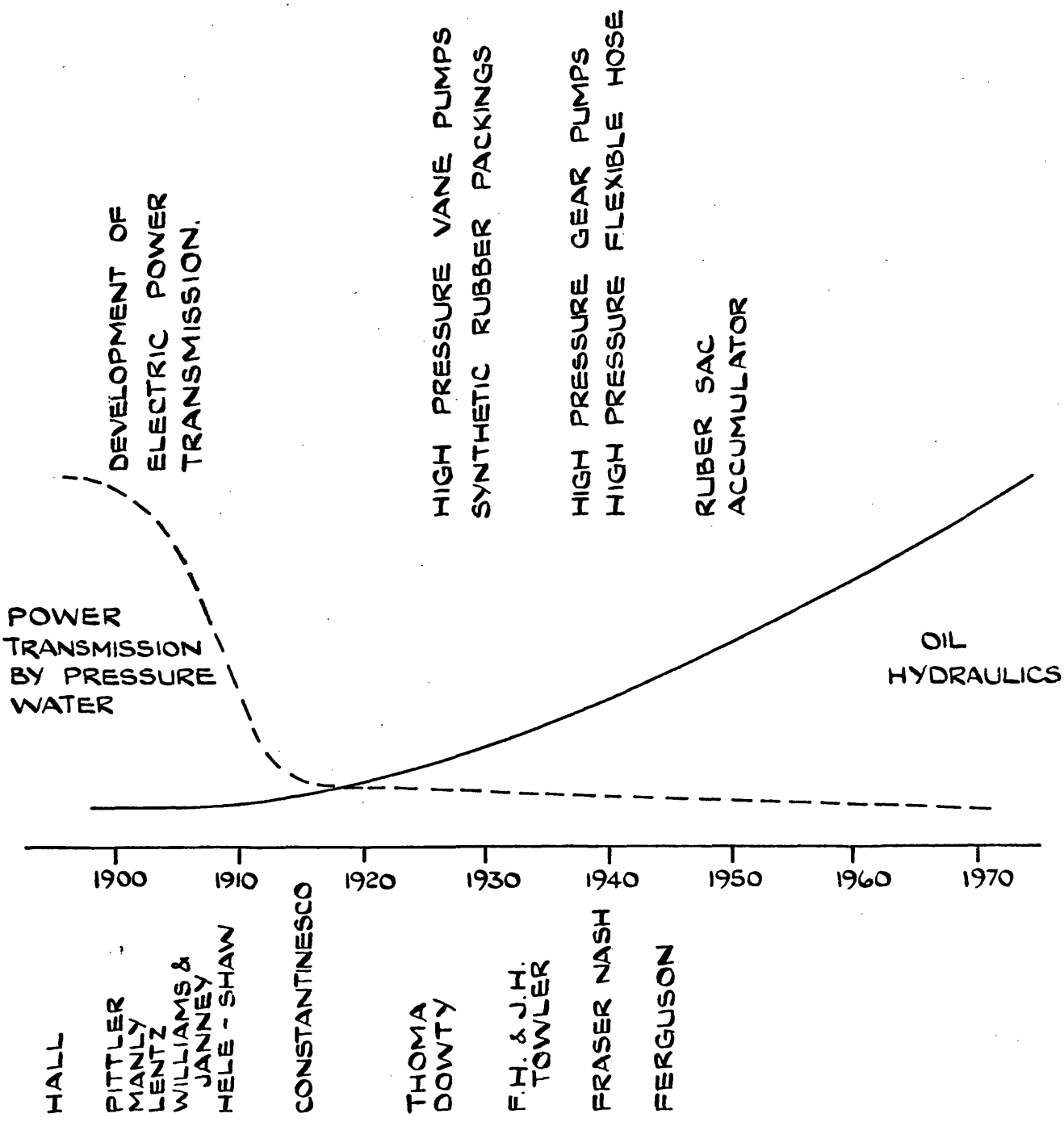

FIG. 1.1. HISTORICAL DEVELOPMENT OF THE OIL HYDRAULICS INDUSTRY.

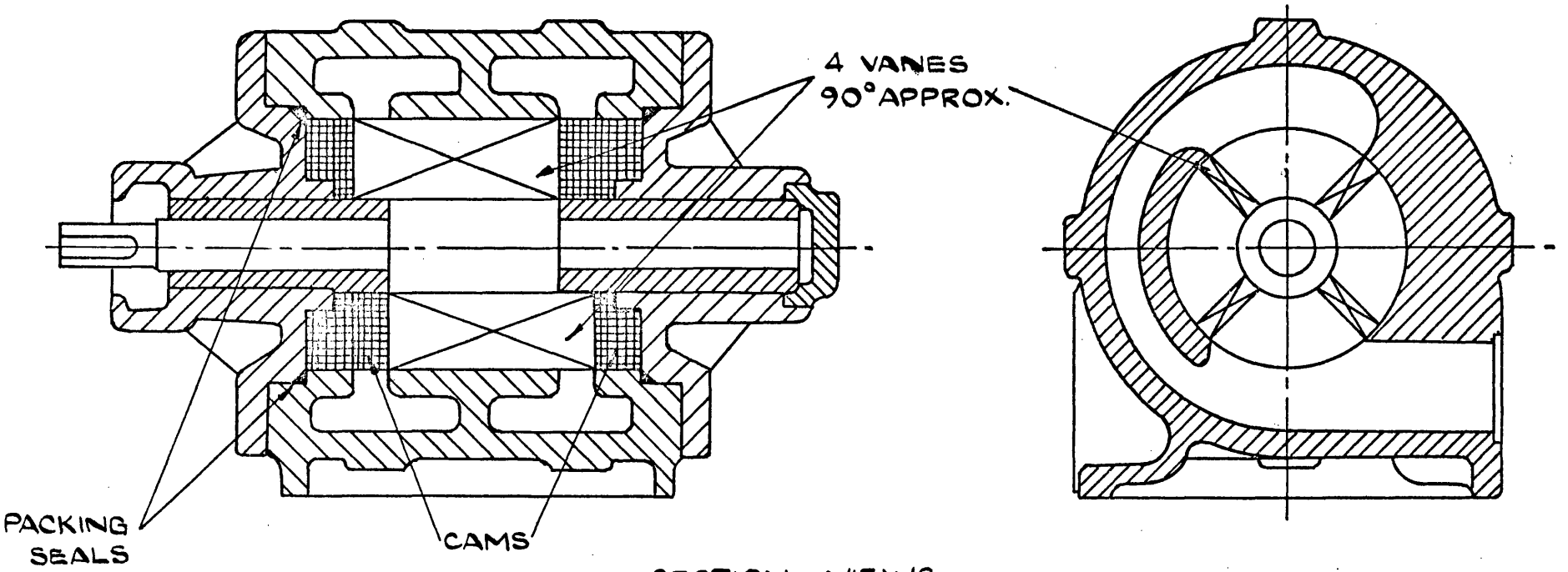

SECTION VIEWS

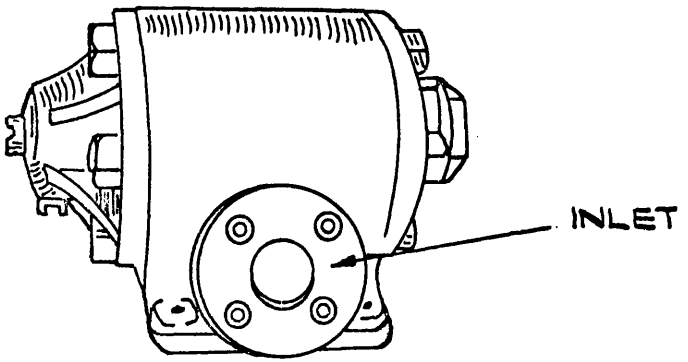

PUMP ASSEMBLY

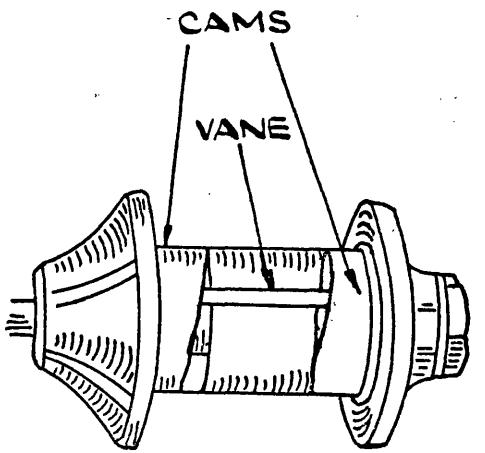

ROTOR & END PLATES.

FIG. 1.2 THE PITTLER ROTARY PUMP & MOTOR.

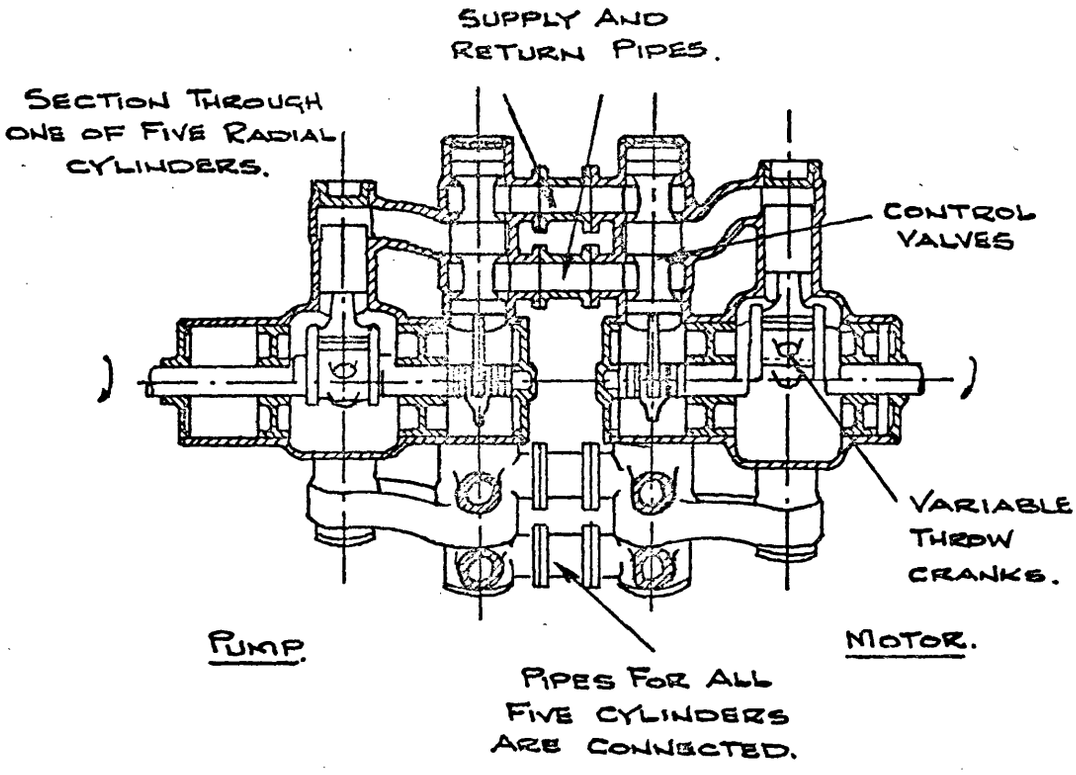

FIG. 1.3 THE MANLY VARIABLE SPEED TRANSMISSION.

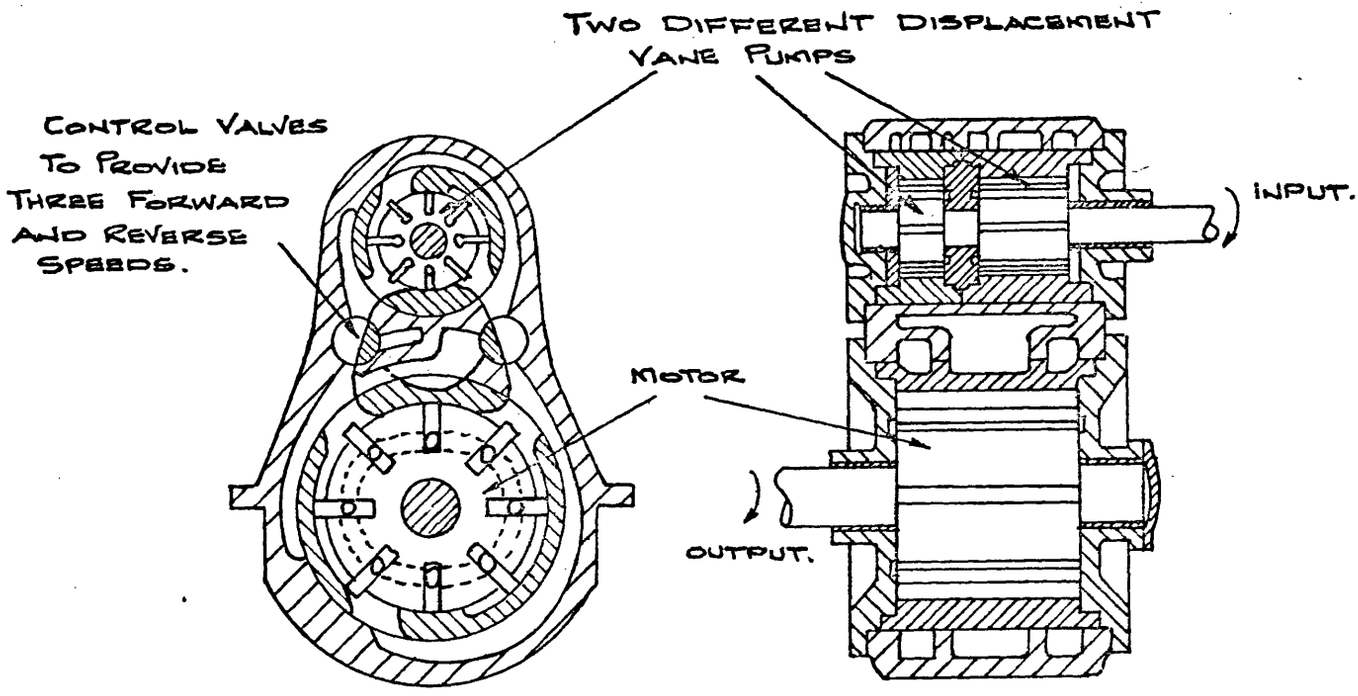

FIG. 1.4 THE LENZ GEAR.

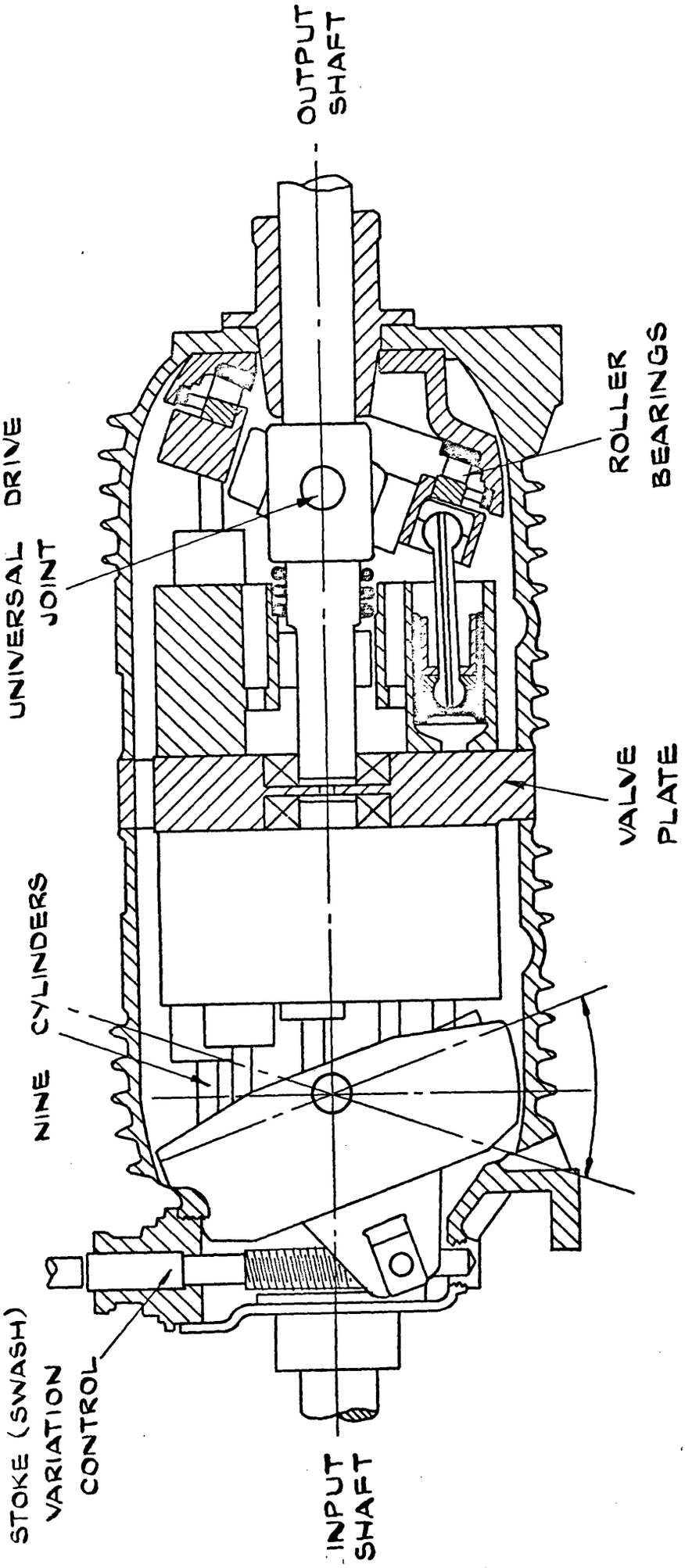

FIG. 1.5 THE 40 H.P. WILLIAMS-JANNEY HYDRAULIC VARIABLE SPEED GEAR - 1913.

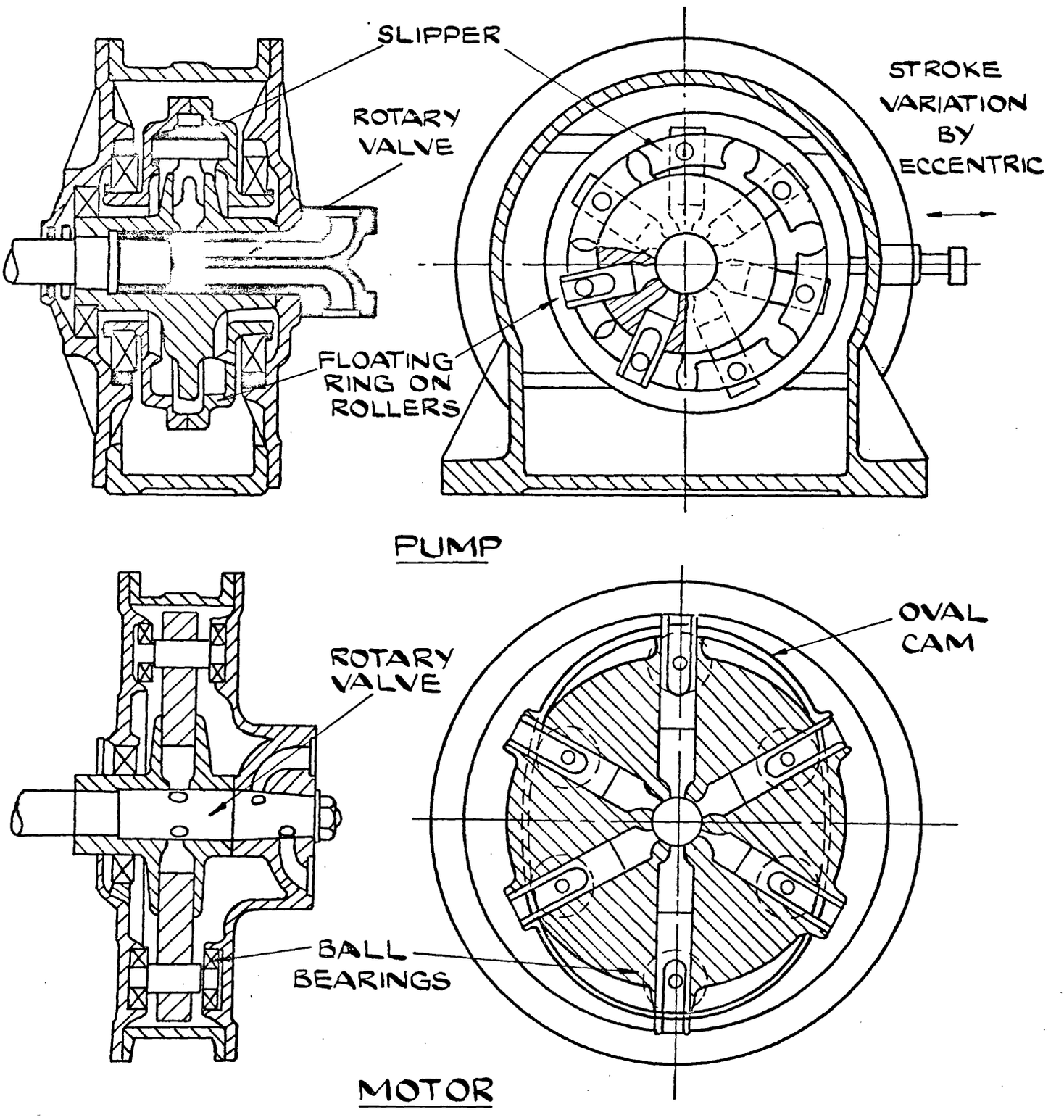

FIG. 1.6. THE HELE - SHAW ROTARY PUMP & MOTOR UNIT.

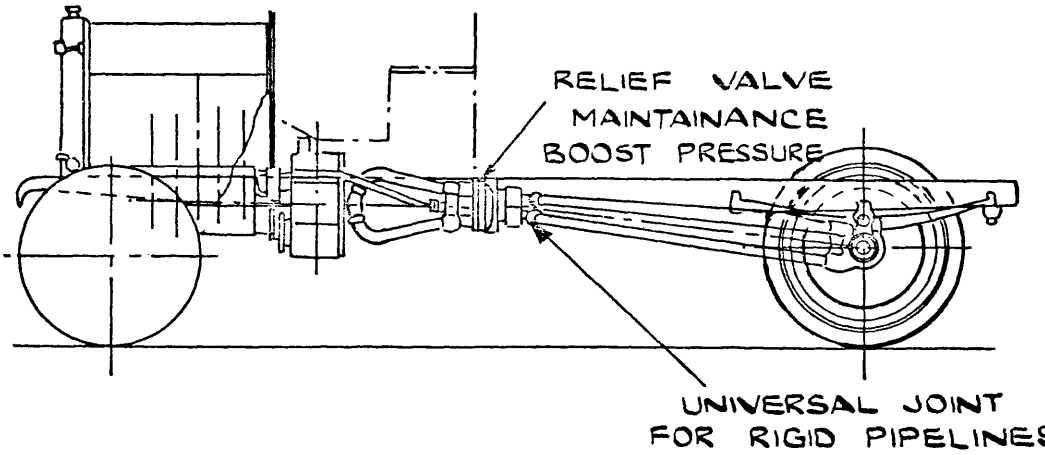

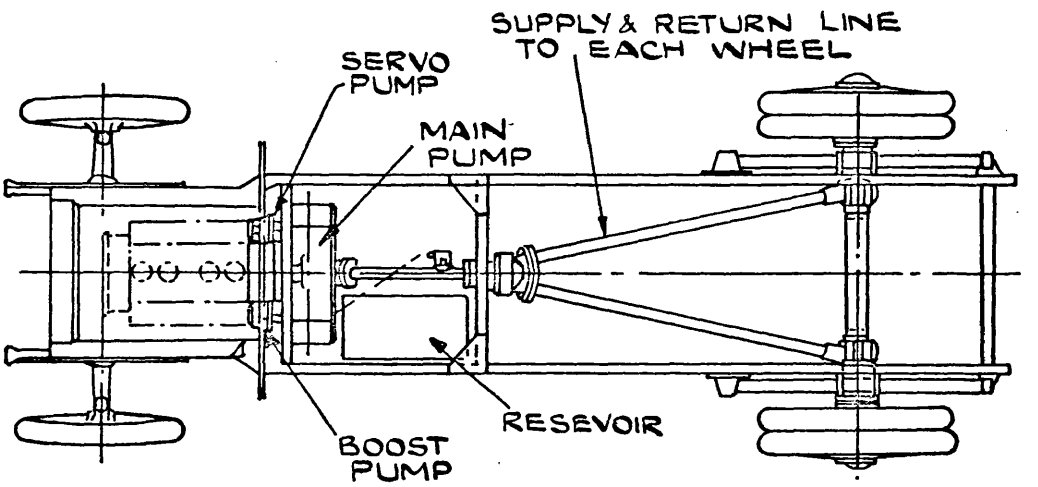

CHASSIS LAYOUT SHOWING HYDROSTATIC TRANSMISSION.

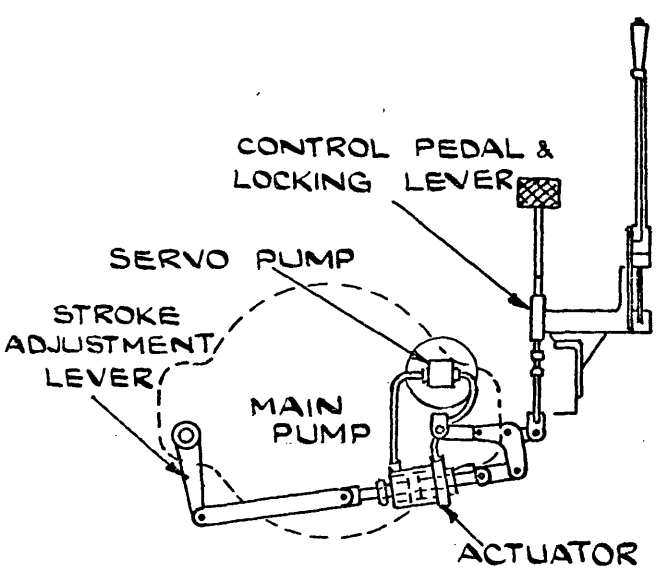

STROKE ADJUSTMENT SERVO
(NOTE MECHANICAL
FEEDBACK LINK)

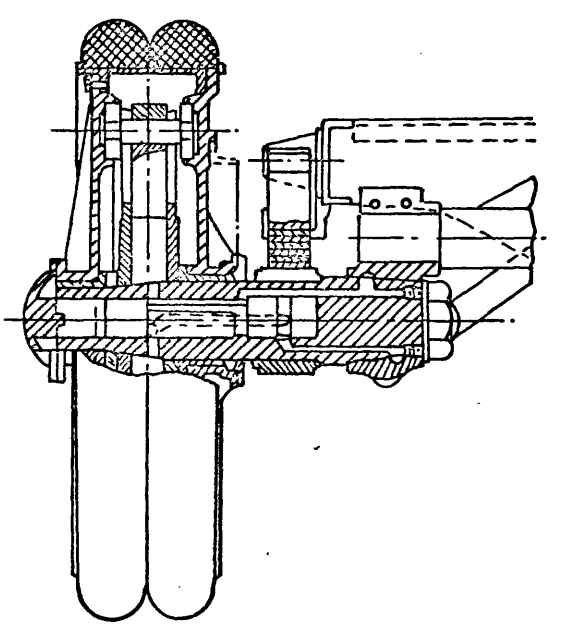

WHEEL MOTOR

FIG. 1.7. MOTOR WAGON FITTED WITH HELE-SHAW TRANSMISSION.

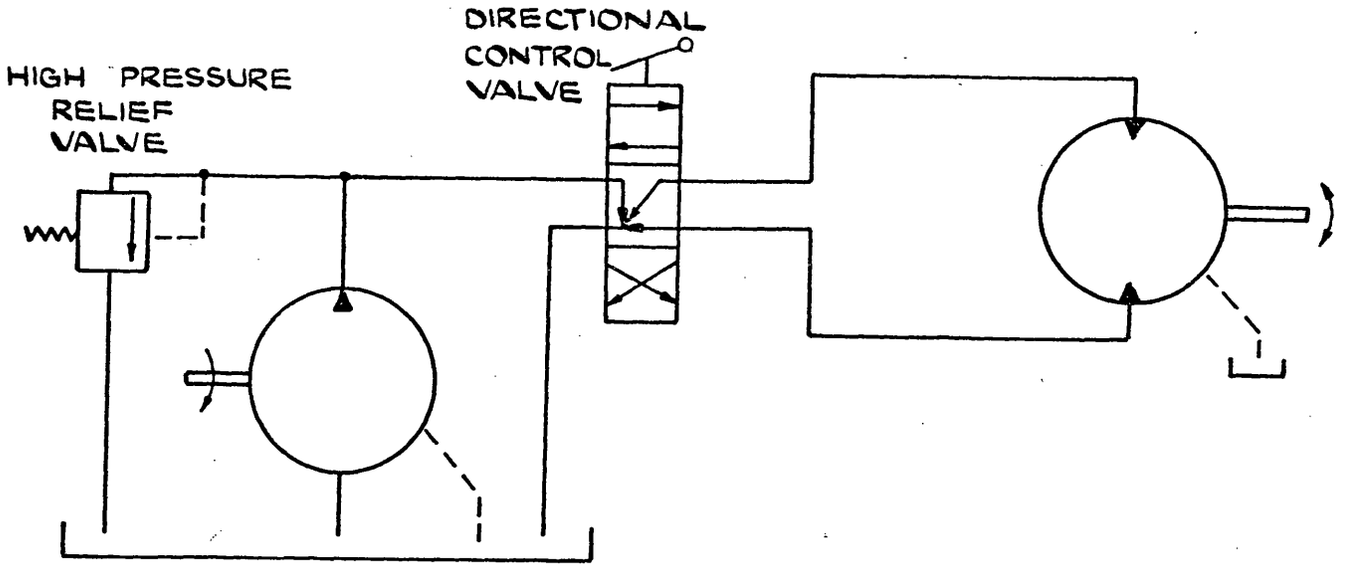

(a) OPEN LOOP HYDROSTATIC TRANSMISSION CIRCUIT WITH DIRECTIONAL CONTROL.

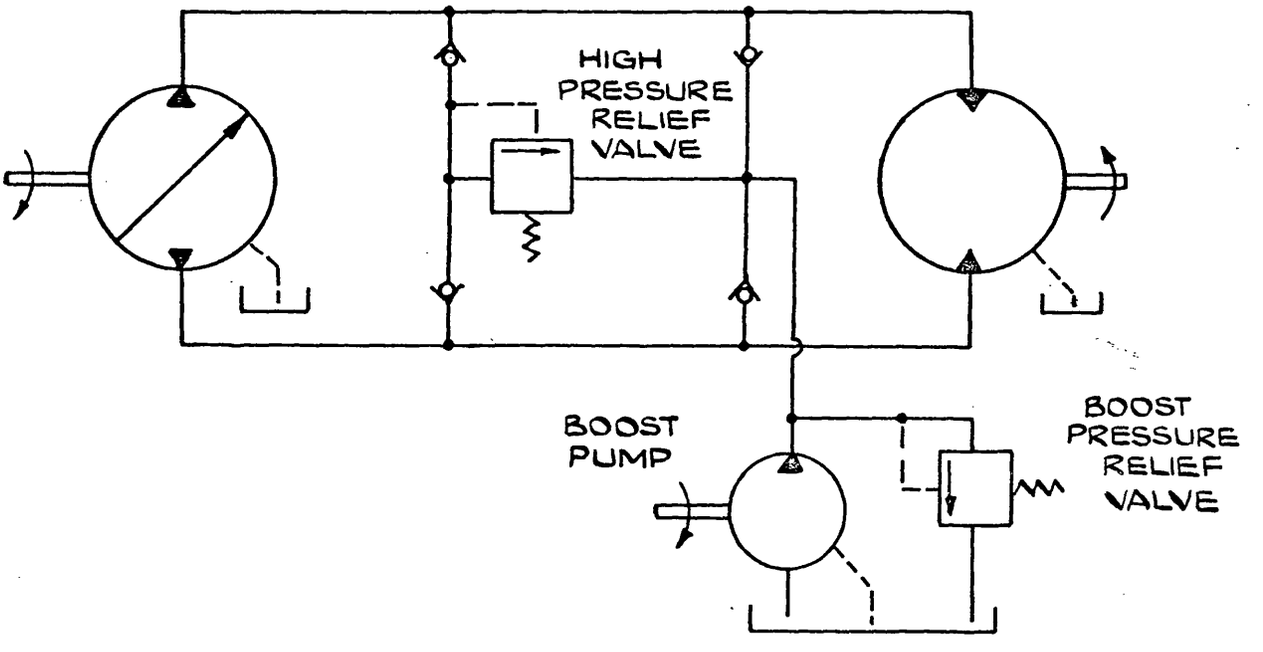

(b) CLOSED LOOP HYDROSTATIC TRANSMISSION CIRCUIT WITH BOOST PUMP.

FIG. 1.8. OPEN & CLOSED LOOP HYDROSTATIC TRANSMISSION CIRCUITS.

CONFIGURATION

PERFORMANCE CURVE FOR CONSTANT INPUT SPEED & SYSTEM PRESSURE.

FIXED RATIO ACCORDING TO PUMP AND MOTOR DISPLACEMENT.

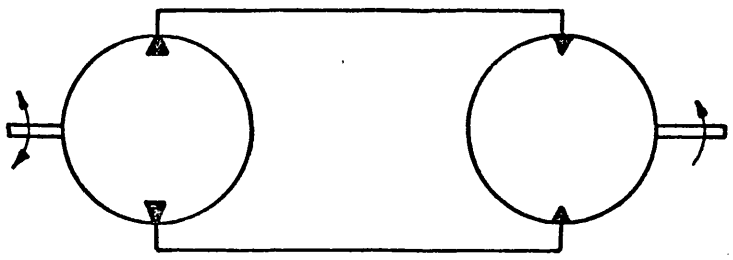

(a) FIXED DISPLACEMENT PUMP & MOTOR.

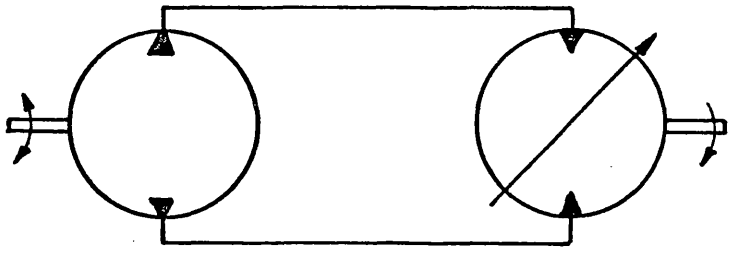

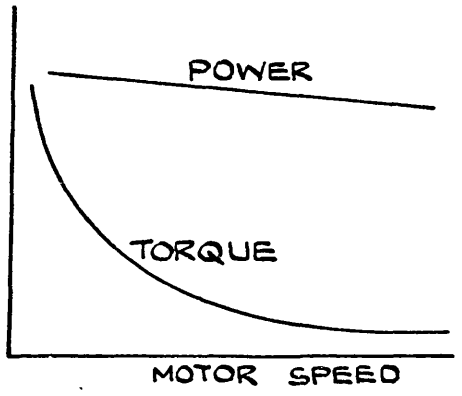

(b) FIXED DISPLACEMENT PUMP VARIABLE DISPLACEMENT MOTOR

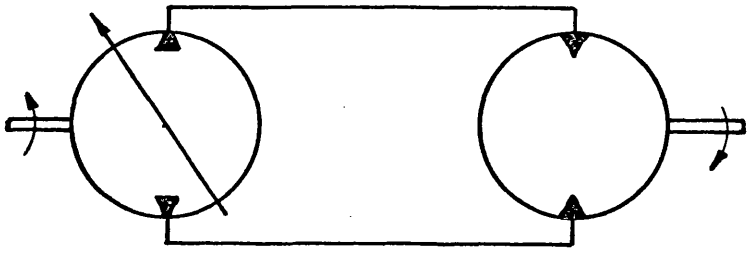

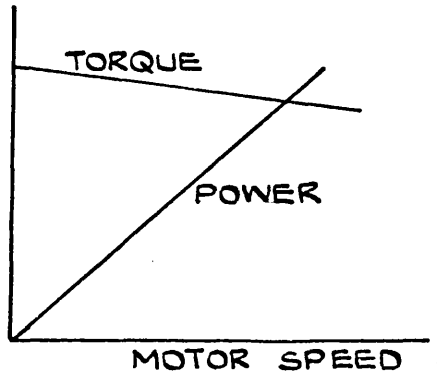

(c) FIXED DISPLACEMENT MOTOR VARIABLE DISPLACEMENT PUMP.

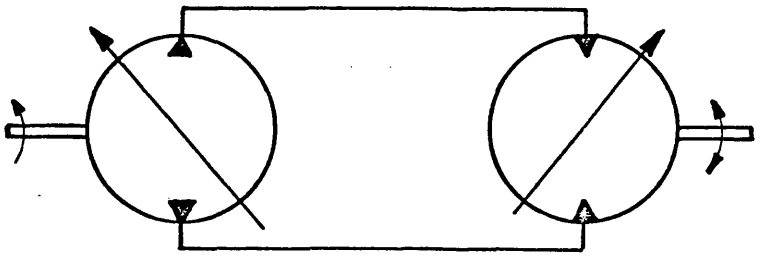

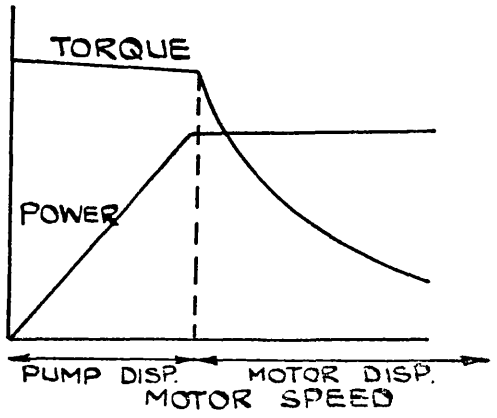

(d) VARIABLE DISPLACEMENT PUMP & MOTOR

FIG. 1.9. THE FOUR BASIC CONFIGURATIONS OF PUMP & MOTOR IN HYDROSTATIC DRIVES & THEIR CHARACTERISTIC PERFORMANCE CURVES.

CHAPTER 2 : POSITIVE DISPLACEMENT PUMPS and MOTORS Used in HYDROSTATIC TRANSMISSIONS and Their PERFORMANCE CHARACTERISTICS

2.1 Positive Displacement Pumps and Motors

A positive displacement pump has been defined as one in which each revolution of the pump shaft is associated with a discrete quantity of fluid being displaced under high pressure. Similarly, a positive displacement motor will produce one revolution when a discrete quantity of fluid is accepted.

In this chapter it is intended to summarize the important steady operating characteristics of pumps and motors which affect their dynamic behavior.

The range of available units can be broadly split into three main types - gear, vane, and piston units. A brief description of each type of unit is as follows.

2.1.1 Vane Units /

2.1.1 Vane Units

A simple vane pump is shown on Fig. 2.1 (a). The pumping action is achieved by vanes moving radially in a rotor which has its centre eccentric to the casing track on which the outer tips of the vanes bear. Because of large out of balance forces the delivery pressure is normally limited to 1000 lbf/in^2, but by balancing the rotor with an additional pair of ports delivery pressures of 3000 lbf/in^2 have been achieved.

A further development of this type of pump is the cam rotor pump which by multiple ports and careful forming of the rotor on which the vanes bear, has been able to achieve balance and a ripple free pump delivery.

2.1.2 Gear Units

By utilising a pair of meshing gears the gear pump shown in Fig. 2.1 (b) displaces fluid between the gears and the inner surface of the pump housing from the inlet to outlet ports. Provision is normally made to bleed off fluid trapped between meshing teeth and in the more sophisticated types of pumps leakage across the faces of the gears is reduced by hydraulically loaded side plates.

Gear units are the most widely used fixed capacity hydraulic pumps and motors in general application.

2.1.3 Piston Units

In this type of unit fluid is displaced by close fitting pistons sliding in cylindrical bores, Fig. 2.1(c). A pumping action is obtained by reciprocating the pistons relative to the bores, and is capable of delivering fluid of higher pressures than the vane and gear units.

The basic reciprocating action of the pistons can be produced in a number of ways and in consequence piston units are available in a wide variety of different designs and configurations. The usual number of pistons is 5, 7, 9, and 11, the odd number being to reduce flow fluctuations as will be seen later. Designs can be broadly broken down into two types, those with radial and those with axial pistons. As the piston unit is of particular interest to the work of this thesis, the basic configurations and their swept volumes will be considered in detail.

Radial Piston Units /

Radial Piston Units

As shown in Fig. 2.2 the pistons in the radial design are set radially around the central driving shaft. The reciprocating motion is produced by either rotating the cylinder barrel whilst the pistons remain in contact with a stationary outer track eccentric to the barrel, Fig. 2.2(a), or by moving the pistons in a stationary barrel using a rotating eccentric cam, Fig. 2.2(b). Rotary valves operated by the main drive shaft direct fluid into the supply and return lines during the appropriate period of the piston strokes.

Both types of radial piston pump can be equally well adopted for use as a hydraulic motor, and many of the low speed high torque motors, in particular wheel motors, have radial pistons.

For a radial piston pump with either a rotating barrel, or a rotating eccentric, the delivery of each piston per revolution

= Area of Piston x Delivery Stroke

$= A \times 2e$ - 2.1

For n pistons:

$$\text{Displacement/rev} = 2Aen \quad \text{- 2.2}$$

Axial Piston Units

There are three main types of axial piston unit whose pistons reciprocate in a direction parallel to the axis of rotation. The wobble plate and swash plate units, Fig. 2.3(a) and Fig. 2.3(b), have in line barrels and drive shafts whilst the third is the bent axis or tilting head type, Fig. 2.3(c).

The wobble plate unit shown in Fig. 2.3(a) has a stationary barrel and the pistons are reciprocated by the inclined wobble plate rotated by the drive shaft. In contrast the swash plate pump, Fig. 2.3(b), has a stationary inclined plate, and the barrel is rotated by the drive shaft. The actions of the two in line units are identical and the delivery of each piston per revolution

$$= \text{Area of Piston} \times \text{Delivery Stroke}$$

$$= A \times 2R \tan X \qquad - 2.3$$

For n pistons:

$$\text{Displacement/rev} = 2AnR \tan X \qquad - 2.4$$

The bent axis unit is shown in Fig. 2.3(c) and it can be seen that as the cylinder barrel axis is tilted from that of the driving shaft the pistons are made to reciprocate in their bores.

Some designs incorporate a constant velocity joint to transmit power to the cylinder barrel and prevent sideloads on the pistons. Unlike the two in line types of unit that are limited to maximum wobble plate and swash plate angles of 15^{o} - 20^{o} the bent axis type of pump is capable of tilt angles of up to 35^{o} with special designs going as high as 45^{o}. A much larger delivery for a given package size is thereby obtained. The delivery of each piston per revolution

$$= \text{Area of Piston} \times \text{Delivery Stroke}$$

$$= A \times 2R \sin X \qquad - 2.5$$

For n pistons:

$$\text{Displacement/rev} = 2AnR \sin X \qquad - 2.6$$

It should be noted that all three units use rotary valves usually in the form of a timing plate as shown in Fig. 2.1(c). However the wobble plate unit with its stationary cylinder barrel sometimes incorporates positive seating valves. Where an axial load is to be transmitted between sliding pistons and swash or wobble plate a slipper pad as shown in Fig. 2.1(c) is often incorporated. The pads are kept in contact with the plate by return springs or boost pressure. These are not required for the bent axis type of unit where both pistons and plate rotate.

2.1.4 Variable Delivery /

2.1.4 Variable Delivery

Most of the positive displacement pumps and motors described above are capable of variable delivery. Exceptions are the gear units where the capacity is fixed by the gear size, and the wobble plate axial piston units where the plate is at a fixed angle to the shaft.

The radial units, both vane and piston can be modified to vary the delivery by having a variable eccentric on the outer track for rotating barrels or the shaft for units with stationary barrels. The delivery of the swash plate and bent axis units can be varied by increasing the angle of the swash plate of the former, and tilting the cylinder barrel of the latter type.

As well as providing a means of varying the capacity of the various units, the process may be taken one stage further to provide pumps that can alternate their delivery and suction ports, and motors their direction of rotation. Provision must be made in all types of variable unit to ensure that they are capable of operating satisfactorily at the many different speeds and pressure that can be introduced as a result of coupling them together to form a hydrostatic transmission.

2.2 The Theoretical Discharge of a Swashplate Pump

2.2.1 Theoretical Discharge with the Swashplate Fixed

The delivery from a reciprocating axial piston pump is not constant, but fluctuates according to the number of pistons, the speed of rotation, and the amplitude of the reciprocating motion. A diagramatic layout of a swashplate pump is shown in Fig. 2.4(a). Consider an ideal pump with n pistons running at an angular velocity of Ω rad/s with a mean swash plate angle X.

Before investigating the affect of oscillating the swash plate it is necessary to consider the flow fluctuations due to the reciprocating pistons. If at time $t = o$ the n^{th} piston is at the bottom of its stroke ($z = o$), and about to commence delivering then at time t the position of the r^{th} piston is given by

$$Z = R \tan X \left(1 - \cos\left(\Omega t + \frac{2\pi r}{n}\right)\right) \qquad - 2.7$$

The flow from the r^{th} piston

$$Qr = AR \tan X \, \Omega \sin\left(\Omega t + \frac{2\pi r}{n}\right) \qquad - 2.8$$

Delivery commencing at $t = \frac{2\pi r}{n\Omega}$ taking place over 180^{o} of the delivery stroke and being completed at time $\frac{\frac{2\pi r}{n} + \pi}{\Omega}$ Fig 2.4(b).

The delivery from n pistons can be added using Fourier Series, the phase relationship between each piston being taken into account. Performing the harmonic analysis the coefficient for the M^{th} harmonic of the series is found to be:

$$C_M = \frac{\Omega}{2\pi} \sum_{r=1}^{n} \int_{-\frac{2\pi r}{n\Omega}}^{\left(\pi - \frac{2\pi r}{n}\right)\frac{1}{\Omega}} AR \tan X \Omega \sin\left(\Omega t + \frac{2\pi r}{n}\right) e^{-jM\Omega t} dt \qquad - 2.9$$

Integrating gives:

$$C_M = \frac{\Omega AR \tan X}{4\pi} \sum_{r=1}^{n} \left\{ \frac{e^{j\frac{2\pi r}{n}M}}{M-1} (e^{-j(M-1)\pi} - 1) - \frac{e^{j\frac{2\pi rM}{n}}}{M+1} (e^{-j(M+1)\pi} - 1) \right\} \qquad - 2.10$$

The co-efficients of all odd harmonics are zero.

If M is even:

$$C_M = -\frac{\Omega AR \tan X}{\pi} \sum_{r=1}^{n} \frac{e^{j\frac{2\pi r}{n}M}}{M^2-1} \qquad - 2.11$$

For /

For harmonics $M < n$ when n is even

$M < 2n$ when n is odd

$$e^{j\frac{2\pi M}{n}} \neq 1$$

$$\therefore \quad C_M = 0$$

For harmonics above:

$$C_M = \frac{-\Omega AR \tan X}{\pi} \frac{n}{M^2-1} \qquad - \ 2.12$$

and all these remaining higher harmonics are identical.

Thoma (13) using a graphical phasor representation demonstrated that the flow ripple:

$$\frac{Q_{T\,Max} - Q_{T\,Min}}{Q_{T\,Max}} = 1 - \cos\frac{\pi}{2n} \text{ if n is odd}$$

$$= 1 - \cos\frac{\pi}{n} \text{ if n is even}$$

Number of Pistons	1	2	3	4	5	6	7	8	9	10
$\frac{Q_{T\,Max} - Q_{T\,Min}}{Q_{T\,Max}}$ %	100	13.4		4.9		2.5			1.5	
		100		29.3		13.4		7.6		4.9

In order to keep flow ripples to a minimum it is usual to find most piston pumps and motors have an odd number of pistons.

For a seven piston pump rotating at 1,200 rpm, the flow ripple produced would be 2.5% of the total delivery at 960 Hz. This is far in excess of any applied frequencies considered in this thesis.

2.2.2 Theoretical Discharge with Swash Plate Oscillating about Zero Swash

In an unpublished report by Vickers Limited, Emmerson (15) investigated the delivery from a swashplate pump when the swashplate was subjected to an oscillatory motion about the zero swash angle. His analytical solution showed that the delivery was reduced as the ratio of the frequency of oscillation of the swashplate to the frequency of rotation was increased. However, it was not possible to relate this analysis to the case where the swashplate was oscillating about a mean swash angle.

2.2.3 /

2.2.3 Theoretical Discharge with Swash Plate Oscillating about a Mean Swash

The effect of subjecting a pump swashplate to a sinusoidal angular displacement about any mean swash angle of amplitude a degrees and frequency $\frac{\omega}{2\pi}$ Hz is considered below.

If the motion commences at time t = o the position of the r^{th} piston from Equ. 2.7 now becomes:

$$Z = R\tan X - R\cos\left(\Omega t + \frac{2\pi r}{n}\right)\tan\left(X - a\sin\omega t\right) \qquad - 2.13$$

$$\dot{Z} = R\Omega\sin\left(\Omega t + \frac{2\pi r}{n}\right)\tan\left(X - a\sin\omega t\right) + a\omega R\cos\left(\Omega t + \frac{2\pi r}{n}\right)\cos\omega t\sec^2\left(X - a\sin\omega t\right) \qquad - 2.14$$

$$Q_r = A\dot{z} \qquad - 2.15$$

To /

To carry out an analytical solution of the series formed by considering a pump with n cylinders would be extremely lengthy and difficult to interpret. As an alternative a graphical solution was obtained by adding the flow from each piston on a delivery stroke at any instant in time. This solution was generalised and a computer programme written to evaluate and plot the output from a positive displacement pump under conditions of an oscillating swashplate. Programme 'DELIV' is shown in Appendix I as

A.1.1 Programme 'DELIV'.

The common approach adopted when analysing variable delivery swashplate pumps and motors is to consider the delivery to be directly proportional to swash angle. The programme 'DELIV' provides a direct comparison between the instantaneous flow as obtained from Equ. 2.14 and the flow derived from the mean flow modified by the sinusoidal variation in swash.

$$Q_T = Q_{T\,Mean} \left(1 - \frac{a}{x} \sin\omega t \right) \qquad - \ 2.16$$

Flows were computed for a pump of nine pistons running at 1,200 rev/min with a mean swash angle of 4.42 degree being subjected to a sinusoidal swashplate oscillation of $\pm$ 1.23 degrees at 6 H_Z. These were conditions typical of those in later test work.

The results indicated the proportional relationship between flow and swash angle was justified under these conditions. The only discrepancy being of the order expected from the normal flow ripple for a nine cylinder pump.

2.3 The Steady State Performance of Positive Displacement Pumps and Motors

If a hydrostatic transmission is to comprise a positive displacement pump and motor before analysis, either steady state or dynamic can be carried out, it is necessary to evaluate the performance characteristics of both pump and motor units. No mention has yet been made of the various losses that can occur in positive displacement pumps reducing the delivery (usually termed slip losses) and increasing the required driving torque (torque losses). The converse will apply to hydraulic motors.

Just over 20 years ago Wilson (16), (17), (18), (19), and (20), presented a comprehensive study of the operation of positive displacement pumps and motors, and the losses experienced when under load. Additional significant contributions have been made by Schlosser, Thoma, and others. The mathematical modelling and simulation of positive displacement units serves two basic needs.

The first is to provide a means of correlating and comparing experimental data for positive displacement machines, and the second is using that data to extrapolate to other conditions and to predict the performance of different sizes of similar machines. Nevertheless errors in performance predictions using these techniques gives rise to considerable discussion on the relative merits of the different models available.

2.3.1 The Volumetric Efficiency of Positive Displacement Pumps and Motors

Considering first the original equation presented by Wilson for positive displacement pump delivery:

$$Q_{AP} = Q_{TP} - Q_{SP} - Q_{CP} \qquad - 2.17$$

where:

Q_{AP} - The Actual Pump Flow.

Q_{TP} - The Theoretical Pump Flow Determined by Pump Geometry.

Q_{SP} - The Slip Flow which is assumed to be Laminar due to Leakage Past Clearances.

Q_{CP} - Flow Losses due to Cavitation or Aeration conditions at the Pump Inlet and Oil Compressibility.

$$Q_{AP} - D_1 X_p \Omega_p - \frac{Csp\, D_1 X_p P_D}{\mu} \qquad - 2.18$$

It is common practice to ignore the cavitation term even though compressibility must play a significant part in the flow losses into a high pressure outlet.

Schlosser (21), (22), and (23), refined Wilson's basic model and pointed out that experimental measurement had shown that if the viscosity of the fluid was halved the leakage flow was not reduced by half. He attributed the discrepancy to the fact that the density effect of the fluid had been ignored and this would be important in areas where leakage flows were turbulent. Equ. 2.18 should be modified to become

$$Q_{AP} = D_1 X_p \Omega_p - \frac{C_{svp} D_1 X_p P_D}{\mu} - C_{stp} \sqrt{\frac{2 P_D}{\rho}} \sqrt[3]{D_1 X_p} \quad - 2.19$$

Despite acceptance of the existence of the density term it is still common practice for many authors to ignore its effect when dealing with experimental results especially over a small working range. Thoma (24) suggested that leakage increasing slower than proportionally with pressure as given by Schlosser, was contrary to his experience.

The two principal models described above although forming the basis of most mathematical models do not cover all aspects of pump operation, and several other extensions to these basic models have been developed.

Toet (25) pointed out the effects of pressure, speed, and temperature on the theoretical discharge. The compressibility of the oil and the dilation of pump and motor housing were taken into account. Schlosser and Hilbrand (22) dealt in detail with the effect of low speeds on slip losses.

The losses for a positive displacement motor are given by

Wilson's Equation:

$$Q_{AM} = D_2 X_M \Omega_M + \frac{C_{SM} D_2 X_M}{\mu} P_D \qquad - 2.20$$

Schlosser's Equation:

$$Q_{AM} = D_2 X_M \Omega_M + \frac{C_{SVM} D_2 X_M}{\mu} P_D + C_{STM} \sqrt{\frac{2 P_D}{\rho}} \sqrt[3]{D_2 X_M} \qquad - 2.21$$

In each case the volumetric efficiency is given by:

$$\eta_v = \frac{Q_{AP}}{Q_{TP}} \quad \ldots \text{ for a pump } \ldots \qquad - 2.22$$

$$\eta_v = \frac{Q_{TM}}{Q_{AM}} \quad \ldots \text{ for a motor } \ldots \qquad - 2.23$$

2.3.1.1 The Effect of Oil Compressibility on Volumetric Efficiency

It is often very difficult to determine whether mathematical models take into account the effects of oil compressibility. Wilson indicated its presence in Equation 2.17, and Schlosser (22) included the compressibility effect as a variation in the swept volume with pressure. The extent of the reduction in the volume of oil delivered as a result of the compressibility effect is determined by the relationship between the swept volume of the unit and the dead volume.

Consider the working cycle of a typical positive displacement pump with a variable stroke piston, Fig. 2.5(a). The cycle commences with the piston at B.D.C. and the fluid is compressed until the delivery pressure is reached and delivery continues until T.D.C. is reached. After T.D.C. the piston starts to retract, the fluid dead volume expanding initially until the pressure of the intake port is reached. With further travel of the piston, fluid is drawn in until B.D.C. is reached. If valving establishes connections to supply and return at exactly T.D.C. and B.D.C. fluid will rush in from the delivery port to compress the fluid already there and is then expelled by the movement of the piston. However, as far as flow and swept volume are concerned this is the same as with ideal valving (valving that connects the piston to the delivery line when a pressure balance is achieved).

If V_1 is the volume of fluid in a cylinder at the moment of switching from the low to high pressure ports:

$$Q_C = \Delta V_c \; n \; \frac{\Omega}{2\pi} \qquad - 2.24$$

For a pump with n cylinders:

Where

$$\Delta V_c = \frac{V_1}{B_o} \; P_D \qquad - 2.25$$

The dilation of the piston bore is ignored.

$$\therefore \; Q_C = V_1 \; n \frac{\Omega}{2\pi} \; \frac{P_D}{B_o} \qquad - 2.26$$

For a variable displacement unit:

$$V_1 = V_D + \frac{V_{Max}}{2} \; \left(1 + \frac{X}{X_{Max}}\right) \qquad - 2.27$$

Where

V_D is the dead volume at maximum swash

V_{Max} is the maximum swept volume at maximum swash X_{Max}.

Combining /

Combining Equ. 2.26 and 2.27:

$$Q_C = n\, V_{Max}\, \frac{\Omega}{2\pi}\, \frac{P_D}{B_o} \left\{ \frac{V_D}{V_{Max}} + \frac{1 + \frac{X}{X_{Max}}}{2} \right\}$$

$$= Q_{Max}\, \frac{P_D}{B_o} \left\{ \frac{V_D}{V_{Max}} + \frac{1 + \frac{X}{X_{Max}}}{2} \right\} \qquad - 2.28$$

Thoma (13) quotes a normal value for $\frac{V_D}{V_{Max}}$ as $\frac{1}{4}$. Therefore at full stroke X = X_{Max} for a pump:

$$Q_{CP} = 1.25\, Q_{Max}\, \frac{P_D}{B_o} \qquad - 2.29$$

However, for a motoring unit switching from low to high pressure takes place at bottom dead centre X = $- X_{Max}$. Therefore at full swash:

$$Q_{CM} = 0.25\, Q_{Max}\, \frac{P_D}{B_o} \qquad - 2.30$$

The compressibility flow is therefore approximately 1.25% and 0.25% of full flow for pumping and motoring respectively at pressure difference of 2,000 lbf/in^2 (taking an approximate value for B_o=200,000 lbf/in^2).

Nevertheless measurement taken from a typical swashplate pump, of the NEL design that had a high dead volume as the pistons had been bored out to reduce inertia, gave a value of $\frac{V_D}{V_{Max}} = 1.00$.

This will give:

$$Q_{CP} = 2.0 \quad Q_{Max} \frac{P_D}{B_o} \quad \text{... for a pump ... - 2.31}$$

$$Q_{CM} = 1.0 \quad Q_{Max} \frac{P_D}{B_o} \quad \text{... for a motor ... - 2.32}$$

Thus the volumetric efficiency has been reduced by approximately 2% for the pump, and 1.0% for the motor when delivering oil at 2,000 lbf/in^2. This is significant when manufactureres talk of volumetric efficiencies of 95% and above.

If the flow output from the pump is allowed to return to atmospheric pressure before the flow is measured, then $Q_{Max} \frac{P_D}{B_o}$ will be recovered.

2.3.2 The Mechanical Efficiency of Positive Displacement Pumps and Motors

Again considering first Wilson's Equation for a positive displacement pump (18):

$$T_{AP} = T_{TP} + T_{DP} + T_{FP} + T_{CP} \qquad - 2.33$$

Where:

T_{AP} - The Actual Pump Torque

T_{TP} - The Theoretical Pump Torque due to Pressure Differential and Pump Swept Volume

T_{DP} - Viscous Torque Loss due to the Shearing of Fluid in Small Clearances

T_{FP} - Pressure Dependent Torque Loss derived from Seals and Bearings, but also includes Pressure Gradient Effect between Sliding Plates.

T_{CP} - Constant Friction Loss

$$\therefore T_{AP} = D_1 X_P P_D + C_{DP} D_1 X_P \mu \Omega_P + C_{FP} 2\pi D_1 X_P P_D + T_{CP} \qquad - 2.34$$

Again after accurate measurement, Schlosser (21) and (22) showed the necessity for the incorporation of a loss dependent on the fluid dynamic pressure.

Thoma (24) is in agreement with its inclusion in the model, pointing out that the many turbulent passages in most hydrostatic units make these hydrodynamic losses significant. Churning losses, as Schlosser described them, are proportional to the square of the shaft speed. Equ. 2.34 was modified by Schlosser to give:

$$T_{AP} = D_1 X_P P_D + C_{DP} D_1 X_P \mu \Omega_P + C_{FVP} 2\pi D_1 X_P P_D + C_{FTP} \rho \Omega_P^2 \sqrt[3]{(D_1 X_P)^5} + T_{CP} \quad - 2.35$$

Similarly the equations for a hydraulic motor are:

Wilson's Equation

$$T_{AM} = D_2 X_M P_D - C_{DM} D_2 X_M \mu \Omega_M - C_{FM} 2\pi D_2 X_M P_D + T_{CM} \quad - 2.36$$

Schlosser's Equation

$$T_{AM} = D_2 X_M P_D - C_{DM} D_2 X_M \Omega_M - C_{FVP} 2\pi D_2 X_M P_D - C_{FVM} \rho \Omega_M^2 \sqrt[3]{(D_2 X_M)^5} + T_{CM} \quad - 2.37$$

The /

The mechanical efficiency η_{Mech} is given by:

$$\eta_{Mech} = \frac{T_{TP}}{T_{AP}} \quad \text{... for a pump ...} \quad - 2.38$$

$$\eta_{Mech} = \frac{T_{AM}}{T_{TM}} \quad \text{... for a motor ...} \quad - 2.39$$

The overall efficiency η_o is given by:

$$\eta_o = \frac{Q_{AP}\, P_D}{\Omega_P\, T_{AP}} = \frac{Q_{AP}}{Q_{TP}} \frac{T_{TP}}{T_{AP}} = \eta_v\, \eta_{Mech}$$

... for a pump ... - 2.40

$$\eta_o = \frac{T_{AM}\, \Omega_M}{P_D\, Q_{AM}} = \frac{T_{AM}}{T_{TM}} \frac{Q_{TM}}{Q_{AM}} = \eta_v\, \eta_{Mech}$$

... for a motor ... - 2.41

2.3.3 /

2.3.3 The Mathematical Model for a Hydrostatic Transmission

The mathematical models for hydrostatic pumps and motors described in the previous section, have been developed for performance predictions of all types of hydrostatic unit. The models may be combined together to provide the overall performance prediction for a hydrostatic transmission, but considerable errors are still experienced in these predictions. Wilson (24) said errors of $\pm$ 20% had been quoted in some published efficiency calculations.

The equations derived from these models are complex and tedious to evaluate. It has been normal practise of most authors to use a digital computer. The equations for overall transmission performance derived from Wilson's equations are given by Wilson & Lemme (20). Korn (26) used a flow graph technique to build up a mathematical model of a transmission that included the load and could be readily computerised.

A further more recent innovation is the development of analogue simulation programmes for use on digital computers. These provide all the advantages of analogue solution without the tedious problems involved with patching and non-linear functions (27) and (28).

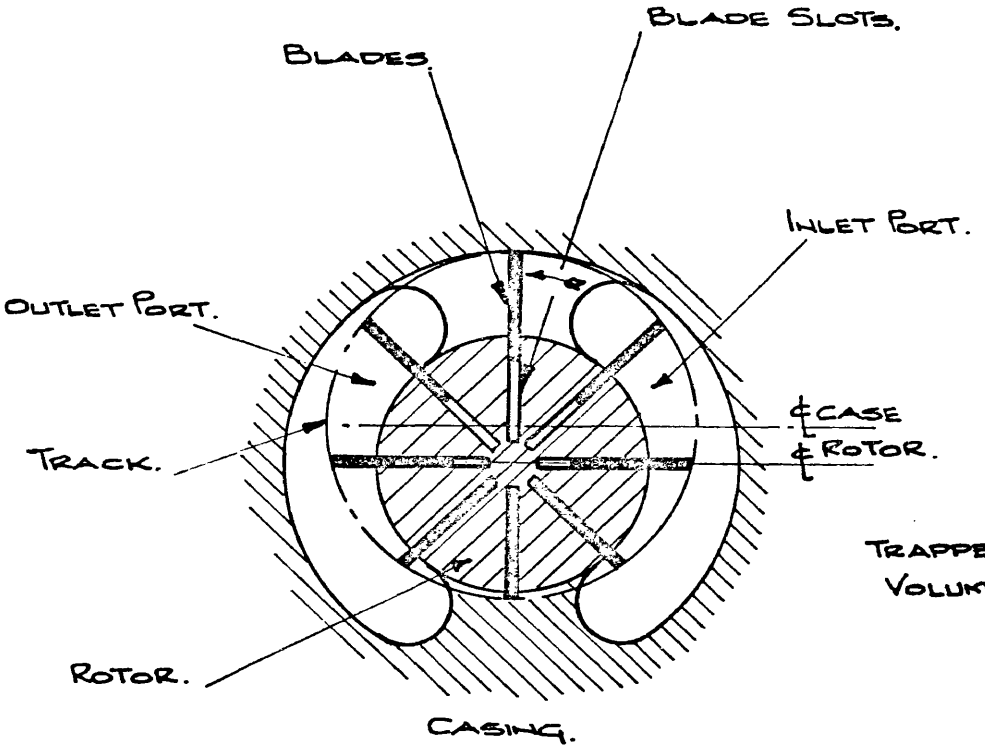

2.1 (a) VANE PUMP.

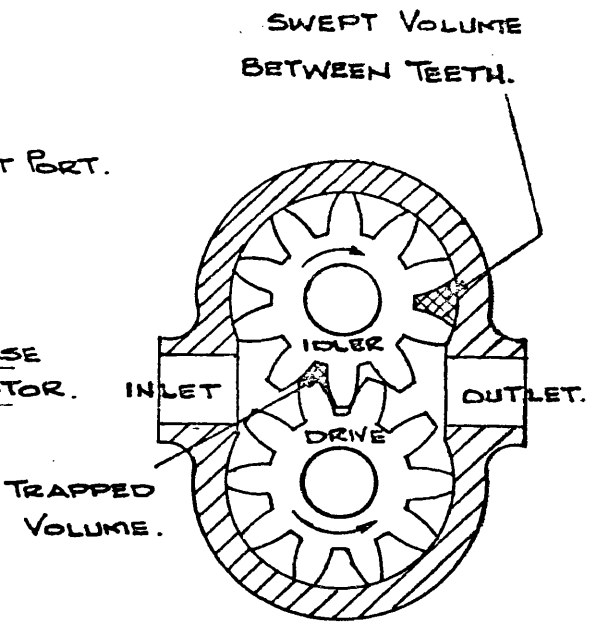

2.1 (b) GEAR PUMP.

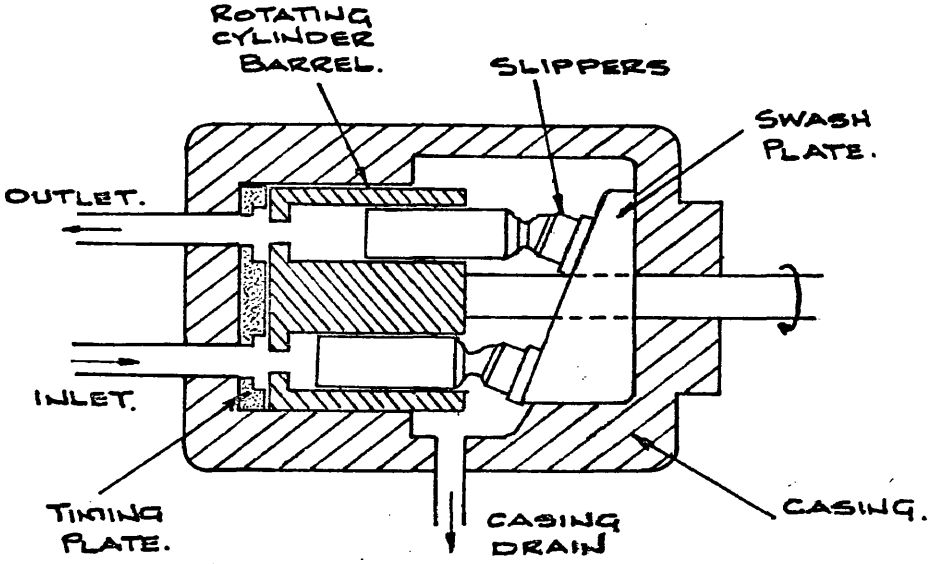

2.1 (c) PISTON PUMP.

FIG. 2.1. THE THREE MAIN TYPES OF POSITIVE DISPLACEMENT PUMP & MOTOR UNITS.

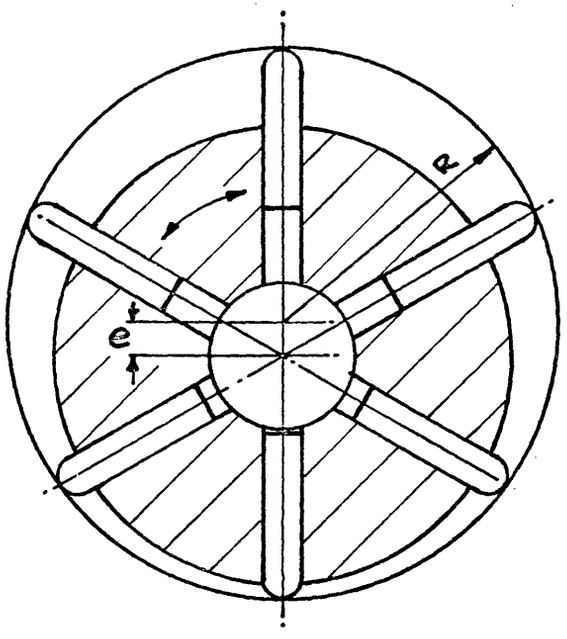

2.2 (a.) ROTATING CYLINDER BARREL. STATIONARY OUTER TRACK.

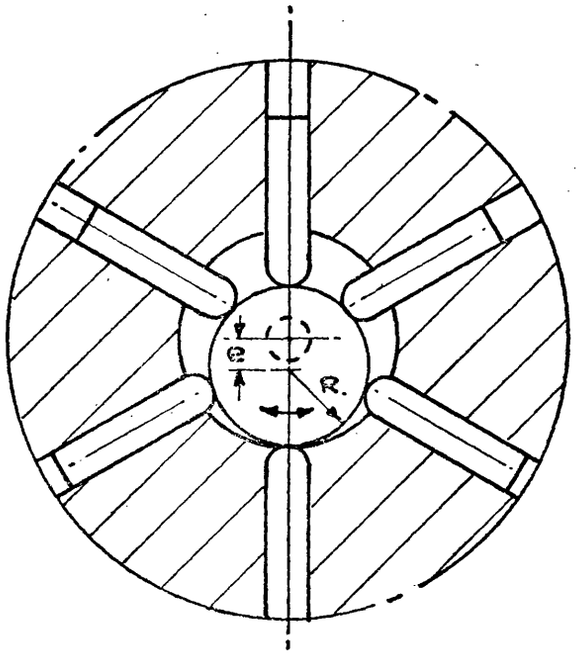

2.2 (b.) STATIONARY BARREL. ROTATING ECCENTRIC.

FIG. 2.2. RADIAL PISTON POSITIVE DISPLACEMENT PUMP & MOTOR UNITS.

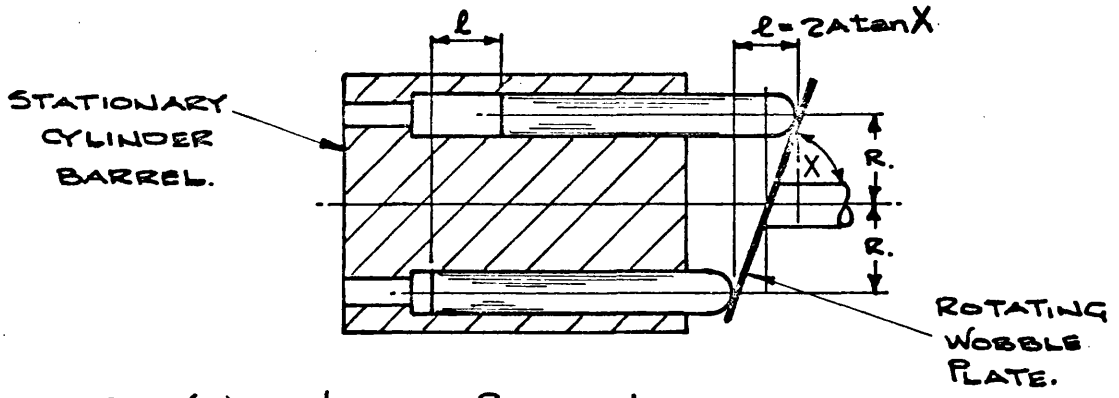

2.3 (a) WOBBLE PLATE UNIT.

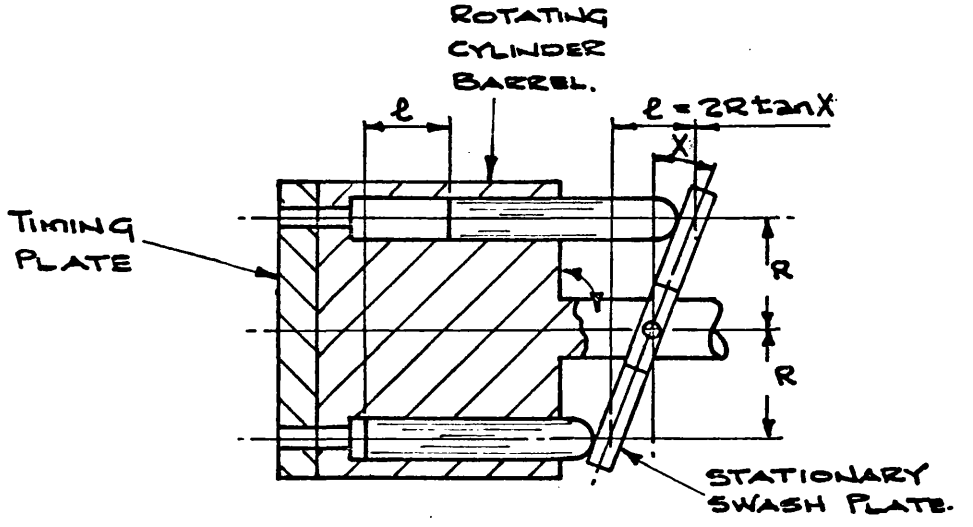

2.3 (b.) SWASH PLATE UNIT.

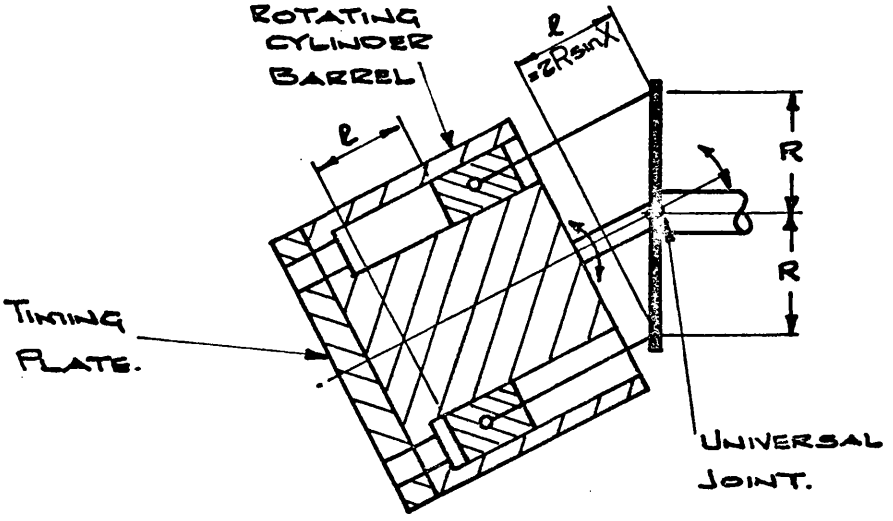

2.3 (c) BENT AXIS UNIT.

FIG 2.3 AXIAL PISTON POSITIVE DISPLACEMENT PUMP & MOTOR UNITS.

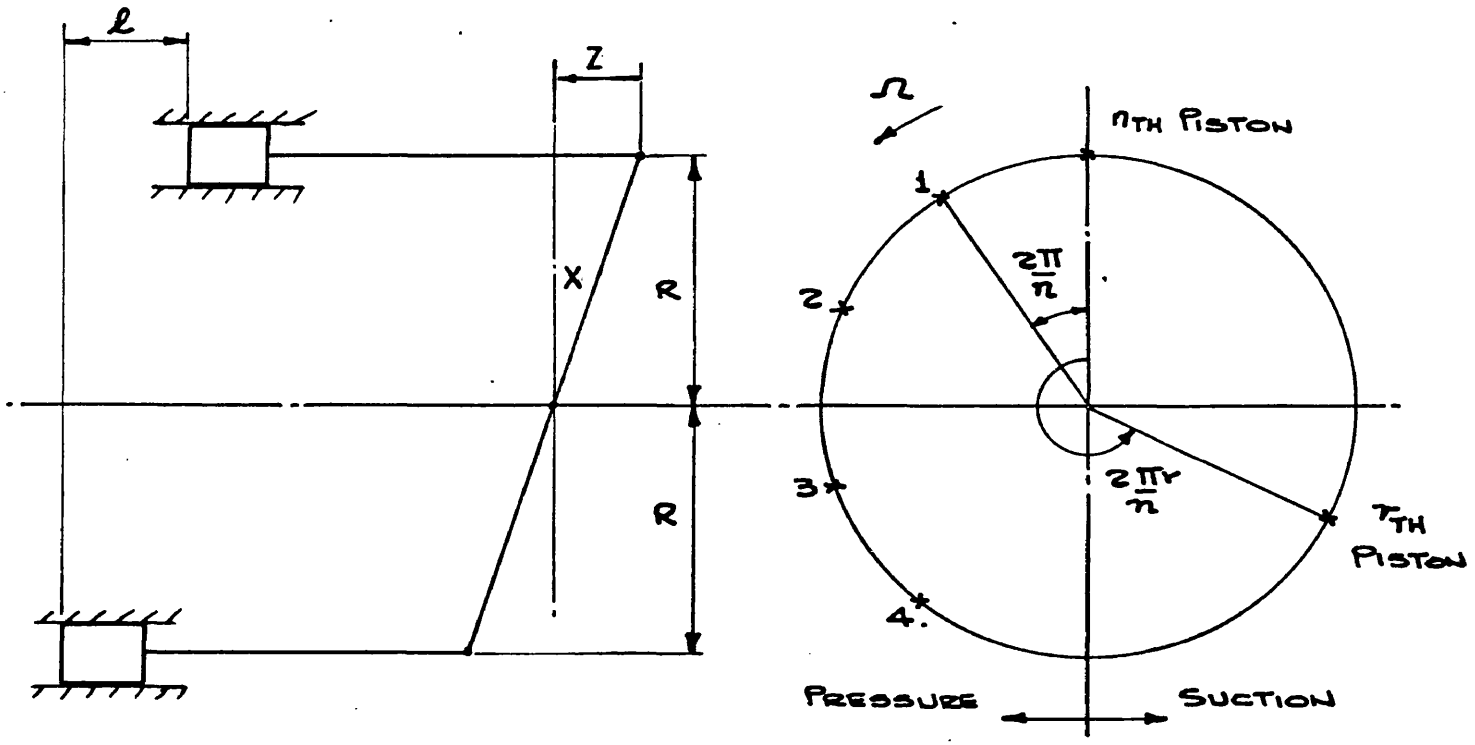

2.4(a) DIAGRAMMATIC LAYOUT OF SWASHPLATE PUMP.

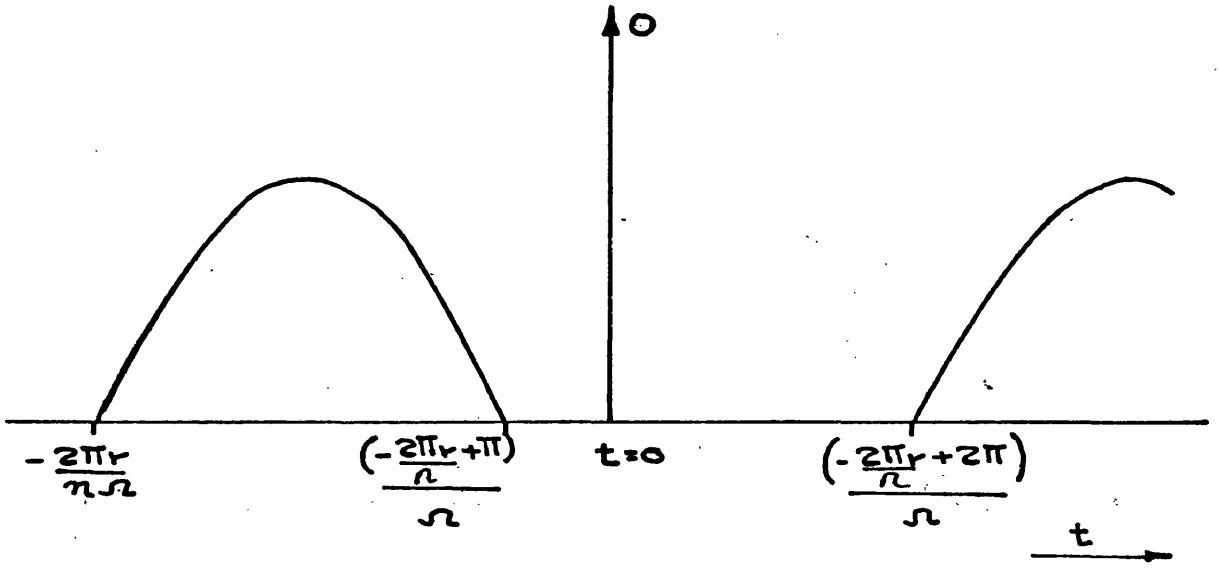

2.4(b) DELIVERY OF r^{th} PISTON.

FIG 2.4 DIAGRAMMATIC LAYOUT OF SWASHPLATE PUMP.
& DELIVERY OF SINGLE CYLINDER.

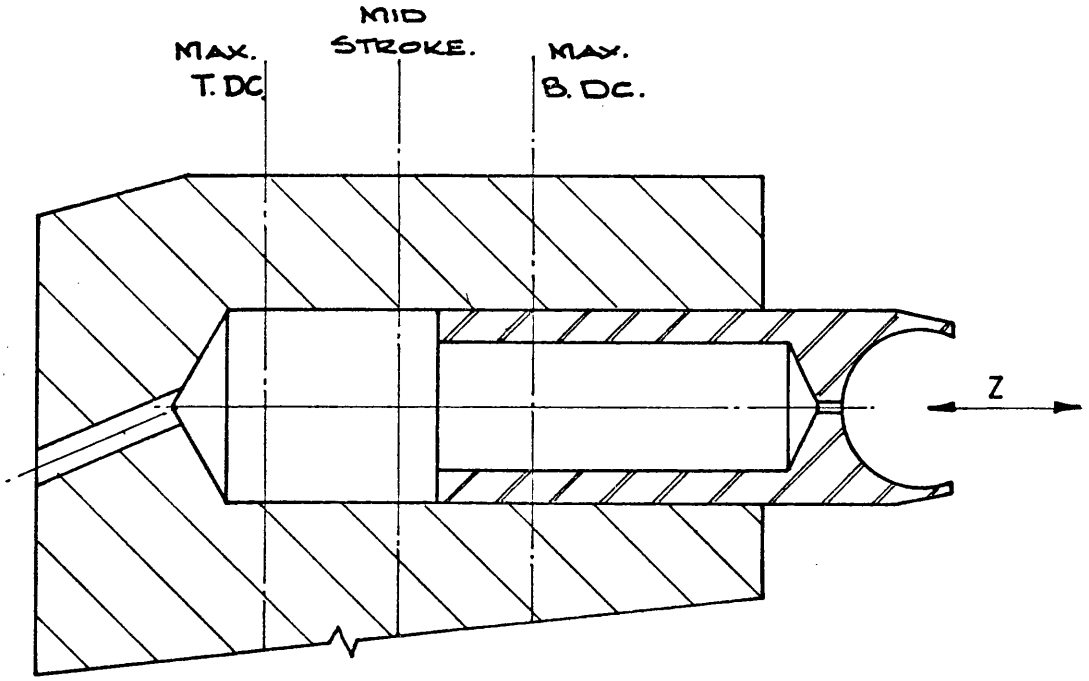

FIG 2.5 (a) SCHEMATIC OF VARIABLE STROKE PISTON.

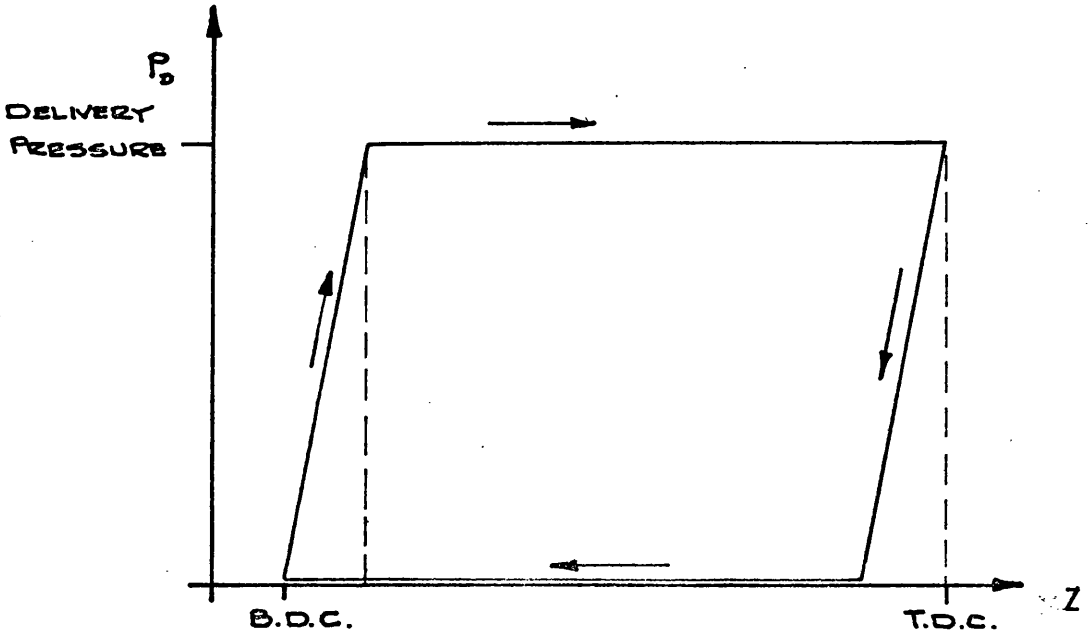

FIG 2.5 (b.) PISTON PUMPING CYCLE.

FIG 2.5. ILLUSTRATION OF COMPRESSIBILITY EFFECTS DURING PISTON PUMP CYCLE.

CHAPTER 3 : The DYNAMIC ANALYSIS of a HYDROSTATIC TRANSMISSION

3.1 Basis of Model

The model presented below is based upon the following assumptions:

1. The hydrostatic transmission is considered to be made up of a hydrostatic pump and motor acting as continuous linear elements connected by a hydraulic link.

2. The pump and motor flows are assumed to be proportional to swashplate position as described in Chapter 2.2.

3. The elasticity of the pipe connecting the pump and motor and the oil compression is assumed to be linear with pressure over the range considered.

4. The distributed parameter approach is ignored.

5. Oil inertia effects are neglected or lumped.

Even though it is common to find the motor or power output element of a hydrostatic transmission remote to the prime mover and pump, in many cases the length of the transmission lines are normally small in comparison with the wavelengths of the pressure signals being transmitted. Therefore as laid down in assumption 4, it is possible to ignore the distributed nature of the system and consider the variables to be lumped.

As the lengths of the transmission lines increase, particular care must be taken to ensure that the inertia of the oil in the pipeline is not playing a significant part by contributing to the transmission load. Healey (29) presented a useful technique for evaluating oil inertia effects.

Healey's approach was applied to the transmission tested. If the inertia of the oil in the pipeline is related to the effective inertia on the motor output shaft, the change in total inertia was less than 0.3% of that of the load and motor alone. This is because for rotary actuators there is no gearing effect due to the arearatio between pipeline and actuator as in linear motion control systems.

A case where the lumped parameter approach was not adopted is given in a recent paper by Knight, McCallion, and Dudley (30). It describes a finite difference approach to pipe flow that has been used to analyse a transmission in a mining application where transmission lines were of the order of several hundred feet long.

A computerised mathematical model of the transmission was used to evaluate its response to step changes in load.

Throughout the analyses presented the transmission has been considered to be acting as a variable speed drive employing a variable displacement pump and fixed displacement motor. It was required to determine the dynamic response of the speed of the output shaft of the transmission to change in pump displacement. However, provided the hydraulic lines are kept full the analysis is equally applicable to the use of a hydrostatic transmission as a position control servo. In addition once the basic transfer function relating output speed changes to pump displacement has been derived and verified, it is only a comparatively small step to develop the analysis to include any other two transmission variables.

Before commencing the linearised analyses several significant assumptions should be pointed out. Except where otherwise stated pressure of the return line has been assumed constant. This implies that the replenishing or boost system is capable of maintaining constant pressure. The implications of this assumption will be discussed later. The shafts connecting the moving members of the motor to the load, and the prime mover to the pump, have been assumed to be of infinite stiffness.

3.2 Linearized Analysis of a Hydrostatic Transmission with Constant Speed Prime Mover

Consider first the transmission shown diagramatically in Fig. 3.1 (a). The simplified analysis given below is standard and assumes a constant speed prime mover, lossless hydraulic pump and motor, compressible fluid, constant return line pressure, and an inertial and viscous load.

Considering small perturbations about a steady state operating condition:

Load: $t_2 = J_2 s \omega_2 + f_L \omega_2$ - 3.1

Motor Torque: $t_2 = p_D D_2 X_M$ for constant return line pressure - 3.2

Pump Flow: $q_p = \Omega_1 D_1 x_p$ - 3.3

Motor Flow: $q_M = \omega_2 D_2 X_M$ - 3.4

Compressible Flow: $q_C = \frac{V}{B_e} s p_D$ - 3.5

The block diagram obtained using the above relations is shown in Fig. 3.1 (b). The following transfer function can be derived:

$$\frac{\omega 2}{x_P} = \frac{D_1 \Omega_1}{D_2 X_M} \cdot \frac{\frac{(D_2 X_M)^2 B_e}{V J_2}}{s^2 + \frac{f_L}{J_2} s + \frac{(D_2 X_M)^2 B_e}{V J_2}} \qquad - 3.6$$

This is a second order equation. The resultant undamped natural frequency of the transmission is:

$$\omega_n = D_2 X_M \sqrt{\frac{B_e}{V J_2}} \qquad - 3.7$$

and damping ratio:

$$\xi = \frac{f_L}{2 D_2 X_M} \sqrt{\frac{V}{J_2 B_e}} \qquad - 3.8$$

Thus if the lossless transmission is used as a speed control, it will have a second order response of output speed to changes in pump displacement and may have a resonance at a frequency determined by the system compressibility, motor size, and the load inertia. Shearer (11), Lewis & Stern (12), Thoma (13), and Gille (14), and several other writers, have all developed this analysis further by including the transmission losses to some extent. Shearer (11) built up a detailed block diagram of the transmission and indicated an analogue computer study as being one method of solution. However, having pointed out that there are lower limits that can occur in line pressure which must be avoided for linearity, he went on to outline Newton's (10) linearized analysis, substantially as follows:

Using the mathematical models for pump and motor performance derived by Wilson (see Chapter 2) and simplifying the loss co-efficients, Equations 3.1 - 3.5 become:

Load: $$t_2 = J_2 \, s \, \omega_2 + f_L \, \omega_2 \qquad - 3.9$$

Motor Torque: $$t_2 = p_D \, D_2 \, X_M - K_{fM} \, p_D - f_M \, \omega_2 \qquad - 3.10$$

Where: $$K_{FM} = C_{FM} \, 2\pi D_2 \, X_M$$

$$f_M = C_{DM} \, D_2 \, X_M{}^{\mu}$$

Pump Flow $$q_P = \Omega_1 \, D_1 \, x_P - K_P \, p_D \qquad - 3.11$$

Where: $$K_P = \frac{C_{SP} \, D_1 \, X_P}{\mu}$$

Motor Flow $$q_M = \omega_2 \, D_2 \, X_M + K_M \, p_D \qquad - 3.12$$

Where: $$K_M = \frac{C_{SM} \, D_2 \, X_M}{\mu}$$

Compressible Flow: $$q_C = \frac{V}{B_e} \, s \, p_D \qquad - 3.13$$

The overall transfer function for the transmission now becomes:

$$\frac{\omega_2}{x_P} = \frac{D_1 \Omega_1 \ (D_2 X_M - K_{fM})}{D_2 X_M \ (D_2 X_M - K_{fM}) + (K_P + K_M)\ (f_L + f_M)} \cdot$$

X

$$\frac{B\left\{\dfrac{D_2 X_M \ (D_2 X_M - K_{fM}) + (K_P + K_M)\ (f_L + f_M)}{V J_2}\right\}}{s^2 + \dfrac{B}{V J_2}\left\{\dfrac{V}{B}(f_L + f_M) + J_2 (K_P + K_M)\right\} s + B\left\{\dfrac{D_2 X_M (D_2 X_M - K_{fM}) + (K_P + K_M)(f_L + f_M)}{V J_2}\right\}}$$

- 3.14

A more complex second order equation where the undamped natural frequency is:

$$\omega_n = \sqrt{B\left\{\frac{D_2 X_M \ (D_2 X_M - K_{fM}) + (K_P + K_M)\ (f_L + f_M)}{V J_2}\right\}} \qquad - 3.15$$

and damping ratio:

$$\zeta = \frac{\dfrac{V}{B}(f_L + f_M) + J_2 (K_P + K_M)}{2\sqrt{\dfrac{V J_2}{B}\left\{(K_P + K_M)\ (f_L + f_M) + D_2 X_M \ (D_2 X_M - K_{fM})\right\}}} \qquad - 3.16$$

3.3 Signal Flow Analysis of a Hydrostatic Transmission Driven by a Prime Mover whose Speed will fall with Torque

Even though Equ. 3.14 gives the transfer function for a linearized hydrostatic transmission where the losses in the pump and motor have been taken into account, it was assumed that the prime mover ran at constant speed despite changes in driving torque. In reality these torque changes would result in changes in speed of the prime mover the extent of which would be determined by the speed droop with load of the prime mover K_E. Signal flow theory facilitates the use of a more complex model to include the prime mover droop.

The signal flow graph is an alternative method of presentation to the block diagram technique and the relation between input and output can be readily obtained by the application of Mason's Rule (31). A significant advantage of the signal flow technique over block analysis is that it enables the transfer characteristic for different points in the system to be readily obtained with very little additional work.

The application of signal flow technique to hydraulics have been demonstrated by Bowns (32) and Korn (26). Korn was concerned with a steady state model of a hydrostatic transmission whilst Bowns suggested signal flow analysis as an aid to dynamic analysis.

Again the transmission was considered to be subject to small perturbations about an operating point. Bowns presented a clear and concise technique for building up the signal flow graph for the overall transmission which has been adopted here. Fig. 3.2 shows graphically the static and dynamic characteristics of the various transmission elements. A sketch of typical speed torque characteristics of a governed I.C. engine for the various governor settings is shown together with linearized equation relating small changes in speed with engine torque variations and governor settings. The quantity $\frac{\delta \Omega_1}{\delta T_E}$ $(= K_E)$ the engine speed droop shows how the speed changes with torque and the quantity $\frac{\delta \Omega_1}{\delta Y}$ $(= K_G)$ the governor speed control constant shows how the engine speed varies with governor setting. Delays in development of the engine developed torque after a change in governor setting have been neglected as relatively insignificant at the frequency of the torque variations considered.

The hydrostatic pump is dealt with in two parts. Firstly the linearized relation between flow, speed, swash plate angle and pressure is obtained, Equ. 2.18. The quantity $\frac{\delta Q_P}{\delta P_D}$ $(= K_P)$ is the pump slip co-efficient. The quantity $\frac{\delta Q_P}{\delta X_P}$ $(= D_1 \Omega_1)$ is the change in flow/unit change in swash angle, and $\frac{\delta Q_P}{\delta \Omega_1}$ $(= D_1 X_P)$ is the flow change/unit change in pump speed.

In a similar manner the change in pump torque for changes in speed, swash plate angle, and pressure, are obtained from Equ. 2.34. $\frac{\delta T_P}{\delta P_H}$ becomes the pump displacement plus the pressure dependent torque co-efficient ($= D_1 X_P + K_{FP}$). $\frac{\delta T_P}{\delta X_P}$ is the change in pump torque/unit change of swash plate angle ($= D_1 P_D$). $\frac{\delta T_P}{\delta \Omega_1}$ ($= f_P$) is the pump viscous torque co-efficient. Once again the return line pressure has been assumed to remain constant. The right hand column of Fig. 3.2 gives the signal flow graph appropriate to each of the elements of the transmission.

The signal flow diagram for the overall transmission is shown in Fig. 3.3, relating changes in output speed ω_2 to changes in input swash angle x_P. The transfer function is derived using Mason's Rule as follows:

$$\frac{\omega 2}{x_P} = T_{\omega_2 x_P} = \frac{T_K \Delta_K}{\Delta} \qquad - 3.17$$

Where

T_K is the path transmittance of the Kth open path between the nodes ω_2 and x_P.

$$\Delta = 1 - \sum_i L_i + \sum_{ij} L_i' L_j' - \sum_{ijk} L_i'' L_j'' L_k'' \quad - 3.18$$

L_i - the loop transmittance of the ith loop in the graph

$L_i' L_j'$ - the loop transmittance of any pairs of non touching loops

$L_i'' L_j'' L_K''$ - the loop transmittance of any trios of non touching loops

Δ_K is the value of Δ for the part of the graph not touching the Kth path.

Signal Paths	Path Transmittance
1. $x_p - q_p - q_m - \omega_2$	$T_1 = \frac{D_1 \Omega_1}{D_2 X_M}$ - 3.19
2. $x_p - t_p - t_e - \omega_1 - q_p - q_m - \omega_2$	$T_2 = \frac{D_1^2 P_D K_E X_P}{D_2 X_M}$ - 3.20

Signal Loops	Loop Transmittance
1. $\omega_1 - t_e - \omega_1$	$I_1 s K_E$ - 3.21
2. $\omega_1 - t_p - t_e - \omega_1$	$f_P K_E$ - 3.22
3. $q_p - q_m - \omega_2 - p_d - q_p$	$\frac{f_M K_P}{D_2 X_M (D_2 X_M - K_{FM})}$ - 3.23

Signal Loops	Loop Transmittance
4. $q_m - \omega_2 - p_d - q_m$	$\dfrac{-f_M \frac{V}{B_e} s}{D_2 X_M (D_2 X_M - K_{FM})}$ - 3.24
5. $\omega_2 - p_d - \omega_2$	$\dfrac{f_M K_M}{D_2 X_M (D_2 X_M - K_{FM})}$ - 3.25
6. $q_p - q_m - \omega_2 - t_m - p_d - q_p$	$\dfrac{K_P (f_L + I_2 s)}{D_2 X_M (D_2 X_M - K_{FM})}$ - 3.26
7. $q_m - \omega_2 - t_m - p_d - q_m$	$\dfrac{-\frac{V}{B_e} s (f_L + I_2 s)}{D_2 X_M (D_2 X_M - K_{FM})}$ - 3.27
8. $\omega_2 - t_m - p_d - \omega_2$	$\dfrac{K_M (f_L + I_2 s)}{D_2 X_M (D_2 X_M - K_{FM})}$ - 3.28
9. $\omega_1 - q_p - q_m - \omega_2 - p_d - t_p - t_e - \omega_1$	$\dfrac{K_E D_1 X_P f_M (D_1 X_P + K_{FP})}{D_2 X_M (D_2 X_M - K_{FM})}$ - 3.29
10. $\omega_1 - q_p - q_m - \omega_2 - t_m - p_d - t_p - t_e - \omega_1$	$\dfrac{K_E D_1 X_P (f_L + I_2 s) (D_1 X_P + K_{FP})}{D_2 X_M (D_2 X_M - K_{FM})}$ - 3.30

1, 2, and 3, 4, 5, 6, 7, 8, are twelve pairs of non touching loops.

$$\Delta = 1 - \sum_{i=1}^{10} L_i \quad L_{13} + L_{14} + L_{15} + L_{16} + L_{17} + L_{18} + L_{23} + L_{24} + L_{25} + L_{26} + L_{27} + L_{28} \qquad - 3.31$$

$$\Delta_1 = 1 - (L_1 + L_2) \qquad - 3.32$$

$$\Delta_2 = 1 \qquad - 3.33$$

$$\therefore \frac{\omega_2}{x_P} = T_{x_P \omega_2} = \frac{T_1 \Delta_1 + T_2}{\Delta} \qquad - 3.34$$

Substitution:

$$T_1 \Delta_1 + T_2 = \frac{D_1 \Omega_1}{D_2 X_M} \left\{ 1 - (J_1 s + f_P) K_E + \frac{D_1 P_H K_E X_P}{\Omega_1} \right\} \qquad - 3.35$$

$$\Delta = 1 - (J_1 s + f_P) K_E - \frac{(f_L + f_M + J_2 s)(K_P - \frac{V}{B_e} s + K_M) + K_E D_1 X_P (D_1 X_P + K_{fP})}{D_2 X_M (D_2 X_M - K_{FM})} + \frac{(f_L + f_M + J_2 s)(K_P - \frac{V}{B_e} s + K_M)(J_1 s + f_P) K_E}{D_2 X_M (D_2 X_M - K_{FM})} \qquad - 3.36$$

$$\frac{\omega_2}{x_P} = \frac{D_1 \Omega_1}{D_2 X_M} \quad \frac{\left\{ 1 - (J_1 s + f_P) K_E + D_1 P_D K_E \frac{X_P}{\Omega_1} \right\}}{1 - (J_1 s + f_P) K_E \frac{-(f_L + f_M + J_2 s)}{D_2 X_M (D_2 X_M - K_{FM})} X}$$

$$\left\{ (K_P - \frac{Vs}{B_e} + K_M)(1 - J_1 K_E s - f_P K_E) + K_E D_1 X_P (D_1 X_P + K_{FP}) \right\}$$

- 3.37

The change in output speed ω_2 due to a change in load torque t_m can be readily obtained once the loop transmittances have been derived. It can be seen that only one path exists between ω_2 and t_m, but many in the opposite direction. It is therefore better to obtain $\frac{t_m}{\omega_2}$ and invert the result.

To determine $\frac{t_m}{\omega_2}$

Signal Path = $f_L + J_2 s$ - 3.38

The loops are as before, and therefore Δ is as given in Equ. 3.36.

There are two non touching loops 1 and 2

$$\therefore \frac{t_m}{\omega_2} = \frac{(f_L + J_2 s)\left\{ 1 - K_E (f_P + J_1 s) \right\}}{\Delta} \quad - 3.39$$

$$\therefore \frac{\omega_2}{t_m} = \frac{\Delta}{(f_L + J_2 s)\left\{ 1 - K_E (f_P + J_1 s) \right\}} \quad - 3.40$$

$$\therefore \frac{\omega_2}{t_m} = 1 - (J_1 s + f_P)K_E - (f_L + f_M + J_2 s)$$

$$\left\{ (K_P - \frac{V s}{B_e} + K_M)(1 - J_1 K_E s - f_P K_E) + K_E D_1 X_P (D_1 X_P + K_{fP}) \right\}$$

$$\frac{}{(f_L + J_2 s)\left\{1 - K_E (f_P + J_1 s)\right\}}$$

- 3.41

It was apparent that the transfer function derived by the signal flow analysis was too involved in the form given by Equ. 3.37 for the significance of the transmission system parameters to be readily appreciated. By comparing with Equ. 3.14 it can be seen that the prime mover droop increased the order of the denominator and was responsible for the additional term in the numerator. The transfer function may therefore be written in the general form:

$$\frac{\omega_2}{x_P} = \frac{K \omega_n^2 (1 + \tau_1 s)}{(1 + \tau_2 s)(s^2 + 2\xi\omega_n s + \omega_n^2)} \qquad - 3.42$$

A digital computer programme was written to enable values of system parameter to be readily substituted into Equ. 3.37 and is shown in Appendix I as A1.2 - Programme 2 'TRDRES'. Two subroutines were written to this main Programme. The first, 'RESP', evaluated the frequency response of the transmission by determining the amplitude ratio and phase angle of output speed to pump swash with frequency of sinusoidal changes in pump swash. The second, 'SOLVE', presented the results in the form of Equ. 3.42 so that values of natural frequency, damping ratio, and other parameters could be determined.

3.3.1 The Effect of a Change in System Parameters on the Natural Frequency and Damping Ratio

The signal flow analysis of a hydrostatic transmission evaluated with the aid of the digital computer programme 'TRDRES' was used to determine the effect of changes in system parameters on the natural frequency and damping ratio. The basic parameters of the transmission were taken to be those of the hydrostatic system tested later.

The first parameter investigated was that of the high pressure (supply line) volume between the pump and motor. Fig. 3.4 shows that the natural frequency rises rapidly with the reduction of supply line volume. It is therefore more difficult to determine accurately when the lines are very short due to the steep slope of the curve, and due to the difficulties in accurately determining small system volumes. In the case of back to back transmissions the natural frequency will be determined by the dead volume in the pump and motor units. The figure also shows how a slight increase in natural frequency occurs with increase in the slope of the torque speed characteristics for the load f_L (termed the load damping co-efficient). The results of the theoretical treatment for a lossless transmission given in Equ. 3.6 is shown dotted. It can be seen that this gives a lower damping ratio than that predicted by the more comprehensive analysis.

Fig. 3.5 examines the effect of load inertia on natural frequency and damping ration. Again the change in natural frequency is large for changes in load inertia at low values of load inertia. The damping ratio is underestimated by the simple theory, and at large values of load inertia the transmission losses predominate causing the damping ratio to increase.

3.3.2 The Effect of Prime Mover Droop

Extensive investigation using Programme 'TRDRES' shows that the fall of speed with load of the prime mover is a secondary effect for systems powered by closely governed engines. The frequency response of a hydrostatic transmission driven by a prime mover with significant droop, Equ. 3.37, is shown in Fig. 3.6. The effect has been to attenuate the low frequency output from the transmission by reducing the overall gain of the system. In effect the prime mover is responding to changes in load; its speed reduces as the output speed of the transmission increases. Hence a movement of the pump swashplate will lead to a reduced change in motor speed.

It can be seen that the low frequency attenuation is increased only when the two break points $\frac{1}{\tau_1}$ and $\frac{1}{\tau_2}$ move apart on the Bode plot. The distance is given by:

$$= \text{Log}\frac{1}{\tau_1} - \text{Log}\frac{1}{\tau_2}$$

$$= \text{Log}\frac{\tau_2}{\tau_1} \qquad - 3.43$$

Therefore provided the ratio $\frac{\tau_2}{\tau_1}$ does not change, the low frequency attenuation will remain the same.

It was found that the ratio $\frac{\tau_2}{\tau_1}$ depended upon the value of the prime mover droop and on the load variations transmitted to the prime mover. These arise from changes in the load damping co-efficient or in the pump or motor displacement. The driving inertia J_1 will affect the time constants τ_1 and τ_2 but does not change their ratio and hence does not affect the amount of attenuation taking place.

However in most cases the natural frequency and damping ratio remain unchanged and the time constants τ_1 and τ_2 in the Equ. 3.42 are close together, thus making little difference to the overall system response.

For example with a 5% droop (no load to full load) the ratio of $\frac{\tau_2}{\tau_1}$ is 1.008 giving an attenuation in the output at low frequencies of only 0.048 dB.

In an extreme case, the low frequency variation of the output is attenuated considerably. If the governor loop gain was reduced to $^1/_{40}$ of that in the above example, the ratio of $\frac{\tau_2}{\tau_1}$ is 1.718, giving an attenuation of 4.3 dB.

3.4 Vector Analysis to determine the Dynamic Response of a Hydrostatic Transmission when the Load cannot be Represented by a Simple Mathematical Model

Many loads which a transmission can be expected to drive cannot be expressed in the form of the first order lag, developed from consideration of an inertial and viscous load, and it may be impossible to obtain simple mathematical models which satisfactorily describe their characteristics. The frequency response of the transmission can however be obtained if the frequency response of the load (change of load torque relative to change in load speed) is known, by plotting the vectors of all relevant quantities.

In Fig. 3.7 an experimental vector locus YXZ has been plotted for a typical load. Let us assume that at a certain input frequency the load vector is $\frac{\overrightarrow{t_L}}{\omega_2}$ terminating at the point X.

We will now work backwards to the input movement of the swashplate, x_p.

Stage (1) .. The torque to accelerate the hydraulic motor must be included as the vector $\frac{\overrightarrow{t_m}}{\omega_2}$. This will be 90^o in advance of the speed vector $\overrightarrow{\omega_2}$.

Stage (2) .. By vector addition the total torque vector $\frac{\overrightarrow{t_2}}{\omega_2}$ is obtained.

$$\frac{\overrightarrow{t_2}}{\omega_2} = \frac{\overrightarrow{t_m}}{\omega_2} + \frac{\overrightarrow{t_L}}{\omega_2} \qquad - 3.44$$

Motor viscous torque losses f_m may be added if significant.

Stage (3) .. The pressure difference across the motor can be predicted by the relation

$$t_2 = P_d D_2 X_M \qquad - 3.45$$

or

$$\frac{\overrightarrow{p_d}}{\omega_2} = \frac{\overrightarrow{t_2}}{\omega_2} \frac{1}{D_2 X_M} \qquad - 3.46$$

It is in phase with $\frac{\overrightarrow{t_2}}{\omega_2}$.

If the return line pressure is considered constant $p_d = p_h$.

Stage (4) .. The slip flow loss q_s in the transmission can now be estimated from the steady state characteristics of the pump and motor.

$$q_s = (K_P + K_M)\, \dot{p}_h \qquad - 3.47$$

Hence $\underset{\omega_2}{\overrightarrow{q_s}} = (K_P + K_M)\, \underset{\omega_2}{\overrightarrow{p_h}}$ and is in phase with $\underset{\omega_2}{\overrightarrow{p_h}}$ - 3.48

Stage (5) .. The compressibility flow loss q_c is

$$q_c = \frac{V}{B_e} \frac{dp_h}{dt} = \frac{V}{B_e}\, j\omega \dot{p}_h \qquad - 3.49$$

or $\underset{\omega_2}{\overrightarrow{q_c}} = \frac{V}{B_e}\, j\omega\, \underset{\omega_2}{\overrightarrow{P_h}}$. This will be 90^o in advance of $\underset{\omega_2}{\overrightarrow{P_h}}$ - 3.50

Stage (6) .. By vector addition the total flow loss $\underset{\omega_2}{\overrightarrow{q_L}}$ may be obtained:

$$\underset{\omega_2}{\overrightarrow{q_L}} = \underset{\omega_2}{\overrightarrow{q_c}} + \underset{\omega_2}{\overrightarrow{q_s}} \qquad - 3.51$$

Stage (7) .. The motor flow vector $\underset{\omega_2}{\overrightarrow{q_m}}$ can be drawn since $q_m = D_2 X_M$ in phase with $\overrightarrow{\omega_2}$.

Stage 8 .. The pump flow vector can now be obtained by vector addition:

$$\frac{\overrightarrow{q_p}}{\omega_2} = \frac{\overrightarrow{q_m}}{\omega_2} + \frac{\overrightarrow{q_L}}{\omega_2} \qquad - 3.52$$

Stage (9) .. The pump flow variation q_p is

$$q_p = D_1 \Omega_1 x_p \qquad - 3.53$$

Hence $$\frac{q_p}{x_p} = D_1 \Omega_1 \qquad - 3.54$$

Hence $$\frac{\overrightarrow{\omega_2}}{x_p} = \frac{\overrightarrow{\omega_2}}{q_p} \cdot \frac{q_p}{x_p} \qquad - 3.55$$

$$= D_1 \Omega_1 \frac{\omega_2}{x_p} \qquad - 3.56$$

Thus the overall response of the transmission can be obtained.

Initially the vector analysis technique was carried out graphically, but as its usefulness became fully appreciated it was decided to incorporate it in a computer programme developed to evaluate experimental results and then compare them with predictions made using the vector analysis technique.

A full description of the programme is given in Appendix I as A1.3 - Programme 3 'VECTAN'.

3.4.1 Vector Analysis Used to Determine the Effect of Return Line Pressure Variations

So far the possibility of return line pressure variations have been ignored; in other words a system supplied by a large capacity boost pump or having an efficient accumulator in the return line has been considered.

Many systems however have a boost pump sufficiently large to make up leakage flows with very little excess capacity, and accumulators are not fitted. In this case a sudden increase in load or swash plate angle can cause suction starvation of the main pump, McCallion, Dudley & Knight (30).

The behaviour of the return line during frequency response tests can be shown by reference to Fig. 3.8(a). This shows the return line pressure as a function of system demand from the boost pump. The relief valve shown has a steeply rising characteristic, and when the system demands no flow the pressure is that which would be given by the relief valve when all the boost pump flow is passing through it (Point A).

During low frequency oscillations there is negligible phase difference between pump and motor flows, and the boost pump has only to make up the leakage. Thus there will be a continuous steady flow through the relief valve, and the pressure appropriate to this will be given at Point A.

At higher frequencies the phase difference in flows between the pump and motor will be considerable and the system demand for flow from the boost system will oscillate at the input frequency from B to B' with a corresponding change in pressure due to the relief valve characteristic. If the flow fluctuation in the return line becomes very large, due to large phase differences and/or large swash plate amplitudes, the instantaneous flow requirement may become greater than the boost capacity and the points may move to C and C', showing that cavitation will occur in the return line. The corresponding pressure time curves for these three conditions are shown on Fig. 3.8 (b), (c), and (d). Oil compressibility will modify this simple argument to some extent.

The effect on system dynamic performance can now be deduced. The vector analysis provides a technique for dealing with return line pressure variations. Taking case (c), the return line pressure variations contribute to the motor torque and hence to the system stiffness. These variations can be included in the signal flow diagram, or can be allowed for in the vector loss approach.

The effective torque vector $\frac{\vec{t_2}}{\omega_2}$ can be converted to a differential pressure vector $\frac{\vec{p_d}}{\omega_2}$. The return line pressure vector $\frac{\vec{p_L}}{\omega_2}$ can be added to this to obtain the supply pressure $\frac{\vec{P_h}}{\omega_2}$. The analysis can then be carried forward as above. Case (d) with cavitation could be analysed in a similar manner using the describing function technique if thought necessary. Extensive cavitation may however reduce the pump performance and the mean motor speed will drop.

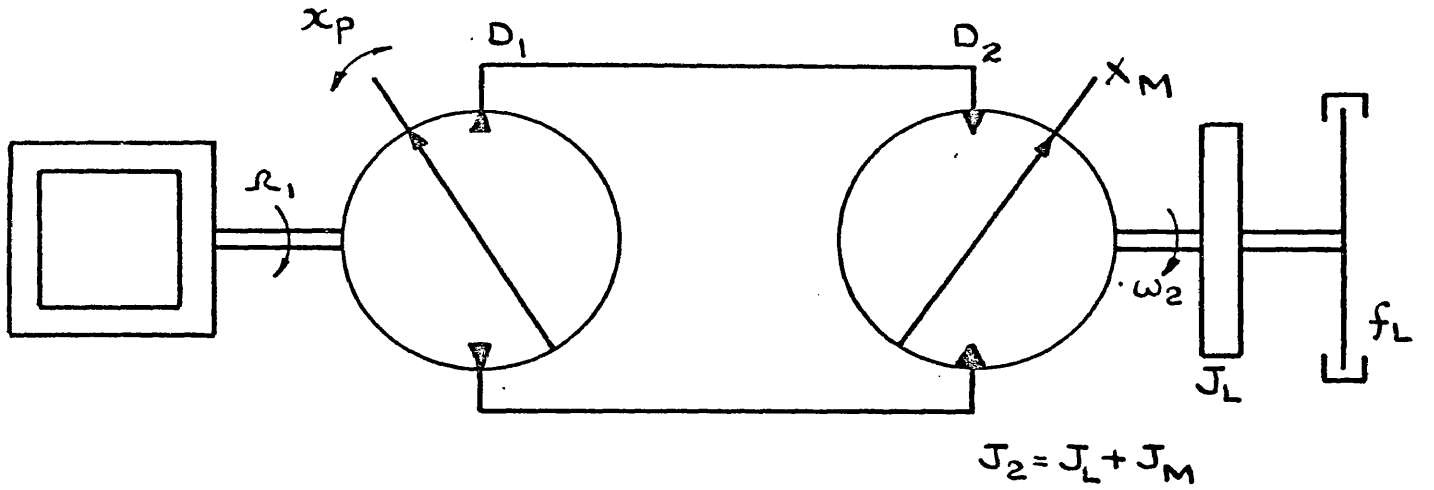

FIG. 3.1(a) DIAGRAMATIC LAYOUT OF HYDROSTATIC TRANSMISSION

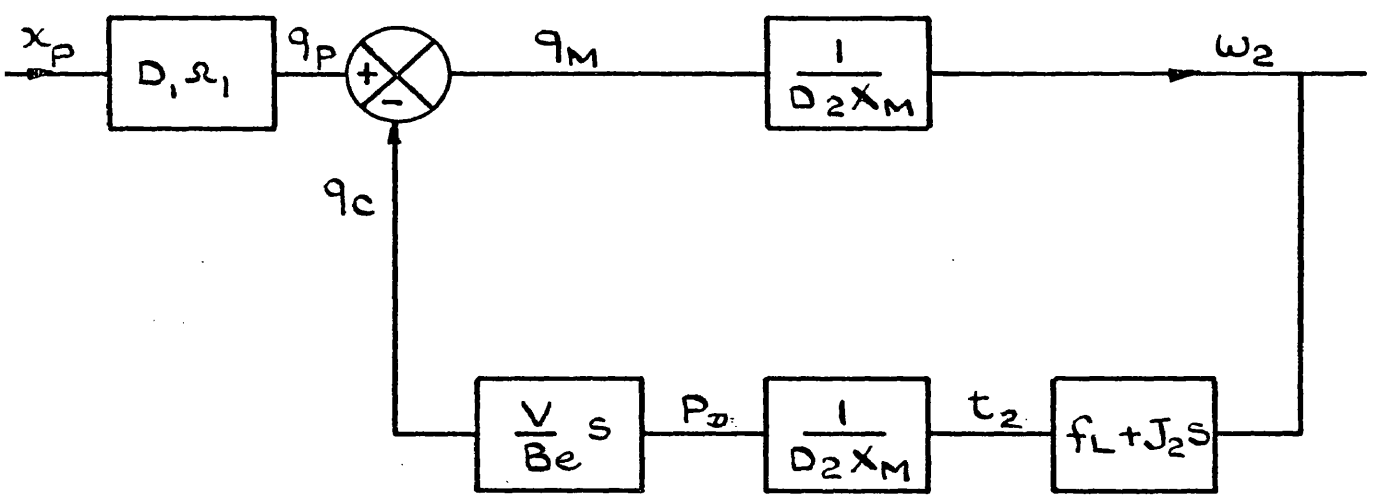

FIG. 3.1(b) HYDROSTATIC TRANSMISSION BLOCK DIAGRAM.

FIG. 3.1. DIAGRAMATIC LAYOUT AND BLOCK DIAGRAM OF A LOSSLESS HYDROSTATIC TRANSMISSION.

FIG.3.2 SIGNAL FLOW ANALYSIS

ELEMENT	STEADY STATE CHARACTERISTIC	TRANSMITTANCE AT OPERATING POINT (LOWER CASE LETTERS REFER TO SMALL CHANGES)	SIGNAL FLOW GRAPH
ENGINE	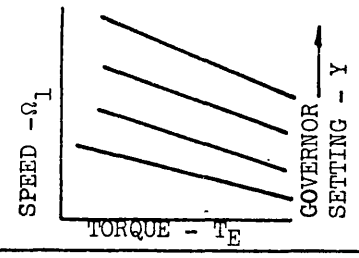	$\Delta\Omega_1 = \frac{\delta\Omega_1}{\delta T_E}.\Delta T_E + \frac{\delta\Omega_1}{\delta Y} . \Delta Y$ OR $\omega_1 = K_E.t_e + K_G.y$	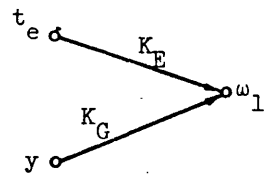
ENGINE & PUMP INERTIA	$T_E = T_P + J_1 \frac{d\Omega_1}{dt}$	$\Delta T_E = \Delta T_P + J_1 s \Delta\Omega_1$ OR $t_e = t_p + J_1 s \omega_1$	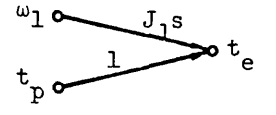
PUMP-FLOW RELATION-SHIP	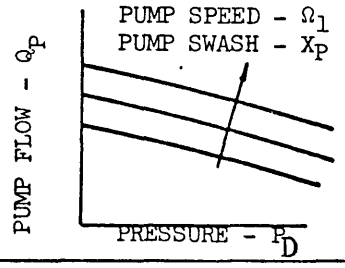	$\Delta Q_P = \frac{\delta Q_P}{\delta P_D}.\Delta P_D + \frac{\delta Q_P}{\delta X_P}.\Delta X_P + \frac{\delta Q_P}{\delta \Omega_1}.\Delta\Omega_1$ OR $q_p = K_P.p_D + D_1.\Omega_1.x_p + D_1 X_P.\omega_1$	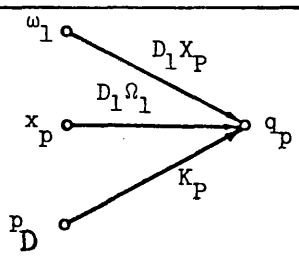
PUMP-TORQUE RELATION-SHIP	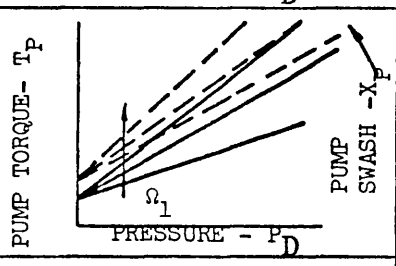	$\Delta T_P = \frac{\delta T_P}{\delta P_D}.\Delta P_D + \frac{\delta T_P}{\delta X_P}.\Delta X_P + \frac{\delta T_P}{\delta \Omega_1}.\Delta\Omega_1$ OR $t_p = (D_1 X_P + K_{FP}) p_D + D_1 P_D x_p + F_P.\omega_1$	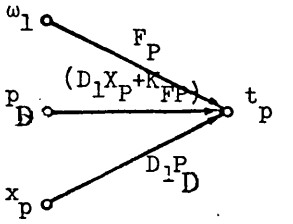
TRANS-MISSION LINE COMPRESS-IBILITY	$Q_C = Q_P - Q_M = \frac{V}{B_e} \frac{dP_D}{dt}$	$\Delta Q_C = \frac{V}{B_e} \frac{d(\Delta P_D)}{dt}$ OR $q_C = \frac{V}{B_e} s\, p_D$	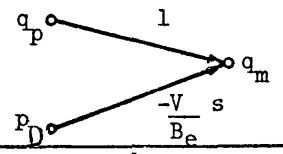
MOTOR-FLOW RELATION-SHIP	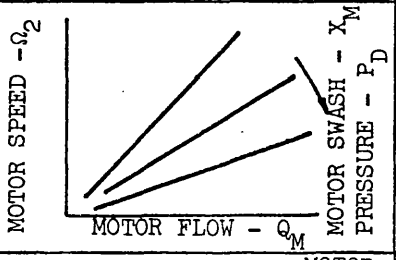	$\Delta\Omega_2 = \frac{\delta\Omega_2}{\delta Q_M}.\Delta Q_M + \frac{\delta\Omega_2}{\delta P_D}.\Delta P_D + \frac{\delta\Omega_2}{\delta X_M}.\Delta X_M$ OR $\omega_2 = \frac{q_m}{D_2 X_M} + \frac{K_M}{D_2 X_M}.p_D - \frac{x_m \Omega_2}{X_m}$	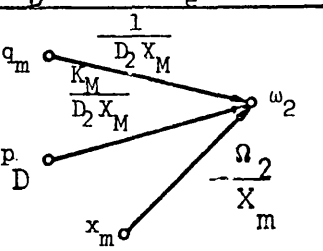
MOTOR-TORQUE RELATION-SHIP	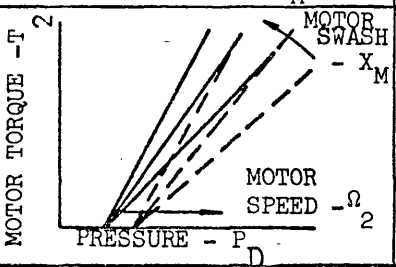	$\Delta T_M = \frac{\delta T_M}{\delta P_D}.\Delta P_D + \frac{\delta T_M}{\delta X_M}\Delta X_M + \frac{\delta T_M}{\delta \Omega_2}.\Delta\Omega_2$ OR $t_m = D_2 P_D x_m - f_m \omega_2 + D_2 X_M p_D - K_{FM} p_D$ $p_h = \frac{t_m + f_M \omega_2 - D_2 P_H x_m}{D_2 X_M - K_{FM}}$	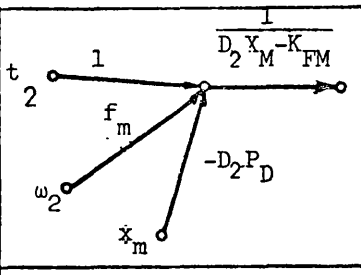
LOAD	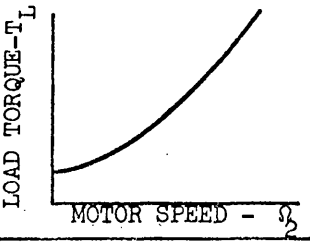	$\Delta T_M = \frac{\delta T_L}{\delta \Omega_2} \Delta\Omega_2 + J_2 \frac{\delta\Delta\Omega_2}{dt}$ OR $t_m = f_L \omega_2 + J_2 s\, \omega_2$	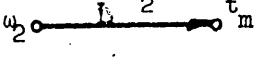

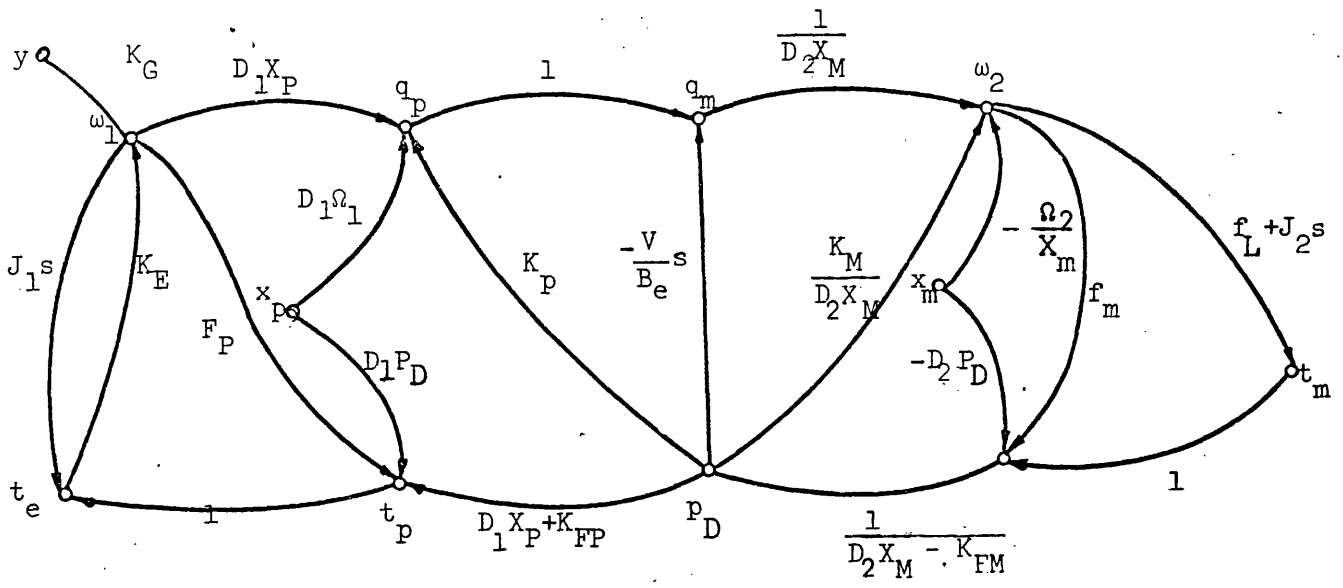

SIGNAL FLOW DIAGRAM.

$$\frac{\omega_2}{x_p} = \frac{D_1\Omega_1}{D_2X_M} \cdot \frac{\left[1-\left(J_1s+f_p\right)K_E+D_1P_DK_EX_P'/\Omega_1\right]}{1-\left(J_1s+f_p\right)K_E-\frac{\left(f_L+f_m+J_2s\right)}{D_2X_M\left(D_2X_M-K_{FM}\right)}\left[\left(K_P\frac{-V}{B_e}s+K_M\right)\left(1-J_1K_Es-f_pK_E\right)+K_ED_1X_P\left(D_1X_P+K_{FP}\right)\right]}$$

TRANSFER FUNCTION RELATING OUTPUT SPEED TO INPUT SWASH ANGLE DERIVED FROM SIGNAL FLOW DIAGRAM.

FIG. 3.3 TRANSMISSION SIGNAL FLOW DIAGRAM AND RESULTANT TRANSFER FUNCTION.

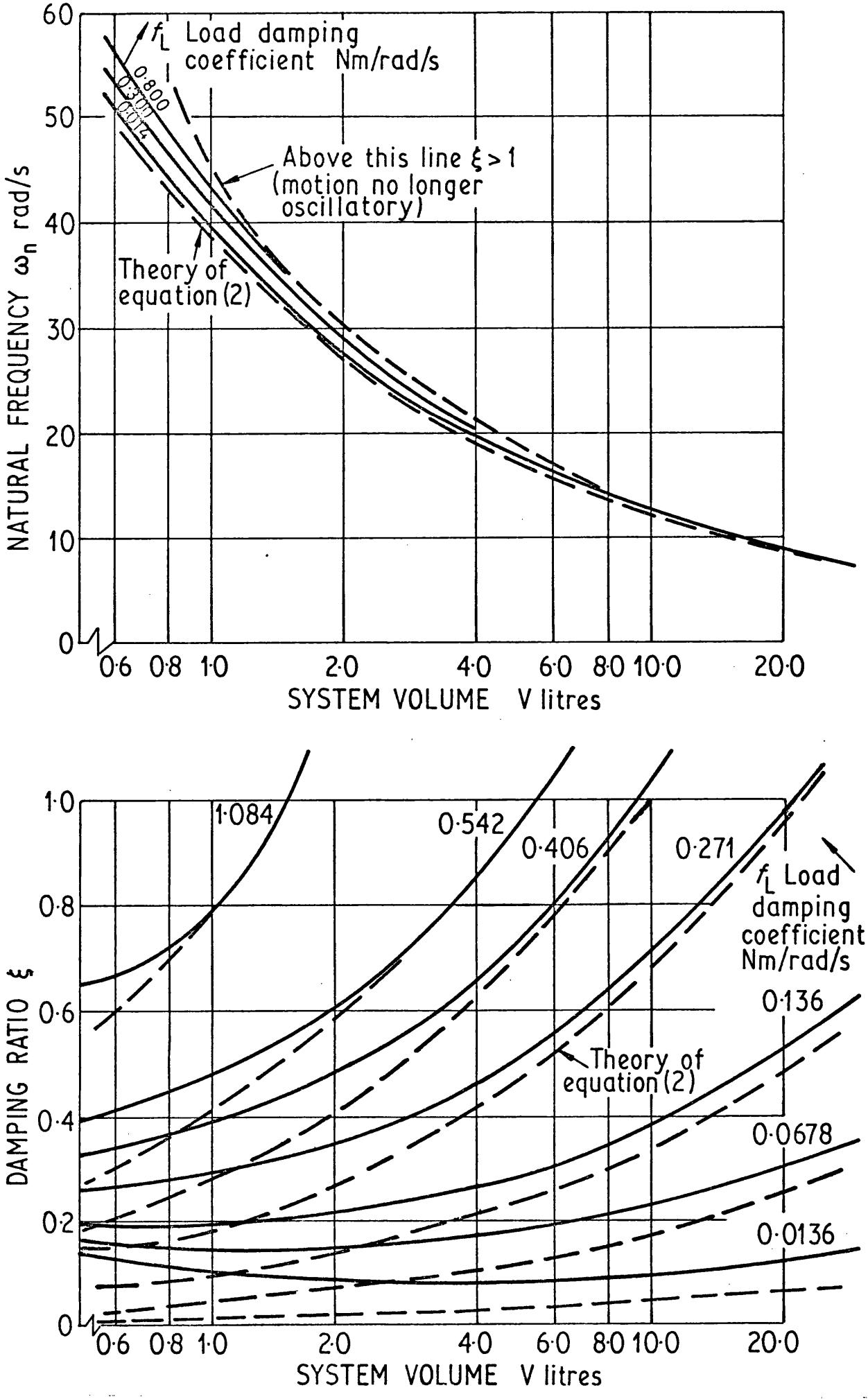

FIG. 3.4 THE EFFECT OF SYSTEM VOLUME ON TRANSMISSION NATURAL FREQUENCY AND DAMPING RATIO.

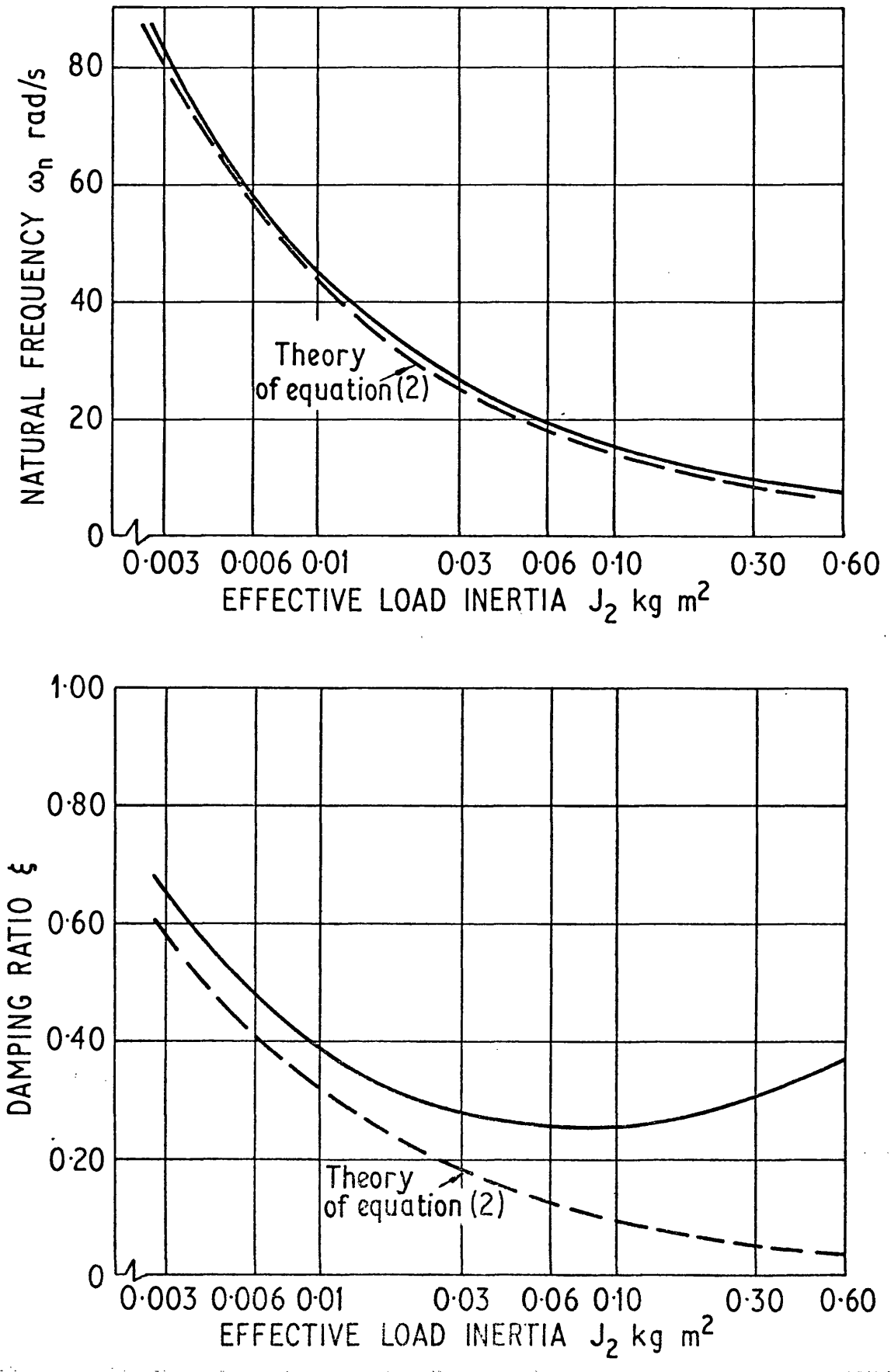

FIG. 3.5 EFFECT OF LOAD INERTIA ON SYSTEM NATURAL FREQUENCY AND DAMPING RATIO.

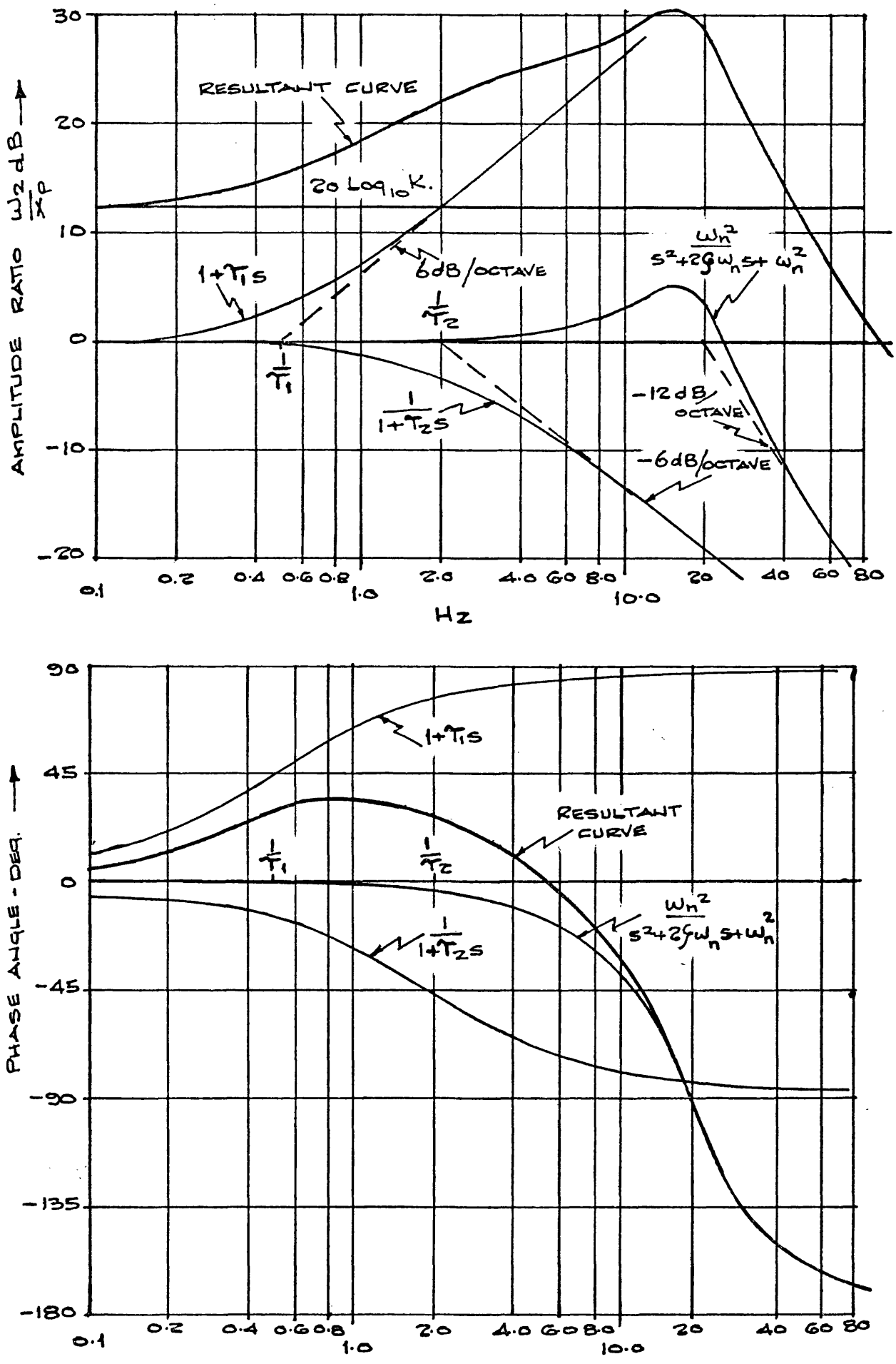

FIG. 3.6 THE FREQUENCY RESPONSE OF A HYDROSTATIC TRANSMISSION DRIVEN BY A PRIME MOVER OF SIGNIFICANT DROOP

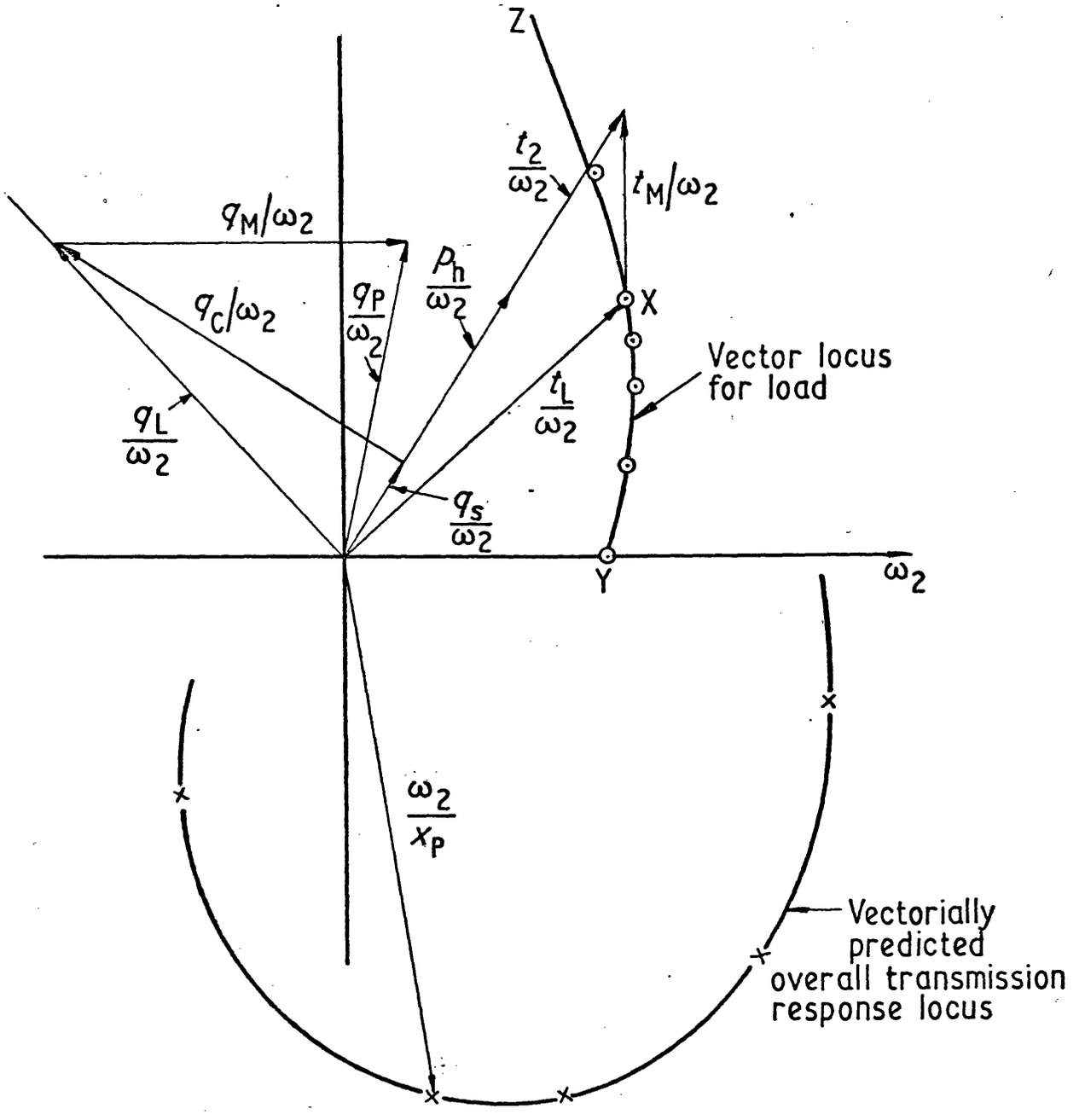

FIG. 3.7 VECTOR ANALYSIS FOR DETERMINING OVERALL TRANSMISSION RESPONSE USING MEASURED LOAD LOCUS.

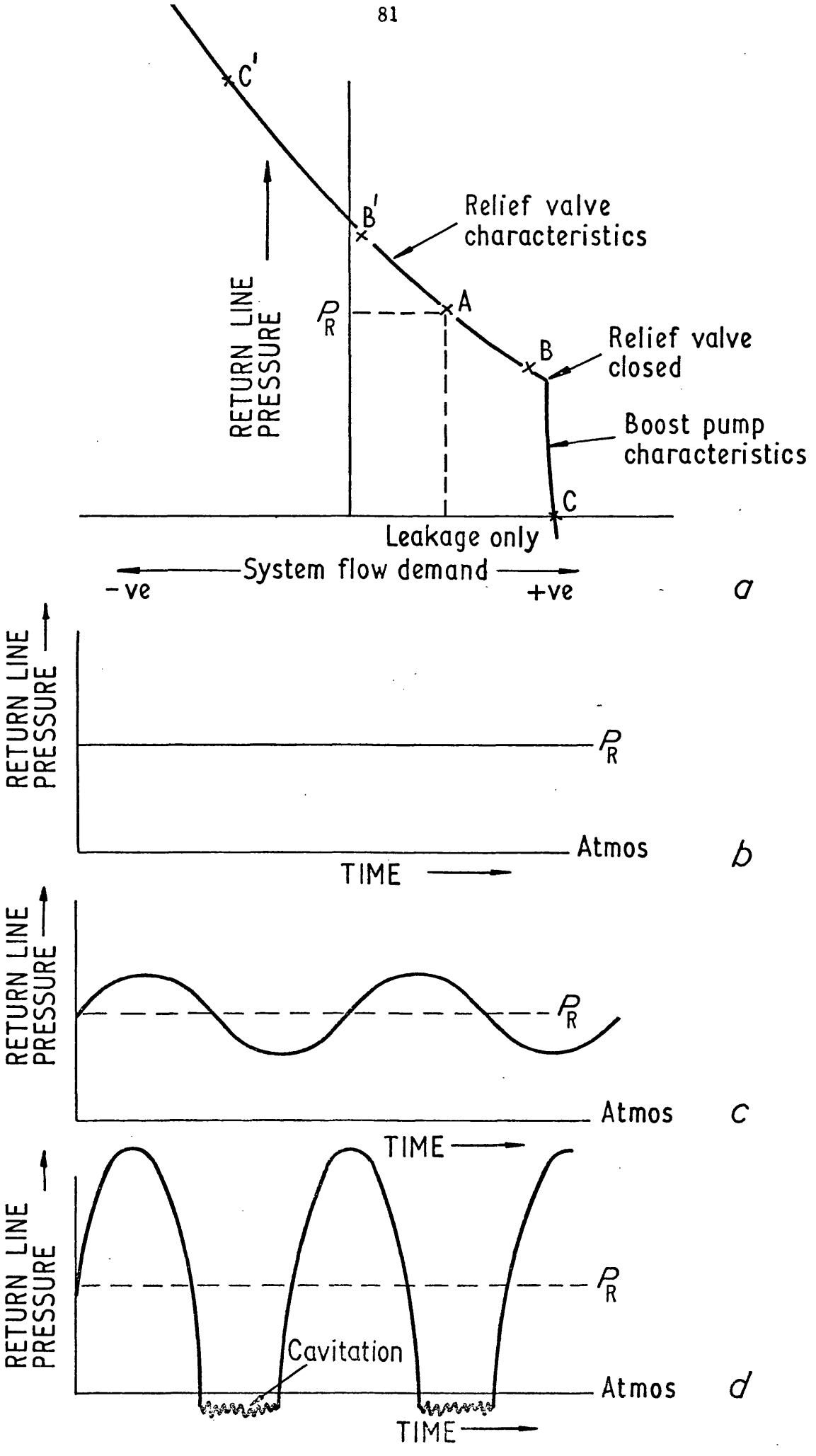

FIG. 3.8 BEHAVIOUR OF RETURN LINE DURING FREQUENCY RESPONSE TESTS.

CHAPTER 4 : OIL COMPRESSIBILITY and its AFFECT UPON HYDRAULIC SYSTEM PERFORMANCE

4.1 Introduction

All fluids are compressible, but because of the relatively low compressibility of liquids, particularly in relation to gases, it has been considered sufficient to treat them as incompressible in many instances. The assumption that fluid density remains constant with changes in pressure considerably simplifies the analysis of many problems of fluid flow, and very often provides satisfactory solutions. However, the high pressures being utilised in oil hydraulic systems make it increasingly important to take into account the reduction in volumetric efficiency that takes place in positive displacement systems due to oil compressiblity.

The necessity of including compressibility effects in component and system design has given rise to a requirement for information on the comprssibility of fluids. Detailed investigations into the compressibility of the whole range of hydraulic media including the fire resistant fluids have been carried out. Besides work by the oil companies, considerable original work and rationalisation of available data has been carried out at the National Engineering Laboratory (33) and (34).

Dynamic tests on hydraulic equipment carried out by many investigators have shown apparent compressibilities of the hydraulic media much greater than the figures obtained by physical measurement of compressibility. However the scatter of figures put forward has been so wide, and the reasons attributed to the discrepancy so varied, that considerable uncertainty continues on this issue.

This chapter defines oil compressibility, examines its affect upon system performance, and investigates the effect of air bubbles upon compressibility. This is the most commonly suggested reason for the discrepancy. The detailed experimental work carried out to investigate the dynamics of a hydrostatic transmission has enabled the compressibility of the oil column trapped between the variable delivery pump and motor to be carefully evaluated and the information presented in this Chapter provides a basis for correlation.

4.2 The Physical Determination of Oil Compressibility

4.2.1 Definitions and Relationships

Hayward (35) outlined many detailed attempts carried out to investigate oil compressibility. He found that the effects of pressure, temperature, and oil chemical composition were not taken fully into account until the 1950^{s}. Even then much of the work was directed towards the evaluation of isothermal compressibility with little or no attention directed towards isentropic compression which is of equal importance to the hydraulics engineer.

The accepted definitions of oil compressibility are obtained as follows. Consider a volume of fluid Vo being compressed by a pressure P. When oil is compressed heat is generated and if it cannot be dissipated then the oil temperature will rise causing a small increase in volume. Therefore the compressibility will be greater if the oil is compressed isothermally rather than isentropically. The type of compression occuring will normally be controlled by the rate of compression as this will affect the heat dissipation process. Fig. 4.1 shows an isothermal and isentropic compression of the oil volume Vo. Vp is the volume of oil at a pressure P. It is apparent that the rate of compression decreases as the oil pressure increases.

There are several methods by which the compression of the oil may be defined. The more common method is to consider the oil to be an elastic medium and determine its resistance to changes in volume known as the Bulk Modulus. As the pressure increases so the slope of the compression curve changes, therefore at any pressure and temperature the slope of the pressure compression curve will define the Bulk Modulus. This slope, known as the Tangent Bulk Modulus, is shown diagramatically for the isothermal compression curve B_T, Fig. 4.2(a):

$$\text{Isothermal Tangent Bulk Modulus } B_T = \left\{ V_p \frac{\delta P}{\delta V} \right\}_T \quad - 4.1$$

$$\text{Isentropic Tangent Bulk Modulus } B_S = \left\{ V_p \frac{\delta P}{\delta V} \right\}_S \quad - 4.2$$

An alternative approach is to evaluate the compression between two defined pressures. This is defined as the Secant Bulk Modulus. It is usual to take atmospheric pressure Po as the reference pressure as shown on Fig.4.2(b), where the isotropic value is illustrated.

$$\text{Isothermal Secant Bulk Modulus } \overline{B_T} = \left\{ \frac{V_o \, P}{V_o - V_p} \right\}_T \quad - 4.3$$

$$\text{Isentropic Secant Bulk Modulus } \overline{B_S} = \left\{ V_o \frac{P}{V_o - V_p} \right\}_S \quad - 4.4$$

The units of bulk modulus are those of pressure.

The inverse of bulk modulus, compressibility, may be defined in a similar manner.

Hayward (35) showed by his comparative study of the available generalised equations that the secant bulk modulus could be satisfactorily expressed as a polynomial of the form:

$$\overline{B} = K_o + gP - hP^2 \qquad - 4.5$$

K_o, g and h depend on the type of oil and its temperature. This equation can be applied to both isothermal and isentropic compression.

To relate secant values obtained from Equ. 4.5 to the Tangent Modulus, consider the general equation for Secant Bulk Modulus:

$$\overline{B} = V_o \left(\frac{P}{V_o - V_p}\right) \qquad - 4.6$$

$$V_p = \frac{V_o}{\overline{B}} \left(\overline{B} - P\right)$$

$$\frac{dV_p}{dP} = V_o \left\{ \frac{P \frac{d\overline{B}}{dP} - \overline{B}}{\overline{B}^2} \right\}$$

The general equation for Tangent Bulk Modulus:

$$B = -V_p \frac{\delta P}{\delta V} \qquad - 4.7$$

In the limit $\delta V \rightarrow O$

$$B = -V_p \frac{dP}{dV}$$

$$= \frac{V_p}{V_o} \left\{ \frac{\overline{B}^2}{\overline{B} - P\frac{d\overline{B}}{dP}} \right\}$$

But $Vo = Vp \frac{\overline{B}}{\overline{B} - P}$

$$\therefore B = \overline{B}\left(\frac{\overline{B} - P}{P\frac{d\overline{B}}{dP} - \overline{B}}\right) \qquad - 4.8$$

From Equ. 4.5

$$\frac{d\overline{B}}{dP} = g - 2hP$$

$$\therefore B = \overline{B}\,\frac{(\overline{B} - P)}{K_o + hP^2} \qquad - 4.9$$

The constants K_o, g, and h, in Equ. 4.5 were evaluated by Hayward by fitting a quadratic curve to a range of isothermal and isentropic compression curves up to 1,400 bar (20,000 lbf/in^2) obtained for a variety of oils of different viscosity. It was found that g and h were independent of the oil viscosity and oil temperature. The same was found to be true for isentropic compression (the temperature in this case was that of the start of the compression). However, due to the low curvature of the compression curves, below pressures of 800 bar (11,600 lbf/in^2) Hayward was able to fit a satisfactory straight line to the compression curve of slope 5.6.

Once the relationship with Bulk Modulus was established it only remained to evaluate the temperature relationship, and the relation: ship between different oils. From experimental data logarithmic relationships were obtained and from these the following generalised relationships for Secant Bulk Modulus derived:

Isothermal Second Bulk Modulus

$$\bar{B}_T = \left\{1.69+0.15\ \text{Log}\nu\right\}\left\{\text{Antilog}\ 0.0018\,(20-T)\right\} \times 10^4 - 5.6\,(690 - P) \qquad - 4.10$$

or:

$$\bar{B}_T = \left\{1.90 +7(\rho - 0.86)\right\}\left\{\text{Antilog}\ \ 0.0018\,(20-T)\right\} \times 10^4 - 5.6\,(690 - P) \qquad - 4.11$$

and:

$$\overline{B}_S = \left\{1.96+0.15\ \text{Log}\nu\right\}\left\{\text{Antilog}\ \ 0.0019\ (20-T)\right\} x\ 10^4 - 5.6\ (690 - P) - 4.12$$

or:

$$\overline{B}_S = \left\{2.17+7\ (\rho - 0.86)\right\}\left\{\text{Antilog}\ \ 0.0019\ (20-T)\right\} x\ 10^4 - 5.6\ (690 - P) - 4.13$$

where:

P - Pressure in bar

T - Temperature ^{o}C

ν - Kinematic Viscosity at $20^{o}C$ in CSt

ρ - Density at $20^{o}C$ Kg/litre.

These /

These generalised relationships gave the Secant Bulk Modulus for the oils used in bar, and are the methods recommended by the oil supplier for determining these values. The Tangent Bulk Modulus was obtained by using Equ. 4.9 where the fit to the compression curve was assumed linear.

Hence $h = o$

$$\therefore \quad B = \bar{B}\,\frac{(\bar{B} - P)}{Ko} \qquad -4.14$$

4.2.2 Experimentally Determined Values of Bulk Modulus

The values obtained by Hayward (35) for his generalised equations for Bulk Modulus were obtained by what are now recognised techniques for measuring Bulk Modulus developed at N.E.L. Curves derived for Bulk Modulus in this way are published as part of the oil technical specifications by several oil companies.

The basis of the N.E.L. testing equipment is to use a standard Hounsfield Tensometer to measure the compression curve of a volume of fluid enclosed in a rigid container into which a plunger is forced.

An isothermal compression is obtained by carring out the loading process very slowly whilst an isentropic compression is obtained by a rapid loading cycle. A further technique employed for determing the isentropic tangent bulk modulus of a fluid is to measure the velocity of wave propegation through the fluid from the equation

$$\overline{B}_S = \rho V^2 \qquad - 4.15$$

where V is the velocity of a sound wave through the fluid under test.

Two oils were used throughout the test work on the Hydrostatic Transmission Shell Tellus 27 and Mobil D.T.E.24. A typical curve for the isentropic tangent bulk modulus of the Shell Oil Tellus 27 is shown in Fig.4.3 and was obtained from (36). It should be pointed out that these figures had been revised following the work at N.E.L. The first edition gave higher values for the oil bulk modulus (37).

It is by definition only correct to use the secant bulk modulus when considering compressibility from an atmospheric starting condition such as would follow the build up of pressure in an hydraulic actuator initially at atmospheric pressure.

The tangent value would be used when considering fluctuations in pressure about some steady state pressure such as might occur in an electro-hydraulic servo system. The use of the isothermal or isentropic value depends upon the rate of compression. A simple assumption is to consider rapid changes as isentropic and slower changes as being isothermal.

As pressure changes occuring during dynamic testing of the hydrostatic transmission were taking place rapidly about a steady state operating pressure, the isentropic tangent bulk modulus was used for calculations. Actual values for the Bulk Moduli were obtained by substituting values in the Generalised Equations, Equ. 4.12 and Equ. 4.14.

4.3 The Use of Oil Bulk Modulus in the Determination of Hydraulic System Performance

In the reported experimental work on hydraulic systems there have been many attempts to obtain a reasonable correlation between the experimental and predicted values of system dynamic performance.

For a loaded hydraulic system that can be represented by a second order differential equation, this means correlating values for natural frequency. The main unknown has been assumed to be the effect of oil compressibility and the resilience of the associated pipework. Most experimenters have claimed good agreement between predicted and experimentally obtained values of natural frequency by assuming a suitable value of effective bulk modulus. A wide range of values have been used to achieve correlation.

Before outlining some of the values used it should be pointed out that many authors failed to clarify which bulk modulus was considered most suitable for the problem under consideration. In addition, in practical systems the effect of wall elasticity has to be taken into account and the extent to which this has been done is often not made clear. The relation for the effective bulk modulus taking into account the hoop stress in thin walled pipes is

$$\frac{1}{Be} = \frac{1}{Bo} + \frac{1}{Bp} \qquad -4.16$$

where $$\frac{1}{Bp} = \frac{d}{t\ E} \qquad -4.17$$

Newton (10) compared his experimental results with theoretical predictions made using what was effectively the simplified analysis presented in Chapter 3.2.

Three different transmissions were used by Newton, two housed in their own reservoir, and all with closed circuit. The theoretical predictions using a bulk modulus of 17,200 bar (250,000 lbf/in^2) gave consistently higher natural frequencies than those obtained during the test work particularly in the case of transmissions with integral reservoirs. Newton proposed that these low values were due to entrained air in the oil and suggested that improved response of the transmission could be obtained by reducing the amount of entrained air present by increasing the boost pressure.

It is interesting to note that Newton's early work recognised many of the problems involved in the analysis and the dynamic testing of the hydrostatic transmission even if he did not manage to investigate their effect. These included return line pressure, replenishing valve characteristic, prime mover droop, and gas solubility.

In 1961 Hansen (38) predicting the resonant frequency of an inertial and viscous load driven by a servo valve controlled hydraulic motor, used an 'average' value for the bulk modulus of oil of 11,600 bar (170,000 lbf/in^2). This resulted in an overestimate of 6% to 10% over the experimentally measured values obtained using frequency response and step response techniques.

Lambert and Davies (39) 1963, who again were concerned with hydraulic servomechanisms under inertial load, quoted a figure which is often put forward of 13,800 bar (200,000 lbf/in^2). The effects of the flexibility of the actuator mounting structure and the actuator dilation reduced this to 7,750 bar (114,000 lbf/in^2). In the theoretical calculation a value of 3,450 bar (50,000 lbf/in^2) was used and provided reasonable correlation with experiment. The reduction by a factor of two was attributed to air entrainment.

In Renner's Paper (40) on the use of hydraulic motors in the machine tool field, he laid down simple procedures for calculating the acceleration capabilities of the hydraulic motor. Like the previous authors he proposed a low value for bulk modulus. In this case, 6,800 bar (100,000 lbf/in^2), due to the likely effects of air entrainment. In addition it was proposed that this value be reduced still further if flexible hydraulic hose was used.

At the other end of the scale Healey and Stringer (41) in 1968 recommended a value of bulk modulus in line with that obtained by physical measurement 18,400 bar (270,000 lbf/in^2). They obtained good agreement between their predicted and experimental results for the dynamic performance of the constant speed drive they were investigating.

Particular attention was paid to the inertia effect of the oil in the pipelines to the actuator, and the authors pointed out the gearing effect on this inertia of the area ratio between the pipelines and the actuators. It should be pointed out that the system employed was of the 'meter out' type giving little possibility of aerated oil affecting the drive performance.

Nevertheless despite the good correlation obtained by Healey and Stringer, some more recent authors have found it necessary to use much lower values for bulk modulus. Green and Crossley (42), and Keating and Martin (43), proposed a value of 6,800 bar (100,000 lbf/in^2).

Amongst the variety of values used for Bulk Modulus there remains a hard core of well known authors who suggest a general value of 13,600 bar (200,000 lbf/in^2) be used despite the fact that this value is considerably lower than that determined by static tests. These authors include Walters(44), Gille (14), and Shearer (11). Shearer stated, "The logical basis of the practice is open to question, but it seems to work".

The picture conveyed by the work of past authors investigating the effect of oil compressibility on hydraulic systems is definitely unsatisfactory.

The detailed experimental work reported here was directed towards clarifying two points. Firstly - were the physically determined values of bulk modulus valid in practical systems, and secondly - what effects if any, could be attributed to oil aeration?

4.4 Aeration of Hydraulic Fluids - The Effect Upon Hydraulic System Performance and Oil Compressibility

4.4.1 The Mechanism of Aeration and Cavitation

The phenomena of air release and cavitation are often confused as both can occur when there is a local reduction in pressure. In the case of air release the pressure must be reduced below the pressure at which air was absorbed into the fluid; in the case of cavitation to below the vapour pressure of the fluid. The vapour pressure of hydraulic mineral oils is well below that of water, usually less than 0.02 bar (0.25 lbf/in^2) absolute.

There are two basic conditions under which low pressures can occur, permitting aeration or cavitation to take place in hydraulic systems. Mechanical movement such as the reciprocating action of pumps and actuators, and the vibration of moving parts such as valve seats, can give rise to high acceleration or retardation forces on the fluid.

Secondly fluid dynamic effects such as local increases in velocity and separation vortices can cause local reductions in pressure.

As air release from the oil can take place anywhere in a hydraulic system when pressures fall below tank pressure and cavitation can also take place when pressures fall further below that level, it can be seen that there is a practical difficulty in separating the two phenomena. A system in which air release is a problem may also be one in which cavitation is occurring.

4.4.1.1 Cavitation

In a cavitating system bubbles of oil vapour form at regions of low pressure, usually round some nucleus which can be a small air bubble or a solid particle. Streeter(45) presents a good review of cavitation phenomena.

An example of a low pressure region suitable for the formation of cavitation bubbles would be the core of a localised vortex. Subsequent collapse would occur when the bubbles enter a region of higher pressure.

The collapse is rapid giving rise to extremely high localised pressures and the familiar cavitation noise. If the collapse occurs in the vicinity of a metal boundary it can give rise to cavitation erosion. It has been established that materials with low strain energy capacity such as aluminium, are more susceptible to erosion than those with a high strain energy capacity such as stainless steel. McCloy (46) gave a good review of the effect of cavitation upon hydraulic systems.

Air in cavitation prone systems has two effects - one being to provide nuclei for the growth of cavitation bubbles - but the other is to cushion the collapse of these bubbles. Air bubbles are sometimes introduced into water systems to prevent cavitation damage. (45).

4.4.1.2 Aeration

Air can be dissolved or entrained in hydraulic fluids, and the physics of gas release and adsorption is governed by Henry's Law which relates gas solubility to pressure. It states that the mass of gas dissolved in a liquid is directly proportional to the pressure of the gas and implies that doubling the gas pressure over an oil will double the amount of gas that can be dissolved in the oil at equilibrium conditions.

Solubility data for hydrocarbon fluids is expressed as Bunsen and Ostwald coefficients and are given in (47), but as an indication most mineral oils have at S.T.P. between 6% to 12% of their volume of air dissolved in them. The type of oil only makes a small difference to the gas solubility, but the type of gas can make a significant change. For instance Carbon Dioxide has a solubility as high as 85% in mineral oils at S.T.P.

The presence of dissolved gas in an oil increases the mass of the oil, but does not increase the volume. Gases in solution have no measurable effect on fluid properties, but once air is dissolved in the hydraulic oil any conditions of low pressure permitting the gas to come out of solution will present problems.

The time taken for release and adsorption is very important since the fluid is moving rapidly through the hydraulic system and exposed to low pressures for only short periods. If the process of release was extremely sluggish, regions of low pressure in a system would cause very little air to come out of solution. Smith, Peeler and Bernd (48) indicated that the time for adsorption is considerably longer than that for release enabling air to come out of solution in hydraulic suction lines and then pass through the pump into the high pressure region where they survived for some time.

Hayward (49) and Magorien (50) and (51), carried out studies on the rate of adsorption of bubbles in hydraulic fluids. The problem is complex with many variables, but two major factors identified by both authors were that the degree of agitation of the fluid and the size of the bubbles were of prime importance. A typical curve obtained by Hayward giving the rate of solution for a typical mineral oil is shown in Fig. 4.4. A controlled rate of agitation was employed.

4.4.2 The Effects of Air Entrainment Upon Oil Compressibility and Hydraulic System Performance

Early workers investigating the effects of air in hydraulic systems were associated with aircraft hydraulic systems. Hydraulic systems in aircraft are subjected to low atmospheric pressures at high altitudes making aeration more likely. Rendel and Allen (52) derived a relationship for the bulk modulus of aerated fluid given by

$$B_{T_{Fluid/Air}} = B_{T_{Fluid}} \frac{\left(\frac{V_o}{V_A} + 1\right)}{\frac{V_o}{V_A} + P_o \cdot \frac{B_{T_{Fluid}}}{P^2}} \qquad - 4.18$$

where V_o - Fluid Volume at Atmospheric Pressure P_o

V_A - Volume of Air at Atmospheric Pressure P_o

P - Fluid Pressure

However, Hayward (49) corrected this relation in 1962 so that it became

$$B_{T_{Fluid/Air}} = B_{T_{Fluid}} \frac{\left(\frac{V_o}{V_A} + \frac{P_o}{P}\right)}{\frac{V_o}{V_A} + \frac{P_o B_{T_{Fluid}}}{P^2}} \qquad - 4.19$$

The discrepancy had occured because of the incorrect definition of tangent bulk modulus used by Rendel and Allen

$$B_T = - V_o \frac{\delta P}{\delta V} \qquad - 4.20$$

instead of the now accepted definition given as Equ.4.7.

$$B_T = - V_P \frac{\delta P}{\delta V} \qquad - 4.21$$

The error in Equ. 4.18 would result in bulk modulus of the mixture higher than that of the fluid alone when P^2 becomes greater than $B_{TFluid}P_o$. This would occur at pressures higher than 120 bar (1750 lbf/in^2). Curves derived from Equ. 4.19 are shown in Fig.4.5, and it can been seen that at low pressure large reductions in bulk modulus can occur due to only a small air content.

It should be pointed out that both formulae are based upon the assumption that air bubbles do not dissolve into the oil when compressed. In fact the air bubbles do dissolve and thus Equ. 4.19 is likely to under estimate bulk modulus.

In 1952 Tourret and White (54) carried out a broad based investigation into the effects of aeration upon hydraulic systems. They were primarily interested in the effects of aeration upon lubricating properties and the rate at which any foam generated could be dissipated both by chemical means and by improvement in hydraulic system construction.

Although most authors investigating aeration have commented upon the losses of volumetric efficiency in hydraulic units that will occur as a result of aeration no quantative information has been presented. One of the most recent authors in the field has been Magorien (50) and (51) who as well as outlining the effects of aeration proposes the use of an instrument for measuring the amount of air in hydraulic systems, and if required, the use of an air separator to remove it. An instance where a separator has been used to improve system performance is given by Livesey and Ettinger (55).

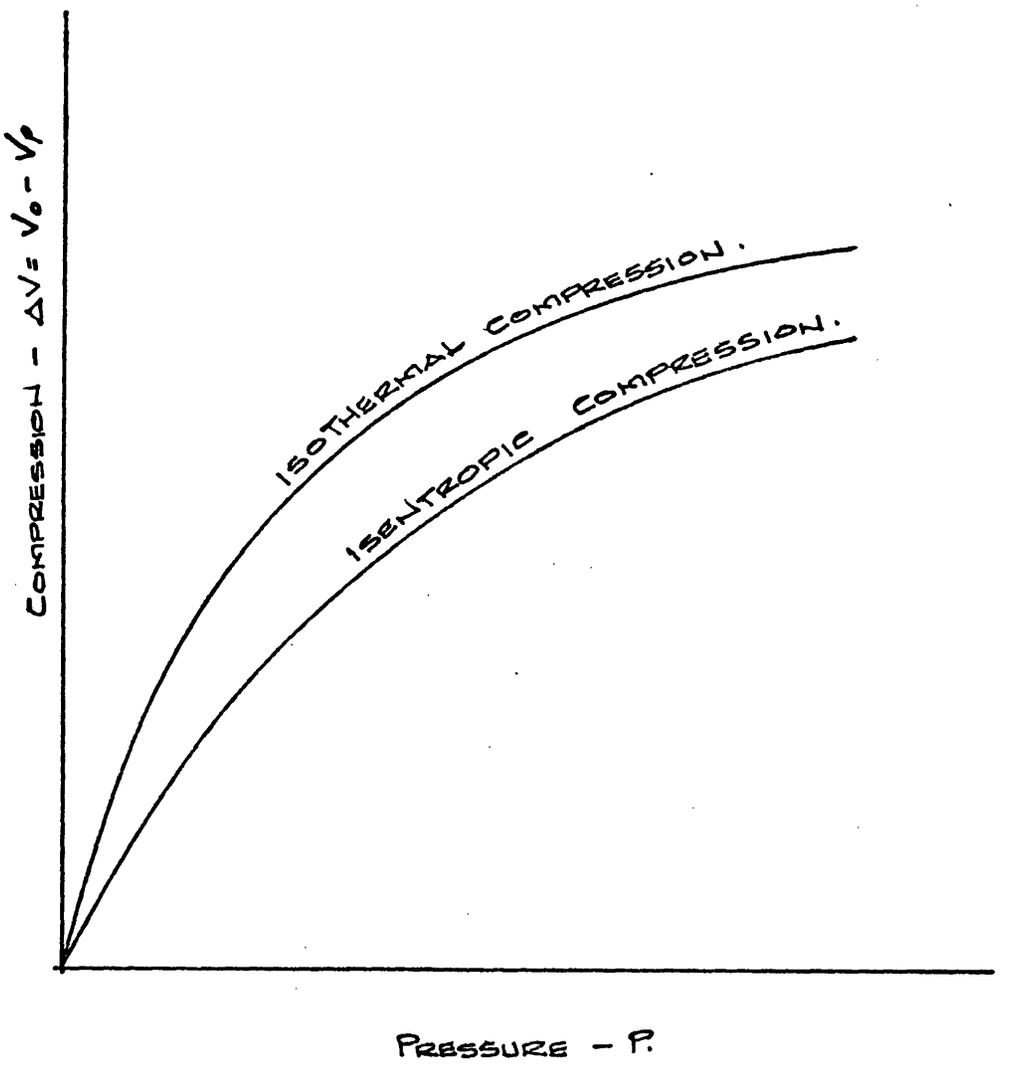

Fig. 4.1 ISOTHERMAL AND ISENTROPIC OIL COMPRESSION CURVES

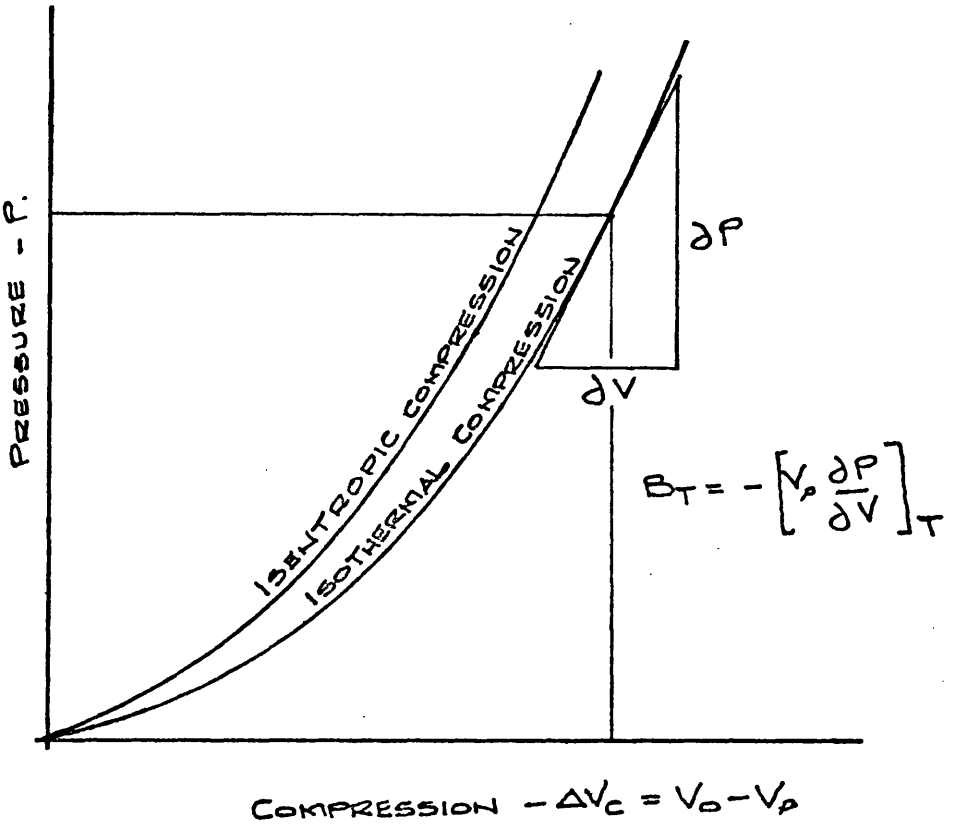

FIG. 4.2(a) ISOTHERMAL TANGENT BULK MODULUS.

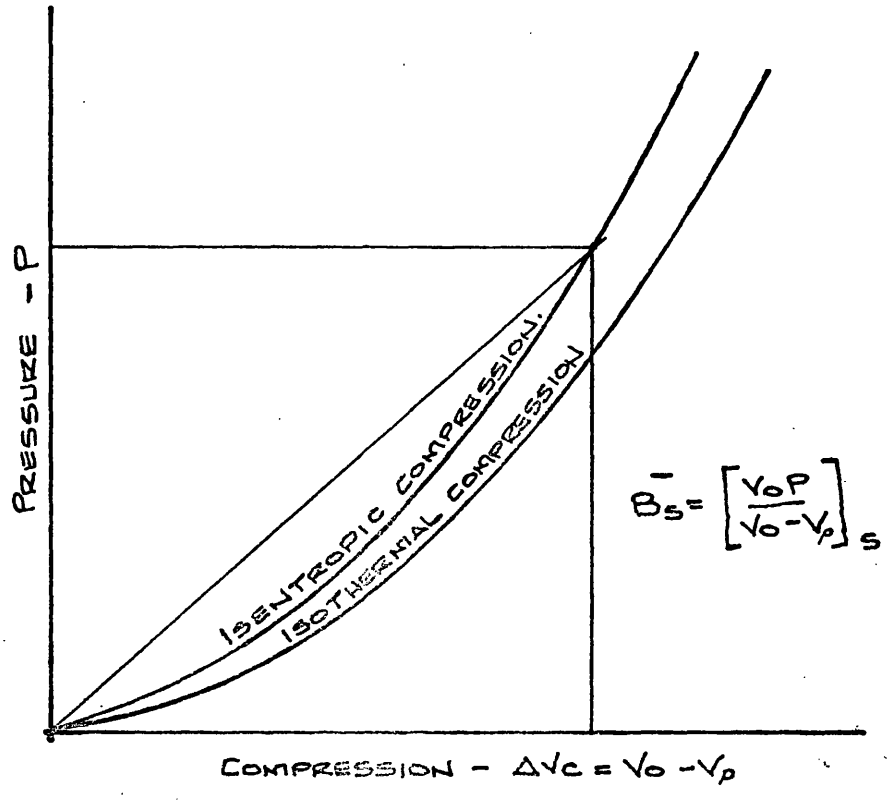

FIG. 4.2(b) ISENTROPIC SECANT BULK MODULUS.

FIG. 4.2 GRAPHICAL REPRESENTATION OF TANGENT AND SECANT BULK MODULUS.

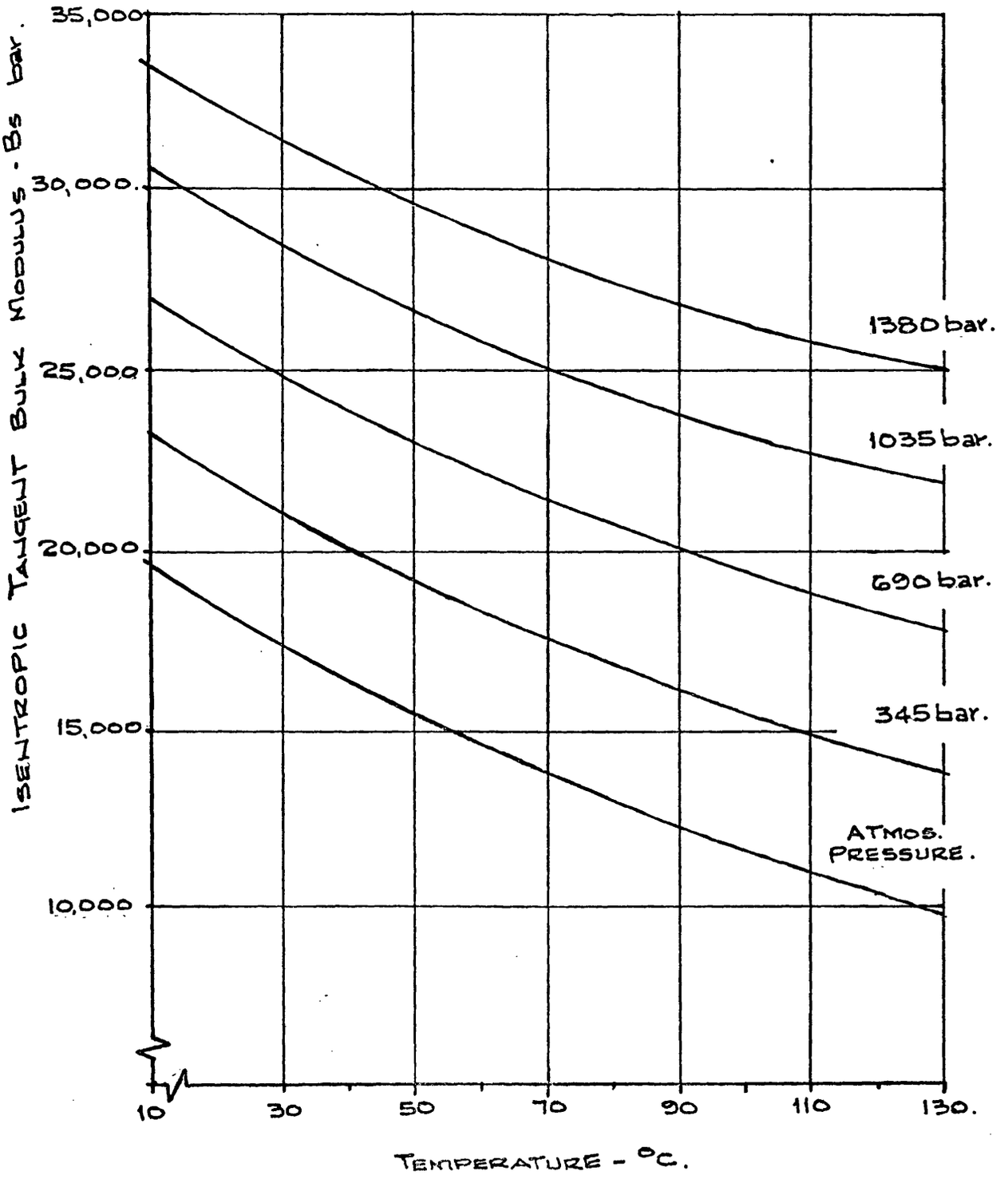

FIG. 4.3 ISENTROPIC TANGENT BULK MODULUS.

AGAINST TEMPERATURE AND PRESSURE FOR

SHELL TELLUS OIL 27.

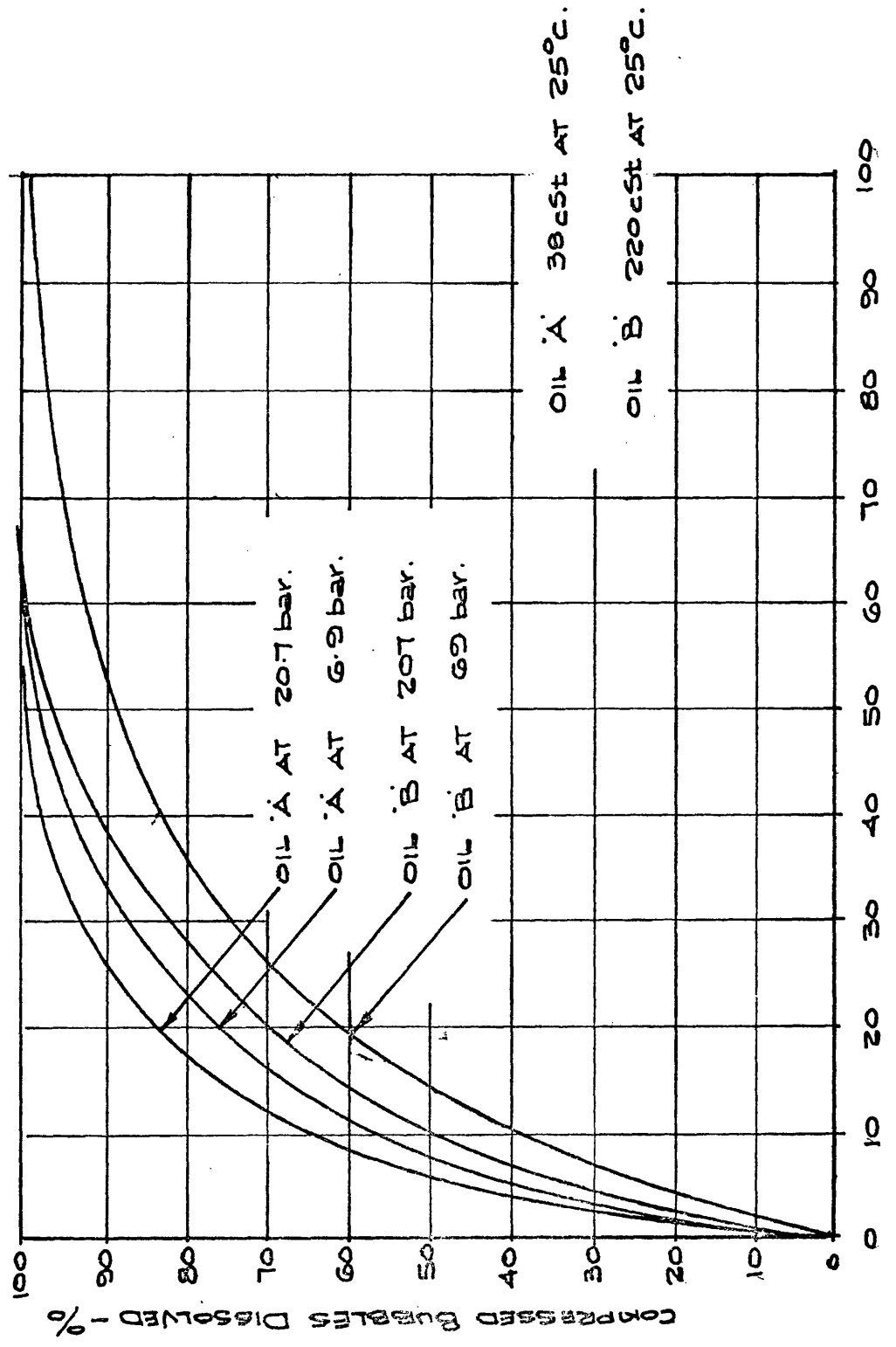

FIG. 4.4 RATE OF SOLUTION OF AIR BUBBLES IN MINERAL OIL

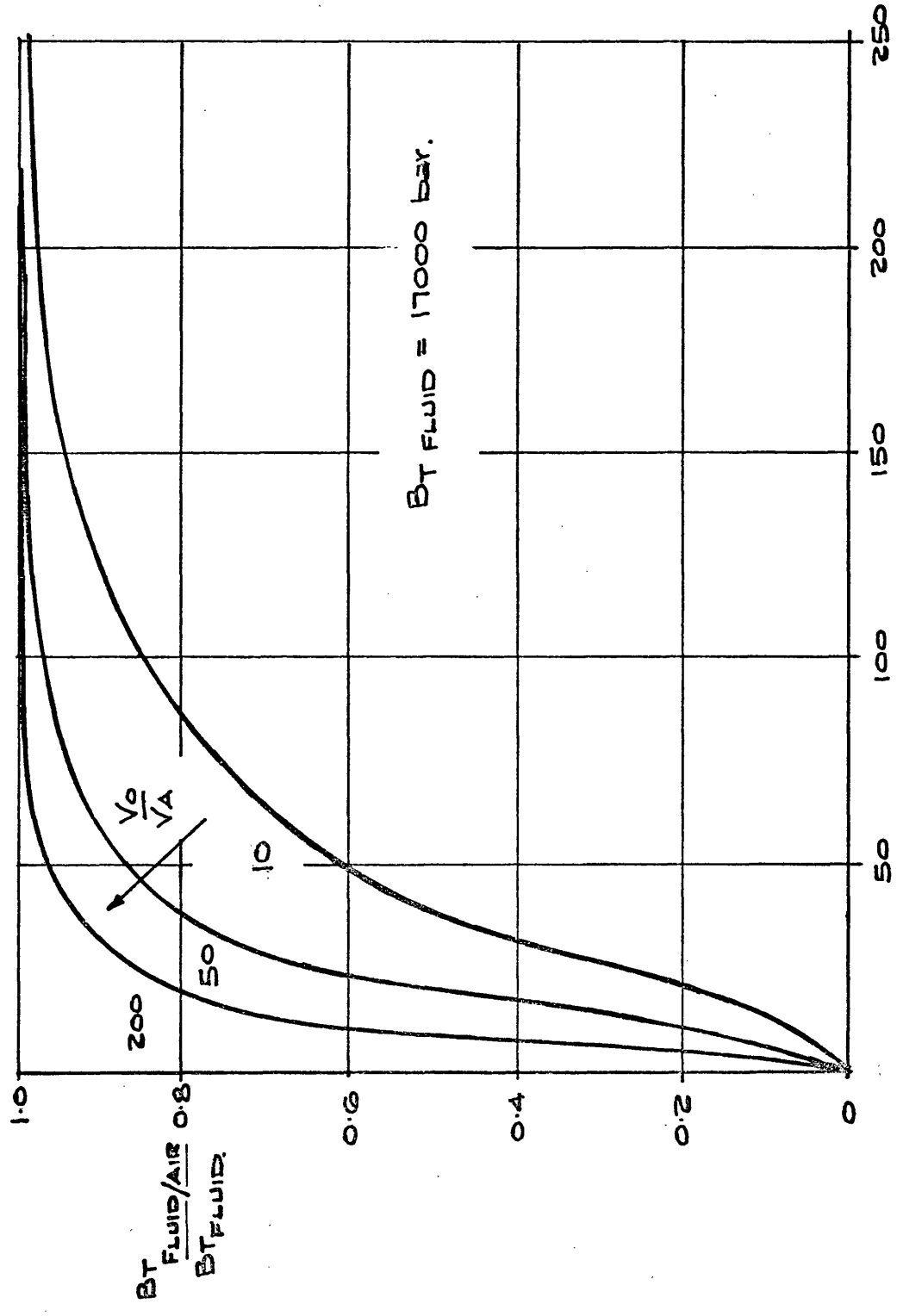

FIG. 4.5 EFFECT OF AERATION ON THE BULK MODULUS OF HYDRAULIC OIL.

CHAPTER 5 : HYDROSTATIC TRANSMISSION TEST RIG and EXPERIMENTAL TECHNIQUES for MEASURING DYNAMIC RESPONSE

5.1 Elements of Hydrostatic Transmission Test Rig

The diagramatic layout of the hydrostatic transmission test rig is shown in Fig. 5.1, and a photograph showing the configuration of the basic elements prior to installation in the test cell facility is shown in Fig. 5.2. The major components of the rig were as follows:

1. A hydrostatic transmission comprising a 3.25 in^3/rev. Downel variable delivery axial piston pump and a similar motor coupled together in a closed loop configuration.

2. A 43 B.H.P. Perkins three cylinder diesel engine prime mover.

3. A variable delivery pressure compensated axial piston pump delivering through a variety of valves to provide hydrostatic load simulation.

A detailed consideration of the various elements of the transmission rig follows, and the methods by which it was used to measure the dynamic response of the transmission under test.

However, a summary of the mechanical equipment, instrumentation and measuring equipment is given in Tables 5.1, 5.2, and 5.3, respectively.

The test rig was designed and built with two essential features in mind.

1. All ancillaries such as servo oil supply and other services were supplied externally to the transmission, load, and prime mover. This was to ensure that no interaction between the various elements might occur other than those due to the inherent characteristics of the transmission.

2. Care was taken to maintain as far as possible the rigidity between the various elements of the transmission by reducing to a minimum shaft flexibility and coupling backlash.

5.2 Selection of Hydrostatic Pump and Motor

The selection of variable displacement hydrostatic pumps and motors to form the principle elements of the hydrostatic transmission was made to provide units most suitable for testwork rather than for any particular application.

The main criterion were that the units should be capable of easy mounting, mechanically as simple as possible, enable external means of varying the displacement to be employed, and capable of being instrumented. The pump was to be driven in line by a 43 B.H.P. diesel engine of maximum rated speed 2400 rev/min, and for compatibility of instrumentation it was decided to use a motor in the medium speed range. The use of axial piston machines was felt to be desirable as these are the most common variable displacement units in use.

A choice was made of Downel variable displacement units of maximum displacement 3.25 in^3/rev. These robust swash plate units, a sectional view of which is shown in Fig. 5.3, are based on a design originated by the National Engineering Laboratory in the early sixties, aimed at producing a range of low cost quiet pumps and motors. The units obtained were readily available and standard except for a minor modification made to the Downel motor. In order to measure the speed of the motor a dummy shaft was fitted to the rear of the motor, between the inlet and outlet ports, a small seal housing having been fitted.

Fig. 5.3 shows that the units comprised a cast iron casing in which a cylinder barrel shrunk onto a drive shaft was mounted between two journal bearings.

The cylinder barrel incorporated nine equally spaced axial pistons each having a ball mounted swivelling slipper, the nine slippers being held against the inclined swash plate by a retaining spider loaded by a central spring. The swash plate is supported between two needle roller bearings with a control shaft for adjusting the angle of the swash plate extending through the side of the unit. The ported end of the cylinder barrel bears against a hydrostatically balanced port or timing plate which communicates fluid in the cylinder bores with either the inlet or outlet ports. Lubrication is provided for the journal bearings by forced feed from the pump outlet. The pump is unidirectional, but the motor rotation is fully reversible. Flow reversal can be achieved on both units as the swash plate angle can be positive or negative.

5.2.1 Hydrostatic Pump and Motor Swash Servos

Many units now incorporate a control servo deriving the servo high pressure oil supply from the output of the unit itself. For the purposes of dynamic test work it was important that the servo should be an element entirely separate from the transmission so that there would be no interaction with the units. There was a second important requirement of the servo and that was that it could be fed with electrical input signals to provide for dynamic measurement.

The pump and motor manufacturer's properietory unit although satisfying the first requirement in that it required an external minimum pressure 17.2 bar (250 lbf/in^2) oil supply, was a mechanical power amplification device that was not capable of receiving an electrical input. The frequency response of the servo at a supply pressure of 208 bar (3,000 lbf/in^2) approximated to a first order lag with a time constant of 0.01s, but the time constant reduced considerably with decrease in supply pressure. A disadvantage of the proprietory servo was that it made direct measurement of swash plate angle difficult. Therefore it was decided that although the proprietory unit could be fitted with an electro-mechanical actuator and just comply with frequency response requirements, it would be more advantageous to design and build two special purpose electro-hydraulic servos. These consisted of trunion mounted actuators mounted in a bracket. Servo control was achieved by a Dowty Moog valve, series 21, mounted on the actuator as can be clearly seen in Fig. 5.4. The design and detailed construction of the servos is given in Appendix II.

Measurement of swash plate angle was carried out by rotary indictive transducers mounted directly on the trunion arm.

5.3 Hydraulic Circuit of the Closed Loop Hydrostatic Transmission

As previously described it had been decided that the hydrostatic transmission should comprise the Downel hydrostatic pumps and motors coupled together in a closed loop.

A conventional hydraulic circuit of the type shown in Fig. 5.5 was to be used, and standard one inch internal diameter rigid steel pipe used for the main loop. This would ensure a maximum fluid speed of 3.7 m/s. (12 ft/sec.) when the pump was on full delivery rotating at 2,000 rev/min. The overall pipe length for the transmission of high pressure oil between the pump and the motor was 1.38 m. (4.5 ft.).

The boost system shown in Fig. 5.5 is typical of the systems adopted for hydrostatic transmissions, and very often these systems form an integral part of either the pump or motor unit and in some cases a combination of the two. It is common to find either a gear or gerotor unit linked to the main drive shaft of the pump to provide the boost flow and the necessary valves mounted in a single block coupled to the timing plate of the pump or motor. The unit used for this rig was one such assembly, mounted on a special plate to enable pipework to be connected. It should be noted that the servo relief valve was removed. A sectional view of the block is shown in Fig. 5.6. The boost pump was a gear pump driven by an induction motor at 1,460 rev/min. delivering 4.5 litre/min. (1.00 gal/min.). This was equal to 6% of the main pump maximum capacity.

For reasons that will be explained in Chapter 6 it was found that during frequency response testing, the boost system described above was not able to maintain a steady boost pressure.

A series of calibrations were carried out to investigate the boost system performance.

As there was a variation of flow to the system during dynamic tests this would cause the flow through the boost pressure relief valve to vary. It was therefore necessary to investigate the pressure flow characteristic of the relief valve. The results of this test are shown in the plot of Fig. 5.7. It was clear from this that the valve had an undesirably steep pressure flow characteristic.

Secondly, during some tests it became apparent that at peak pressures galvanometer recordings of the variation in pressure during frequency response tests showed a cut off indicating that the cross line relief valves were opening despite the use of springs rated at 208 bar (3,000 lbf/in.^{2}) well above the maximum pressure being experienced. A pressure flow test was carried out on the cross line relief valve being subjected to high pressure and the results are shown in Fig. 5.8. The figures showed clearly that the valve was beginning to crack at 138 bar (2,000 lbf/in.^{2}), far below the expected value, and in addition the valve was failing to seat properly.

A sample calculation was carried out on the boost pressure relief valve to ensure its response was sufficient to cope with the transient pressures likely to be experienced.

Calibration of the valve spring gave a stiffness of 46,400 N/m (3190 lbf/ft.), and the valve poppet mass was 0.0739 Kg. (0.0334 lbs). This gave a natural frequency of 1761 rad/s. Since the maximum test frequency used was 20 Hz the valve dynamic response was quite adequate for the application, and would not lead to any resonances as a result of frequency response testing.

5.3.1 Improved Boost System

To overcome the difficulties experienced with the proprietory valve block described in the previous section an improved boost system was developed in the following way.

To provide for the maximum flow demands being made upon the boost system during frequency response testing, a 22.6 litre/min. (5.0 gal/min.) nominal delivery gear pump was used. This capacity was equivalent to 30% of the main pump maximum capacity. However, the increase in flow necessitated the use of a boost system relief valve capable of passing the large quantity of excess flow in the steady state condition.

To obtain the required improvement the standard relief valve block was removed and replaced by the simplified circuit shown in Fig. 5.9. The circuit protection high pressure relief valves were not included, to remove any possibility of cross line leakage.

The removal of the ball and spring non-return valves meant that the circuit was no longer reversible, having one line as the high pressure supply, whilst the other was continuously connected to the boost system. However, this was not a significant penalty as the rig instrumentation and load pump did not permit a reversal of the rotation of the motor shaft.

To maintain a constant return line pressure it was necessary to obtain a relief valve with as flat a pressure flow characteristic as possible. This was achieved using a two stage relief valve of the type shown in Fig. 5.10. As the pressure at the valve rises to the relief valve setting the pilot valve cracks causing a bleed flow to tank down the centre of the piston. This bleed flow causes a pressure drop across the piston restriction sufficient to lift it against a light spring and flow forces, dumping the main flow to tank. However, to raise the piston further and increase the flow to tank requires an increase in the bleed flow that can only be obtained by an increased pressure acting on the piston. Therefore this type of two stage relief valve has a pressure flow curve with a significant positive slope.

By the addition of an unloader plunger of the type shown it is possible to reduce the slope of the pressure flow characteristic of the valve. As the diameter of the plunger increases so the slope of the pressure flow characteristic of the valve becomes negative causing it to be unstable and act as an unloader valve.

It is often found that proprietory valves sold as unloaders just border on the edge of instability and if carefully chosen can provide a valve with a slightly positive pressure flow characteristic. One such valve was obtained and the pressure flow characteristic measured. The results are shown on Fig. 5.11, and it can be appreciated that despite the positive slope this valve gave a much better characteristic than the poppet in the valve block used for the conventional boost system.

5.3.2 System Filtration

As the hydrostatic transmission test rig was assembled under laboratory conditions, it was decided that a full flow filter would not be included in the main loop during the rig running in period as the additional expense would not warrant its use. However, for both the conventional and improved boost system the flow from the boost pump was passed through a paper element 50 l/min. (11 gal/min.) 10 micron pressure filter between the pump and the main loop. After any instance where it was found necessary to break the main loop of the transmission circuit fluid was bled from the main loop back to tank to permit circulation and filtration of the fluid.

5.4 The Prime Mover

The prime mover used for driving the hydrostatic transmission was a three cylinder four-stroke diesel engine of 2,500 cm^3 capacity developing a maximum of 32.1 Kw. (43 B.H.P.) at 2.400 rev/min. This was the basic unit rigidly mounted that had been used for a detailed research programme carried out by Bowns (56) to investigate the transfer characteristics reciprocating engines. The experimental work associated with this programme had required that frequency response tests be carried out on the engine and to permit this the conventional engine governor had been removed and replaced by an electro-hydraulic governor.

The provision of an electro-hydraulic governor makes the diesel engine a very versatile prime mover. Firstly it is possible to control the speed of the engine at all points in its operating range (800-2400 rev/min), and secondly because of the type of governing provided it is possible to vary the sensitivity of the engine speed to load changes by adjusting the governor loop. This made the engine ideal for driving a hydrostatic transmission where it was required to measure the effect of the prime mover characteristic upon the overall transmission response.

5.4.1 Electro-Hydraulic Governing of Diesel Engine /

5.4.1 Electro-Hydraulic Governing of Diesel Engine

Fig. 5.12 shows a simplified block diagram for the electro-hydraulic governor relating changes in speed of the reciprocating engine to changes in load torque. It has been assumed that the delays in developed engine torque following a change in fuel rack position are relatively insignificant.

Consider first the electro-hydraulic position control servo on the engine fuel rack. Fig. 5.13 shows the mounting of the electro-hydraulic servo valve, actuator displacement feedback transducer, and fuel rack, along with the block diagram and resulting transfer function. Substitution of values into the transfer function gave a time constant for the servo used of 0.003 secs. The response of the servo is a first order lag which has an attenuation of $^{1}/K_{F}$.

The transfer function of the position control servo is shown as part of governor block diagram on Fig. 5.14. The time constant of engine and load $\frac{J_1}{f_E}$ is of the order of seconds and is large enough to make the response of the position control servo negligible. The overall response of the governor and engine is therefore given approximately by the transfer function

$$\frac{t_p}{\omega_1} = \frac{1}{(f_E + \frac{K_E K_T}{K_F}) + J_1 S} \qquad - 5.1$$

In the steady state the load torque speed characteristic of the engine can be controlled by varying the governor parameters K_T or K_F. It was found most convenient to place a potentiometer on the output from the speed feedback tachogenerator thereby varying K_T.

Typical speed load characteristics of the diesel engine with variable feedback eletro-hydraulic speed governing are shown in Fig. 5.15. Six different characteristics have been selected from the experimental measurements made whilst testing the hydrostatic transmission covering a wide range of engine speed load droops 0.057 - 3.200 Rad/s/Nm. (0.042 - 2.360 Rad/s /lbf ft.). The droop has been evaluated as the percentage change in speed, about a mean speed of 1,200 rev/min. between no load and full load, and for the range of droops given is 4 - 212 %. The characteristics have not been presented about the same operating torque at 1,200 rev/min, but are a range of load torques measured during transmission testing.

5.4.2 Installation of Diesel Engine

There were several significant features about the installation of the diesel engine that should be pointed out. In order to prevent any flexibility between the prime mover and the hydrostatic pump both were mounted in a rigid steel frame and then the whole mounted on anti-vibration material.

To prevent any influence of ancillaries normally found on diesel engines from affecting the performance of the engine, these had all been removed. Therefore in the absence of such things as a dynamo, fan belt and radiator, and fuel pump it was necessary to provide an external means of charging a battery for starting, a laboratory supply of cooling water, and a gravity fuel feed. A safety device for stopping the engine in the event of a governor failure was provided in the form of a remote operation valve lift.

5.5 Load Simulation

The hydrostatic transmission was loaded by connecting a hydrostatic loading pump to the transmission motor output shaft, and loading the output from this pump with suitable loading valves. This method provides a very versatile answer to the problem of speed dependant load simulation although several limitations were encountered.

Simulation of coulomb, viscous, windage torque and constant horsepower loads was achieved, and in addition inertial loads could be provided by securing a flywheel to the transmission output shaft either in addition to, or in place of, the hydrostatic loading pump. Different size flywheels were used and their inertias determined by run down tests carried out between centres.

The hydrostatic loading circuit employed did not permit flow reversal and care had to be taken to ensure that no reversal of the motor rotation took place during dynamic testing.

A 38.5 cm^3/rev. (2.35 in^3/rev.) axial piston pump originally developed for use with aircraft ground equipment, and incorporating variable delivery and pressure compensation, was used. Fig. 5.16 shows a schematic of the pump which was of the tilting head design. The method by which swash control and pressure compensation overide was achieved can be seen. An outline specification for the pump is also given.

The inlet to the pump was connected to a reservoir with several feet of positive head by a large bore pipe and the outlet fed directly into a pilot operated pressure relief valve and needle valve connected in series. Initial work using hydrostatic load simulation for dynamic testing had shown clearly the need for removing the compressibility effect of the oil trapped between the pump and the loading valve by reducing the trapped volume to a minimum and maintaining the distance between the pump and valve as short as possible. Calculation of the time constant of the first order lag due to the compressible oil column introduced into the transfer function relating load pressure and flow in loading circuit gave a value of 0.000556 secs for the oil column used. This represents a break point of 300 Hz.

The circuit diagram for the load pump is shown in Fig. 5.1. Return line filtration and an oil cooler to dissipate the lost power were employed.

5.5.1 Coulomb Friction plus Viscous Load Torque Simulation

The output from the loading pump was connected to a pilot operated pressure relief valve having a typical pressure flow characteristic as shown in Fig. 5.17(a). This enabled a load torque that varied linearly with speed changes to be simulated. Considering the ideal flow and pressure relationships for the load pump:

The output flow from the load pump is given by:

$$Q_{LP} = D_{LP1} X_{LP} \Omega_2 \qquad - 5.2$$

The torque required to drive the load pump is:

$$T_{LP} = D_{LP1} X_{LP} P_{LP} \qquad - 5.3$$

Fig 5.17(a) shows a straight line fitted to the pressure flow characteristic of the relief valve at an operating point on the linear portion of the characteristic. This straight line can be given by:

$$P_{RV} = C_{RV} + K_{RV} Q_{RV} \qquad - 5.4$$

Assuming incompressible oil between the load pump and loading valves:

$$Q_{LP} = Q_{RV}$$

and

$$P_{LP} = P_{RV}$$

Therefore combining Equ.s 5.2, 5.3, and 5.4:

$$T_{LP} = D_{LP1} C_{RV} + K_{RV} D_{LP1} X_{LP} \Omega_2 \quad - 5.5$$

The load torque therefore comprises a constant or coulomb value plus a component proportional to speed usually termed viscous load.

5.5.2 Windage Load Simulation

From the previous section it was determined that the characteristic of the load simulation depended upon the characteristic of the loading valve. As the square law relationship for flow through an orifice is similar to that of a typical square law windage load this type of load was simulated using a needle valve the typical characteristics for which are shown in Fig. 5.17(b). Initially it was deduced that in order to increase the slope of the windage load all that would be necessary would be to reduce the swash of the load pump thereby moving to a steeper characteristic orifice as shown.

However if this assumption is considered more closely, the pressure drop due to flow through a needle valve can be given by

$$P_{NV} = K \frac{Q_{NV}^2}{a_{NV}^2} \qquad - 5.6$$

where a_{NV}^2 is a value depending upon the needle valve opening

$$\frac{dP_{NV}}{dQ_{NV}} = 2 \frac{K}{a_{NV}^2} Q_{NV} \qquad - 5.7$$

Again assuming

$$Q_{LP} = Q_{NV}$$

and

$$P_{LP} = P_{RV}$$

the torque speed relationship is

$$\frac{t_L}{\omega_2} = (D_{LP1} X_{LP})^2 \frac{2KQ_{NV}}{a_{NV}^2} \qquad - 5.8$$

Now if it is required to maintain the mean load constant then

$$\frac{KQ_{NV}^2}{a_{NV}^2} D_{LP1} X_{LP} = \text{Constant} = K \qquad - 5.9$$

$$\therefore \frac{t_L}{\omega_2} = \frac{K}{\Omega_2}$$

Thus using the combination of a variable displacement pump and variable orifice it is not possible to obtain a variable slope load torque speed simulation whilst maintaining the same mean torque and load speed.

To achieve a variable slope load torque speed simulation it is necessary to employ the combination of a pilot operated pressure relief valve and needle valve in series. The use of the pressure relief valve enables a different needle setting to be used whilst still achieving the same mean load. Typical examples are shown on Fig. 5.18.

5.5.3 Constant Horsepower Loads

In order to achieve a constant horsepower loading of the transmission it is necessary to ensure that the power dissipated by the load pump is constant no matter what the pump speed. The power output of the pump is given by

$$= P_{LP} \quad Q_{LP} \qquad - 5.10$$

If the pressure compensation overide of the loading pump is employed this will ensure pump output pressure is maintained constant, and if fluid is passed through a fixed orifice and the pressure drop maintained constant a constant flow will be achieved.

As the pump speed increases the load pump output flow will be maintained level by a reduction in the pump swash.

The significance of constant horsepower loading is that it provides a decrease in load torque with speed making it a destabilising factor in any control system driving this type of load. However, it was found that when cyclic loads were applied over the test frequencies the pressure compensator would not respond satisfactorily and the load deviated from the characteristic measured under steady state conditions. For this reason dynamic testing of the hydrostatic transmission employing constant horsepower loading could not be satisfactorily undertaken using hydrostatic load simulation.

5.5.4 Experimental Determination of Simulated Load

The previous sections have outlined the different types of speed dependent load that could be simulated using the hydrostatic pump and loading valves. However, to determine the values of these loads the following experimental techniques were adopted.

The transmission was loaded to some steady state operating condition employing one of the techniques outlined in the previous section.

The speed of the transmission output shaft would then be varied about this mean condition and steady values of the load torque and speed recorded. Typical loads that have been simulated are shown in Fig. 5.19.

5.6 Instrumentation and Measuring Equipment

To provide for the measurement of dynamic changes in the hydrostatic transmission parameters it was necessary to instrument the transmission with electrical transducers. The frequencies of disturbances applied to the transmission and the subsequent responces of the various parameters under consideration were up to 20 Hz. However, the frequency of the pressure ripple generated by the nine piston axial piston unit was 450 Hz at a speed of 1,500 rpm. It was therefore decided to use inductive transducers driven by a carrier frequency of 3 KHz giving a handwidth of 1,000 Hz for pressure and displacement measurement. Strain gauge transducers were used for torque measurement which were recommended for use at frequencies up to approx. 2,000 Hz.

The inductive pressure transducers were fitted midway between the pump and motor units of the transmission to both the supply and return lines, and in addition a differential transducer fitted across the lines at this point.

The transducers were driven by a carrier amplifier integral with a demodulator unit termed an oscillator-demodulator.

The pump and motor swash angles were measured by rotorary A.C. pick-offs constructed with a soft iron slug rotating in the four arms of an inductive bridge. An oscillator demodulator unit was used similar to those used with the inductive pressure transducers, but wired to take the four arms of the A.C. pick-off bridge instead of the more common two arms employed by the pressure transducers. The small soft iron slug was coupled directly to the end of the trunnion shaft extending from the pump and motor units.

Speed measurement of the input and output shafts of the transmission was made with high quality D.C. tachogenerators especially developed to provide the feedback voltage to high impedance circuits. The tachogenerators were especially constructed to provide freedom from ripple, both brush ripple and the more difficult to remove low frequency 1 and $\frac{1}{2}$ cycle ripple due to the non-uniform field generated by the machine. However, these improvements were not obtained without making the units large in size with a relatively high armature inertia.

It was felt the poor correlation that was obtained from early dynamic testing could have resulted from the flexibility of the small shaft connecting the motor to this high inertia tachogenerator armature. A smaller less accurate transducer was fitted, but no measurable change determined.

The torque transducers incorporated a strain gauge rosette mounted on a reduced diameter shaft in the form of a bridge network. They were fed with 10 volts by dry cells through high quality slip rings and the output signal again obtained through slip rings amplified 100 times for signal correlation. To enable any system parameter to be measured quickly either for static or dynamic measurement, all the signals were brought to a common two pole switch.

In addition to the electronic instrumentation for dynamic measurement steady state instruments were incorporated. These included bourdon pressure gauges that could be shut off from the transmission during response testing, visual swash indication, impulse shaft speed counters, and mercury in steel temperature gauges. Full details of the instrumentation for both steady state and dynamic measurement is given in Table 5.2.

The development of digital equipment for frequency response testing has enabled the dynamic testing of systems to be carried out to higher accuracy and due to the reduced testing time in far greater depth. The Solartron Digital Transfer Function Analyser used for measuring the dynamic response of the transmission comprised two basic elements, a signal generator and a signal correlator. The correlator could measure the amplitude of the response of a system to a generated sine wave and the phase angle between the generated signal and its response.

An alternative method of response testing could have been the use of pseudo random binary sequences. This recently developed technique allows the impulse response of the system to be measured, which can be subsequently decomposed to obtain the frequency response. As yet this is not as familiar or direct a technique as frequency response testing and the results might be difficult to assess, particularly in the presence of non-linearities. Despite the advantages of the very small disturbances that need to be applied to a system using this technique, it was decided to remain with the more familiar frequency response technique.

In addition to the acquisition of digital response data for the system, an analogue signal was recorded using galvanometers recording on U - V paper. A detailed listing of the measuring equipment is shown in Table 5.3.

Unit	Type	Range & Capabilites	Type No. & Ser. No.
Hydrostatic Pump Hydrostatic Motor	Downel Variable Displacement Units Maximum Capacity 53.2 cm^3/rev. (3.25 in^3/rev.)	Maximum Speed - 1,500 rev/min. Max. Cont. Press. - 208 bar (3,000 lbf/in^2) Swash Angle - $\pm 15^o$ Rotation - Pump Clockwise/Motor Dual	Type: 3.25 B.438 Ser. No. H570 MkIA Type: 3.25 H381S Ser. No. H579 MkIA
Engine	Perkins 3.152 Industrial Diesel Fitted With Electro-Hydraulic Governor	3 Cylinder 2,500 cm^3 (152,7 in^3 capacity) Developing 26.1 Kw (35 BHP) continuous at 2,000 rev/min.	Engine No. 1129027H
Electro-Hydraulic Governor			
Servo Valve	Pegasus Industrial Servo Valve	Maximum Flow 82 cm^3/s. (5 in^3/rev.) Band Width - 100 Hz	Type No. 30.800.30.1000.3000 Ser. No. T.5786
Displacement Feedback	Pye Transducer & Fenlow Oscillator Demodulator	(0 - 3 ins.) 0 - 76 mm.	-
Actuator	Double Acting, Single Ended, End Bolt Mounting	Bore Dia. - 25.4 mm. (1.0 in.) Rod Dia. - 39.0 mm. (.325 in.)	-
Operational Amp.	Telehoist Valve Amp. & Power Supply	Maximum Current - 35 mA	Type: 4029
Load Pump	Vickers Pressure Compensated Axial Piston Pump - Maximum Capacity 38.5 cm^3/rev. (2.35 in^3/rev.)	Maximum Speed - 3,750 rev/min. Maximum Pressure - 345 bar (5,000 lbf/in^2) Maximum Tilt - 30^o	Type No. A12900R Ser. No. X446377

TABLE 5.1 EQUIPMENT USED ON HYDROSTATIC TRANSMISSION TEST RIG

Unit	Type	Range & Capabilities	Type No. & Ser. No.
Loading Valves			
Needle Valve	$\frac{1}{2}$ Inch Bore Standard Needle Valve	-	-
Pilot Operated Pressure Relief Valve	Keelavite Relief Valve	Maximum Flow - 136 l/min (30 gal/min.) Maximum Pressure - 345 bar (5,000 lbf/in^2)	Type No. VDV 0608 GT/ 4/1/5000 Ser. No. P6533 T8
Swash Servos	See Appendix II		
Boost System			
Small Boost Pump	Dowty Gear Pump	Nom. Capac. 4.54 l/min (1.0 gal/min.) at 1,500 rev/min.	Type: GRP 1T/10CT Ser No. CP/049/66/12
Large Boost Pump	Salami Gear Pump	Nom. Capac. 22.2 l/min. (4.9 gal/min.) at 1,500 rev/min.	Type: 2P 15 Ser No. 1200/40030/50
Transmission Valve	Vicker Racine Valve Block	Cross Line R/V Setting 208 bar (3,000 lbf/in^2) Boost Press. Setting Valve 6.9 bar (100 lbf/in^2)	Type: S5-71A
Unloader Valve	B & G Hydrocone Valve Based on Vickers Design	36.3 l/min. (8.0 gal/min.) Pressure Setting 3.45-690 bar (50-1000 lbf/in^2)	Type: BGRP 081.1 J
Boost Pump Motor	Newman 3-Phase Induction Motor	1.12 Kw (1.50 HP) 1,425 rev/min.	M. 9264

TABLE 5.1 CONT.

Unit	Type	Range & Capabilites	Type No. & Ser. No.
Filters			
Transmission Filter	Fairey Micro Filter Series 820	10 micron 50 l/min. (11 gal/min.)	Type No. 820A/2R/B/125
Servo Valve Filter	Fairey Micro Filter Series 525	2.5 micron 25 l/min. (5.5 gal/min.)	Type No. 525A/2L/B/4020T
Load Circuit Filter	Permanent Filter Corp.- Previously Used with Load Pump in Missile Trailer Application	Max.Press. 208 bar (3,000 lbf/in^2) 151 l/min. (34 gal/min.)	-
Accumulators	Greir Mercer Bag Type	Capacity - 1.12 litre (1 quart) Max.Press. 345 bar (5,000 lbf/in^2)	

TABLE 5.1 CONT.

Parameter To Be Measured	Equipment	Range	Calibration	Transducer Type and Serial No.
Pump Speed - Ω_1	(A.E.I. D.C. Tachogenerator (Inductive Pick-Up Coupled to Pulse Counter	0 → 4000 rev/min	0.1 volts/rev/min	Type: 8D 2510B
Motor Speed - Ω_2	(A.E.I. D.C. Tachogenerator	0 → 4000 rev/min	0.1 volts/rev/min	Type: 8D 2510B
	(Evershed & Vignal D.C. Tachogenerator	-	0.01 volts/rev/min	Type:FAD 102/94/8D
	(Used to Investigate Tacho Inertia Effect			Ser.No. 1689797
Pump Torque -Tp	)Saunders Roe Strain Gauge Torque	0 → 133.5 Nm	.0149 volts/Nm	Type: TT2/4CA
	)Transducers. Bridge Supplied By Accumulators	(0 → 100 lbf ft)	(.0199 volts/lbf ft)	Ser.No. S2/20704
Load Torque - T_L	)and Output Signal Amplified using Operational	0 → 133.5 Nm	.0147 volts/Nm	Type: TT2/4/CA
	)Amplifier	(0 → 100 lbf ft)	(.0197 volts/lbf ft)	Ser.No. S2/E/295
Supply Line Press - P_H	0 - 276 bar (0 - 4000 lbf/in^2)) Pressure Trans:	0 - 138 bar	.00515 volt/bar	SE Type 150D
	Bourdon Gauge) ducers listed in	(0 → 2000 lbf/in^2)	(.000356 volts/lbf/in^2)	Ser.No. 48562
Return Line Press - P_L	0 - 276 bar (0 - 4000 lbf/in^2)) conjunction with	0 - 34.5 bar	-.01020 volt/bar	NEP Type: 1028
	& 0 - 138 bar (0 - 200 lbf/in^2)) either S.E. or	(0 → 500 lbf/in^2)	(-.000704 volts/lbf/in^2)	Ser.No. C686/106
	Bourdon Gauges) Fenlow			
Differential Line Pressure - P_D	) Demodulator	0 - 276 bar	.00577 volt/bar	NEP Type: 1028
	) Units	(0 → 4000 lbf/in^2)	(.00003975 volts/lbf/in^2)	Ser.No. C686/18 3
Load Pressure	Bourdon Gauge	0 - 276 bar (0 → 4000 lbf/in^2)	-	-
Engine Oil Press	Bourdon Gauge	0 - 69 bar (0 → 100 lbf/in^2)	-	-
Pump Swash	)Graduated Visual Indicator and Elliot Rotary		- .110 volts/deg	Type: 400-2B-1
Motor Swash	)A.C. Pick-Off Coupled to Fenlow Demodulator Unit.		.113 volts/deg	Type: 4000-2B-1
Oil Temperature	Budenberg Mercury in Steel Thermometer	0 - 100°C	-	Ser.No. 163871
Oil Temperature Probe	Electronic Temperature Probe for Hydraulic Circuit Investigation	-	-	-

TABLE 5.2 HYDROSTATIC TRANSMISSION TEST RIG INSTRUMENTATION

Unit	Type		Parameter	Calibration	Type and Serial No.
Counter	Venner				TSA 3436
Digital Voltmeter	Advance DVM/1				Ser.No. 145
Dual Beam Oscillascope	Tektronix				Type 502
U - V Recorder	S.E. 12 Channel Type Galvanometers Listed for Five Channels in Use. (S.E. 3006/D2)	1.	Return Line Press		Type B450 Ser.No. 8/5606
		2.	Motor Speed		Type 900 Ser.No. S/913
		3.	Pump Swash		Type B160 Ser.No. S/7982
		4.	Differential Line Press		Type B450 Ser.No. 8/5360
		5.	Supply Line Pressure		Type B450 Ser.No. 9/1100
Transfer Function Analyser	Solatron Digital T.F.A. J.M. 1600				Ser.No. 173704

TABLE 5.3 MEASURING EQUIPMENT USED ON HYDROSTATIC TRANSMISSION TEST RIG

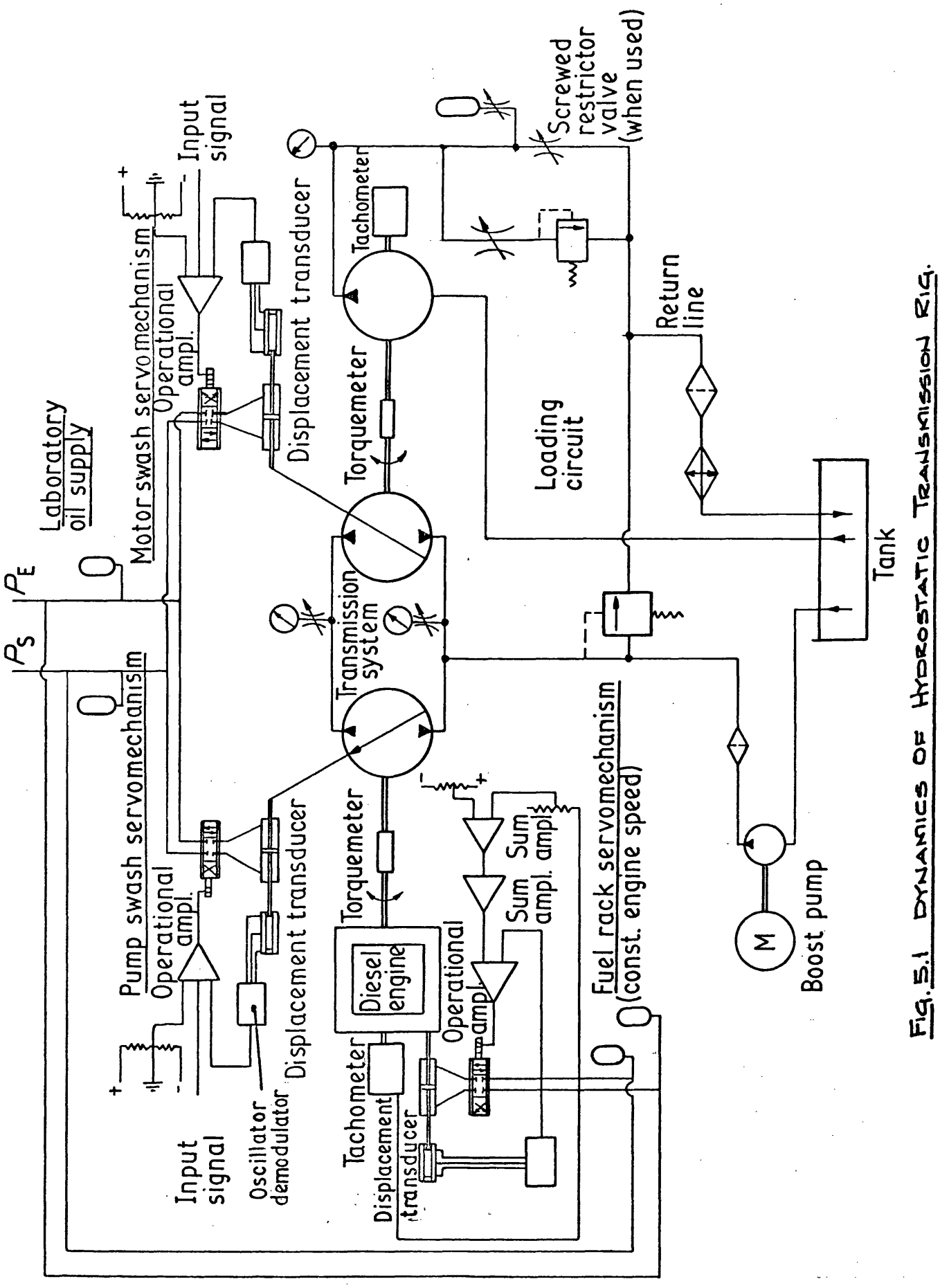

Fig. 5.1 DYNAMICS OF HYDROSTATIC TRANSMISSION RIG.

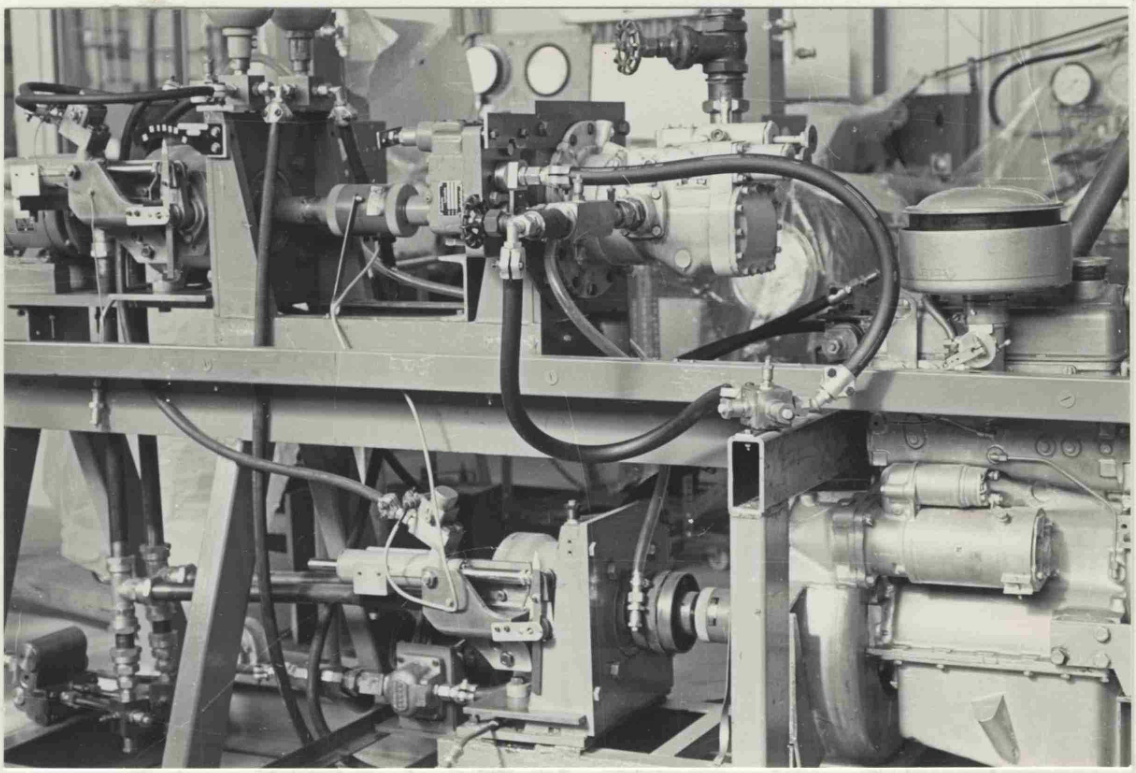

Fig. 5.2 LAYOUT OF ENGINE DRIVEN HYDROSTATIC TRANSMISSION AND LOAD PUMP

(The pumps and motor swash servos can be clearly seen)

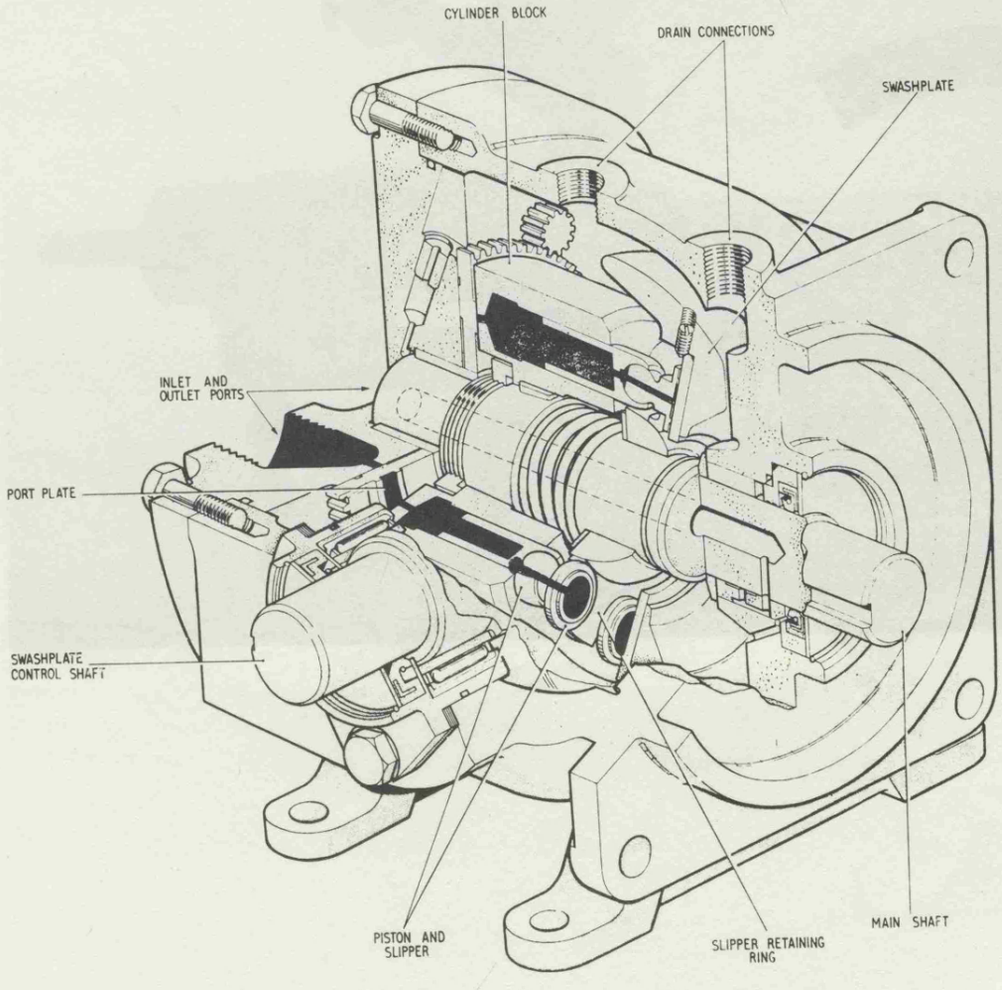

FIG. 5.3 SECTIONAL VIEW of DOWNEL VARIABLE DISPLACEMENT PUMP / MOTOR

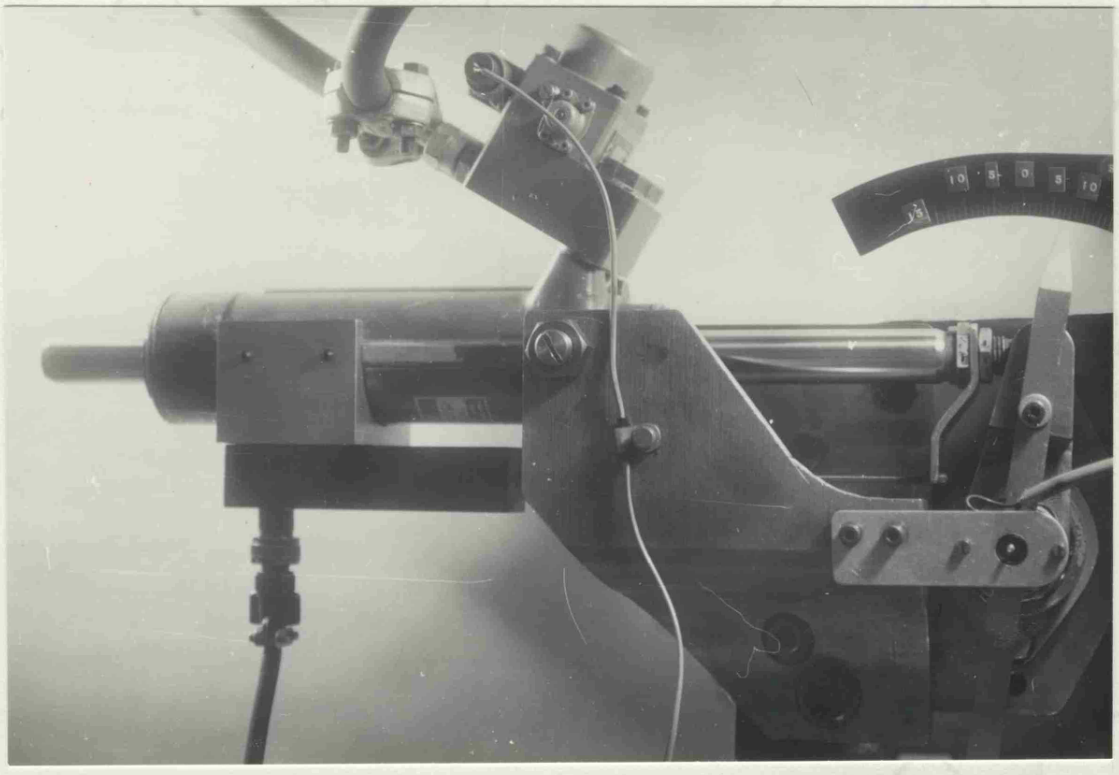

FIG. 5.4 PUMP AND MOTOR SWASH SERVOS

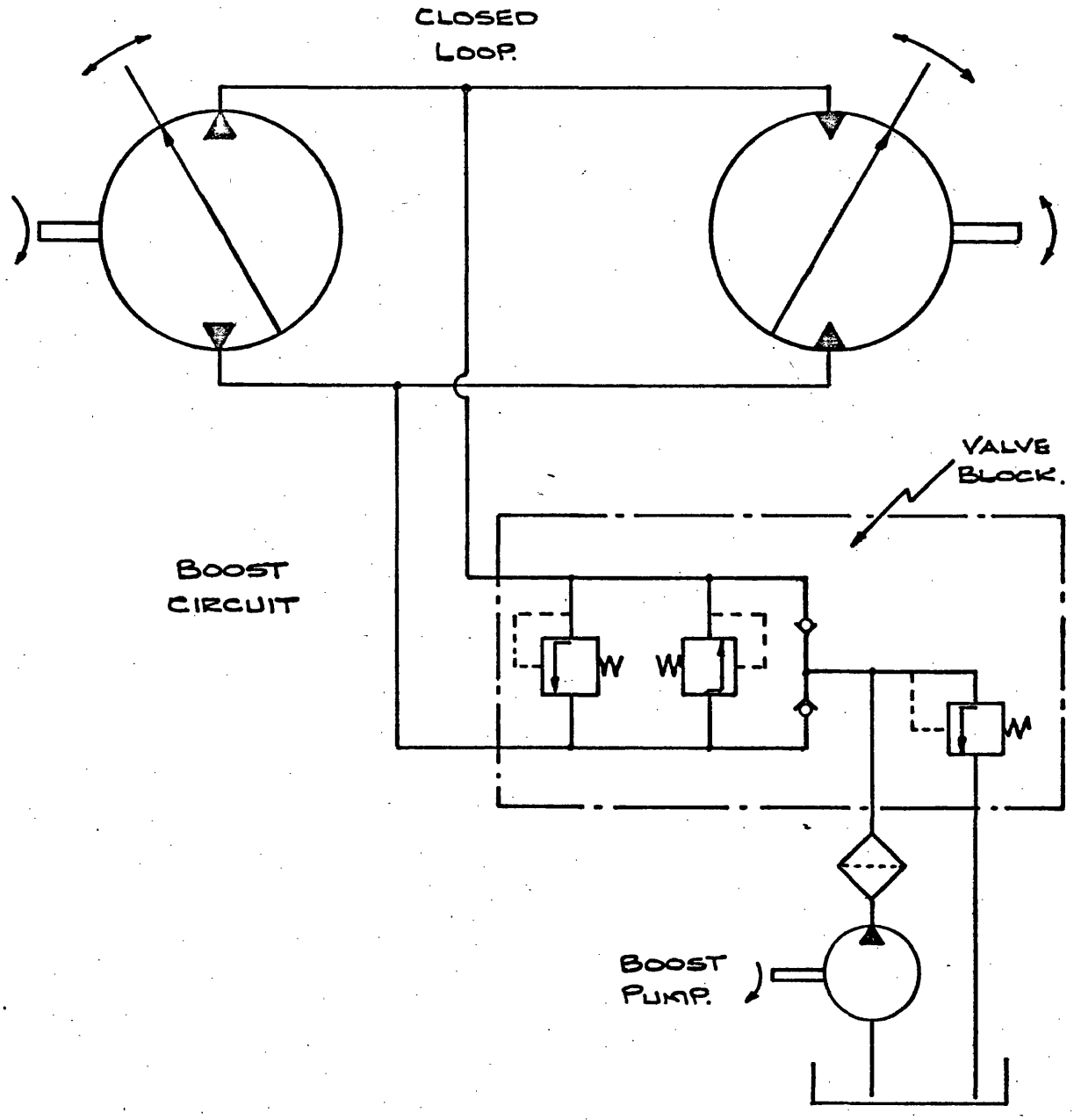

FIG. 5.5 CLOSED LOOP HYDROSTATIC TRANSMISSION CIRCUIT AND BOOST CIRCUIT.

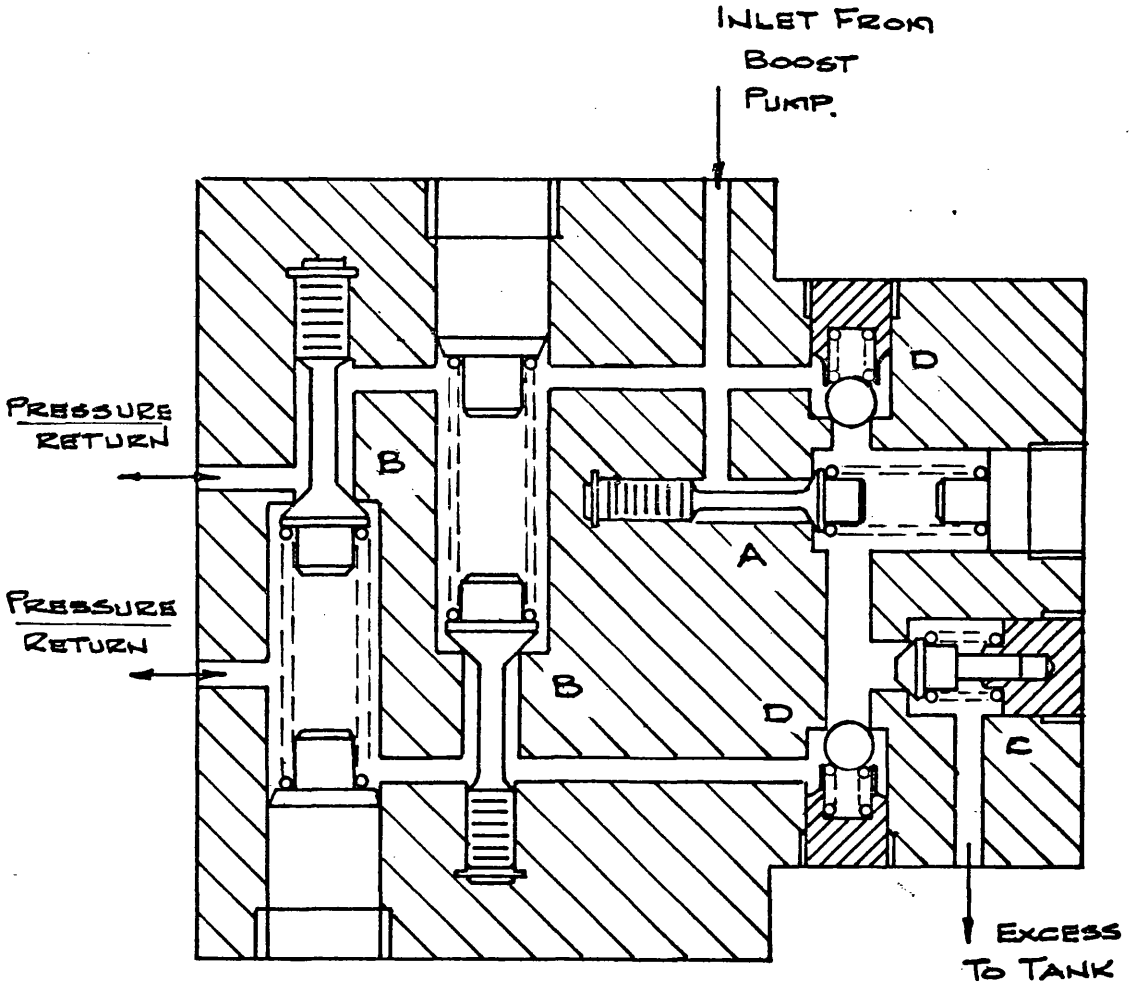

	VALVE	SETTING
A	SERVO PRESSURE VALVE	REMOVED
B	RELIEF VALVE	208 bar.
C	BOOST PRESSURE VALVE	7 bar Approx.
D	REPLENNISHING NON-RETURN VALVE.	———

FIG. 5.6 VALVE BLOCK FOR BOOST SYSTEM.

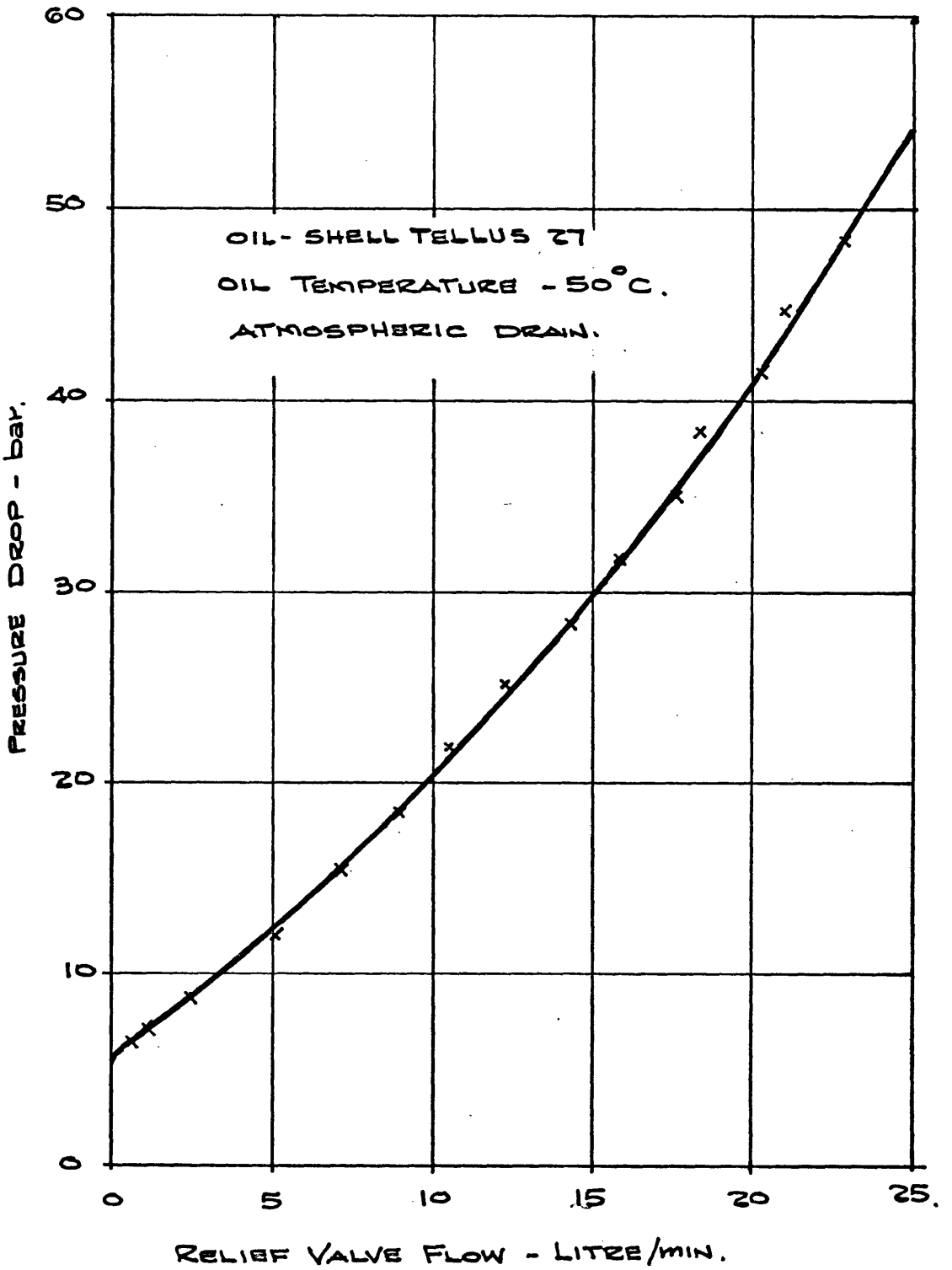

FIG. 5.7 PRESSURE / FLOW CHARACTERISTIC OF BOOST PRESSURE VALVE IN VALVE BLOCK.

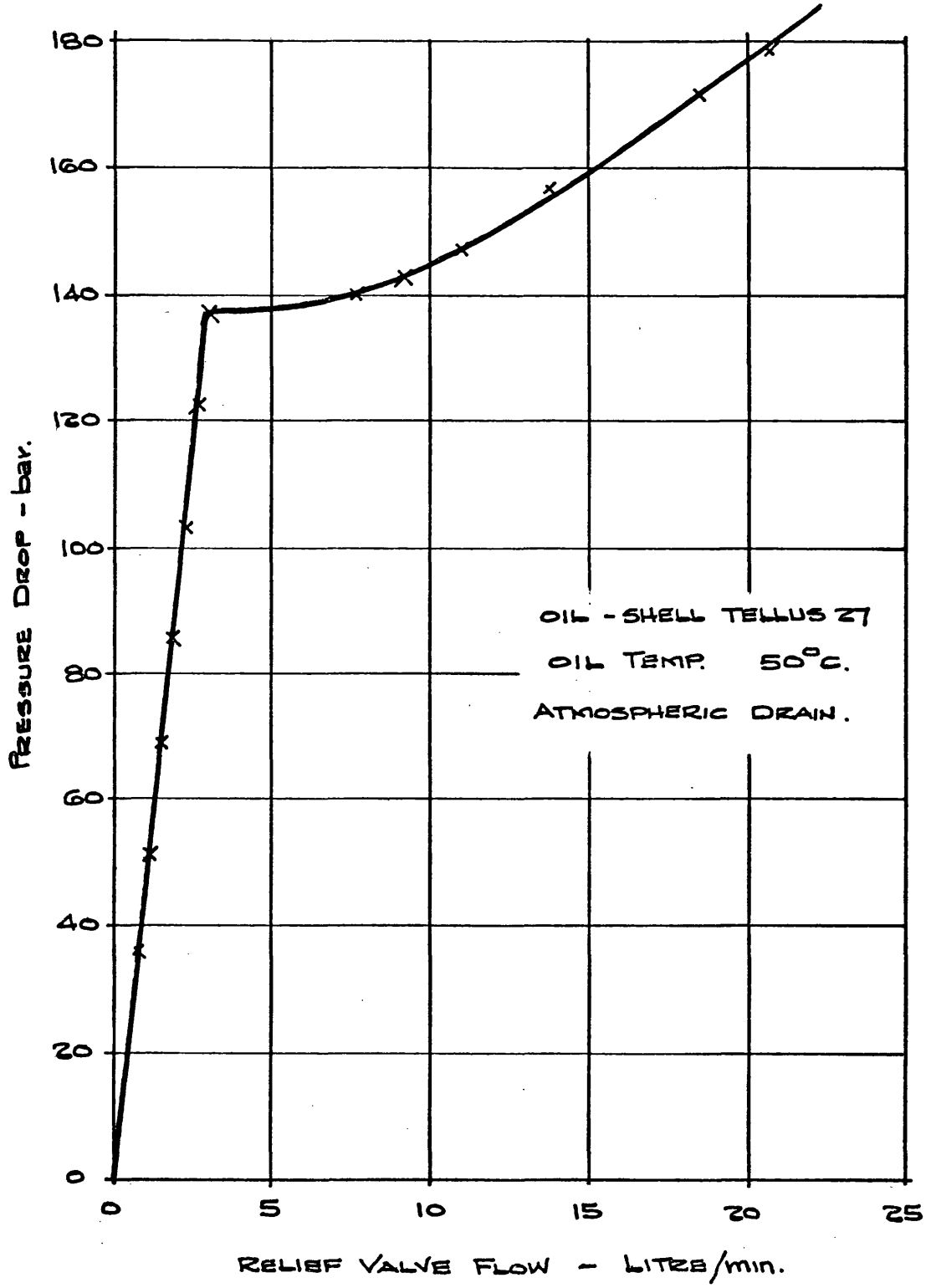

FIG. 5.8 PRESSURE - FLOW CHARACTERISTIC OF CROSS LINE HIGH PRESSURE RELIEF VALVE IN VALVE BLOCK.

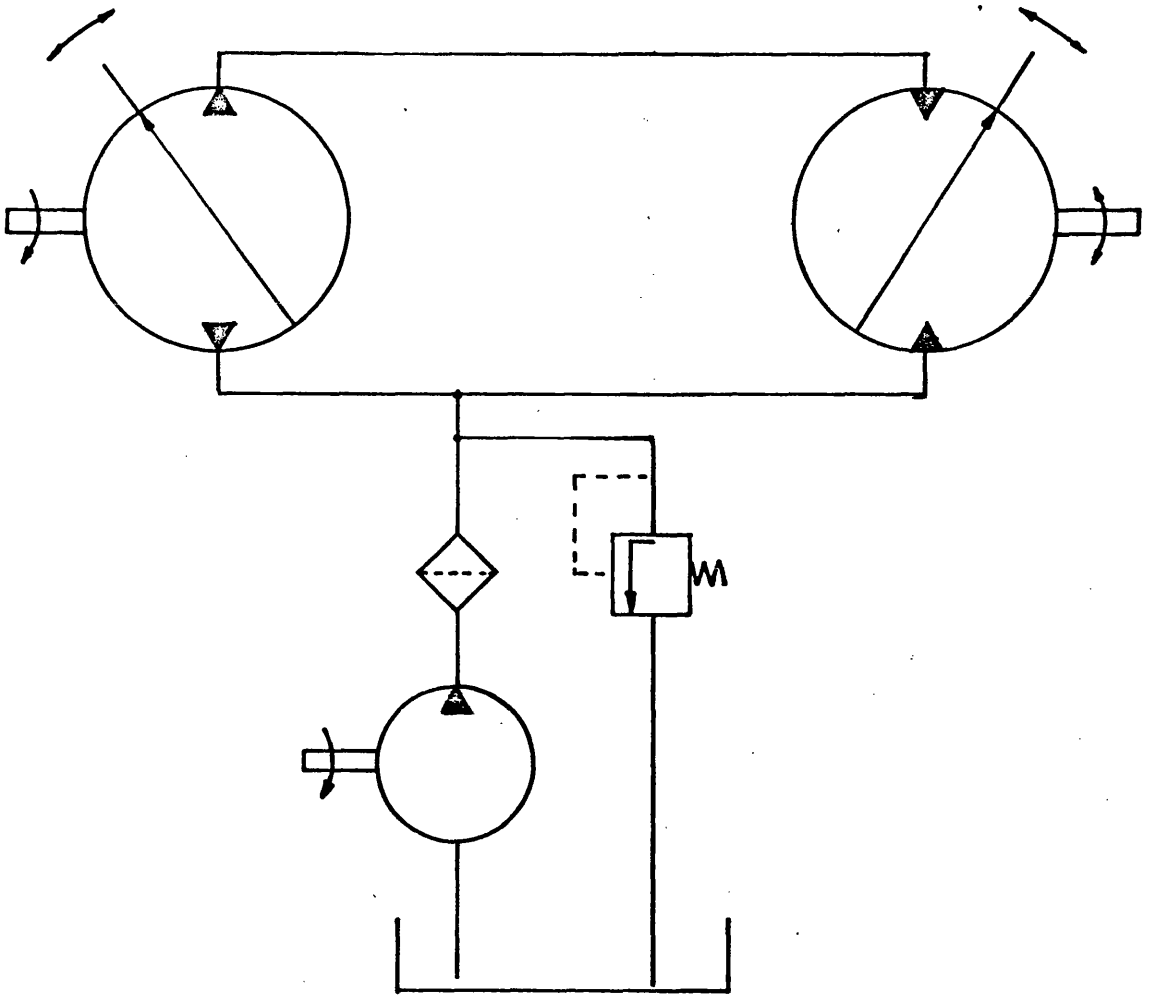

FIG. 5.9 CLOSED LOOP HYDROSTATIC TRANSMISSION CIRCUIT WITH SIMPLIFIED LARGE CAPACITY BOOST SYSTEM.

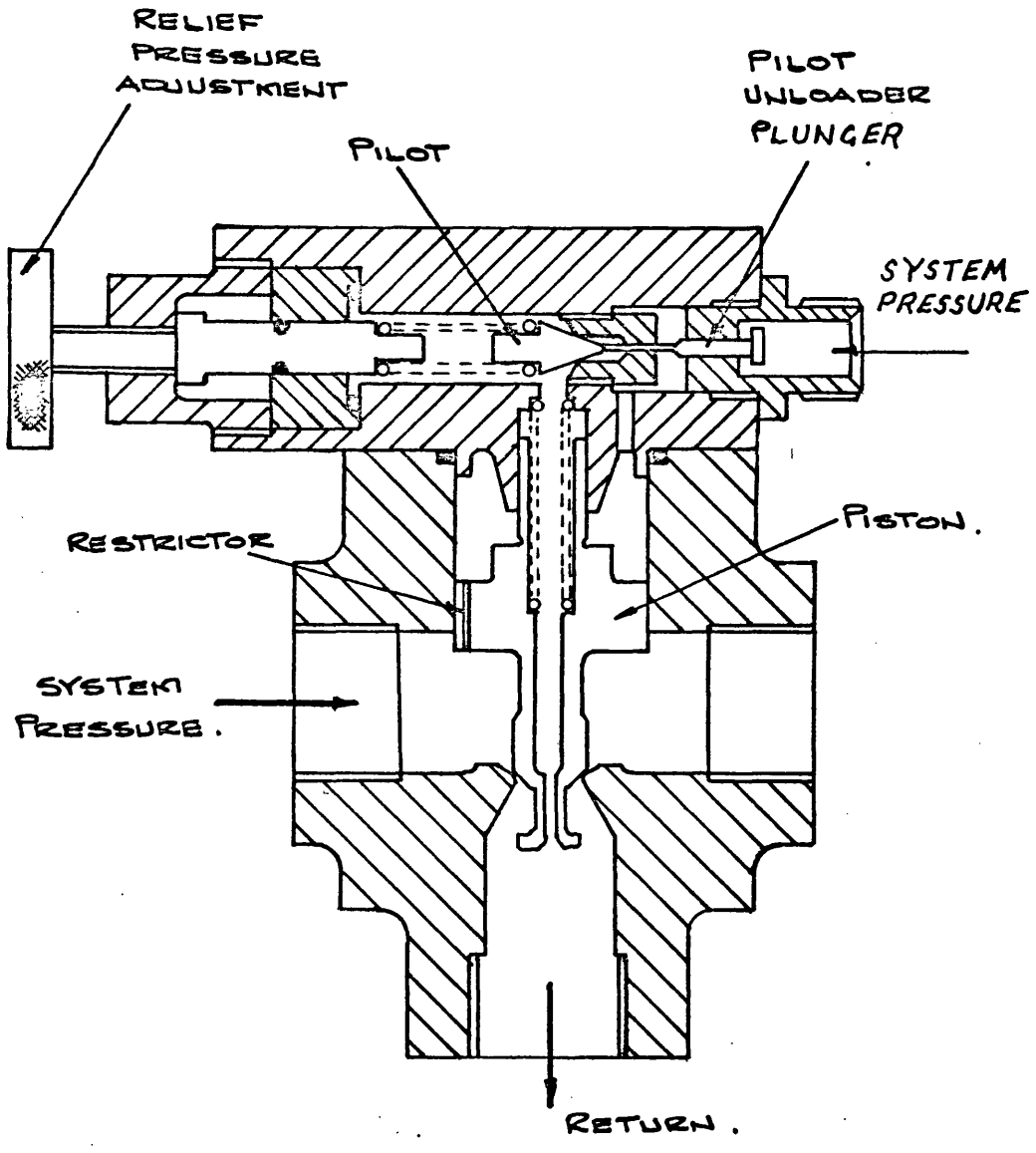

FIG. 5.10 PILOT OPERATED UNLOADER VALVE.

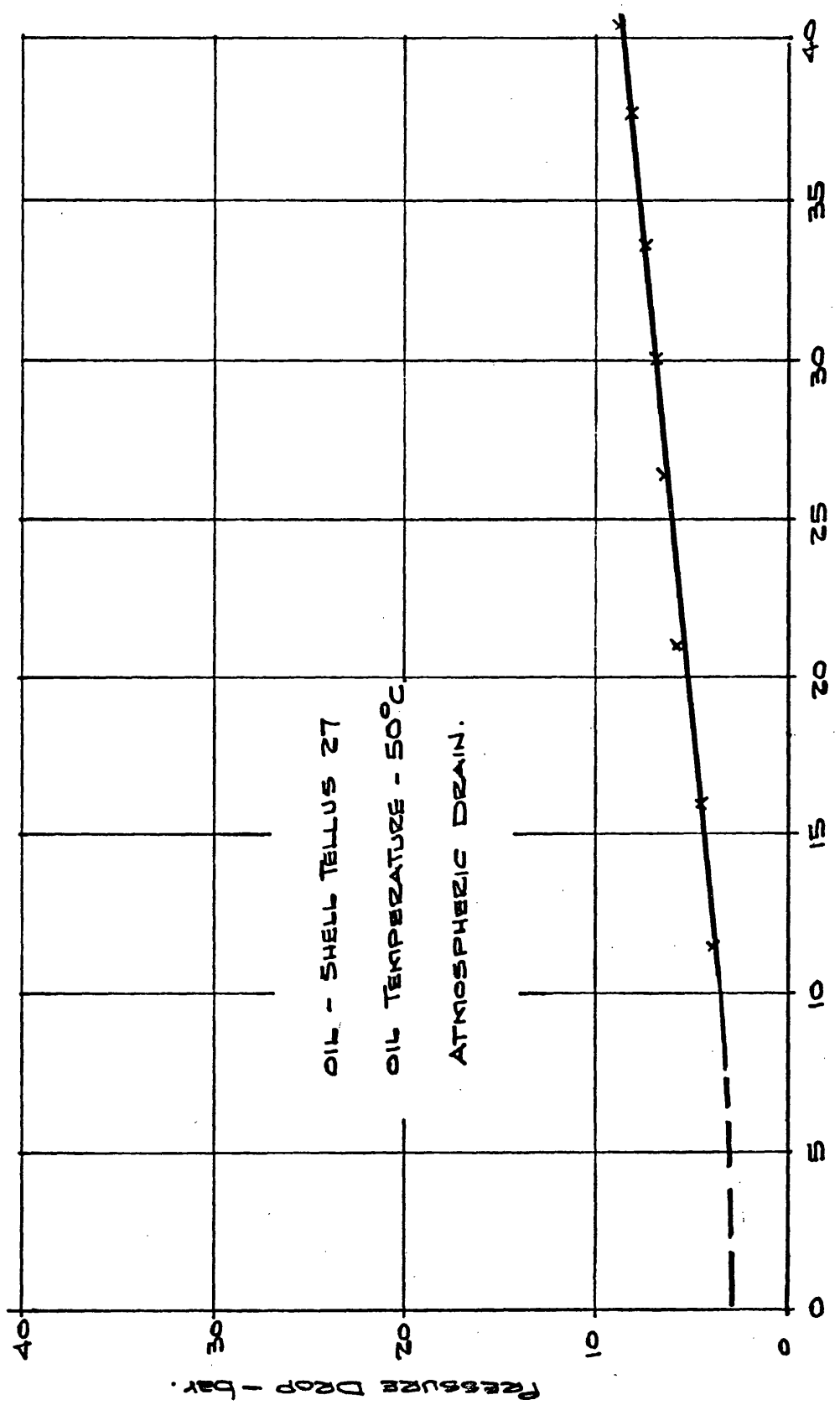

Fig 5.11 Pressure / Flow Characteristic of Relief Valve Used in High Capacity Boost System.

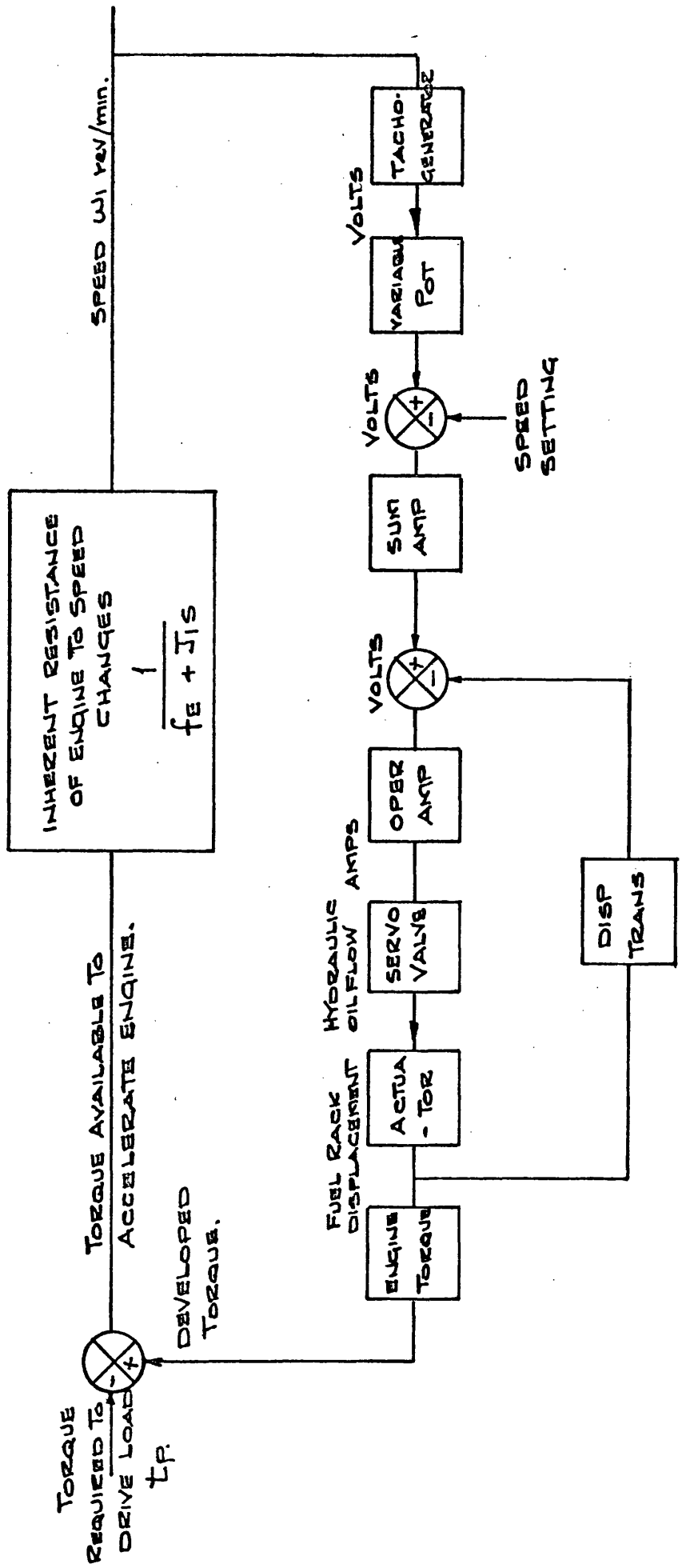

Fig. 5.12. Block Diagram of Diesel Engine with Electro-Hydraulic Speed Governor.

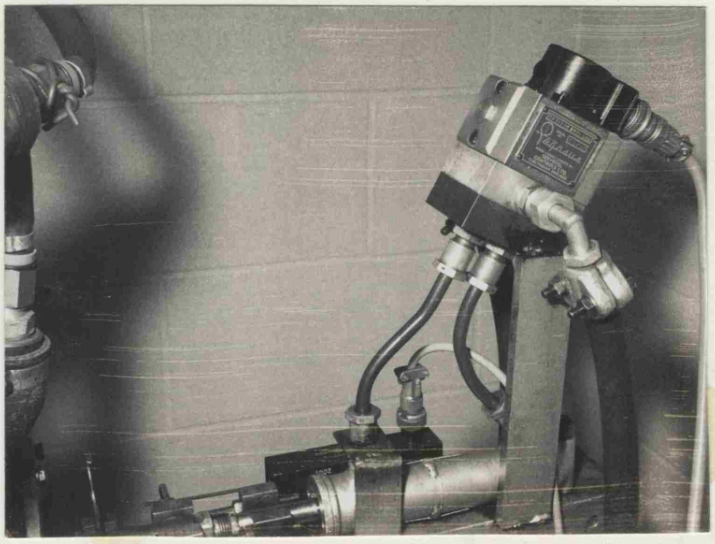

Fig. 5.13 (a) Close Up of Fuel Rack Servo.

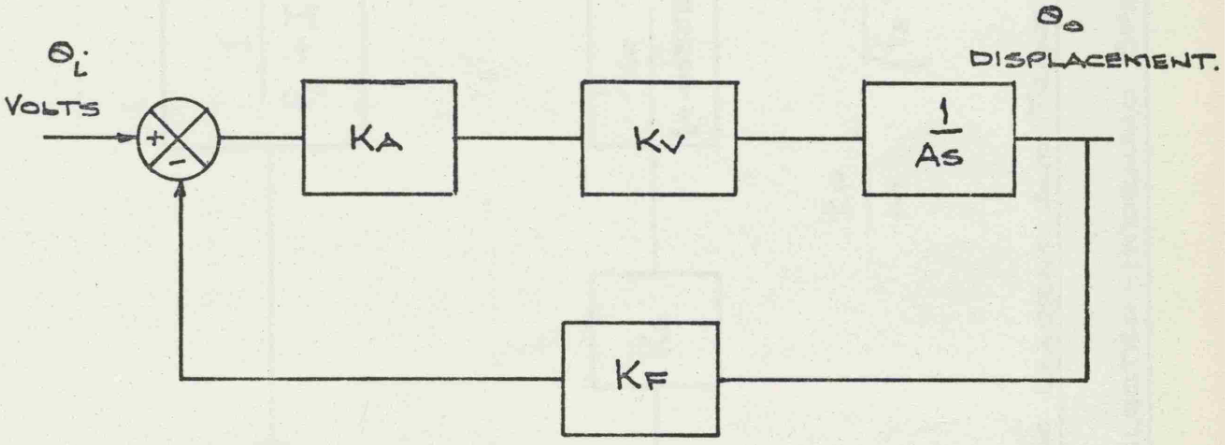

$$\frac{\theta_o}{\theta_i} = \frac{\frac{1}{K_F}}{1 + \frac{As}{K_A K_V K_F}}$$

$$= \frac{\frac{1}{K_F}}{1+Ts}$$

WHERE T IS THE TIME CONSTANT OF THE FUEL RACK SERVO.

Fig 5.13 (b.) Fuel Rack Block Diagram and Resultant Transfer Function.

Fig 5.13. Photograph Block Diagram and Transfer Function of Fuel Rack Servo.

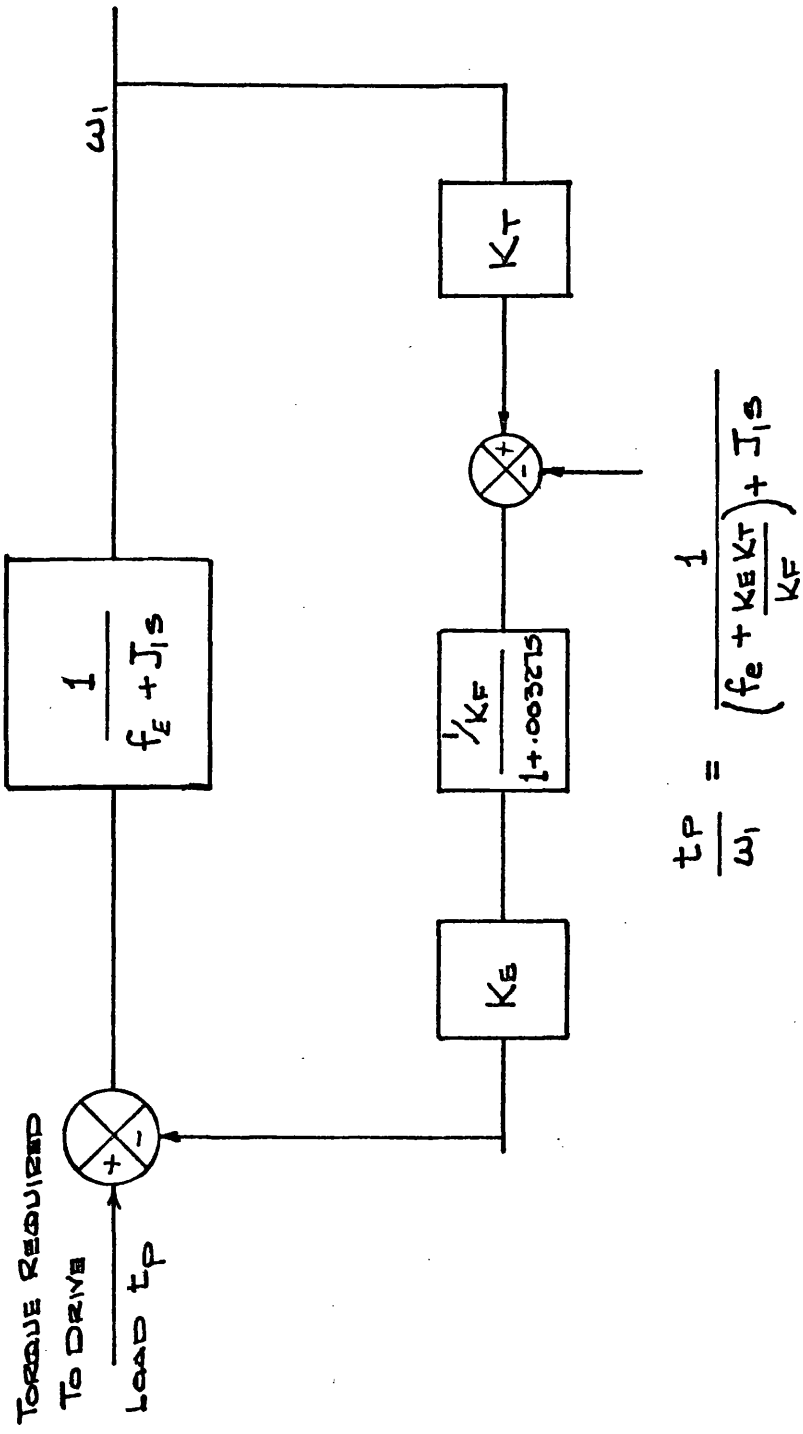

$$\frac{t_P}{\omega_1} = \frac{1}{\left(f_e + \frac{K_E K_T}{K_F}\right) + J_1 s}$$

Fig. 5.14 Block Diagram and Transfer Function of Diesel Engine Electro-Hydraulic Speed Governor.

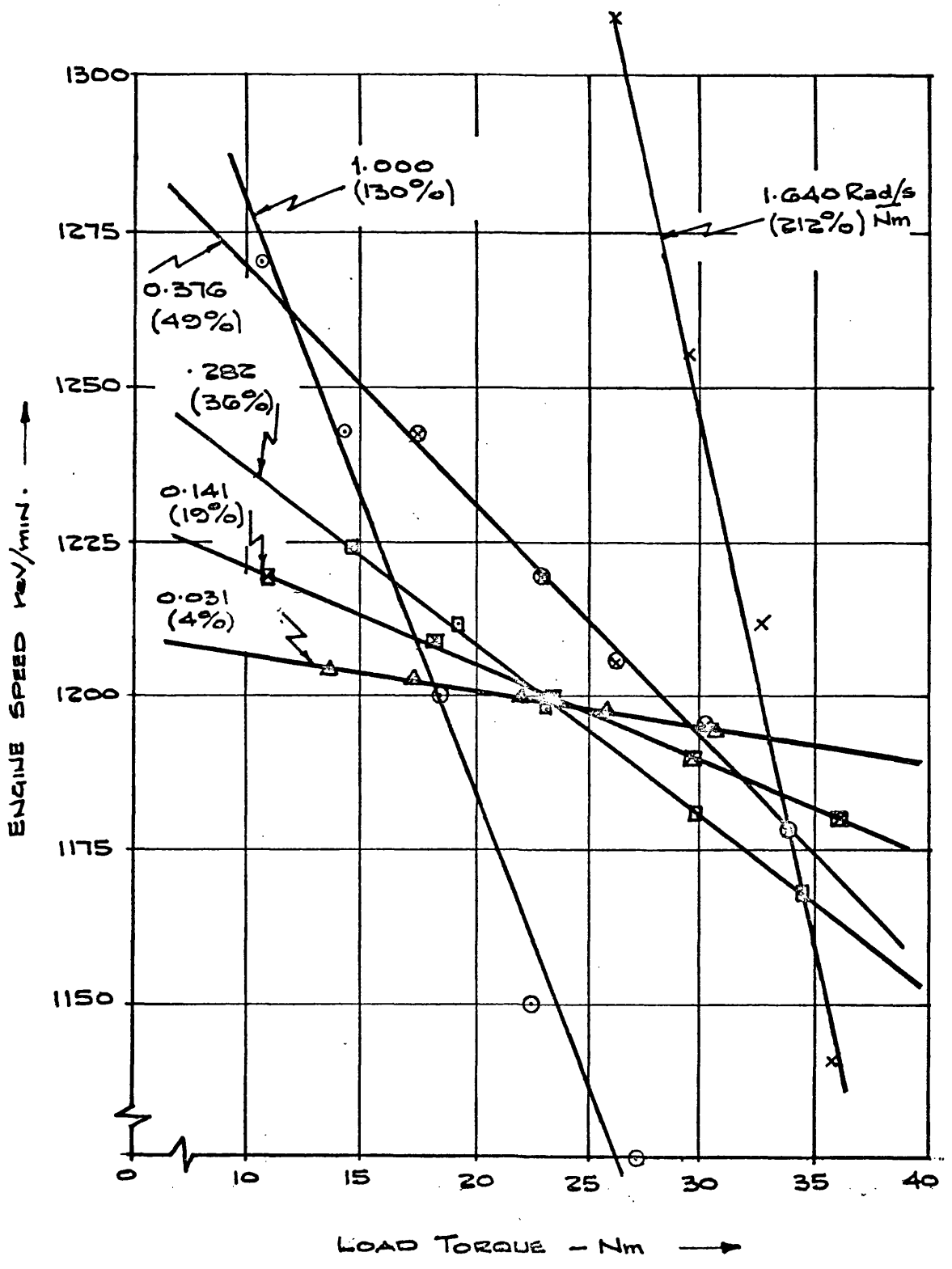

FIG. 5.15 TYPICAL SPEED & LOAD CHARACTERISTICS OF DIESEL ENGINE WITH VARIABLE FEEDBACK ELECTROHYDRAULIC GOVERNOR.

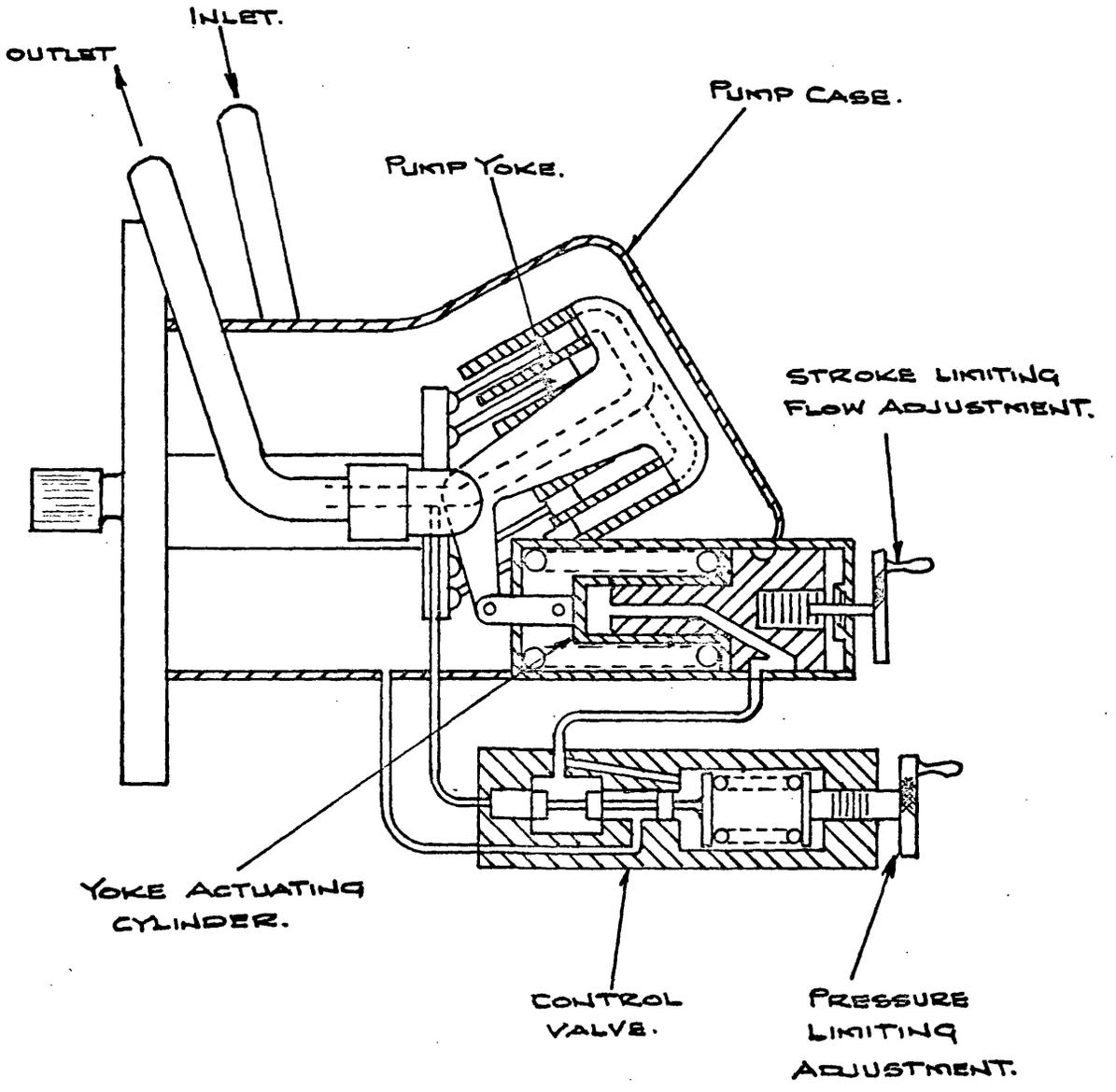

DISPLACEMENT	= 38·5 cm^3/rev.
MAX. CONTINUOUS PRESSURE	= 208 bar.
MAX CONTINUOUS SPEED	= 3750 rev/min.
MAX YOKE ANGLE	= 30°

Fig. 5.16 VICKERS VARIABLE DELIVERY PRESSURE COMPENSATED AXIAL PISTON LOAD PUMP.

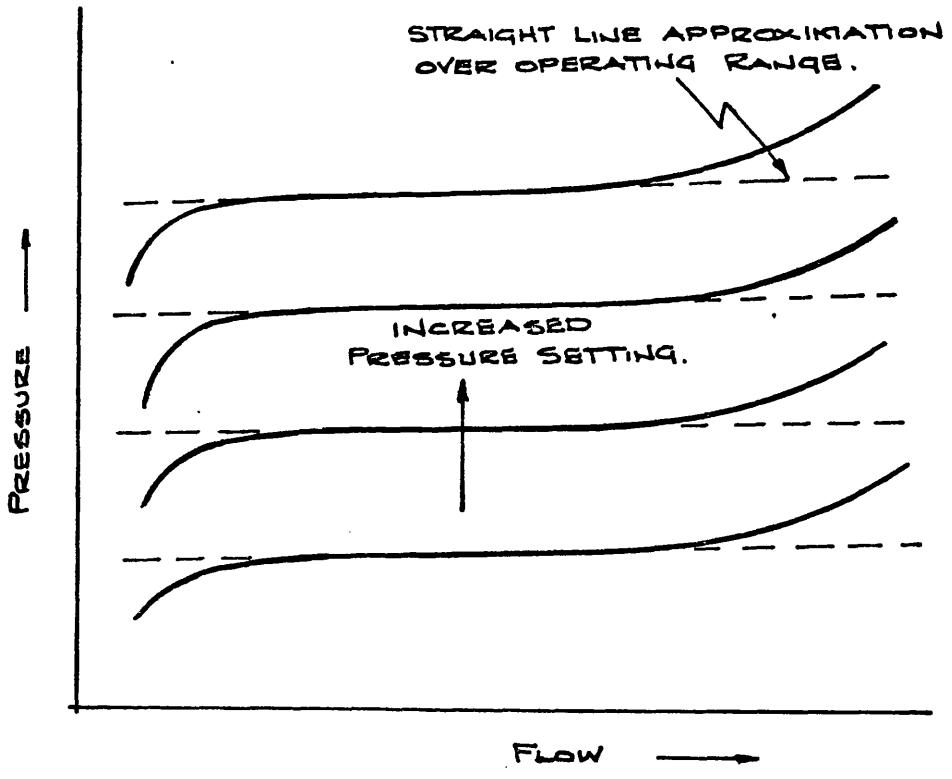

FIG. 5.17 (a) TYPICAL PRESSURE FLOW CHARACTERISTIC OF PILOT OPERATED PRESSURE RELIEF VALVE.

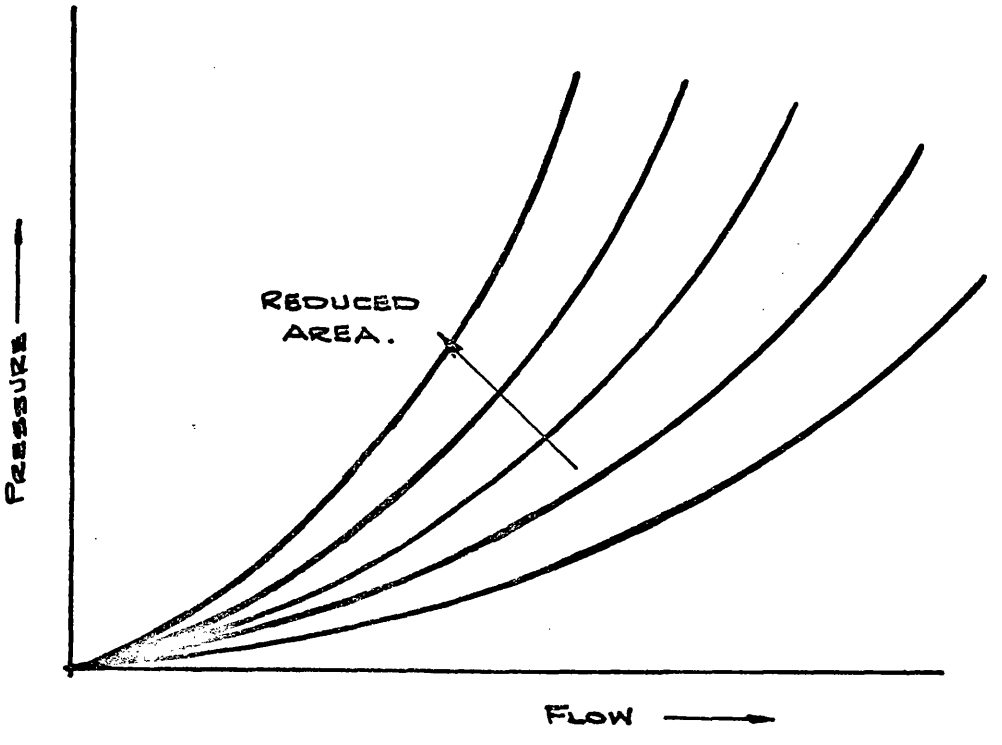

FIG. 5.17 (b.) TYPICAL PRESSURE FLOW CHARACTERISTIC FOR NEEDLE VALVE.

FIG. 5.17 PRESSURE FLOW CHARACTERISTICS FOR LOADING VALVES.

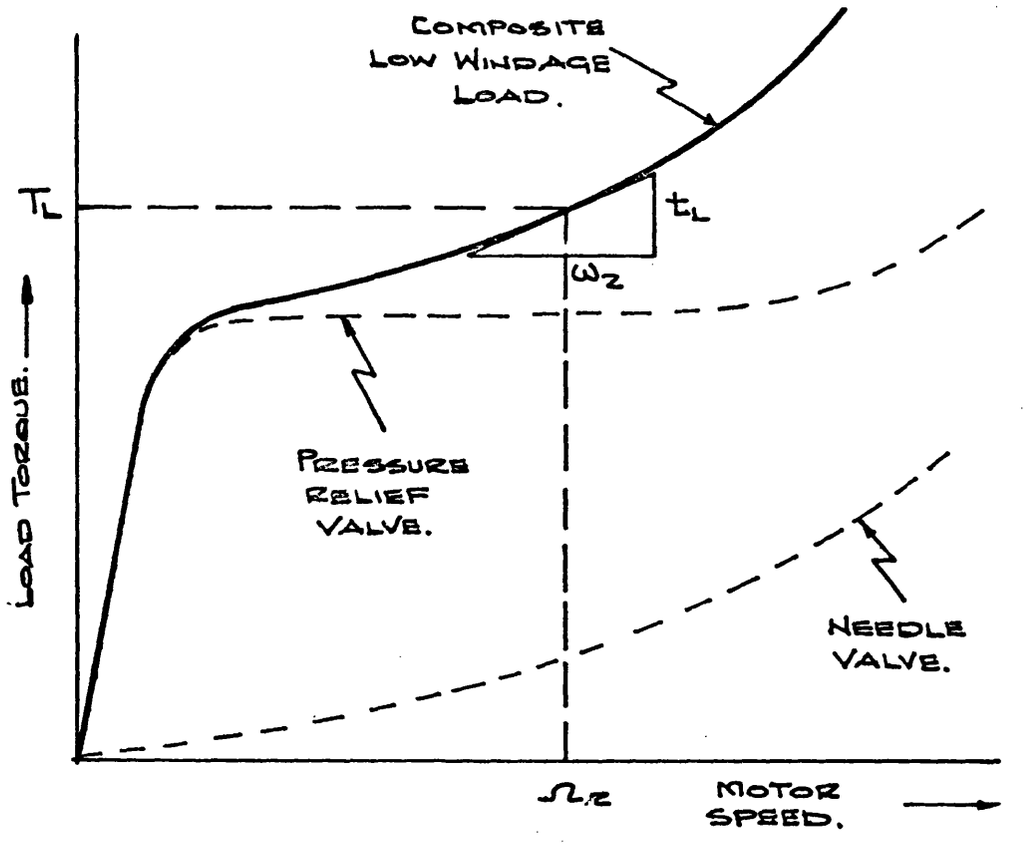

FIG. 5.18(a) SIMULATION OF LOW WINDAGE LOAD.

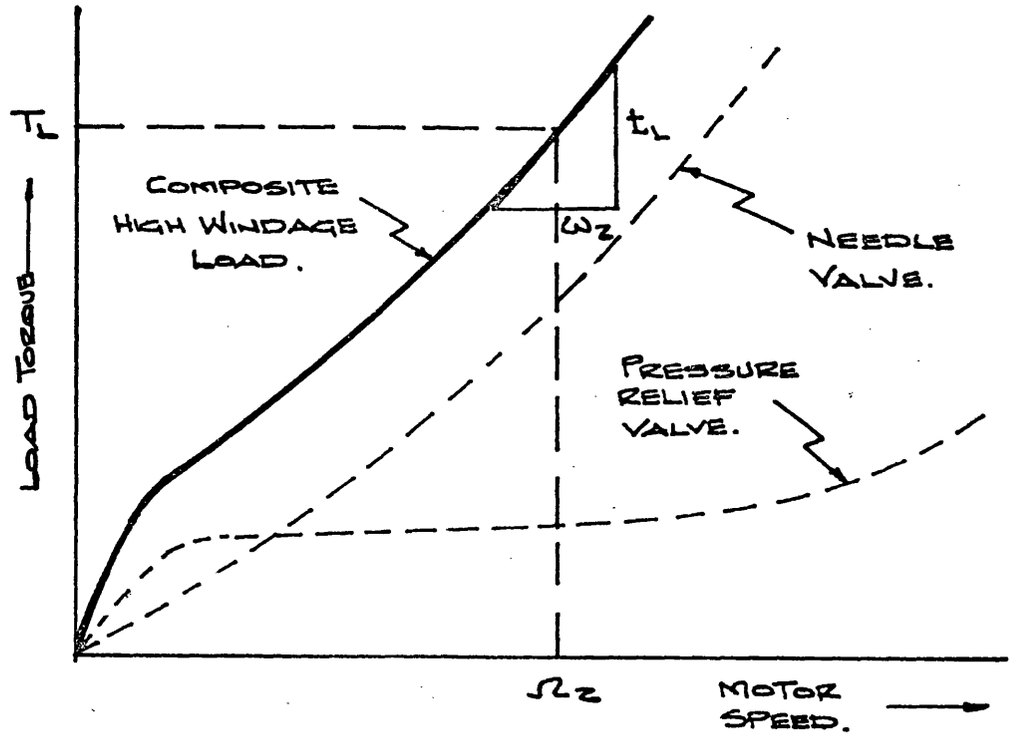

FIG. 5.18(b) SIMULATION OF HIGH WINDAGE LOAD

FIG. 5.18 THE SIMULATION OF VARIABLE SLOPE LOAD TORQUE & MOTOR SPEED WINDAGE LOADS.

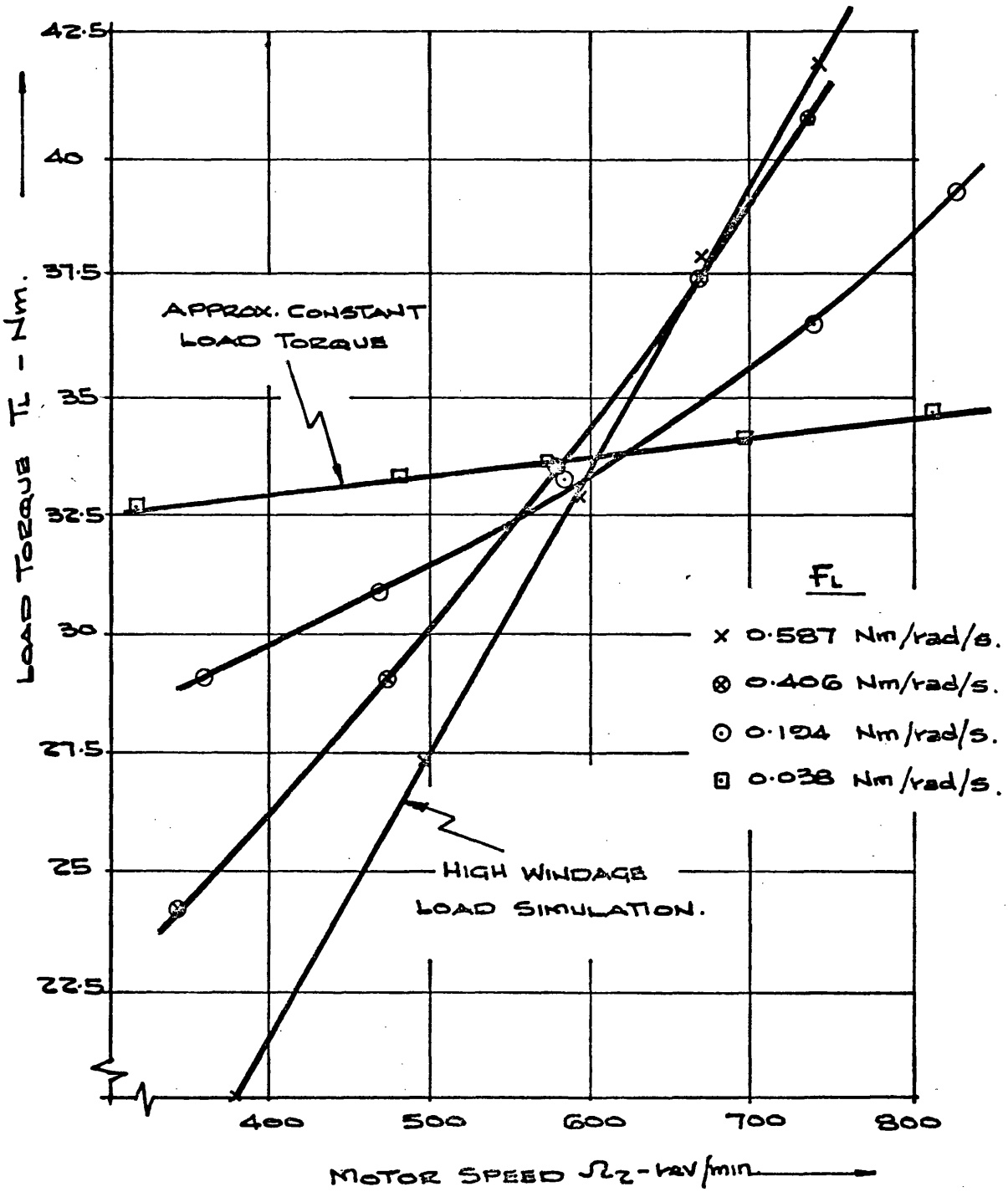

FIG. 5.19 TYPICAL EXPERIMENTALLY DETERMINED LOAD SIMULATIONS.

CHAPTER 6 : The EXPERIMENTAL DETERMINATION of the DYNAMIC RESPONSE of a HYDROSTATIC TRANSMISSION

6.1 Experimental Determination of Transmission System Parameters and Steady State Operating Conditions

6.1.1 System Physical Parameters

Pump and Motor Capacity D_1 and D_2

The displacements of the pump and motor units were obtained from the manufacturer's literature and were expressed as the displacement per radian of rotation and radian of swash. The pump and motor units were of the same capacity $3.19 \times 10^{-5} m^3$/rad/rad swash ($1.14 \times 10^{-3} ft^3$/rad/rad swash).

Total Supply Line Volume - V

The volume of oil trapped in the supply line between the pump and the motor was measured directly by removing the entire rigid pipe assembly from the transmission, and measuring the oil required to fill the assembly. The dead volume trapped in the pump and motor units was measured using the following displacement technique.

The pump unit was stripped and the piston and barrel assembly and port plate drained of oil. The unit was then reassembled and two short lengths of flexible clear P.V.C. tubing fitted to the inlet and outlet ports. The free ends were then immersed in a previously measured volume of oil, and the pump turned by hand until no further air was seen to escape from the pipes. The remaining volume of oil was then determined and the difference attributed to the dead volume of the pump. The dead volume exposed to the supply line by the pump and motor was then assumed to be the total dead volume of one unit, and the total supply line volume obtained by adding this value to the pipe volume. For one of the transmission systems used, the total volume was 1,099 cm^3 (67.04 ins^3) of which the dead volume of the pump and motor contributed 18%.

Driving Inertia $J_1 = J_E + J_p$

The driving inertia of the transmission comprised the inertia of the diesel engine prime mover J_E and the inertia of the hydrostatic transmission pump J_p. The inertia of the engine had been determined by run down tests to be 0.854 Kg m^2 (0.63 slug ft^2) when complete with a lightweight flywheel. The inertia of the hydrostatic pump was obtained from manufacturer's information as 0.00731 Kg m^2 (0.0054 slug ft^2) giving a total value J_1 of 0.860 Kg m^2 (0.635 slug ft^2).

Driven Inertia $J_2 = J_M + J_L$

The inertia of the transmission motor J_m and the inertia of the load pump when no additional load was applied J_L, were both obtained from manufacturers information giving a total load inertia J_2 of 0.0167 Kg m^2 (0.0123 slug ft^2).

Any changes in inertia of the axial piston units due to the displacement changes were ignored.

6.1.2 Loss Co-efficients for Pumps and Motors

To enable any of the mathematical models of pump and motor performance presented in Chapter 2 to be used for predicting the dynamic performance of a hydrostatic transmission it was necessary to determine co-efficients for the slip flow and torque losses of the pump and motor. The models described in Chapter 2 were simplified as the same working fluid was used at a constant temperature throughout the tests. As the pump and motor units were geometrically similar, it was decided to carry out our performance tests on the pump only and refer the results to both the pump and motor.

Before performance tests could be undertaken it was necessary to modify the hydrostatic transmission test rig as shown in Fig. 6.1. The hydraulic circuit was similar to that for the closed loop hydrostatic transmission, but the motor was replaced by a loading valve, flowmeter, and heat exchanger. The boost pressure was maintained during performance tests to prevent volumetric loss due to cavitation. The pump flow was measured at the boost pressure.

To determine the slip losses and the pressure dependent torque co-efficients the pump was run at constant speed and the pump torque and flow measured at different pressures. This was repeated at speeds throughout the working range of the pump. The viscous torque co-efficient was determined by measuring the torque required to drive the pump at different speeds while the delivery pressure was held constant. This was carried out at varying delivery pressures over the pump working range.

The variation in pump flow with pressure is shown in Fig. 6.2 and using Wilson's linear relationship Equ. 2.18, straight lines fitted to the results. The slopes of these lines, the pump slip co-efficient K_p where

$$K_p = \frac{C_{SP}\, D_1\, X_P}{\mu} \quad \text{from Equ. 2.18}$$

were evaluated at each speed.

It must be pointed out that as all flow measurements were made at a boost pressure of 8.3 bar (120 lbf/in^2) a large proportion of the slip losses due to the compressibility have been recovered, and were not taken into account in measurement.

For a hydrostatic unit on half displacement with a ratio of dead volume to maximum swept volume of 1.0, Equ. 2.28 gives:

$$Q_{CP} = \frac{Q\,Max}{2} \quad \frac{P_D}{B_o} \left(1 + \tfrac{3}{4}\right) \qquad \ldots \text{ for a pump } \ldots \quad - 6.1$$

$$Q_{CM} = \frac{Q\,Max}{2} \quad \frac{P_D}{B_o} \left(1 + \tfrac{1}{4}\right) \qquad \ldots \text{ for a motor } \ldots \quad - 6.2$$

The flow measurement at boost pressure means that $\frac{Q_{T\,Max}}{2} \frac{P_D}{B_o}$ has been recovered from the compressible flow loss. To determine the actual slip losses $\frac{Q_{T\,Max}}{2} \frac{P_D}{B_o}$ must be added to the measured slip losses for the pump, and half that value for the motor. The resultant values obtained for the pump and motor are plotted against speed on Fig. 6.3.(a).

Neither Wilson's nor Schlosser's Equations suggest any variation in the slip co-efficient with speed. It can be appreciated however that at high speed the pump pistons may be eccentric to their bores due to centrifugal force thereby increasing the effective leakage path and hence the slip co-efficient.

Schlosser (22) draws attention to the high leakage flows that can occur at low pump speeds due to large temperature rises. When working well below the normal efficiency of the pump, power is lost in heat to the working fluid, and if flow rates are small this can mean high temperature rises that will rapidly increase the leakage flow rate producing an unstable situation.

To enable the torque variations at different speeds to be plotted on one graph pump torque/pump speed has been plotted against differential pressure on Fig. 6.4. Again, using Wilson's Equ. 2. 34 at constant speed:

$$T_{AP} = D_1 X_P (1 + 2\pi C_{FP}) P_D + C_{DP} D_1 X_P \mu \Omega_P + T_{CP} \quad - 6.3$$

$$\therefore \frac{T_{AP}}{\Omega_P} = \frac{D_1 X_P}{\Omega_P} (1 + 2\pi C_{FP}) P_D + C_{DP} D_1 X_P + \frac{T_{CP}}{\Omega_P} \quad - 6.4$$

Using the measured swept volume of the pump no significant value for the pressure dependent torque co-efficient K_{fP} could be determined.

Where

$$K_{fP} = 2\pi \frac{D_1 X_P}{\Omega_P} C_{FP} \quad - 6.5$$

Korn (26) states that speed dependent torque losses are predominent and other losses may be neglected. The results indicated that pressure dependent torque losses could be neglected for this pump. The constant torque losses $\frac{T_{cP}}{\Omega_P} + C_{DP} X_P D_1$ are clearly shown on Fig. 6.4 and were seen to be between 5.4 - 6.8 Nm (4 - 5 lbf ft.).

The variation of pump torque with speed at constant delivery pressure is shown in Fig. 6.5. The slope of the straight lines fitted to the points gave the pump viscous torque co-efficient

$$f_P = C_{DP} D_1 X_P \mu \qquad - 6.6$$

which has been plotted against pressure on Fig. 6.3(b). The decrease in viscous torque losses with pressure could be attributed to an increase in clearances between bearing surfaces with pressure.

6.1.3 The Steady State Condition for Dynamic Testing

Prior to starting up the hydrostatic transmission test rig the desired torque speed characteristic of the prime mover was selected by adjusting the feedback potentiometer of the diesel engine electro-hydraulic governor as described in Chapter 5.4.1.

The required displacement of the transmission pump and motor was then set by adjusting the swash servo input potentiometers and measured using a vernier micrometer against the angular position straight edge. The boost pump was then switched on and the engine started.

Load was applied to the transmission and the characteristic determined as described in Chapter 5.5.4 (when the correct running temperature was achieved). As all test work was carried out at an oil temperature of $50^{o}C$. a warm up period was required which was sometimes reduced by running the transmission at a highly loaded condition. It was found that once the running temperature had been achieved it was a comparatively simple task to adjust the flow rate of water through the oil cooler to maintain $50^{o}C. \pm 2^{o}C.$ Sophisticated temperature control systems were not required.

Once the required conditions were achieved and the prime mover and load characteristics measured the following readings were taken:

1. Supply Line Pressure
2. Return Line Pressure
3. Load System Pressure
4. Input Speed of Transmission
5. Output Speed of Transmission
6. Input Torque
7. Output Torque

6.2 Dynamic Testing Procedures

The input variable for the dynamic testing of the hydrostatic transmission was the pump swash plate angle and the swash control servo enabled any form of electrical signal to be used to disturb the system. Frequency response and step response tests were carried out.

6.2.1 Frequency Response Testing

One method of frequency response testing using electro-hydraulic servos for applying a sinusoidal input is to carry out a closed loop frequency response test of the servo and subsequently allow for this after obtaining the overall frequency response of the system and electro-hydraulic servo mechanism. This method is time consuming as a change of input signal would require a repeat of the servo frequency response test and can lead to errors as it is not always possible to ensure that the servo dynamic performance has not been affected by a change in system variables such as the oil temperature.

However, the use of the digital transfer function analyser has not only facilitated dynamic testing, but also enabled the frequency response testing technique to be improved.

It was possible to record the response of the electro-hydraulic servo and the overall transmission, which includes the servo, consecutively at any frequency and then by division immediately obtain the net transmission response. This is shown in simple block diagram form in Fig. 6.6.

It is also a simple matter to continuously monitor the servo output to ensure a constant amplitude of pump swash plate angular movement throughout the test frequency range. This is necessary because output from the swash servo per unit electrical signal input will change with frequency of input. In addition by means of the selector switch the response of a number of system parameters including output speed of the transmission, line pressure variations, and torque variation, could be measured consecutively. All results from the tests were tabulated and any particular frequencies of interest fully investigated.

The digital transfer function analyser measures the sinusoidal variation of a signal about a D.C. level. The maximum D.C. signal the instrument can accept is 200% of the maximum range of the sensitivity setting. It carries out measurement by an iteration process either over an automatically selected or pre-set number of cycles. It is a relatively noise insensitive instrument and searches for the frequency of the applied signal. However it will not indicate any distortion in the measured sinusoidal signal and an analogue galvanometer recording was used to indicate non-linearities.

6.2.2 Step Response Testing

An alternative method of dynamic testing is to apply a step disturbance to the transmission and from the analogue record of the transient response of the system parameters, determine the dynamic response characteristics of the transmission. By comparing the transient response curve of the transmission with the characteristic response of a second order system an effective natural frequency and damping ratio can be calculated.

6.3 Preliminary Dynamic Testing of Hydraulic Transmission (Tests 1 - 19)

6.3.1 Test Programme

Preliminary frequence response tests were carried out to determine the correlation between the theoretical predictions of dynamic response made using the signal flow analysis presented in Chapter 3.3, with experimentally measured values. The input variable for the tests was a sinusoidal disturbance applied to the pump swash plate. The effect of the following parameters were investigated:

1. Pump swash plate angle
2. Motor swash plate angle
3. Mean load torque and the slope of the torque speed curve
4. The slope of the engine torque speed curve
5. Load inertia
6. System volume

The amplitude of the input signal was also varied, but care was taken to ensure that the pump swash plate did not reverse at low mean pump swash angles causing the motor shaft to reverse its rotation.

The details of the first test series are shown in Table 6.1. Unless otherwise stated, all tests were carried out at a nominally constant engine speed of 1,200 rev/min. and at a mean return line pressure of 6.9 bar (100 lbf/in^2) using the restricted boost system described in Chapter 5.3. The predicted values of the transmission natural frequency and damping ratio together with experimentally measured values for these tests are given in Table 6.2.

The experimental values were obtained from the results of the frequency response test by comparing the measured response with the standard response of a second order system.

The apparent natural frequency was defined as the frequency at which 90^{o} of phase lag occurred between the pump swash variation and the variations in motor speed. The damping ratio was obtained by comparing the shape of the phase lag curve with standard curves. The shape of the amplitude response curve was used for verification.

The theoretical predictions of the dynamic performance shown in Table 6.2 were made using Programme TDRES and the values for the natural frequency ω_n and damping ratio ξ are given. The system parameters measured as previously described were used. The effective oil bulk modulus of 13,800 bar (200,000 lbf/ins^2) put forward by Shearer as the most realistic for use in practical systems was adopted and used in the computation. It was hoped that any error in the assumed value for effective bulk modulus would be determined by a consistent error between predicted and experimental values of natural frequency.

6.3.2 Discussion of Preliminary Test Results

The results shown in Table 6.2 provided very poor correlation between predicted and experimental results, but several significant factors were determined providing a basis for further test work.

The effect of varying the torque speed droop of the diesel engine was to significantly reduce the low frequency gain of the transmission, in effect producing a lower speed variation of the motor per unit charge of swash of the pump. The measured frequency response of Test 5 and that predicted using subroutine RESP of Programme TDRES are shown in Fig. 6.7. The low frequency attenuation obtained experimentally correlated well with the computed value, but there was a discrepancy in both amplitude and phase between the predicted and measured curves over the remaining frequency range. However, the error between the tabulated values for apparent natural frequency and damping ratio and the computed values for Tests 1 - 5 could not be correlated with the change in engine droop.

Tests 6 - 10 showed the effect of varying the transmission pump swash plate angle. The theoretical predictions showed very little change in transmission natural frequency with the pump swash plate angle, except for Test 6 whose natural frequency was reduced by a reduction in motor swash. However, these predictions were not borne out by the experimental results. It was found that the error between the predicted and experimental natural frequency ranged from 37.4% for Test 6 down to -2.7% for Test 9. The reverse trend was shown by the damping ratio whose error increased from -8.1% for Test 6 up to 52% for Test 10.

The possibility that the mean swash plate angle of the pump could effect the assumption that the pump was delivering flow as a linear element when the swash was varied sinusoidally prompted the theoretical investigation described in Chapter 2.2. This computer analysis verified that the proportional relationship between flow and swash angle under the test conditions was a valid assumption.

To assess the experimental technique Test 7 was repeated three times over a time span of several days. The results shown as Tests 11 - 13 gave a 5% discrepancy between the upper and lower value obtained for apparent natural frequency and damping ratio. The 25% difference between computed and measured values for natural frequency varied little.

The remaining Tests 14 - 19 gave errors of under 10% between predicted and measured natural frequency, except for Test 18 which gave 28%. Comparative errors for damping ratio were also obtained, but no real basis for correlation could be determined.

An investigation of the galvanometer recordings of the pressures in the supply and return line of the transmission during frequency response testing showed that considerable variation in the return line pressure was occurring.

As the signal flow analysis had assumed a constant return line pressure the boost system was improved in a somewhat artificial manner compared with most practical systems in order to maintain a near constant return line pressure. The improved system is described in Chapter 5.3.1. All subsequent testing employed this improved boost system at a mean return line pressure of 13.8 bar (200 lbf/in^2) except where otherwise stated.

This preliminary investigation demonstrated that the theoretical analysis that had been adopted to analyse the dynamic response of the hydrostatic transmission was insufficiently accurate. No clear indication had been given as to the validity of using a value 13,800 bar (200,000 lbf/in^2) for the bulk modulus of the oil, and it was necessary to extend the dynamic testing to determine the source of error.

6.4 Test Programme (Tests 20 - 54) Using Modified Procedure to Investigate Scatter in Previous Tests

6.4.1 The Effect of Cycle Loading on Transmission Performance (Tests 20 - 24)

Frequency response tests 11, 12, and 13, had been carried out using the method described as discreet short duration tests over a period of several days to ensure that the results obtained from dynamic testing were repeatable.

However, even though this had been found to be the case it had not been established whether the cyclic loading of the hydrostatic transmission during dynamic testing was in any way affecting the transmission performance and hence the results of frequency response tests carried out consecutively.

The transmission was set up according to Test 20 shown in Table 6.3, and a frequency response test carried out. The pump swash was then oscillated sinusoidally at a peak to peak amplitude of 2.5^{o} for the following periods:

Test No.	Frequency H_Z	Duration Mins.
20		
	1.0	15.0
21		
	4.0	15.0
22		
	6.5	15.0
23		
	12.0	15.0
24		

Total Cycling Running Time Including Frequency Response Tests - 3.4 Hours.

At the end of each period the frequency response of the transmission was measured and the results are given as Tests 20 - 24 in Table 6.3 and Table 6.4. Full steady state and load determinations were only carried out at the start and finish of the tests. No significant variation in the error between the theoretically predicted and experimentally measured values was obtained.

6.4.2 The Effects of Load Torque Speed Characteristics

6.4.2.1 A Typical Windage Load (Tests 25 - 28)

The transmission was set up with the load pump delivering through a needle valve, to simulate a typical windage type load, and frequency response tests carried out on the transmission at four different pump swash angles. The results are tabulated as Tests 25 - 28 in Tables 6.3 and 6.4 and are shown graphically on Fig. 6.8. From the frequency response plot of Fig. 6.8 a variation of 30% between the experimentally determined values for natural frequency was again obtained giving at one extreme an 8.4% underestimate of the predicted value of natural frequency and at the other 14.8% overestimate. However, although this type of load is typical of many of those found in practise, it was obvious that many of the system parameters such as pump swash, system pressure, and load damping co-efficient had been altered. It was therefore not possible to establish which of these parameters was causing the discrepancy between the theoretically predicted and experimentally measured dynamic response of the transmission. It was therefore necessary to carry out further tests in a more artificial manner ensuring the transmission was only subjected to the change of one parameter.

6.4.2.2 Variation of Load Damping Co-efficient - f_L (Tests 29 - 32)

Using the technique described in Chapter 5.5.2 the transmission load torque speed characteristic, load damping co-efficient f_L, was varied whilst holding the mean swash plate angles of the pump and motor, mean pump and motor speed, load torque and hence system pressure all constant (Tests 29 - 32). The effects upon the dynamic response of the transmission are shown on Fig. 6.9. The apparent natural frequency as determined from the 90^o phase lag point alters with the load damping co-efficient from 4.8 HZ at 0.037 Nm/rad/sec. to 6.5 H_Z at 0.587 Nm/rad/sec. This suggests a considerable increase in natural frequency with increase in load damping co-efficient. As can be seen from Table 6.4 this is not in agreement with the theoretical predictions made using Programme TDRES.

6.4.2.3 Effect of Amplitude of Input Signal (Tests 33 - 36)

Tests 33 - 36 were carried out at the same steady state conditions as Tests 29 - 32, but at a reduced amplitude of pump swash plate oscillation. The results are shown on Fig. 6.10, and are similar in all respects to those shown on Fig. 6.9 indicating that there were no significant non-linearities present.

6.4.2.4 Step Response Tests for a Variety of Load Damping Co-efficients (Tests 37 - 54)

Having established the effect of varying the load damping co-efficient upon the transmission dynamic response by frequency response testing similar tests were carried out using the step response technique for measuring dynamic response described in Chapter 6.2.2. It was found to be very difficult to set up the transmission with pre-determined values of load damping co-efficient and therefore three different typical windage load curves were set up and step response tests carried out on the transmission at different pump swash angles.

The transmission was driven at 1,200 rev/min. and with a load inertia J_2 of 0.0167 Kg m^2 (0.0123 slug ft^2), system volume V of 0.957 litres (0.0338 ft^3) and an engine speed load droop K_E of 0.147 rad/sec/Nm (0.200 rad/sec/lbf ft) the same conditions as Tests 20 - 36.

The steady state test condition for the step response was determined and the pump swash stepped. The response was measured at the conditions at the end of the step corresponding to the steady state previously determined. The conditions for Tests 37 - 54 are shown on Table 6.5. The natural frequency ω_n and the damping ratio ξ measured from the galvonometer recordings at these conditions are given. A typical galvanometer recording is shown for Test 44 on Fig. 6.11.

To investigate the effect of varying the load damping co-efficient f_L upon the step response, the natural frequency ω_n and damping ratio ξ measured were plotted against load damping co-efficient on Fig. 6.12 and 6.13. As a comparison the results of dynamic response measurement by frequency response testing for Tests 29 - 32 have been plotted and show less scatter than these obtained by the step response method. However, the same increase in natural frequency ω_n and damping ratio ξ with load damping co-efficient f_L was observed.

The step response technique did not permit detailed studies of the various system parameters during transients to be readily undertaken. It was not possible to determine whether any of the elements in the transmission were giving rise to non-linearities, and all the results obtained to date pointed to the need for detailed studies of the loading simulations. It was therefore decided to curtail further step response tests in favour of frequency response testing.

6.4.2.5 The Dynamic Characteristics of the Load

Whilst carrying out the frequency response tests the torque on the load shaft was also measured and hence the frequency response for the actual load used obtained. In the theoretical analysis the load was assumed to comprise a viscous and inertial component, the response of the load torque to changes in speed being a first order lead.

i.e./

i.e. $t_L = (f_L + J_L s)\,\omega_2$ - 6.7

It is convenient to rearrange this and put it in the form:

$$\frac{t_L}{\omega_2 f_L} = 1 + \frac{J_L}{f_L} s \quad \text{- 6.8}$$

i.e. $$\frac{t_L}{\omega_2 f_L} = 1 + \frac{J_L}{f_L} j\omega \quad \text{- 6.9}$$

If this is plotted on a vector locus it gives the vertical line shown on Fig. 6.14. The actual values obtained during Tests 29 - 32 which departed significantly from this line are also shown on Fig. 6.14. This shows that the load was not by any means the inertial and viscous load first assumed. The causes for these deviations from the assumed load were not determined, but it is apparent that particular care must be taken to evaluate the actual load imposed upon a transmission under dynamic conditions.

6.5 /

6.5 Correlation

6.5.1 Assessment of Methods Used to Determine Transmission Dynamic Performance

Four methods have been presented to determine system dynamic performance:

the simple theory of Equ. 3.6
the signal flow graph method using Programme TDRES
vector analysis
and experiment.

The results shown in Tables 6.2 and 6.4 compared predicted values obtained using Programme TDRES with experimental results, the value of 13,800 bar (2×10^5 lbf/in^2) for effective bulk modulus suggested by Shearer being used.

Table 6.6 shows a comparison of the four methods applied to Tests 29 - 32. To obtain values for the first three the isentropic tangent bulk modulus for the oil of 18,300 bar (2.65×10^5 lbf/in^2) obtained from the manufacturer's literature (37) was used. The pipe resilience was taken into account using Equ. 4.16 and Equ. 4.17.

All the methods give natural frequencies within 30% of each other and if this type of accuracy is all this is required, then any of the methods can be used. However, when it is considered that variations in natural frequency are proportional to the square root of most of the system parameters it shows that very wide discrepancies have occurred.

Simple Theory

The simple theory of Equ. 3.6 gave a value of natural frequency that did not vary with load damping co-efficient f_L, and only provided good correlation with the experimental results at the higher load damping co-efficients. The damping ratio was very much underestimated.

Signal Flow Analysis

The signal flow analysis predicted a small change in natural frequency with load damping co-efficient, but not to the extent of the values obtained experimentally (see Table 6.6). The prediction of damping ratio was very much improved.

Vector Locus Technique /

Vector Locus Technique

The theoretically predicted natural frequencies ω_n and damping ratios ξ obtained using the vector locus technique are shown on Table 6.6, and give the most accurate correlation with the experimental values. The vector locus technique would appear to be the most valuable tool for prediction of dynamic performance, but slightly overestimates the natural frequency of the system and slightly underestimates the damping ratio.

The effectiveness of the vector analysis approach for predicting the dynamic performance of a hydrostatic transmission suggested that the technique could be well employed for investigating in more detail the effect of various system parameters on dynamic performance. However, as described in Chapter 3 to improve the usefulness of the technique a computer programme was written, 'VECTAN' (Appendix I - Programme 3). In addition to providing the predicted dynamic response of the hydrostatic transmission using vector analysis the Programme was adapted to handle experimental data and present it in a manner suitable for correlation.

6.5.2 Bulk Modulus Evaluation

As described in Chapter 4, most investigators carrying out dynamic testing of hydraulic systems when confronted with a discrepancy between their theoretical and experimental results, have worked backwards to determine the effective bulk modulus of the oil in the system. This procedure has also been adopted here for a large number of tests with different load damping co-efficients, but all have the same volume of oil in the steel pipe supply line. Over a range of frequencies between 0.1 Hz and 12.0 Hz, the load vector has been obtained, and by using the vector diagram of Fig. 3.7 starting from both ends the compressible flow vector $\frac{\tilde{q}_c}{\omega_2}$ determined. The effective bulk modulus of the oil in the steel pipe B_e was then evaluated.

The mean value of the effective bulk modulus of the oil in the pipe was found to be 15,700 bar (2.28×10^5 lbf/in^2) and a statistical analysis of the results showed a standard error of only 7.3% over the 79 determinations carried out. When the elasticity of the steel pipe line was allowed for (using Equ. 4.16 and Equ. 4.17) the bulk modulus for the oil was determined to be 16,400 bar (2.38×10^5 lbf/in^2). This value was compared with the oil manufacturer's physical test tangent values at the temperature and pressure of the tests, 50°C. and 82.7 bar (1,200 lbf/in^2). Initially, use of the first edition of the oil manufacturer's data (37) suggested this experimentally measured value of bulk modulus lay between the isentropic and isothermal values. However, subsequent use of Hayward's Equations (Equ. 4.12 and Equ. 4.13) and the oil manufacturer's second edition of published data (36) gave isentropic tangent

bulk modulus of oil 16,500 bar (2.40×10^5 lbf/in^2). The experimentally determined value for the bulk modulus of oil was therefore in very close agreement with the physically measured isentropic tangent value.

Using the vector locus technique and the isentropic tangent bulk modulus of the oil, it is therefore possible to predict the natural frequency of the transmission to within 5%. In order to provide a clear procedure for the designer to adopt when predicting the dynamic performance of a transmission, Appendix III has been presented.

6.5.3 The Effect of Oscillating the Pump Swash Upon its Performance

All the methods of analysis described had assumed the pump and motor to be continuous linear elements, but from the outset it had been considered possible that the piston slippers might leave the swash plate under some oscillatory conditions. This would lead to a reduction in flow from the pump and the impact occurring when the slippers strike the swash plate at the start of the pressure stroke could cause damage to the unit. The experimental results showed no sign that this had happened and on stripping the units after the tests no sign of excessive wear of the slipper pads or swash plate surface could be determined.

Effect of Slip

The flow loss from the pump, motor and valves in the system shows as a flow loss which is in phase with the pressure pulsations and 90^{o} out of phase with the compressibility term. Careful tests were carried out on the pump and motor units to determine whether the mean leakage altered with swash plate frequency by measuring the drain flow from the casing of the units. No change was recorded up to a frequency of 12 Hz.

At low frequencies the slip losses cause a reduction in the amplitude of the response of the transmission. The amount of this reduction could be predicted by the vector analysis using values of pump and motor slip obtained by experimental measurement as described in Chapter 6.1.2. At higher frequencies slip losses are insignificant in comparison with compressibility losses.

6.6 Further Investigations of the Effect of System Parameters upon Hydraulic Transmission Dynamic Performance

Following the adoption of the vector analysis technique it was possible to make accurate theoretical predictions of hydrostatic transmission performance.

Investigations previously carried out were repeated and extended using the computerised analysis. It was necessary to measure the frequency response of the load applied to the transmission and the subsequent line pressure variations to enable the vector analysis to be used. Details of the tests carried out are given in Table 6.7 along with each test objective. All tests were at a nominal engine speed of 1,200 rev/min. and engine speed load droop of 0.160 rad/sec/Nm (0.217 rad/sec/lbf ft.).

6.6.1 The Effect of Load Inertia

The load inertia applied to the transmission output was increased by securing a large lathe chuck to the output shaft. The inertia of the chuck was measured prior to installation by mounting between centres and using the run down technique. Subtracting the inertia of the mandrel, determined by calculation, the inertia of the flywheel was found to be 0.174 Kg m^2 (0.128 slug ft^2). When added to the load pump and transmission motor inertia this gave a total value of 0.190 Kg m^2 (0.140 slug ft^2).

Frequency response tests were carried out at two input amplitudes the conditions for which are listed as Tests 55 and 56.

The reduction in apparent natural frequency with increased load inertia is shown on Fig. 6.15 by comparing the results of Tests 55 and 56 with Test 32 a test with the same load damping co-efficient f_L, but 0.0167 Kg m^2 (0.0123 slug ft^2) load inertia. The vector locus technique was used to predict the response and good correlation obtained. Since the load was now predominantly inertia the simple mathematical model for the load was satisfactory. Using a value for the bulk modulus of the oil 16,200 bar (2.38×10^5 lbf/in^2) the natural frequency of the transmission was predicted to be 1.66 Hz using the simple theory of Equ. 3.6, and 1.75 Hz using the signal flow analysis. The apparent natural frequency measured experimentally was 1.70 Hz..

6.6.2 Mean Return Line Pressure Effects

Many of the previous authors described in Chapter 4.3 working on the dynamic response of hydraulic systems, indicated that aeration effects were causing a reduction in oil bulk modulus, and consequently reducing the natural frequency of the system. It was felt likely that the degree of aeration taking place in a hydrostatic closed loop transmission system would be influenced by the mean return line pressure.

Tests 57, 58, and 59, were carried out at similar conditions, but at reduced mean return line pressures, to those of Test 30. By carrying out the vector analysis to predict the response of the transmission and then using the procedure described to evaluate the effective bulk modulus of the oil, no significant change in the effective bulk modulus of the oil could be determined when the return line pressure was varied between 6.0 bar and 25.0 bar.

6.6.3 Effect of Boost System

From the completion of the first series of tests the tests reported have been carried out with a return line supplied by an artificially large boost pump, to ensure the return line pressure was kept as constant as possible during frequency response testing. A more practical boost system was now fitted with a boost pump capacity of 6% of the main pump maximum capacity. A single stage pressure relief valve was installed.

Tests 60 - 63 were carried out at the conditions similar to those of Tests 33, 29, 35, and 31 respectively, but with this restricted boost system. The mean return line pressure was left constant at 13.8 bar. Galvanometer recordings of swash plate angle x_p, output speed ω_2 and return line pressure p_L are shown on Fig. 6.16 for Tests 60 and 63. The tests correspond to the smallest and largest pressure variations in the return line obtained in this series with the restricted boost supply.

When the amplitude of the flow fluctuations was large, cavitation was marked and cut off the bottom of the sine wave for reasons shown in Fig. 3.8. There was however an intermediate stage which occurred with smaller flow fluctuations in the return line (at correspondingly lower frequencies, see Test 61, at 2Hz) where the pressure appears to rise exponentially after cavitation. This could be due to the purging of voids in the return line following local cavitation.

The increase in apparent natural frequency due to the restricted boost supply is shown on Fig. 6.17 by comparing the result of Test 61 with those of a similar test incorporating the larger capacity boost system - Test 29. By adding the return line pressure variations $\frac{\overrightarrow{P_L}}{\omega_2}$ vectorially to the differential line pressure variations $\frac{\overrightarrow{P_D}}{\omega_2}$ to give the supply line pressure variations $\frac{\overrightarrow{P_H}}{\omega_2}$ the response of the transmission was predicted using the vector locus technique. The predicted response vector loci for Tests 60 - 63 were in very good agreement with the experimental loci for all tests. It was significant that despite considerable cavitation taking place in the return line there was nevertheless a marked increase in apparent natural frequency compared with the tests where the return line pressure was held constant by use of the large boost system.

It should be noted that the maximum increase in system stiffness would occur if the relief valve had a very steep pressure flow characteristic and there was no cavitation in the return line. In that case both line pressures would then vary equally and provided the mean return line pressure was high enough to prevent cavitation the natural frequency of the transmission would be increased by 40%.

6.6.4 Effect of Flexible Hose

One of the many advantages of hydrostatic drives is their ability to transmit power to normally inaccessible places and very often flexible hose is incorporated to facilitate this. To determine the effect of the use of flexible hose upon the dynamic response of a hydrostatic drive the steel pipes used up until this time were removed and replaced by a length of 25.4 mm (1.0 in) internal bore, double braided flexible hose.

Tests 64 - 67 were carried out with a hose of length 2.44 m (8 ft.) and the overall effect was to reduce the natural frequency of the transmission to approximately $\frac{1}{3}$ of the value recorded with the steel pipes. The measured frequency response of Test 66 is compared with the response obtained with steel pipes for a similar value of load damping co-efficient Test 31 on Fig 6.18.

Again the vector locus technique was used to work back from the measured response of the transmission to determine the effective bulk modulus of the oil in the flexible pipe. A value of 4,350 bar (64,000 lbf/in^2) was obtained from the vector analysis applied to 26 operating points for the four tests - Tests 64 - 67, giving standard error of 8%.

A static test was carried out on the same hose by coupling it to a deadweight tester and pressurising to 69 bar (1,000 lbf/in^2). An additional load of 0.69 bar (10 lbf/in^2) was then applied to the deadweight tester, and by measuring the depression of the load carriage with time due to the leakage past the loading ram the compressibility of the oil in the flexible hose determined. The measured compression time characteristic and hence the calculated compressibility of the oil on the flexible hose is shown on Fig. 6.19. A measured tangent bulk modulus of 6,600 bar (97,000 lbf/in^2) was obtained at 20^{o}C. and 69 bar (1,000 lbf/in^2). Applying the Hayward temperature correction, Equ.s 4.12 and 4.13, a value of 5,790 bar (84,000 lbf/in^2) was obtained at 50^{o}C.

The error between the static and dynamic test results for the flexible hose were significant when compared with the good correlation achieved with the overall test programme. A detailed study of the dynamic behaviour of flexible hose would be desirable. Initial work using a pressure loading valve (58) has been commenced, but needs extending.

6.6.5 Effect of Pressure Gauges

Most practical hydraulic transmission systems are fitted with Bourdon gauges with snubbers incorporated if pressure fluctuations are likely to be damaging to the gauge. Tests 29 - 32 were repeated with a 300 bar (4, 350 lbf/in^2) Bourdon tube gauge fitted to supply line (Tests 68 - 71). It was connected to the transmission supply line by an 8 m. length of 3.17 mm (.125 in.) internal diameter pipe and a snubber. The gauge line was carefully bled of all air and the frequency response tests carried out.

The average reduction in natural frequency resulting from the inclusion of the pressure gauge and line was $3\frac{1}{2}\%$.

Test No.	Amp. of Input Swash Deg.	Mean Pump Swash Deg.	Mean Motor Swash Deg.	Mean Load Torque Nm	Load Damping Co-eff. Nm/rad/sec	Engine Droop $\frac{\text{Rad/sec}}{\text{Nm}}$	Load Inertia Kg m^2	System Volume l	Overall Efficiency η_{ov} %	Test Feature
1	2.50	7.50	7.50	27.85	.681	.031	.0167	1.292	64.0	
2	2.50	7.17	7.42	30.05	.440	.739	.0167	1.292	76.0	Variation of Engine
3	2.50	7.50	7.50	28.50	.694	.429	.0167	1.292	59.0	Speed Load Droop
4	2.50	7.17	7.33	32.00	.400	1.056	.0167	1.292	70.0	
5	2.50	7.50	7.50	42.50	.524	1.645	.0167	1.292	63.5	
6	2.50	3.08	6.00	29.00	.948	.294	.0167	1.292	58.3	
7	2.50	4.75	7.50	20.60	.740	.150	.0167	1.292	64.8	Increasing
8	2.50	5.08	7.42	29.10	.690	.325	.0167	1.292	72.0	Pump Swash
9	2.50	7.33	7.42	34.90	.362	.202	.0167	1.292	79.0	
10	2.50	9.42	7.33	28.20	.286	.330	.0167	1.292	80.0	
11	2.50	4.42	7.50	20.00	.667	.295	.0167	1.292	65.0	Repeats of Test 7 to
12	2.50	4.42	7.33	20.10	.661	.294	.0167	1.292	63.5	check repeatability of
13	2.50	4.42	7.33	20.60	.677	.306	.0167	1.292	63.0	results
14	5.00	7.33	7.66	34.50	.444	.189	.0167	1.292	77.5	Increased input swash variation
15	2.50	5.00	10.00	25.40	1.380	.775	.0167	1.292	-	Increased motor swash
16	2.50	7.50	7.50	13.27	.264	.775	.0167	1.292	-	Low load damping co-efficient
17	2.50	7.50	7.50	24.40	.598	.775	.0167	2.990	-	Large System
18	2.50	9.42	7.25	28.90	.279	.303	.0167	2.990	81.0	Volume
19	2.50	7.50	7.50	23.40	.640	.775	.3150	1.292	-	Increased Load Inertia

TABLE 6.1 STEADY STATE CONDITIONS for FIRST SERIES of DYNAMIC RESPONSE TESTS

Test No.	Natural Frequency - Rad/sec ω_n			Damping Ratio - ξ			Test Feature
	Predicted	Measured	Error % + ve Underestimate	Predicted	Measured	Error % + ve Underestimate	
1	36.89	35.2	- 4.8	0.629	0.65	3.0	Variation of Engine Speed Load Droop
2	35.44	39.8	12.0	0.443	0.70	82.0	
3	36.51	36.1	- 1.2	0.637	0.70	9.4	
4	34.88	39.1	12.0	0.417	0.65	56.0	
5	36.36	36.3	- 0.3	0.601	0.58	- 3.4	
6	31.35	43.1	37.4	0.991	0.91	- 8.1	Increasing Pump Swash
7	36.88	46.2	25.7	0.667	-	-	
8	35.37	41.4	14.5	0.658	0.80	21.3	
9	35.07	34.1	- 2.7	0.380	0.55	45.0	
10	34.80	35.1	0.9	0.329	0.50	52.0	
11	36.41	45.6	25.3	0.623	0.80	29.0	Repeats of test 7 to ensure repeatability of test results
12	35.69	43.9	23.0	0.630	0.78	24.0	
13	35.36	45.3	28.0	0.649	0.80	23.1	
14	36.66	38.5	5.0	0.509	0.65	27.5	Increased input swash variations
15	35.90	34.6	- 3.6	0.510	0.65	27.5	Increased motor swash
16	35.19	32.0	- 9.1	0.304	0.35	16.4	Low load damping coefficient
17	21.90	25.1	14.6	0.890	0.80	- 10.1	Large system volume
18	22.53	29.0	28.8	0.433	0.65	28.0	
19	15.80	16.7	5.4	0.370	0.35	- 5.4	Increased load inertia

TABLE 6.2 RESULTS of FIRST SERIES of DYNAMIC TESTS

Test No.	Amp. of Input Swash Deg.	Mean Pump Swash Deg	Mean Motor Swash Deg.	Mean Load Torque Nm	Load Damping Co-eff. Nm/rad/sec	Mean Motor Speed Rev/min	Load Inertia Kg m^2	System Volume Litres	Eng. Speed Load Droop Rad/sec/Nm	Test Feature
20	2.50	4.42	7.42	38.6	.602	588	.0167	.957	0.147	
21	2.50	4.42	7.42	-	-	-	.0167	.957	0.147	To determine the
22	2.50	4.42	7.42	-	-	-	.0167	.957	0.147	effect of cycle
23	2.50	4.42	7.42	-	-	-	.0167	.957	0.147	loading on
24	2.50	4.42	7.42	38.6	.592	584	.0167	.957	0.147	transmission.
25	2.50	3.40	7.42	7.1	.288	245	.0167	.957	0.147	
26	2.50	5.20	7.42	18.1	.365	625	.0167	.957	0.147	Typical windage
27	2.50	7.00	7.42	36.2	.405	910	.0167	.957	0.147	load simulation.
28	2.50	8.80	7.42	52.0	.471	1158	.0167	.957	0.147	
29	3.76	4.75	7.42	33.0	.587	594	.0167	.957	0.147	Effect of load damping
30	3.76	4.75	7.42	33.5	.407	578	.0167	.957	0.147	coefficient variation.
31	3.76	4.75	7.42	33.3	.194	585	.0167	.957	0.147	Other parameters
32	3.76	4.75	7.42	33.6	.037	572	.0167	.957	0.147	held constant.
33	1.25	4.75	7.42	33.6	.544	579	.0167	.957	0.147	
34	1.25	4.75	7.42	33.9	.415	582	.0167	.957	0.147	Tests 29 - 32 repeated
35	1.25	4.75	7.42	33.4	.176	564	.0167	.957	0.147	with smaller input
36	1.25	4.75	7.42	33.6	.035	579	.0167	.957	0.147	amplitude.

TABLE 6.3 STEADY STATE CONDITIONS for SECOND SERIES of DYNAMIC TESTS

TEST NO.	Natural Frequency - ω_n Rad/sec.			Damping Ratio - ξ			TEST FEATURE
	Predicted	Measured	Error % + ve Underestimate	Predicted	Measured	Error % + ve Underestimate	
20	41.4	49.6	+ 19.8	.54	.85	57.5	
21	-	49.6	-	-	.85	-	To determine
22	-	46.8	-	-	.75	-	effect of cycling
23	-	47.7	-	-	.90	-	loading on
24	41.4	46.9	+ 13.0	.53	.70	32.0	transmission.
25	40.7	34.5	- 14.8	.31	.40	29.0	
26	41.2	37.7	- 10.9	.36	.48	33.3	Typical windage
27	41.4	39.5	- 2.2	.38	.52	36.8	load simulation.
28	41.7	45.2	8.4	.42	.58	38.2	
29	37.6	40.2	+ 7.1	.55	.60	9.1	Effect of load
30	36.9	37.6	+ 1.9	.42	.50	19.0	damping coefficient.
31	36.0	32.0	- 11.0	.26	.30	15.4	Other parameters
32	35.3	30.1	- 15.0	.14	.20	43.0	held constant.
33	37.6	40.8	+ 8.5	.55	.60	9.1	Tests 29 - 32
34	36.9	37.6	+ 1.9	.42	.40	- 4.8	repeated with
35	36.0	35.0	- 2.8	.26	.28	7.2	smaller input
36	35.3	32.3	- 8.5	.14	.26	86.0	amplitude.

TABLE 6.4 RESULTS of SECOND SERIES of DYNAMIC TESTS

TEST NO.	Pump Swash Step Input Degrees	Pump Swash Degrees	Fixed Motor Swash Degrees	Load Torque Nm	Motor Speed Rev/min.	Load Damping Coefficient Nm/Rad/Sec	Measured Step Response		TEST FEATURE
							Natural Frequency - ω_n Rad/Sec	Damping Ratio - ξ	
37	1.77	2.20	7.42	18.8	271	.408	33.3	.51	
38	3.54	2.20	7.42	18.8	270	.408	33.9	.54	Windage
39	1.77	4.00	7.42	30.6	522	.491	39.8	.55	Load
40	3.54	4.00	7.42	30.3	515	.491	35.3	.59	Simulation No.1
41	1.77	5.80	7.42	43.8	771	.630	40.7	.51	
42	3.54	5.80	7.42	42.8	760	.630	42.3	.51	
43	1.77	2.20	7.42	21.8	255	.275	35.6	.47	
44	3.54	2.20	7.42	22.3	262	.275	32.9	.50	Windage
45	1.77	4.00	7.42	32.7	500	.333	36.5	.51	Load
46	3.54	4.00	7.42	32.7	500	.333	33.8	.54	Simulation No.2
47	1.77	5.80	7.42	45.1	754	.382	36.4	.51	
48	3.54	5.80	7.42	44.9	751	.382	36.4	.53	
49	1.77	2.20	7.42	28.0	243	.101	29.5	.26	
50	3.54	2.20	7.42	28.0	248	.101	28.5	.26	Windage
51	1.77	4.00	7.42	32.2	504	.155	31.2	.30	Load
52	3.54	4.00	7.42	32.2	504	.155	30.2	.33	Simulation No.3
53	1.77	5.80	7.42	38.1	772	.174	29.9	.33	
54	3.54	5.80	7.42	38.1	781	.174	29.8	.33	

TABLE 6.5 STEP RESPONSE TEST SERIES

TABLE 6.6 COMPARISON BETWEEN THEORETICALLY PREDICTED AND EXPERIMENTALLY MEASURED DYNAMIC RESPONSE OF HYDROSTATIC TRANSMISSION

TEST NO.	Natural Frequency - ω_n Hz				Damping Ratio - ξ			
	Simple Theory of Equation 3.6	From Signal Flow Analysis	Vector Analysis	Experimental	Simple Theory of Equation 3.6	From Signal Flow Analysis	Vector Analysis	Experimental
29	6.20	6.63	6.54	6.4	0.44	0.50	0.55	0.60
30	6.20	6.50	6.06	6.0	0.28	0.38	0.48	0.50
31	6.20	6.36	5.45	5.1	0.15	0.24	0.30	0.30
32	6.20	6.24	4.93	4.8	0.03	0.13	0.20	0.20

TEST NO.	Amp. of Input Swash Angle Deg.	Mean Pump Swash Deg.	Mean Motor Swash Deg.	Mean Load Torque Nm	Load Damping Co-eff. Nm/Rad/S	Mean Motor Speed Rev/min.	Load Inertia Kg m^2	System Volume Litres	Mean Return Line Press. Bar	TEST FEATURE
55	1.25	4.75	7.42	42.1	.035	563	.1900	.957	13.8	Large Load
56	1.88	4.75	7.42	42.1	.037	560	.1900	.957	13.8	Inertia
57	3.76	4.75	7.42	25.7	.415	562	.0167	.957	6.1	Mean Return
58	3.76	4.75	7.42	24.3	.419	574	.0167	.957	20.7	Line Pressure
59	3.76	5.12	7.42	24.4	.422	624	.0167	.957	25.4	Varied
60	1.25	4.75	7.42	18.8	.595	595	.0167	.957	13.8	Tests with
61	3.76	4.75	7.42	22.3	.540	585	.0167	.957	13.8	Restricted
62	1.25	4.75	7.42	21.9	.230	597	.0167	.957	13.8	Boost
63	3.76	4.75	7.42	22.3	.234	596	.0167	.957	13.8	System
64	3.76	4.75	7.42	26.4	.557	589	.0167	.957	13.8	Supply Line
65	3.76	4.75	7.42	26.7	.447	582	.0167	.957	13.8	Replaced by
66	3.76	4.75	7.42	26.8	.204	587	.0167	.957	13.8	Rubber
67	3.76	4.75	7.42	25.7	.037	580	.0167	.957	13.8	Flexible Hose
68	3.76	4.75	7.42	28.6	.597	591	.0167	.957	13.8	Pressure
69	3.76	4.75	7.42	28.0	.460	582	.0167	.957	13.8	Gauge
70	3.76	4.75	7.42	28.0	.324	577	.0167	.957	13.8	Connected into
71	3.76	4.75	7.42	27.6	.037	583	.0167	.957	13.8	Supply Line

TABLE 6.7 THIRD SERIES OF FREQUENCY RESPONSE TESTS

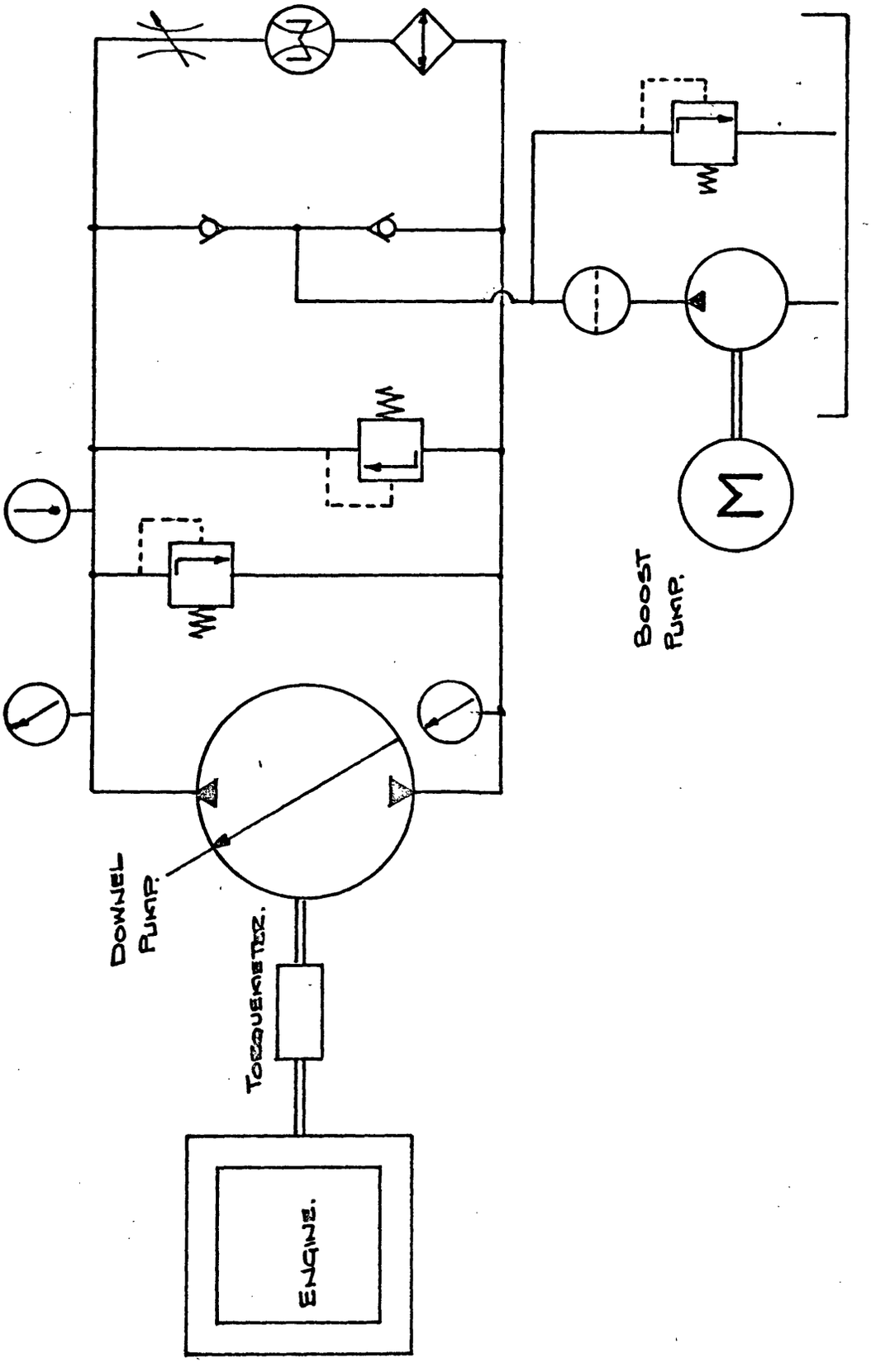

FIG. 6.1 TEST RIG FOR MEASURING STEADY STATE PERFORMANCE CHARACTERISTICS OF DOWNEL PUMP.

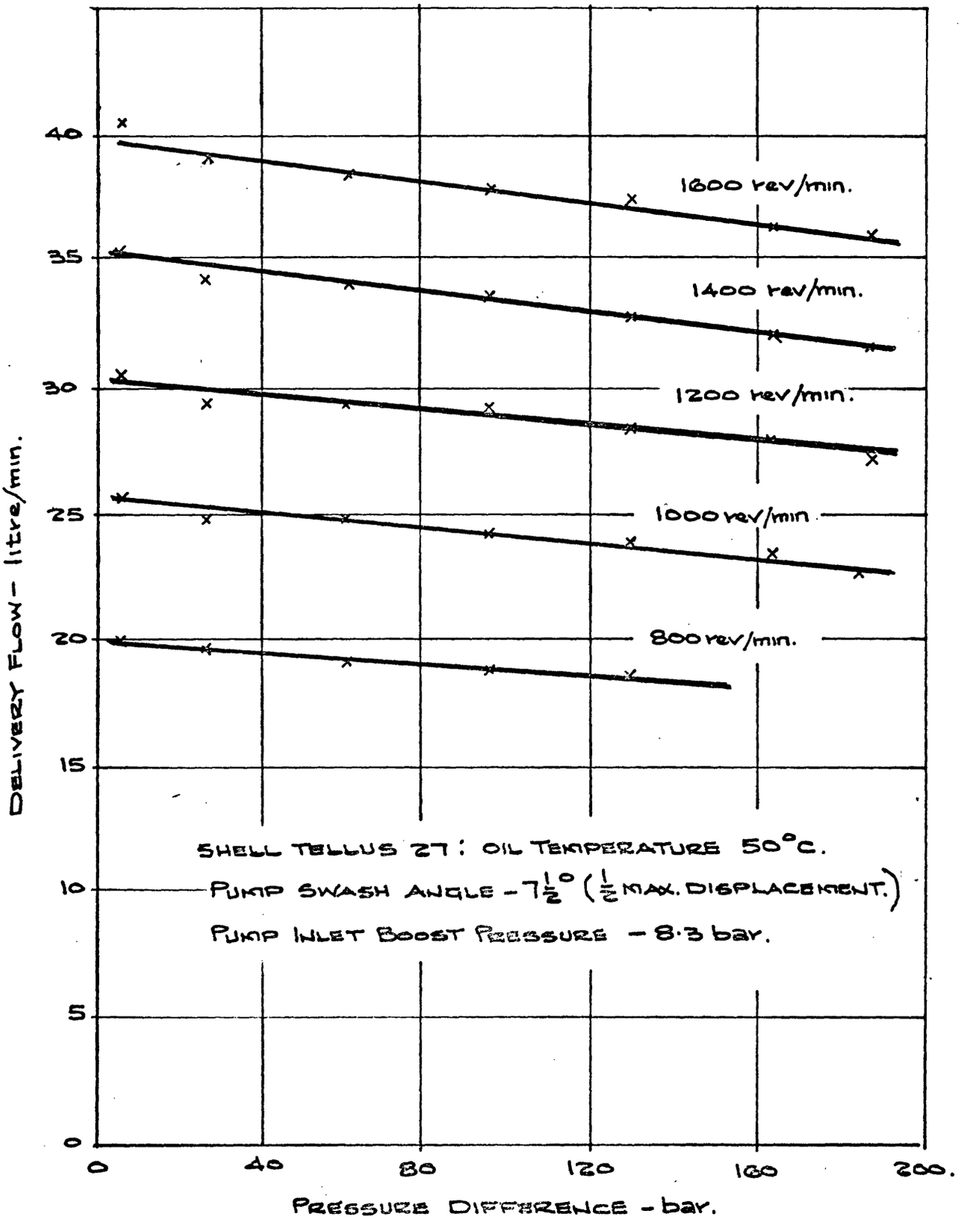

FIG. 6.2 VARIATION OF PUMP FLOW WITH PRESSURE AT CONSTANT SPEED.

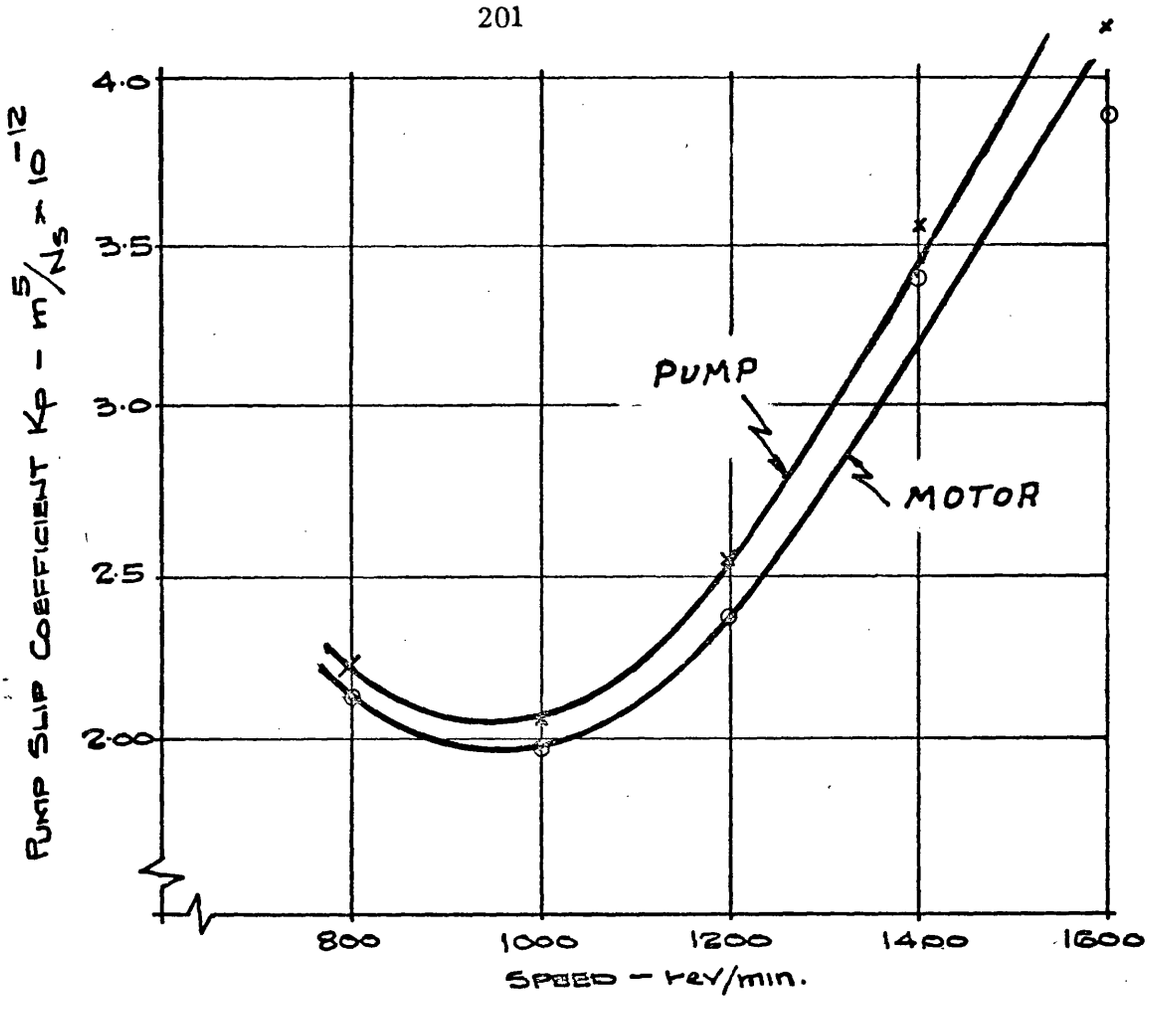

FIG. 6.3 (a) VARIATION OF PUMP SLIP COEFFICIENT WITH SPEED.

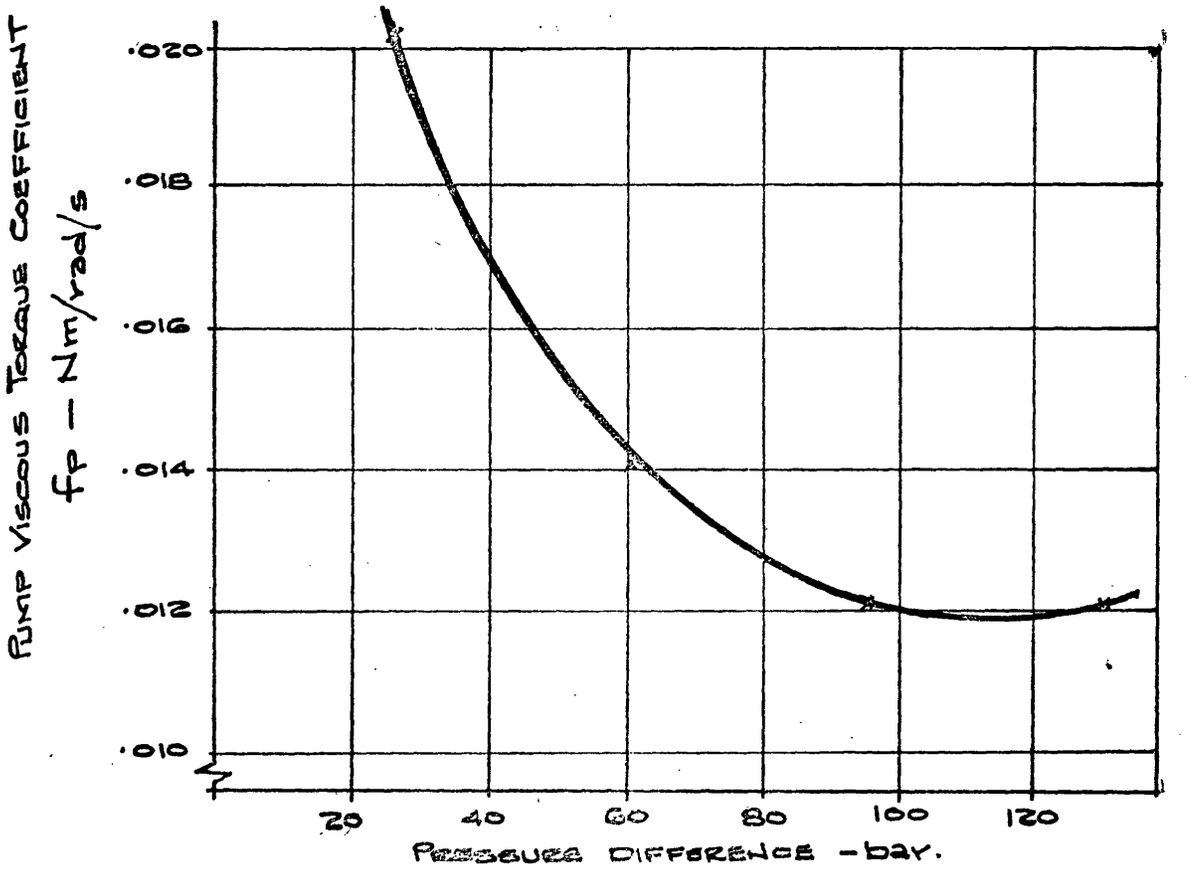

FIG. 6.3 (b) VARIATION OF PUMP VISCOUS TORQUE COEFFICIENT WITH PRESSURE.

FIG. 6.3 PUMP SLIP AND VISCOUS TORQUE LOSS COEFFICIENTS

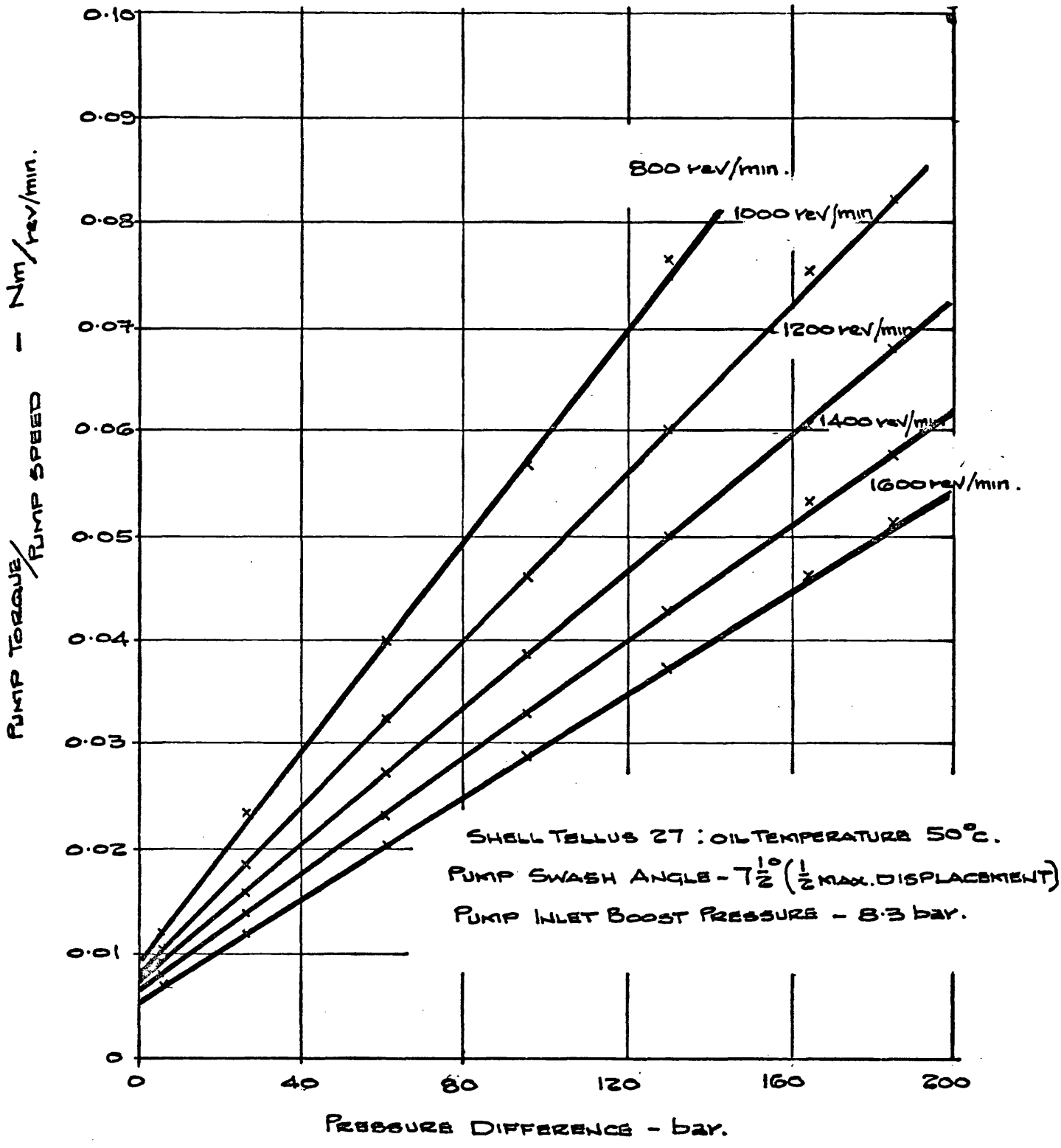

FIG 6.4 VARIATION OF PUMP TORQUE WITH PRESSURE DIFFERENCE AT CONSTANT SPEED.

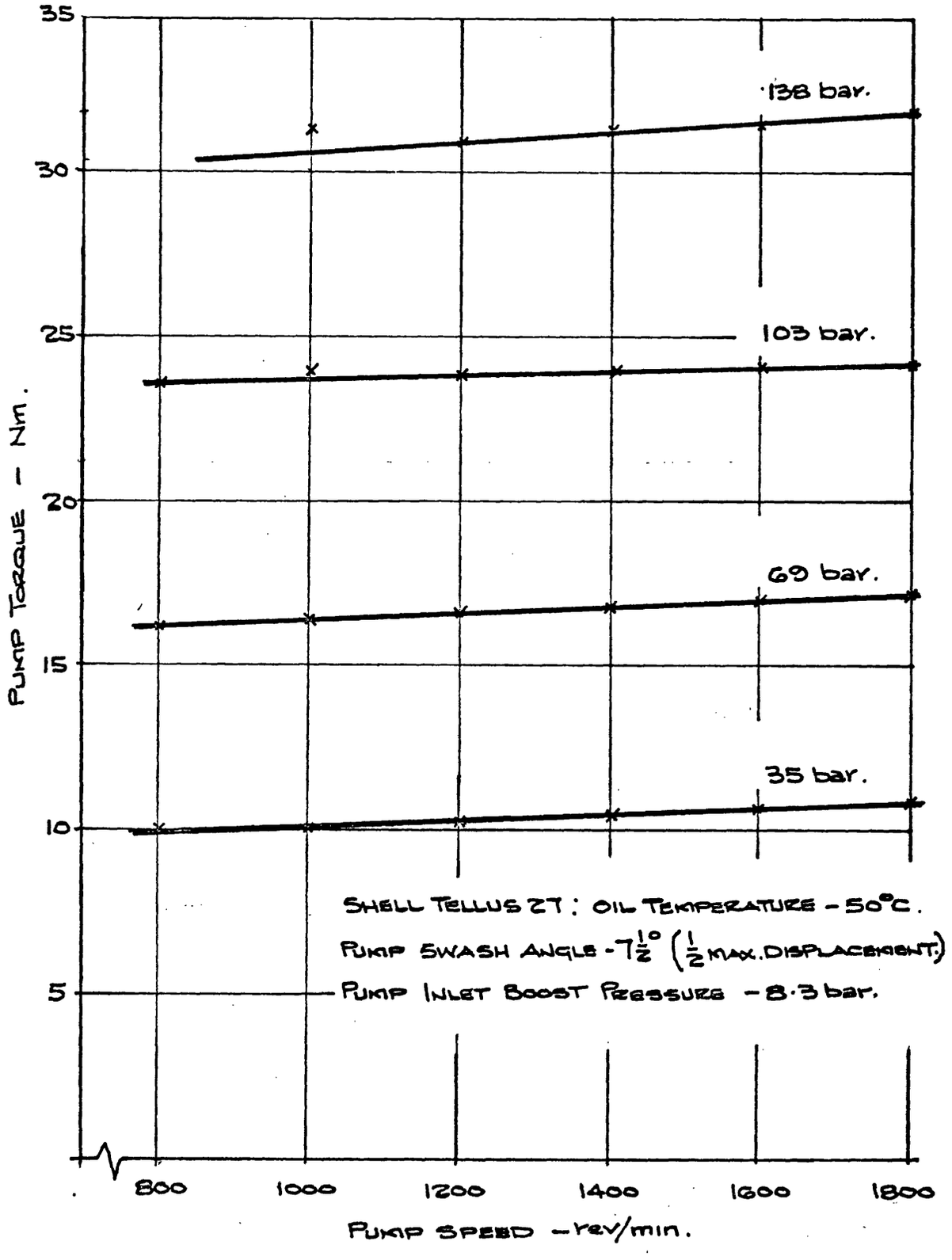

FIG. 6.5 VARIATION OF PUMP TORQUE WITH SPEED AT CONSTANT PRESSURE.

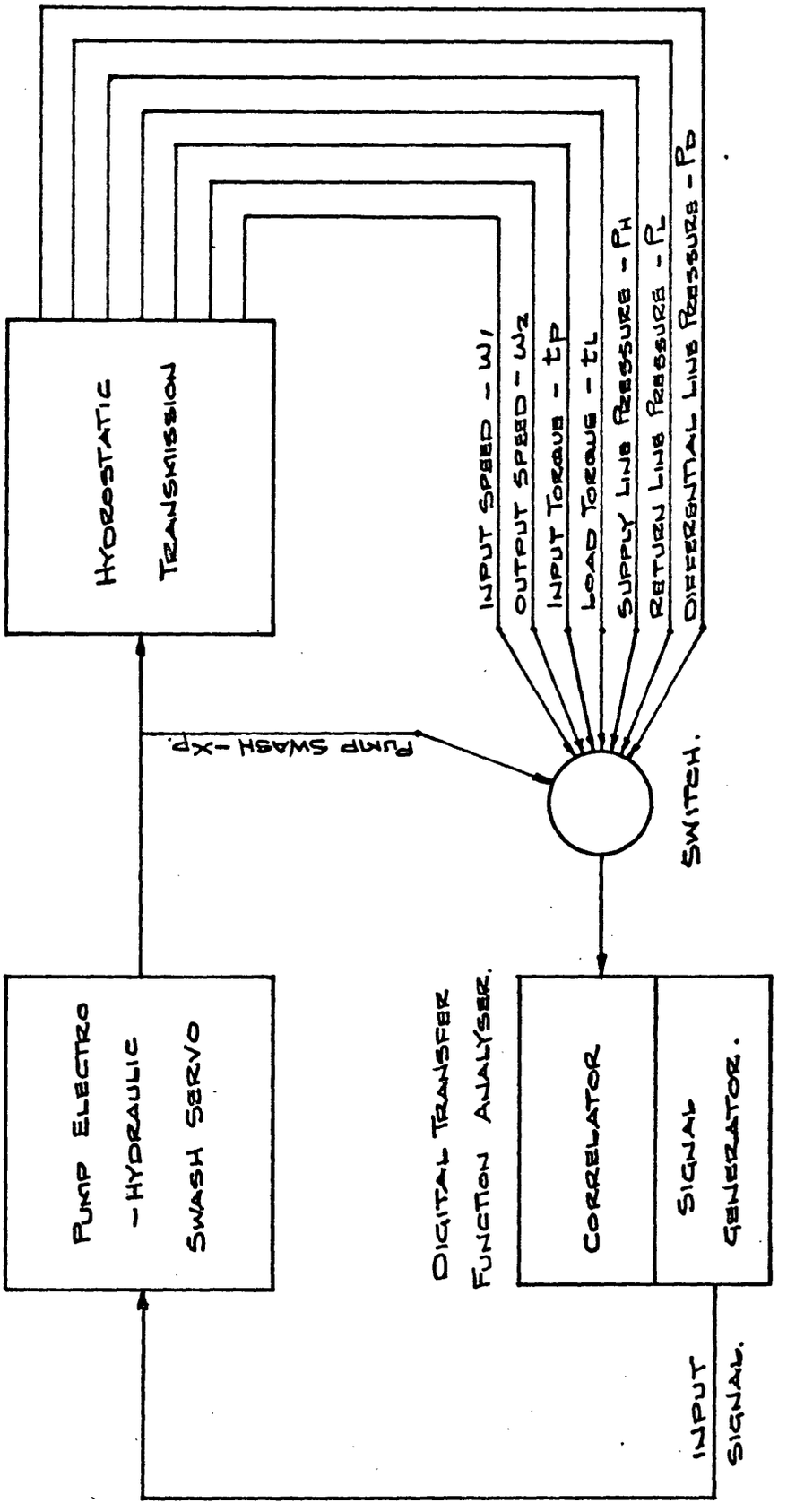

Fig. 9.6 Schematic illustrating technique for frequency response testing.

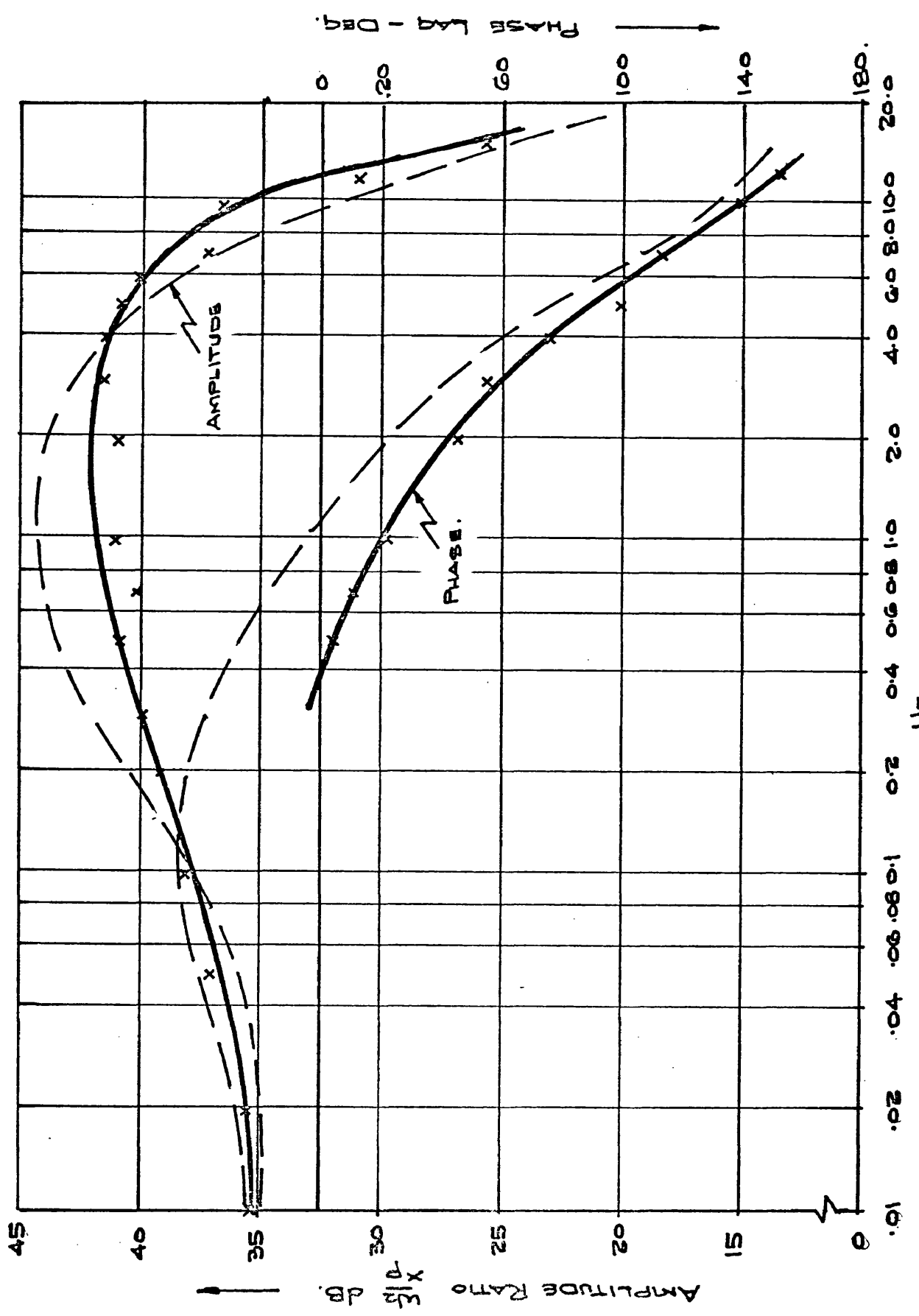

Fig. 6.7 Experimentally Determined Frequency Response For Test 5 Compared With Theoretically Computed Results.

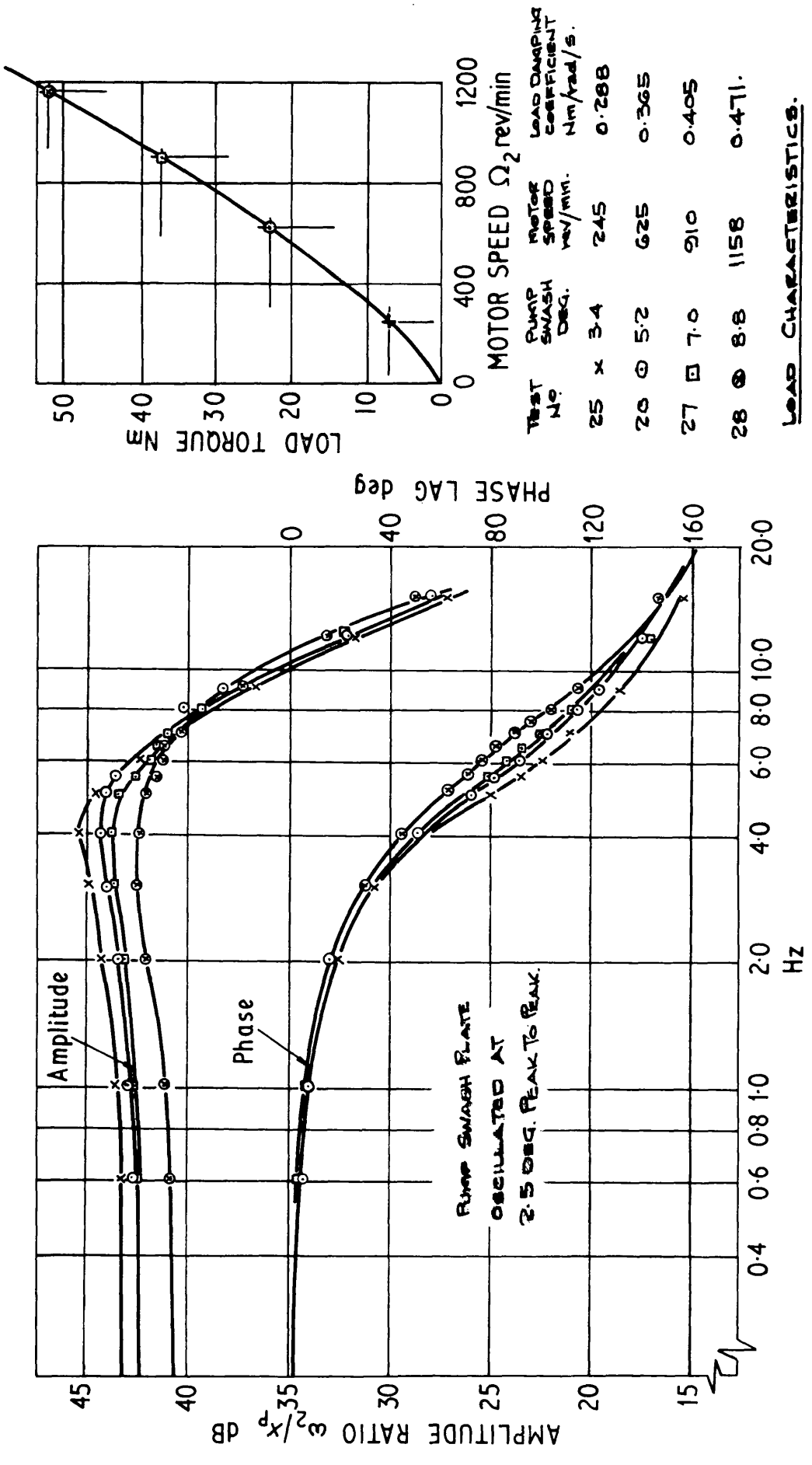

FIG. 6.8 OVERALL FREQUENCY RESPONSE OF TRANSMISSION WITH WINDAGE LOAD.

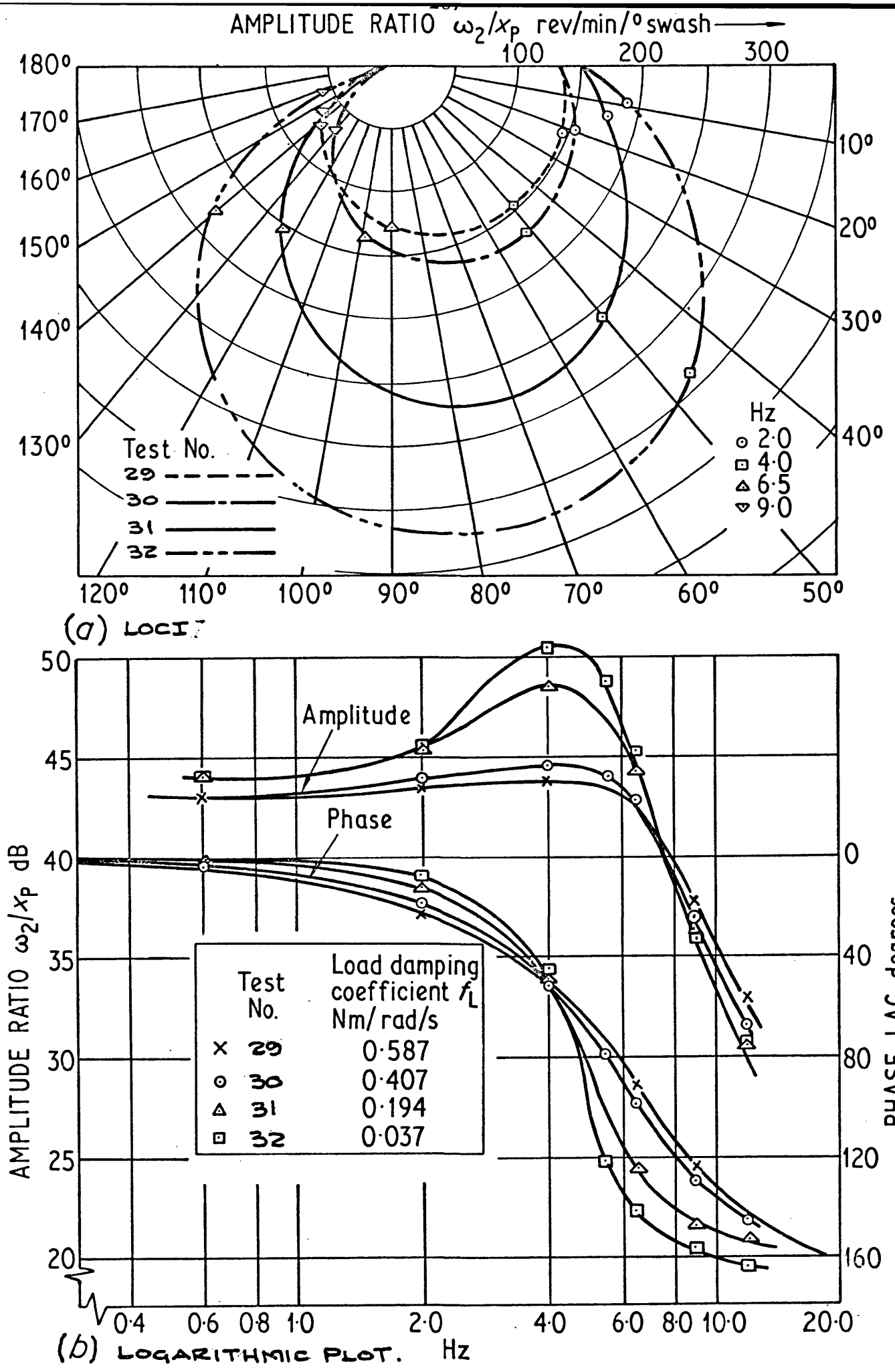

FIG. 6.9 EFFECT OF LOAD DAMPING COEFFICIENT ON TRANSMISSION DYNAMIC RESPONSE.

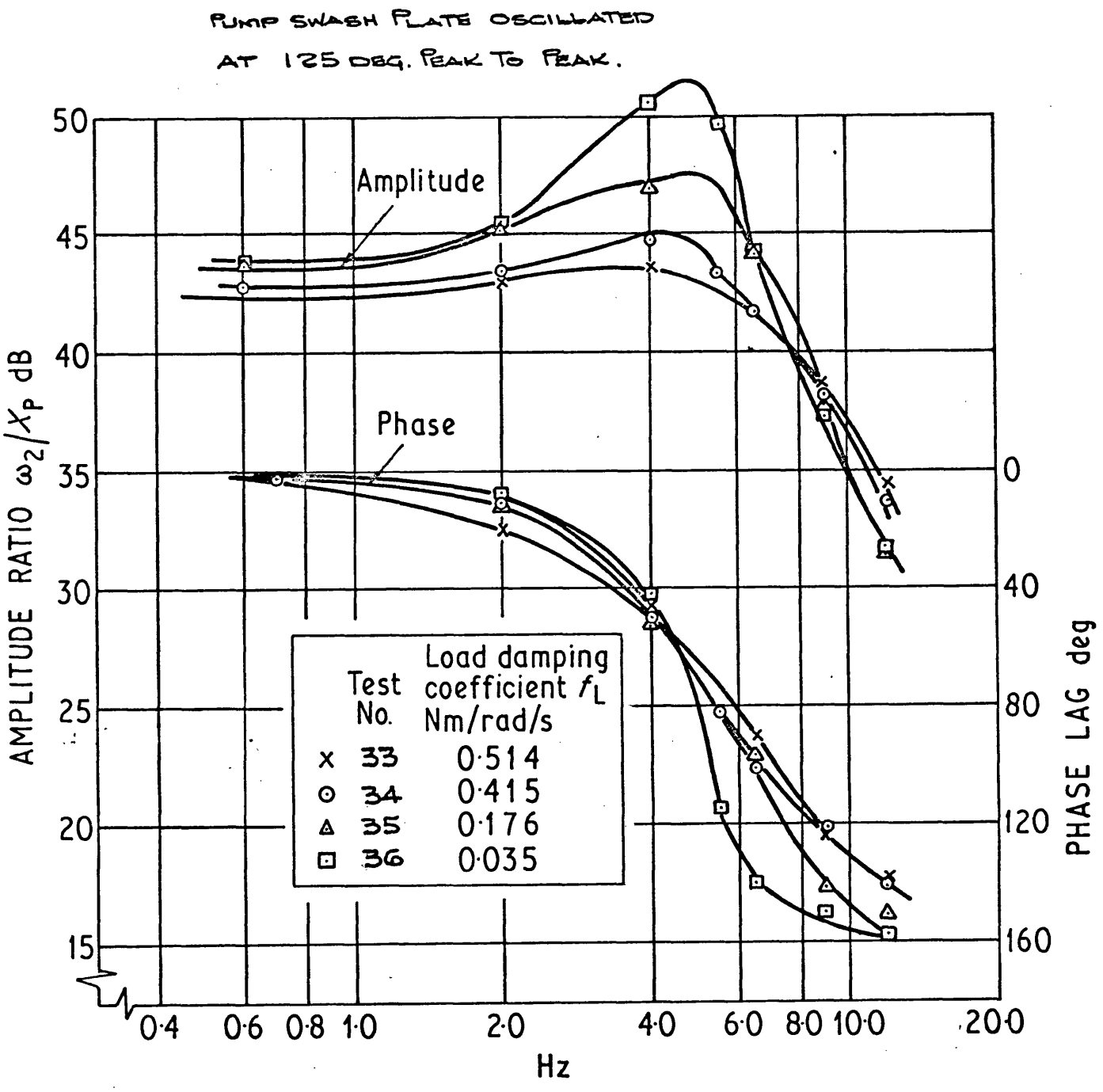

Fig. 6.10 The Effect of Load Damping Coefficient on Overall Transmission Response Using Smaller Input Amplitude.

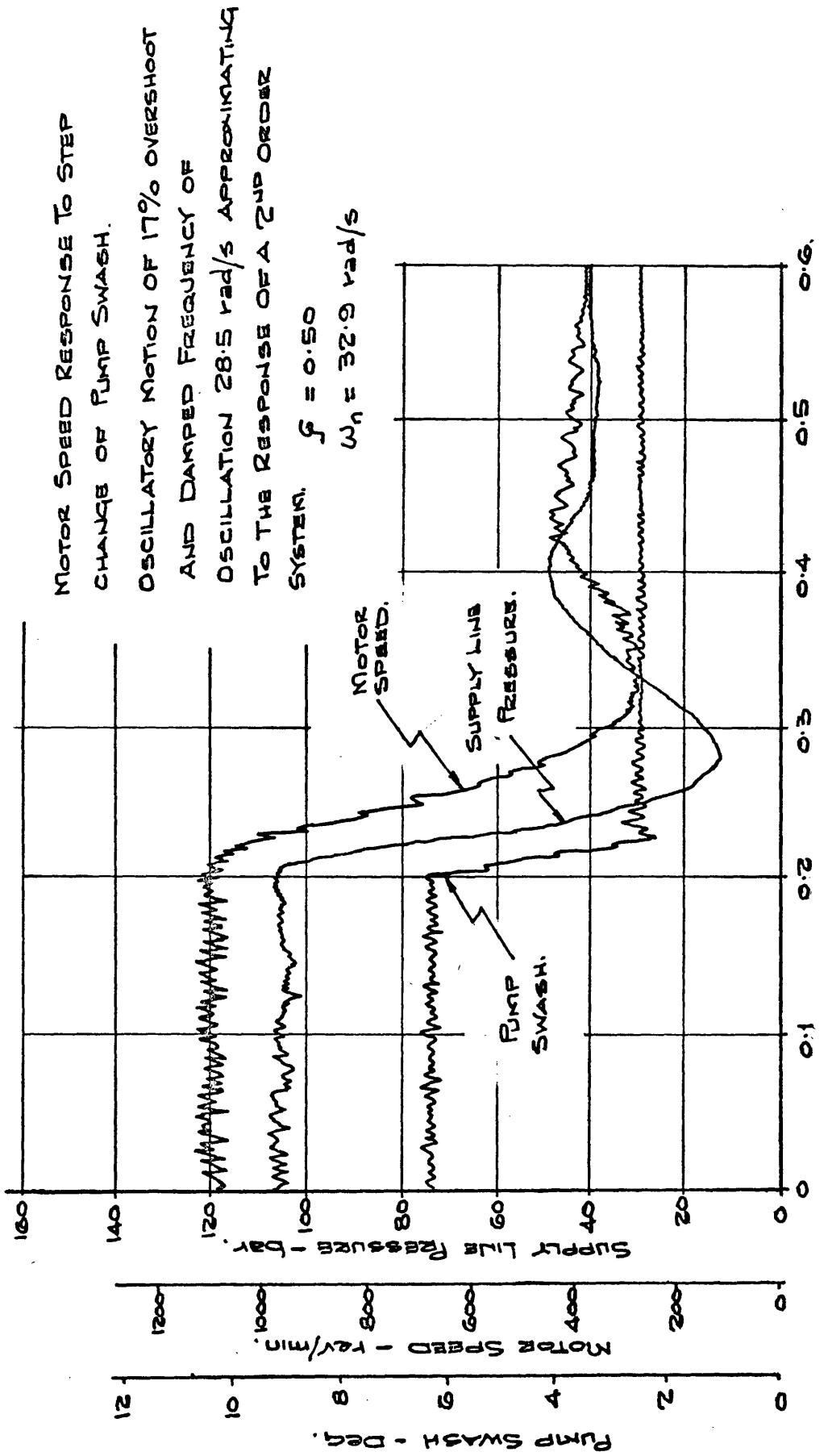

Fig. 6.11 Step Response Galvanometer Recording For Test 44.

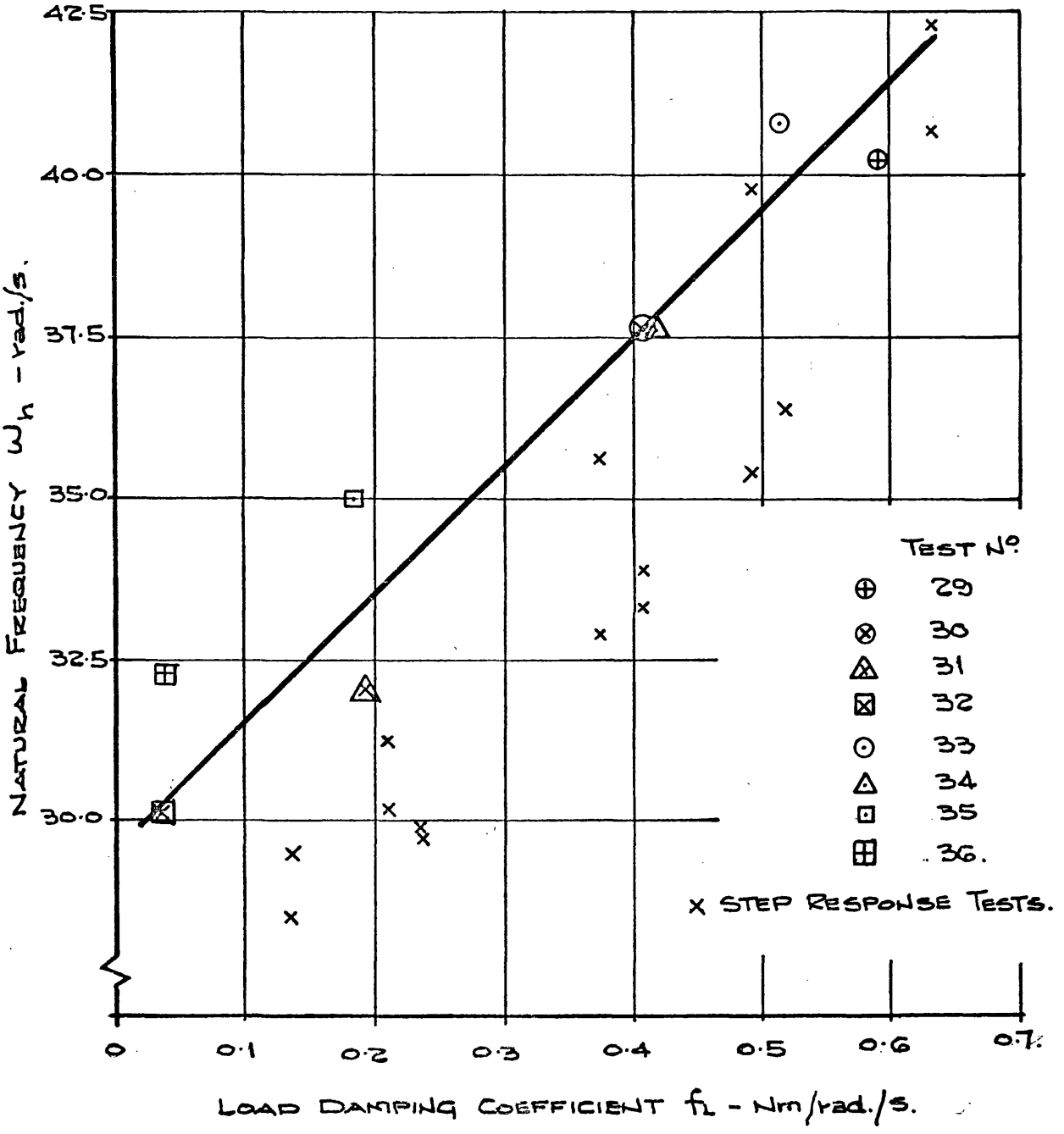

FIG 6.12 VARIATION OF TRANSMISSION APPARENT NATURAL FREQUENCY WITH LOAD DAMPING COEFFICIENT f_L MEASURED BY STEP RESPONSE TECHNIQUE.

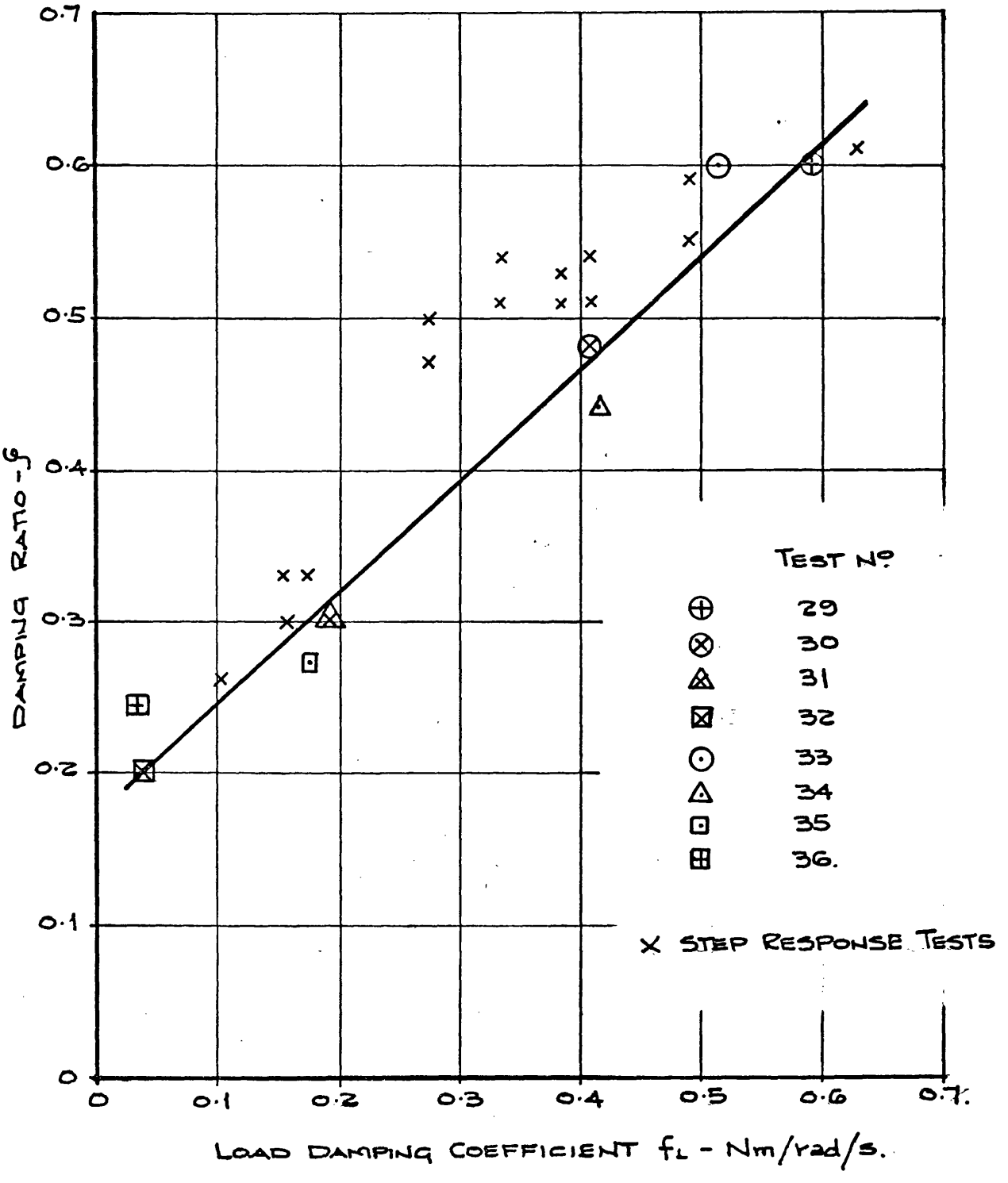

Fig. 6.13 Variation of Transmission Damping Ratio with Load Damping Coefficient Measured by Step Response Technique.

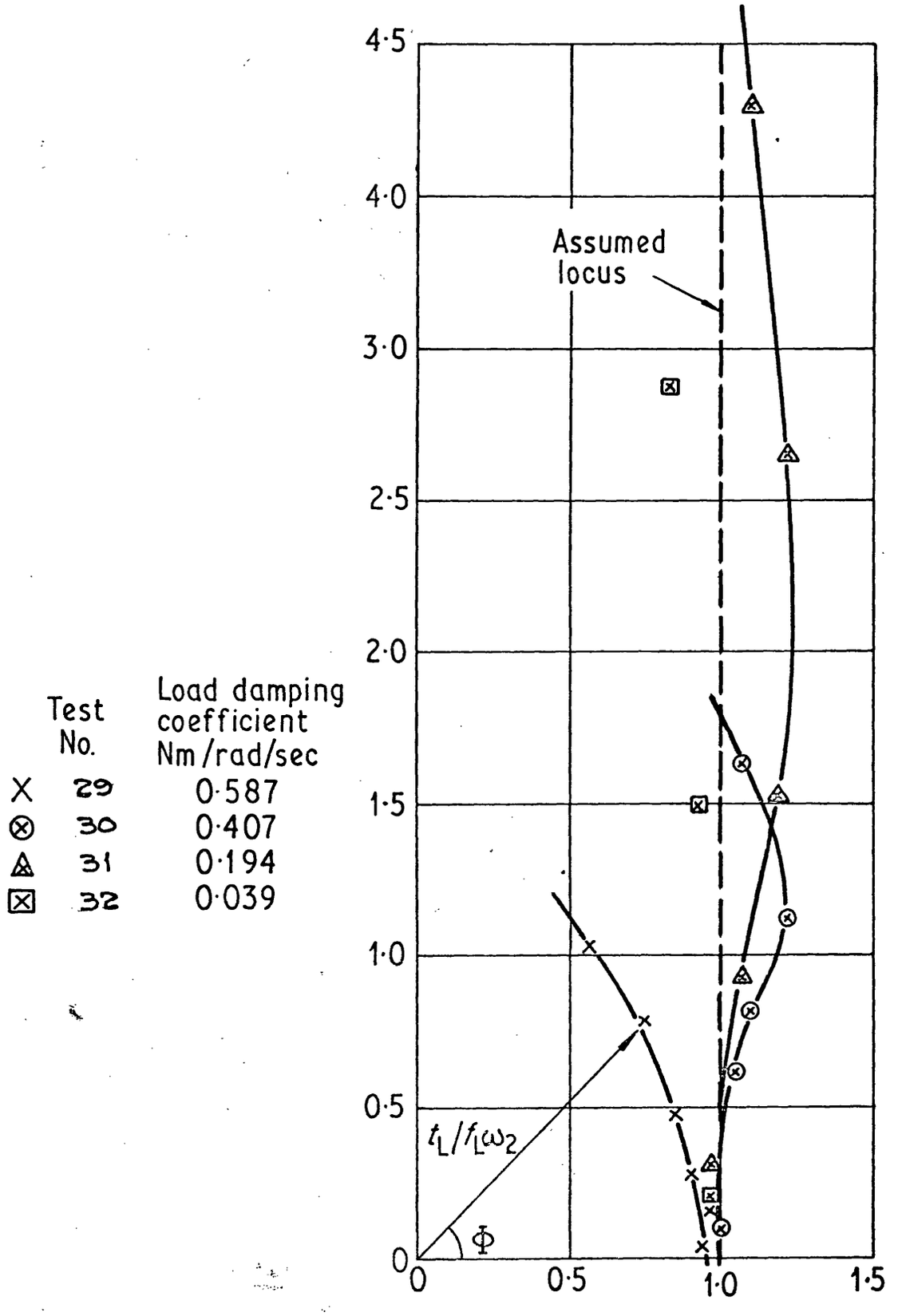

FIG 6.14 THE LOCUS OF THE MEASURED HYDROSTATIC LOAD.

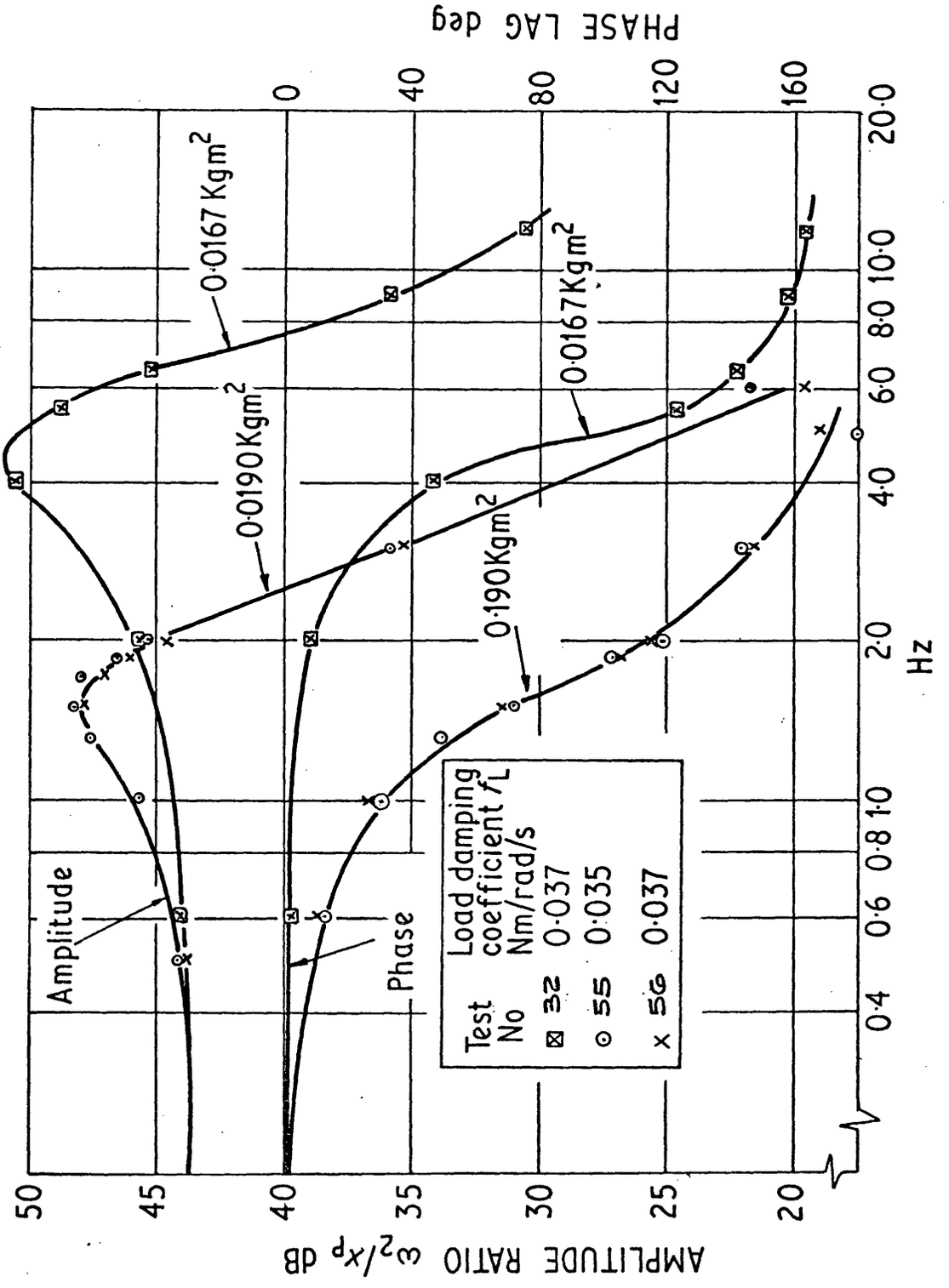

FIG. 6.15. THE EFFECT OF AN INCREASED INERTIAL LOAD ON OVERALL TRANSMISSION RESPONSE.

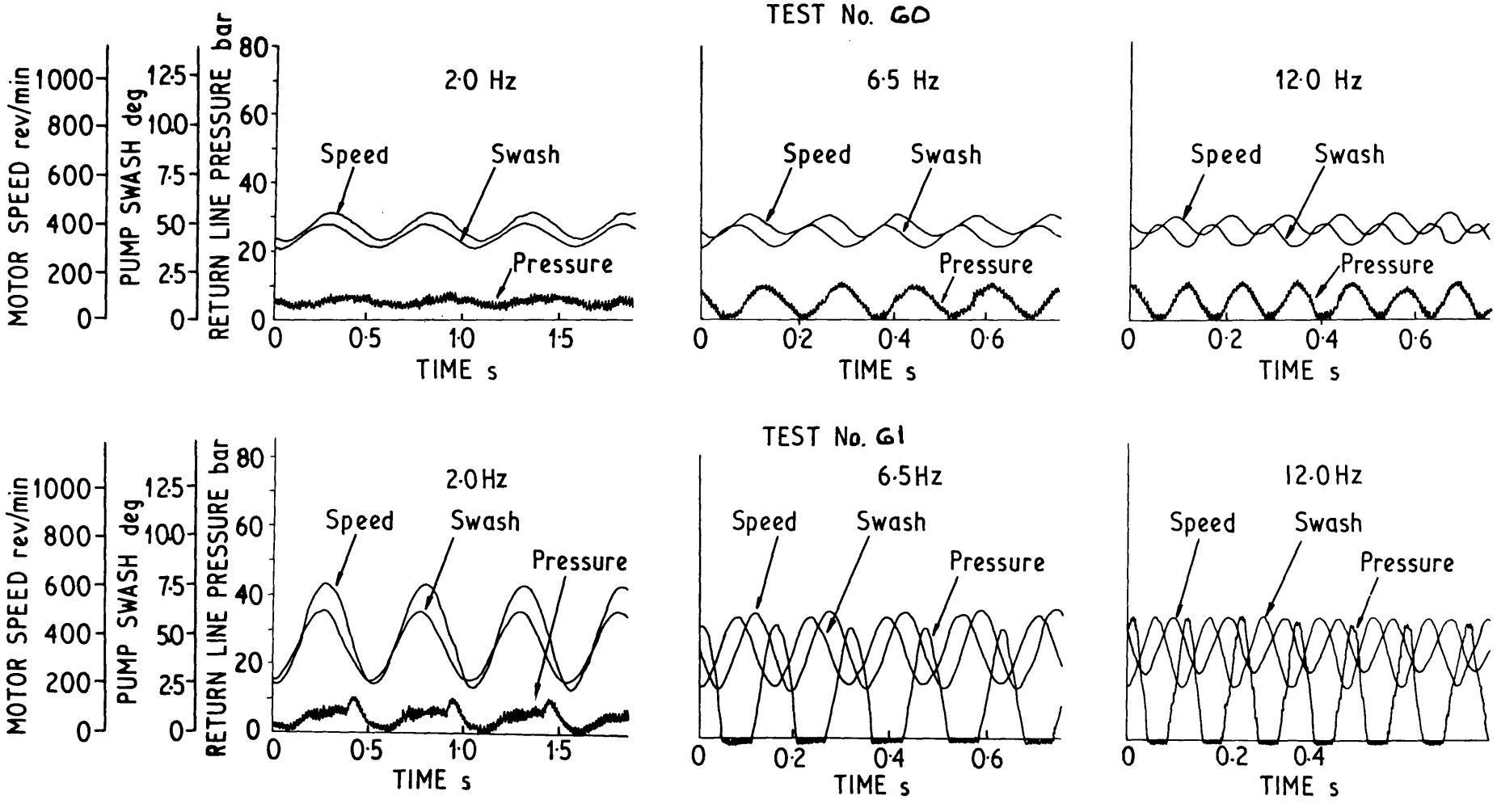

FIG. 6.16 GALVANOMETER READINGS OF SWASH PLATE ANGLE, OUTPUT SPEED RETURN LINE PRESSURE FOR RESTRICTED BOOST SYSTEMS.

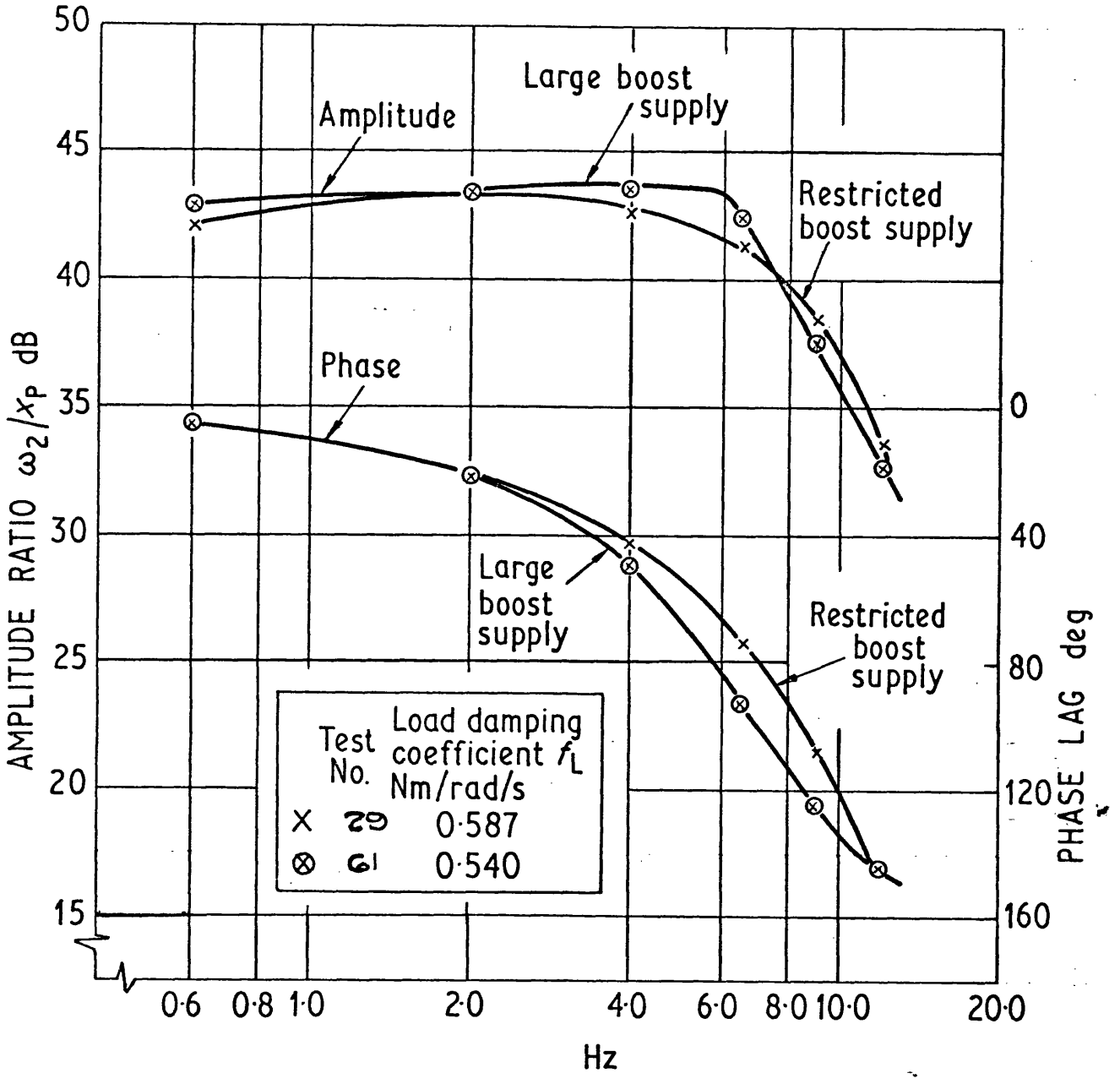

FIG. 6.17 THE EFFECT OF RESTRICTED BOOST SUPPLY UPON OVERALL TRANSMISSION RESPONSE.

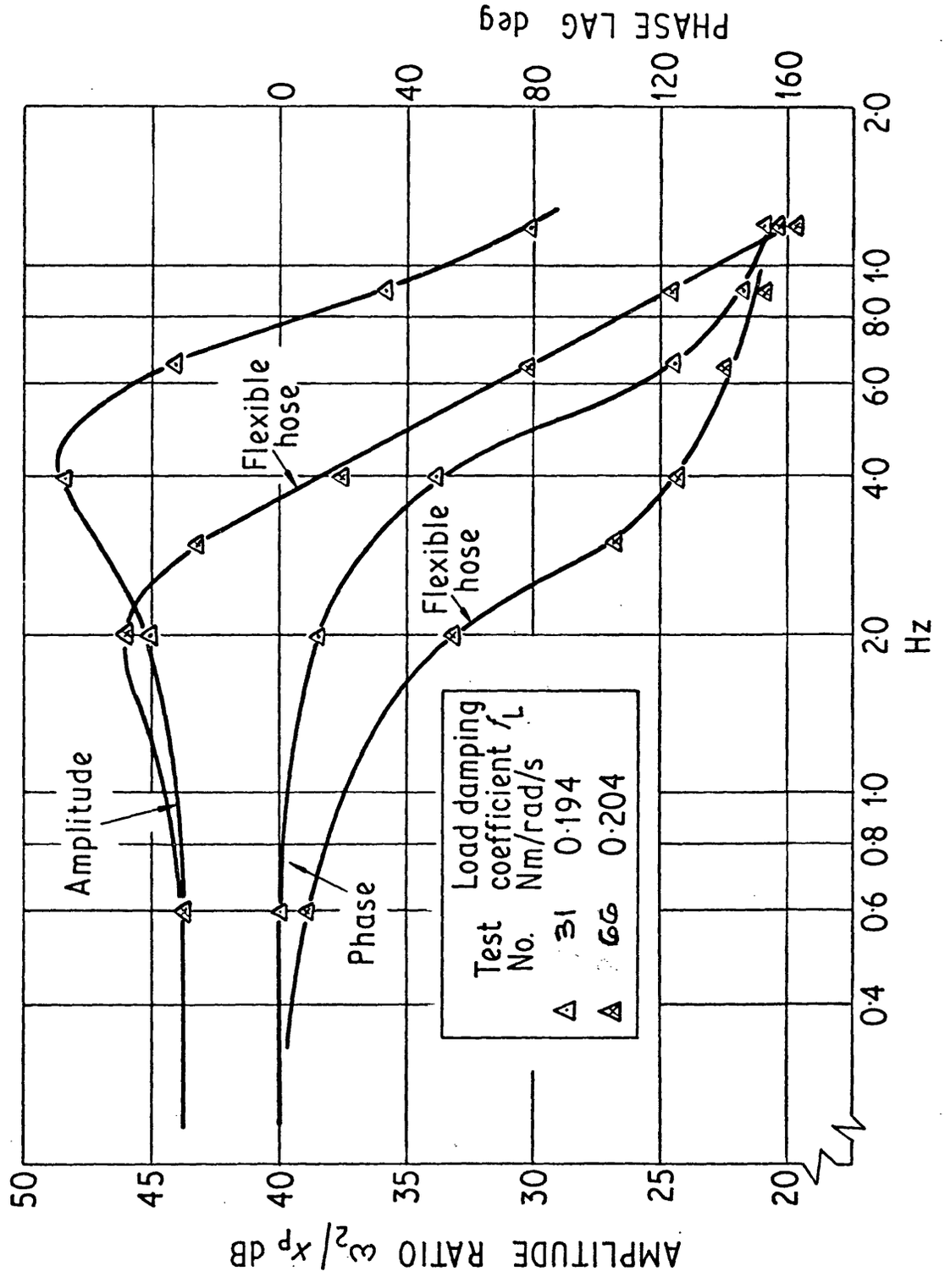

Fig. 6.18 The Effect of Using a Flexible Hose Supply Line on Overall Transmission Response.

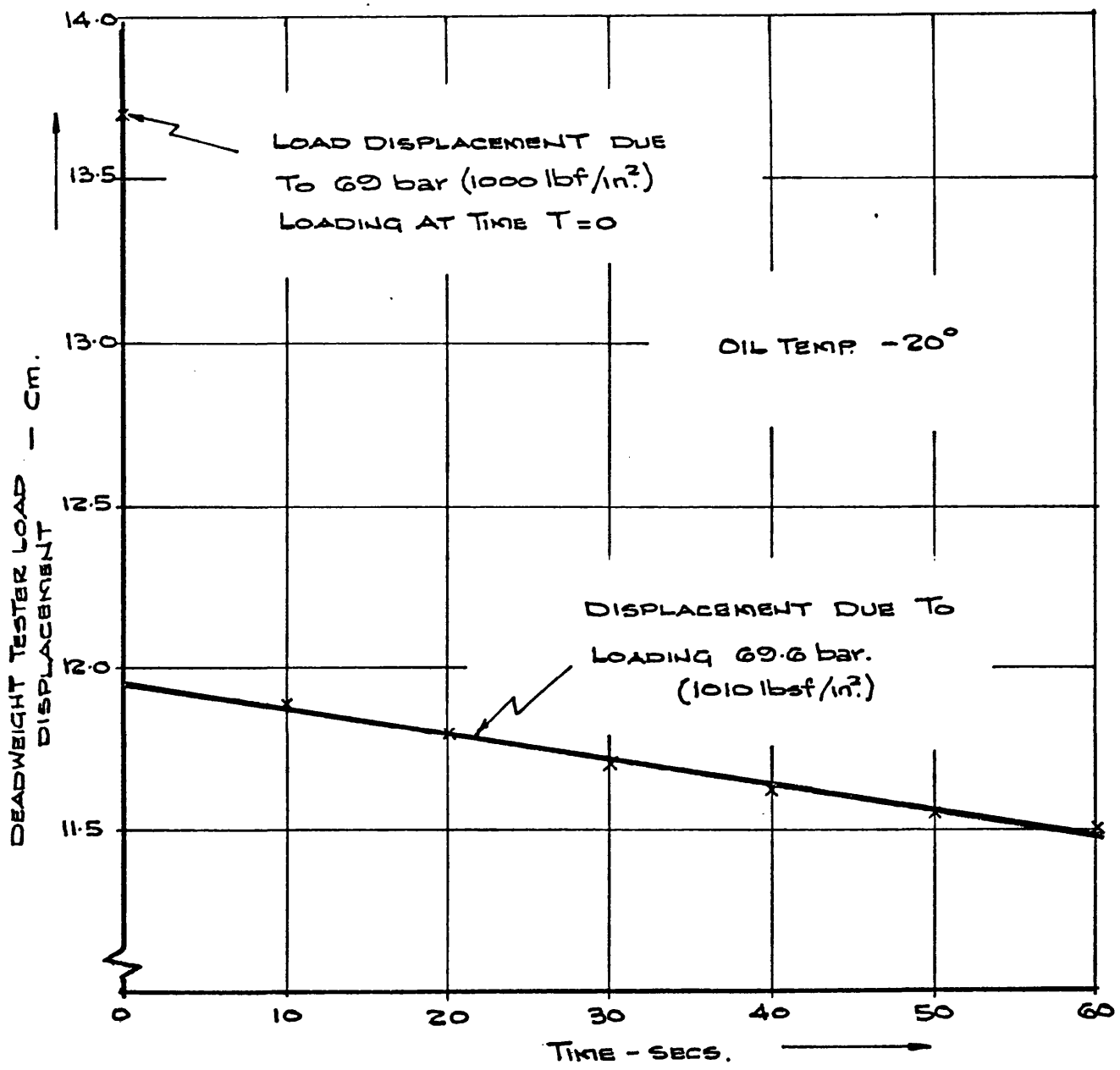

EXTRAPOLATING TO TIME $T=0$.

$$\delta V = \frac{13.70 - 11.95}{4.88}\ cm^3$$ DUE TO ADDITIONAL LOAD.

EFFECTIVE ISENTROPIC TANGENT BULK MODULUS OF OIL IN FLEXIBLE HOSE AT 69·0 bar AND 20°C

= 6,600 bar. (97,000 lbf/in².)

FIG 6.19 STATIC TEST DETERMINATION OF EFFECTIVE BULK MODULUS OF OIL IN FLEXIBLE HOSE USING DEADWEIGHT TESTER.

CHAPTER 7 : The DYNAMICS of HYDROSTATIC TRANSMISSIONS TEST RIG used to INVESTIGATE AERATION EFFECTS

7.1 The Effects of Aeration upon Hydrostatic Transmission Performance and the Proposed Experimental Investigation

As described in Chapter 4.4, the presence of air in hydraulic systems can cause considerable reduction in system performance, and has very often been blamed for causing any discrepancy between the theoretically predicted and experimentally measured dynamic performance of hydraulic systems.

The experimental work on hydrostatic transmissions and the subsequent development of the vector analysis technique for the theoretical determination of dynamic performance provided an excellent tool with which to investigate the effects of aeration upon dynamic performance.

Since dissolved air has no effect on system performance and any pockets of free air present would soon be flushed out of a properly designed system, the main interest is in the air dissolved in the system fluid which can subsequently be released in bubble form and then redissolved (adsorbed).

Bernd (58) reported in depth on air-oil cavitation effects in the L.G.C. drive - a typical closed loop transmission of the type used for a constant speed alternator drive. He was investigating the possible causes of cavitation erosion and excessive slip occurring in the transmission. The report commented in general on the many possible causes and results of aeration, but described in depth the difference between local and general aeration. Extensive calculations were made to ascertain the level of boost pressure required to prevent both general and localised aeration, but these were specific.

Bernd's experimental work was principally concerned with determining the required boost pressure to prevent cavitation. An interesting factor was that it was noted that although cavitation commenced immediately the boost pressure was dropped, it took in the order of 15 secs. to cease after the pressure in the L.P. line had again been increased.

To determine to what extent air release is a problem in practical systems it was decided to run the hydrostatic transmission test rig with oil into which air had been dissolved at a higher pressure than the normal atmospheric pressure. To exaggerate the problem further, carbon dioxide was to be used, which has a solubility in oil approximately five times that of air. It had been made known by the oil supplier that in the long term the presence of carbon dioxide in the oil would accelerate the oxidation process of the oil.

However this was felt not to be a problem for the short term tests being undertaken. In this way any changes in system performance would be brought to light more readily and would provide data for extrapolation to cases where only small quantities of gas are present.

The likely effects of aeration upon the closed loop transmission would be loss of system stiffness giving a reduced system natural frequency, reduction in volumetric efficiency causing the transmission to slip, foaming, and erosion caused by local cavitation.

The effect of surface tension in the air release mechanism is important as it will alter the rate of bubble growth. Anti-foaming additives reduce surface tension and assist in the breaking of foams. However, there will be a reduction in the rate of bubble growth and overdosing with anti-foaming additives will reduce the rate at which air bubbles rise from and clear the body of the fluid.

In conjunction with an oil producer it was therefore arranged to obtain the basic hydraulic oil without defoament additives, so that the effects of additives upon aeration in the closed loop transmission could be investigated.

7.2 Modifications to Hydraulic Transmission Test Rig

To investigate the effect of gas content upon the hydrostatic transmission performance the first requirement was to provide a means of applying pressure to the transmission oil and thereby vary the amount of gas dissolved in the oil. It was therefore necessary to separate the transmission circuit from that of the loading pump and supply the transmission from a new tank. The new tank was to be capable of containing oil under pressure up to values of 17.0 bar (247 lbf/in^2).

The diagramatic layout of the transmission oil circuit is shown in Fig. 7.1. The servos and prime mover remained unchanged and the load pump was supplied from the existing reservoir and returned through the same loading valves as before. It can be seen from Fig. 7.1 that two methods of applying a boost pressure to the closed loop hydrostatic transmission can be adopted.

7.2.1 Test Set-Up for Atmospheric Tests

To use the boost pump with modified pressure relief valve as for previous tests, the pressure tank was used as a normal reservoir vented to atmosphere.

Refering to Fig. 7.1 valve 1) was closed and valves 2), 3), and 4) opened. Valve 5) was used where necessary to bleed oil from the closed loop of the transmission to maintain an oil temperature of $50^{o}C. \pm 2^{o}C.$

7.2.2 Test Set-Up to Pressurise Supply Oil with Gas

To supply the closed loop transmission with oil under pressure valves 2), 3), and 4) were closed and valve 1) opened. The boost pressure was applied to the closed loop transmission by connecting the oil under pressure in the tank directly to the return line of the transmission. The pressure of the return line was therefore maintained nominally at the pressure of the oil on the tank. The pipeline between the tank was constructed of $\frac{3}{4}$ in. rigid pipe, and gate valves used to provide an unrestricted passage between the tank and return line. The bleed valve 5) was used for temperature control as before.

To maintain the oil level in the pressurised tank depleted by the leakage losses of the pump and motor units and the oil bled off for cooling purposes, a method had to be devised for returning oil to the pressurised tank. A second smaller overflow tank at atmospheric pressure was provided.

All leakage flows were fed to this tank which was fitted with a level control switch to actuate a small pump to return oil to the pressure tank when the overflow tank became full.

A full list of the additional system components and their specification is given in Table 7.1.

7.2.2.1 Design and Installation of Pressurised Oil Reservoir

The lack of restraints upon installation size and weight of the reservoir enabled the reservoir to be built using readily available standard pipe and flanges. To provide a maximum operating pressure of 17.0 bar (247 lbf/in^2) the tank was designed to withstand a test pressure of 26.0 bar (377 lbf/in^2). For an oil capacity of 45 litres (9.9 gal.) the total capacity of the tank required was 68 litres (14.9 gal.) to ensure sufficient volume of gas above the oil to cause only small changes in pressure when oil was withdrawn from the reservoir.

The tank was constructed with an internal diameter of 35.5 cms. (12.0 in.) and length of 91.5 cms. (36.0 in.) using flange sizes laid down by BS.10 on pressure vessels. A sketch of the tank is shown in Fig. 7.2. Additional features were a 125 micron suction strainer and pepper pot return, both fitted 3 in. below the minimum expected oil level. A 60 mesh copper gauge was used according to standard practise to remove aeration bubbles from the circulating fluid.

Three ports were available on the top of the tank to which were fitted a pressure gauge, a safety valve set to 15 bar (218 lbf/in^2) and gas pressure regulator incorporating relief valve which was fed with gas at high pressure - via a length of 6.35 mm. (0.25 in.) bore pipe for safety reasons. When air was used it was obtained from a 5.9 bar (85 lbf/in^2) service supply and when carbon dioxide was used it was from a cylinder of liquified gas with no dip tube fitted. A standard regulator set fully open was incorporated.

The reservoir was mounted on a cradle in a position necessitating only approximately 50 cms. (19.7 in.) of pipe between the tank outlet and the T into the transmission return line at the pump inlet. The cradle raised the tank 30 cms. (11.8 in.) above the ground level to enable the tank to be easily drained via a fitted cock at the lowest point of the tank.

7.2.2.2 Design and Installation of Atmospheric Overflow Reservoir

The overflow tank designed to have a capacity of 24 litres (5.3 gal.) is shown sketched on Fig. 7.3. The tank constructed from 14 S.W.G. stainless steel and incorporating the standard features of 125 micron suction strainer, pepper pot return, and 60 mesh copper gauze, had in addition a filter strainer and air vent.

A miniature level control switch was fitted to the tank to actuate the return pump through a relay and starter box. The control switch was wired to actuate the pump when the oi level approached the top of the atmospheric reservoir and cut out when the level fell to 2 in. from the bottom of the reservoir.

7.3 Test Programme

7.3.1 Dynamic Response Tests with the Oil at Atmospheric Pressure

Initially the high pressure tank was charged with oil without defoament additives and the tank vented to atmosphere. The test set-up described in section 7.2.1 was employed, which was similar to that used for earlier test work and the dynamic response of the transmission (the response of motor output speed to changes in pump swash) measured at different mean return line pressures.

By the use of a lower stiffness pilot spring in the relief valve it was possible to reduce the level of the mean return line pressure to 1.4 bar (20 lbf/in^2). These tests therefore provided further correlation to earlier work and extended the investigation of mean return line pressure effects described in Chapter 6.6.2.

Frequency reponse tests were carried out with the transmission loaded to simulate a high and low load damping co-efficient f_L at each mean return line pressure. The transmission was tested at mean return line pressures of 8.3 bar (120 lbf/in^2), 5.5 bar (80 lbf/in^2), 2.8 bar (40 lbf/in^2) and 1.4 bar (20 lbf/in^2). The steady state conditions of the eight tests carried out, Tests 80 - 87, are shown on Table 7.2.

The results of the frequency response tests were analysed with the aid of VECTAN, the computer programme developed to analyse frequency response data and carry out the vector analysis. As described in Appendix I, Programme 3, the printout from Programme VECTAN contains a complete record of the frequency response test carried out developed from the instrumentation output using the appropriate calibration constants in both S.I. and Imperial Units. In addition the transmission response predicted using the vector analysis is given. The results are also compared in graphical form by plotting the predicted and measured response of the motor output speed to changes in pump swash on Bode and Nyguist diagrams.

At the time this work was undertaken it was felt that the best correlation could be obtained if the arithmetic mean of the isothermal and isentropic tangent bulk moduli were used for the theoretical predictions. (As described in Chapter 6.5.2 these values were based on information obtained from Ref. 37).

As a result the theoretically predicted response is lower than obtained experimentally. However, VECTAN also evaluates an effective bulk modulus for the oil in the pipe from the experimental results.

To illustrate the use of the programme the entire computer printout for Test 86 is shown on Table 7.3. The computed Bode and Nyguist Plots are shown on Figs. 7.4 and 7.5. The effective bulk modulus evaluated from results of the response at twelve frequencies for each test is given in Table 7.2, together with the standard error.

7.3.2 Dynamic Response Tests with the Oil in the Reservoir Pressurised with Air

Utilising the same charge of oil as that used for the atmospheric pressure tests (oil without defoament additives) the transmission was set up in manner described in 7.2.2. The use of air pressure above the oil level to maintain a boost pressure in the return line was found to be very successful and at low pressures provide a steadier mean return line pressure than possible with the boost pump and relief valve used previously. Fig. 7.6 shows galvanometer recordings of Tests 84 and 92 comparing the effectiveness of the two techniques for providing a boost system.

To enable the oil in the reservoir to become saturated with dissolved air at the pressure applied, the tank was allowed to stand for one hour and then the transmission run for half an hour with oil being circulated by bleeding off through valve 5). The dynamic response of the transmission was measured with the oil in the tank pressurised to 0.7 bar (10 lbf/in^2), 1.4 bar (20 lbf/in^2), 2.8 bar (40 lbf/in^2) and 5.5 bar (80 lbf/in^2). The upper limit of pressure applied to the oil in the reservoir was governed by the available pressure from the service air supply. Again two frequency response tests were carried out at each oil reservoir pressure. The conditions of the eight tests, Test 88 - 95, are shown on Table 7.4. The results of the frequency response tests were again analysed with the aid of VECTAN and for correlation purpose the evaluated effective bulk modulus for the oil for each test, Tests 88 - 95, is given in Table 7.4, together with the standard deviation.

An observed phenomena during the frequency response tests was the foaming of any oil bled from the closed loop of the transmission. If a quantity of oil was bled from the closed loop of the transmission and then trapped in a length of transparent hose it was observed that after a period of several seconds the oil turned milky due to the presence of small air bubbles in the oil. As time progressed these bubbles grew and slowly rose until after coalescing large static bubbles existed. However, it was not possible to carry out any quantitive studies as to the growth rate of these bubbles, but it should be said that a several second delay before the formation of any indication of aeration was long enough to suggest that the possibility of aeration due to the mean return line pressures used was unlikely.

However, the possibility of local aeration due to vortex formation or other low pressure areas still existed.

7.3.3 Dynamic Response Tests with the Oil in the Reservoir Pressurised with Carbon Dioxide

Using the same charge of oil without defoament additives the transmission was again set up to enable gas pressure above the oil to maintain a boost pressure in the return line. A cylinder of carbon dioxide was connected to the reservoir via a regulator and the oil pressurised for a minimum period of one hour prior to starting up the transmission, and for half an hour with the oil circulating as carried out with the previous tests.

The dynamic response of the transmission was measured with the oil pressurised to 0.7 bar (10 lbf/in^2), 1.4 bar (20 lbf/in^2), 2.8 bar (40 lbf/in^2), and 4.2 bar (60 lbf/in^2). Two frequency response tests were carried out at each oil reservoir pressure, the conditions of the eight tests, Tests 96 - 103, and the effective bulk modulus of the oil evaluated by VECTAN are shown on Table 7.5.

7.4 Correlation of Test Results

7.4.1 The Effect of Low Mean Return Line Pressures with the Oil at Atmospheric Pressure

At a mean return line pressure of 8.3 bar (125 lbf/in^2) the evaluated effective bulk modulus for the oil in the steel pipe was 15,500 and 14,950 bar (2.24 x 10^5 and 2.17 x 10^5 lbf/in^2) at the high and low load damping co-efficients respectively. These values compare extremely well with the previously determined value, Chapter 6.5.2, of 15,700 bar (2.28 x 10^5 lbf/in^2).

As the mean return line pressure was reduced down to 1.38 bar (20 lbf/in^2) again no appreciable change in the effective bulk modulus of the oil could be determined, Table 7.2, with no suggestion of a reduction in effective bulk modulus of the oil as the mean return line pressure was reduced.

The removal of defoament additives from the oil did not affect the effective bulk modulus of the oil either by changing the physical nature of the fluid, or by introducing air bubbles into the fluid. However, it was observed during the charging of the system that the oil was more inclined to foam when being poured and this foam took an appreciable time to disappear when compared to the oils used previously.

7.4.2 The Effect of Oil in the Reservoir being Pressurised with Air

The results of the tests carried out with the oil reservoir pressurised with air shown in Table 7.4 have volumetric efficiencies in the range 83 - 86%, the same as those carried out with the boosted system. However, as in the case of the previous tests considerable scatter was obtained with the valves for overall efficiencies. These were found to be due to zero errors in the measurement of the pump torque, but as these measurements were not used for the dynamic analysis the tests were not repeated.

A particular feature of the tests carried out on the transmission with oil under gas pressure was the air release taking place from the oil bled from the closed loop transmission circuit. However, the presence of the additional air did not appear to affect the dynamic performance of the transmission. The values obtained for effective bulk modulus of the oil in the pipe again compared well with the previously determined value with no apparent trends within the scatter of values obtained.

The steady return line pressure maintained during frequency response tests when compared with pressure fluctuation obtained with a large boost pump and flat characteristic relief valve suggest a pressurised reservoir as a very suitable technique for providing a boost system for closed loop systems.

The results of the frequency response tests suggest that the transmission performance is in no way affected. The implementation of such a system would therefore depend upon the economics of a pressurised reservoir versus that of a boost pump and associated relief valve.

7.4.3 The Effect of Oil in Reservoir being Pressurised with Carbon Dioxide

It could be argued that local low pressure regions in a closed loop hydrostatic transmission circuit would have a fixed pressure level below that of the mean return line pressure whatever that level provided the transmission was operating under the same conditions. If this was true the extent to which the return line is pressurised with air would not increase the volume of gas coming out of solution to a large degree.

The use of a gas many more times more soluble than air should increase the amount of gas coming out of solution over the given pressure drop by the same ratio as the solubility.

Again as the results in Table 7.5 show, the use of oil pressurised with carbon dioxide did not reduce the response of the transmission. The evaluated values of effective bulk modulus for the oil in the pipe showed a slight increase over previous values.

An average value of 17,000 bar (2.42×10^5 lbf/in^2) was obtained compared to the previously determined value of 15,700 bar, an increase of 7%. However, there was no indication of a relationship between the value obtained and the pressure of the oil in the reservoir and return line. No reason could be ascertained for the increase.

7.5 Further Work

The work described set out to accentuate any possible effects upon a practical transmission resulting from the aeration of working fluid. No measurable change in the performance of the transmission could be found despite the use of oil with abnormally high quantities of carbon dioxide dissolved in it. However, the work in no way indicated the effects that a poorly designed transmission system with local areas of low pressure would have upon the performance.

It is suggested that the next stage of the investigation would be to use the pressurised reservoir for the boost system in conjunction with a valve or similar device to provide a step down in pressure between the reservoir and return line.

This would therefore artificially create a low pressure region promoting additional gas to come out of the solution in the return line.

Unit	Type	Range & Capabilities	Type No. & Serial No.
Pressurised Oil Reservoir	Designed and Built to Requirements - See Section 7.2.2.1	Total Capacity - 68 litres (14.9 gal.) Max. Cont. Pressure - 17.0 bar (247 lbf/in^2)	-
Safety Valve	Bristol Pneumatics	$\frac{1}{2}$" B.S.P. Set to Blow at a Pressure of 21.0 bar (305 lbf/in^2)	Type No. 8305
Integral Regulator and Relief Valve	APCO Valve Designed for Use with Nitrogen Pressurised Oil Reservoirs	Inlet - Max. Pressure - 310 bar (4,500 lbf/in^2) Outlet - 1.0 – 21.0 bar (15 – 305 lbf/in^2)	Model 10102 Ser. No. 129
Atmospheric Over Flow Reservoir	Designed and Built to Requirements - See Section 7.2.2.2	Capacity - 24 litres (5.3 gal.)	-
Level Control Switch	Alan Cobham Miniature Level Control Switch and Relay	High Level Control - Close on Rising Low Level Control - Open on Falling	-
Return Pump	Dowty Gear Pump (Originally Small Boost Pump)	Nominal Capacity 1.0 gpm at 1,500 rev/min.	Type: GPP1T/10CT Ser. No: CP049/66/12
Control Valves 1 2 3 4	Full Bore Gate Valves for $\frac{3}{4}$ in. Pipe	-	-
Bleed Valve 5	$\frac{1}{4}$" Bore Standard Needle Valve	-	-

TABLE 7.1 ADDITIONAL TRANSMISSION COMPONENTS USED FOR WORK ON AERATION

TEST NO.	Mean Pump Input Torque Nm	Mean Load Torque Nm	Mean Motor Speed Rev/min	Volumetric Efficiency η Vol - %	Overall Efficiency η Ov - %	Mean Return Line Pressure bar	Mean Effective Bulk Modulus bar x 10^4	Standard Deviation %
80	21.3	27.7	659	84.1	71.2	8.63	1.550	2.5
81	19.8	28.2	659	84.3	78.6	7.94	1.495	4.0
82	21.1	28.2	672	85.7	74.9	5.51	1.479	2.4
83	20.3	29.1	666	85.0	79.4	5.51	1.472	6.0
84	19.3	28.5	673	85.9	83.2	2.76	1.483	2.3
85	18.2	30.0	676	86.3	93.1	2.76	1.481	4.4
86	18.4	28.8	667	-	87.0	1.38	1.508	3.4
87	18.3	27.6	656	83.7	82.0	1.38	1.410	3.3

All Tests Carried Out At:

Mean Pump Swash	=	4.90 Deg.	Pump Speed	=	1200 rev/min
Mean Motor Swash	=	7.50 Deg.	Oil Temp	=	$50^oC \pm 2C^o$
Load Inertia	=	.0167 Kg m^2	Amplitude of Pump Input Swash Angle	=	3.76 Deg. Peak to Peak
System Volume	=	1.27 litres			

TABLE 7.2 TESTS CARRIED OUT TO INVESTIGATE THE EFFECT OF LOW MEAN RETURN LINE PRESSURES ON TRANSMISSION DYNAMIC RESPONSE

TRANSMISSION COMPONENT DATA

PRIME MOVER SPEED	=	1.200E 03	RPM
	=	1.257E 02	RAD/SEC
PUMP DISPLACEMENT/RADIAN SWASH/RADIAN	=	1.140E-03	FT3/RAD SWASH/RAD
	=	3.228E-02	LITRE/RAD SWASH/RAD
MOTOR DISPLACEMENT/RADIAN SWASH/RADIAN	=	1.140E-03	FT3/RAD SWASH/RAD
	=	3.228E-02	LITRE/RAD SWASH/RAD
MAXIMUM PUMP SWASH	=	1.500E 01	DEGREES
	=	2.618E-01	RADIANS
MAXIMUM MOTOR SWASH	=	1.500E 01	DEGREES
	=	2.618E-01	RADIANS
HYDRAULIC MOTOR INERTIA	=	5.000E-03	SLUG FT2
	=	6.779E-03	KG M2

PUMP AND MOTOR LOSS COEFFICIENTS

PUMP SLIP LOSS	=	3.720E-09	FT3/SEC/LBF/FT2
	=	2.200E-04	LITRE/SEC/BAR
MOTOR SLIP LOSS	=	3.900E-09	FT3/SEC/LBF/FT2
	=	2.306E-04	LITRE/SEC/BAR
PUMP VISCOUS TORQUE LOSS COEFFICIENT	=	1.130E-02	LBF FT/RAD/SEC
	=	1.532E-02	NM/RAD/SEC
MOTOR VISCOUS TORQUE LOSS COEFFICIENT	=	1.130E-02	LBF FT/RAD/SEC
	=	1.532E-02	NM/RAD/SEC

TABLE 7.3 PROGRAMME "VECTAN" PRINTOUT FOR TEST 86 - INPUT DATA

RIG CALIBRATION CONSTANTS

PUMP SWASH	=	1.098E-01	VOLT/DEGREE
MOTOR SWASH	=	9.500E-02	VOLT/DEGREE
PUMP TORQUE	=	1.990E-02	VOLT/LBF FT
	=	1.468E-02	VOLT/NM
MOTOR TORQUE	=	1.965E-02	VOLT/LBF FT
	=	1.449E-02	VOLT/NM
PUMP SPEED	=	1.000E-01	VOLT/RPM
MOTOR SPEED	=	9.560E-03	VOLT/RPM
SUPPLY LINE PRESSURE	=	3.555E-04	VOLT/LBF/IN2
	=	5.156E-03	VOLT/BAR
RETURN LINE PRESSURE	=	7.040E-04	VOLT/LBF/IN2
	=	1.021E-02	VOLT/BAR
DIFFERENTIAL LINE PRESSURE	=	3.975E-05	VOLT/LBF/IN2
	=	5.765E-04	VOLT/BAR

TABLE 7.3 PROGRAMME "VECTAN" PRINTOUT FOR TEST 86 - INPUT DATA (Cont.)

STEADY STATE TEST CONDITIONS

PUMP TORQUE	=	1.357E 01	LBF FT
	=	1.840E 01	NM
PUMP SPEED	=	1.200E 03	RPM
MOTOR TORQUE	=	2.122E 01	LBF FT
	=	2.877E 01	NM
MOTOR SPEED	=	6.674E 02	RPM
SUPPLY LINE PRESSURE	=	1.120E 03	LBF/IN2
	=	7.722E 01	NM
RETURN LINE PRESSURE	=	2.000E 01	LBF/IN2
	=	1.379E 00	NM
DIFFERENTIAL LINE PRESSURE	=	1.100E 03	LBF/IN2
	=	7.584E 01	NM
PUMP SWASH	=	4.900E 00	DEGREE
MOTOR SWASH	=	7.500E 00	DEGREE

TRANSMISSION EFFICIENCIES

VOLUMETRIC EFFICIENCY	=	8.512E 01	%
MECHANICAL EFFICIENCY	=	1.022E 02	%
OVERALL EFFICIENCY	=	8.698E 01	%

TABLE 7.3 PROGRAMME "VECTAN" PRINTOUT FOR TEST 86 - INPUT DATA (Cont.)

ADDITIONAL SYSTEM INFORMATION FOR DYNAMIC ANALYSIS

PUMP DEAD VOLUME	=	5.270E 00	IN3
	=	8.636E 01	CCS
MOTOR DEAD VOLUME	=	5.270E 00	IN3
	=	8.636E 01	CCS
SUPPLY PIPE LENGTH	=	6.620E 00	FT
	=	2.018E 00	METRES
SUPPLY PIPE INTERNAL DIAMETER	=	1.000E 00	IN
	=	2.540E 00	CM
SUPPLY PIPE WALL THICKNESS	=	1.625E-01	IN
	=	4.128E-01	CM
TOTAL SUPPLY LINE VOLUME(CALCULATED)	=	4.221E-02	FT3
	=	1.195E 00	LITRE
TOTAL SUPPLY LINE VOLUME(MEASURED)	=	4.490E-02	FT3
	=	1.271E 00	LITRE
KINEMATIC VISCOSITY	=	8.000E 01	CENTISTOKES AT 20DEG CENTIGRADE
OIL TEMPERATURE	=	5.000E 01	DEG CENTIGRADE

TABLE 7.3 PROGRAMME "VECTAN" PRINTOUT FOR TEST 86 - INPUT DATA (Cont.)

PIPE MATERIAL YOUNGS MODULUS	=	3.000E 07	LBF/IN2
	=	2.068E 06	BAR
OIL ISENTROPIC BULK MODULUS	=	2.347E 05	LBF/IN2
	=	1.618E 04	BAR
OIL ISOTHERMAL BULK MODULUS	=	2.021E 05	LBF/IN2
	=	1.394E 04	BAR
MEAN OIL BULK MODULUS	=	2.184E 05	LBF/IN2
	=	1.506E 04	BAR
PIPE BULK MODULUS	=	4.875E 06	LBF/IN2
	=	3.361E 05	BAR
MEAN BULK MODULUS OF OIL IN PIPE	=	2.091E 05	LBF/IN2
	=	1.441E 04	BAR

TABLE 7.3 PROGRAMME "VECTAN" PRINTOUT FOR TEST 86 - INPUT DATA (Cont)

E PERIME TAL RESULTS - ENGLISH UNITS

FRE UENCY		W2/XP		TL/W2		PH/W2		PL/W2		PD/W2	
HZ	RAD/SEC	RPM/DEG	DEG LAG	LBF FT/RPM	DEG LAG	LBF/I 2/RPM	DEG LAG	LBF/IN2/RPM	DEG LAG	LBF/IN2/RPM	DEG LAG
.000E- 1	6.283E-01	1.348E 02	1.000E-01	2.847E-02	3.582E 02	1.238E 00	3.572E 02	0.000E 00	0.000E 00	1.407E 00	3.565E 02
.000E- 1	3.770E 00	1.371E 02	2.900E 00	2.908E-02	3.516E 02	1.277E 00	3.473E 02	0.000E 00	0.000E 00	1.451E 00	3.468E 02
.000E 0	6.283E 00	1.380E 02	6.200E 00	3.017E-02	3.477E 02	1.382E 00	3.382E 02	0.000E 00	0.000E 00	1.559E 00	3.388E 02
.000E 0	1.257E 01	1.534E 0	1.600E 01	3.252E-02	3.360E 02	1.581E 00	3.246E 02	0.000E 00	0.000E 00	1.777E 00	3.246E 02
.000E 0	1.885E 01	1.683E 0	3.140E 01	3.643E-02	3.278E 02	1.916E 00	3.126E 02	0.000E 00	0.000E 00	2.196E 00	3.110E 02
.000E 0	2.513E 01	1.727E 0	4.950E 01	3.953E-02	3.211E 02	2.449E 00	-5.390E 01	0.000E 00	0.000E 00	2.566E 00	-5.420E 01
.500E 0	2.827E 01	1.981E 0	6.050E 01	4.013E-02	3.186E 02	2.323E 00	-5.420E 01	0.000E 00	0.000E 00	2.704E 00	-5.550E 01
1.000E 00	3.142E 01	1.950E 0	7.340E 01	4.231E-02	3.170E 02	2.519E 00	-5.620E 01	0.000E 00	0.000E 00	2.833E 00	-5.740E 01
5.500E 00	3.456E 01	1.796E 0	8.450E 01	4.427E-02	3.163E 02	2.701E 00	-5.640E 01	0.000E 00	0.000E 00	3.097E 00	-5.740E 01
6.000E 00	3.770E 01	1.603E 02	9.520E 01	4.701E-02	3.160E 02	2.922E 00	-5.650E 01	0.000E 00	0.000E 00	3.318E 00	-5.870E 01
6.500E 00	4.084E 01	1.394 02	1.045E 02	4.858E-02	3.142E 02	3.118E 00	-5.760E 01	0.000E 00	0.000E 00	3.502E 00	-6.160E 01
7.000E 00	4.398E 01	1.210 02	1.118E 02	5.111E-02	3.144E 02	3.268E 00	-5.730E 01	0.000E 00	0.000E 00	3.699E 00	-6.060E 01
8.000E 00	5.027E 01	9.495E 01	1.239E 02	5.375E-02	3.093E 02	3.622E 00	-6.020E 01	0.000E 00	0.000E 00	3.995E 00	-6.470E 01
9.000E 00	5.655E 01	7.657 01	1.323E 02	5.595E-02	3.032E 02	3.819E 00	-6.300E 01	0.000E 00	0.000E 00	4.281E 00	-6.620E 01
1.000E 01	6.283E 01	6.161 01	1.360E 02	5.886E-02	3.016E 02	4.084E 00	-6.300E 01	0.000E 00	0.000E 00	4.691E 00	-6.620E 01
1.200E 01	7.540E 01	4.107 01	1.474E 02	7.118E-02	2.956E 02	4.831E 00	-6.810E 01	0.000E 00	0.000E 00	5.790E 00	-7.360E 01

TABLE 7.3 PROGRAMME "VECTAN" PRINTOUT FOR TEST 86 - OUTPUT

EXPERIMENTAL RESULTS - S.I. UNITS

FREQUENCY		W2/XP		TL/W2		PH/W2		PL/W2		PD/W2	
HZ	RAD/SEC	RPM/DEG	DEGLAG	NM/RPM	DEG LAG	BAR/RPM	DEG LAG	BAR/RPM	DEG LAG	BAR/RPM	DEG LAG
1.000E-01	6.283E-01	1.348E 02	.000E-01	3.860E-02	3.582E 02	8.633E-02	3.572E 02	.000E 00	0.000E 00	9.704E-02	3.565E 02
6.000E-01	3.770E 00	1.371E 02	3.900E 00	3.843E-02	3.516E 02	8.704E-02	3.473E 02	0.000E 00	0.000E 00	1.000E-01	3.468E 02
1.000E 00	6.283E 00	1.380E 02	6.200E 00	4.090E-02	3.477E 02	9.530E-02	3.382E 02	0.000E 00	0.000E 00	1.075E-01	3.388E 02
2.000E 00	1.257E 01	1.534E 02	.600E 01	4.409E-02	3.360E 02	1.090E-01	3.246E 02	0.000E 00	0.000E 00	1.225E-01	3.246E 02
3.000E 00	1.885E 01	1.688E 02	3.140E 01	4.840E-02	3.278E 02	1.321E-01	3.126E 02	0.000E 00	0.000E 00	1.514E-01	3.110E 02
4.000E 00	2.513E 01	1.727E 02	3.950E 01	5.359E-02	3.211E 02	1.639E-01	-5.390E 01	0.000E 00	0.000E 00	1.769E-01	-5.420E 01
4.500E 00	2.827E 01	1.981E 02	4.050E 01	5.441E-02	3.186E 02	1.692E-01	-5.420E 01	0.000E 00	0.000E 00	1.865E-01	-5.550E 01
5.000E 00	3.142E 01	1.950E 02	7.340E 01	5.736E-02	3.170E 02	1.787E-01	-5.620E 01	0.000E 00	0.000E 00	1.953E-01	-5.740E 01
5.500E 00	3.456E 01	1.796E 02	8.450E 01	6.002E-02	3.163E 02	1.852E-01	-5.640E 01	0.000E 00	0.000E 00	2.135E-01	-5.740E 01
6.000E 00	3.770E 01	1.603E 02	9.520E 01	6.374E-02	3.160E 02	2.015E-01	-5.650E 01	0.000E 00	0.000E 00	2.288E-01	-5.870E 01
6.500E 00	4.084E 01	1.394E 02	1.045E 02	6.560E-02	3.142E 02	2.150E-01	-5.760E 01	0.000E 00	0.000E 00	2.414E-01	-6.160E 01
7.000E 00	4.398E 01	1.210E 02	1.118E 02	6.930E-02	3.144E 02	2.253E-01	-5.730E 01	0.000E 00	0.000E 00	2.550E-01	-6.060E 01
8.000E 00	5.027E 01	9.495E 01	1.239E 02	7.288E-02	3.093E 02	2.497E-01	-6.020E 01	0.000E 00	0.000E 00	2.755E-01	-6.470E 01
9.000E 00	5.655E 01	7.657E 01	1.323E 02	7.586E-02	3.032E 02	2.633E-01	-6.300E 01	0.000E 00	0.000E 00	2.952E-01	-6.620E 01
1.000E 01	6.283E 01	6.161E 01	1.360E 02	7.981E-02	3.016E 02	2.816E-01	-6.300E 01	0.000E 00	0.000E 00	3.235E-01	-6.620E 01
1.200E 01	7.540E 01	4.107E 01	1.474E 02	9.650E-02	2.956E 02	3.331E-01	-6.810E 01	0.000E 00	0.000E 00	3.992E-01	-7.360E 01

TABLE 7.3 PROGRAMME "VECTAN" PRINTOUT FOR TEST 86 - OUTPUT (Cont.)

EFFECTIVE LOAD TORQUE & PRESSURE DIFFERENCE CALCULATED FROM EXPERIMENTAL RESULTS
ENGLISH UNITS

FREQUENCY		TL/W2		T /W2		T2/W2		CAL-PD/W2	
HZ	RAD/SEC	LBF FT/RPM	DEG LAG	LBF FT/RPM	DEG LAG	LBF FT/RPM	DEG LAG	LBF/IN2/RPM	DEG LAG
1.000E-01	6.283E-01	2.847E-02	3.582E 02	3.290E- 4	-9.000E 01	2. 67E-02	-2.365E 00	1.381E 00	-2.365E 00	2.848E-02	-2.463E 00
6.000E-01	3.770E 00	2.908E-02	3.516E 02	1.974E- 3	-9.000E 01	3. 59E-02	-1.174E 01	1.424E 00	-1.174E 01	2.944E-02	-1.221E 01
1.000E 00	6.283 00	3.017 -02	3.477E 02	3.290E- 3	-9.000E 01	3.216E-02	-1.759E 01	1.497E 00	-1.759E 01	3.104E-02	-1.825E 01
2.000E 00	1.257E 01	3.252E-02	3.360E 02	6.580E-03	-9.000E 01	3.669E-02	-3.267E 01	1.708E 00	-3.267E 01	3.570E-02	-3.369E 01
3.000E 00	1.885E 01	3.643E-02	3.278E 02	9.870E-03	-9.000E 01	4.339E-02	-4.245E 01	2.019E 00	-4.245E 01	4.252E-02	-4.353E 01
4.000E 00	2.513E 01	3.953E-02	3.211E 02	1.316E-02	-9.000E 01	4.963E-02	-4. 93E 01	2.310E 00	-4.993E 01	4.888E-02	-5.100E 01
4.500E 00	2.827E 01	4.013E-02	3.186E 02	1.480E-02	-9.000E 01	5.185E-02	-5.288E 01	2.413E 00	-5.288E 01	5.114E-02	-5.394E 01
5.000E 00	3.142 01	4.231E-02	3.170E 02	1.645E-02	-9.000E 01	5.554E-02	-5.466E 01	2.584E 00	-5.466E 01	5.486E-02	-5.567E 01
5.500E 00	3.456E 01	4.427E-02	3.163E 02	1.809E-02	-9.000E 01	5.891E-02	-5.572E 01	2.742E 00	-5.572E 01	5.826E-02	-5.668E 01
6.000E 00	3.770E 01	4.701E-02	3.160E 02	1.974E-02	-9.000E 01	6.301E-02	-5.626E 01	2.932E 00	-5.626E 01	6.236E-02	-5.716E 01
6.500E 00	4.084 01	4.838E-02	3.142E 02	2.138E-02	-9.000E 01	6.605E-02	-5.809E 01	3.074E 00	-5.809E 01	6.544E-02	-5.897E 01
7.000E 00	4.398E 01	5.111E-02	3.144E 02	2.303E-02	-9.000E 01	7.008E-02	-5.818E 01	3.261E 00	-5.818E 01	6.946E-02	-5.901E 01
8.000E 00	5.027E 01	5.375E-02	3.093E 02	2.632E-02	-9.000E 01	7.651E-02	-6.258E 01	3.560E 00	-6.258E 01	7.597E-02	-6.338E 01
9.000E 00	5.655E 01	5.595E-02	3.032E 02	2.961E-02	-9.000E 01	8.278E-02	-6.740E 01	3.853E 00	-6.740E 01	8.234E-02	-6.816E 01
1.000E 01	6.283E 01	5.886E-02	3.016E 02	3.290E-02	-9.000E 01	8.900E-02	-6.891E 01	4.142E 00	-6.891E 01	8. 58E-02	-6.962E 01
1.200E 01	7.540E 01	7.118E-02	2.956E 02	3.948 -02	-9.000E 01	1.085E-01	-7.288E 01	5.046E 00	-7.288E 01	1. 81E-01	-7.348E 01

TABLE 7.3 PROGRAMME "VECTAN" PRINTOUT FOR TEST 86 - OUTPUT (Cont.)

EFFECTIVE LOAD TORQUE & PRESSURE DIFFERENCE CALCULATEDFROM EXPERIMENTAL RESULTS
S.I. UNITS

FREQUENCY		TL/W2		TM/W2		T2/W2		CAL-PD/W2	
HZ	RAD/SEC	NM/RPM	DEG LAG	NM/RPM	DEG LAG	NM/RPM	DEG LAG	BAR/RPM	DEG LAG
1.000E-01	6.283E-01	3.860E-02	3.[illegible]2E 02	4.460E-04	-9.000E 01	4.460E-04	-2.365E 00	9.519E-02	-2.365E 00
6.000E-01	[illegible].770E 00	3.943E-02	3.516E 02	2.676E-03	-9.000E 01	2.676E-03	-1.174E 01	9.816E-02	-1.174E 01
1.000E 00	[illegible].283E 00	4.090E-02	3.[illegible]7E 02	4.460E-03	-9.000E 01	4.460E-03	-1.759E 01	1.032E-01	-1.759E 01
2.000E 00	[illegible].257E 01	4.409E-02	3.[illegible]0E 02	8.921E-03	-9.000E 01	8.921E-03	-3.267E 01	1.177E-01	-3.267E 01
3.000E 00	[illegible].885E 01	4.940E-02	3.278E 02	1.338E-02	-9.000E 01	1.338E-02	-4.245E 01	1.392E-01	-4.245E 01
4.000E 00	[illegible].513E 01	5.359E-02	3.211E 02	1.784E-02	-9.000E 01	1.784E-02	-4.993E 01	1.592E-01	-4.993E 01
4.[illegible]00E 00	[illegible].627E 01	5.441E-02	3.1[illegible]E 02	2.[illegible]07E-[illegible]	-9.000E 01	2.007E-02	-5.[illegible]38E 01	1.664E-01	-5.288E 01
5.[illegible]00E 00	3.142E 01	5.736E-02	3.170E 02	2.230E-02	-9.000E 01	2.230E-02	-5.466E 01	1.782E-01	-5.466E 01
5.[illegible]00E 00	3.456E 01	6.002E-02	3.163E 02	2.453E-02	-9.000E 01	2.453E-02	-5.572E 01	1.890E-01	-5.572E 01
6.000E 00	3.770E 01	6.374E-02	3.160E 02	2.676E-02	-9.000E 01	2.676E-02	-5.626E 01	2.022E-01	-5.626E 01
6.500E 00	4.084E 01	6.560E-02	3.142E 02	2.899E-02	-9.000E 01	2.899E-02	-5.809E 01	2.119E-01	-5.809E 01
7.000E 00	4.398E 01	6.930E-02	3.144E 02	3.122E-02	-9.000 01	3.122E-02	-5.818E 01	2.249E-01	-5.818E 01
8.000E 00	5.027E 01	7.288E-02	3.093E 02	3.568E-02	-9.000E 01	3.568E-02	-6.258E 01	2.455E-01	-6.258E 01
9.000E 00	5.655E 01	7.586E-02	3.032E 02	4.014E-02	-9.000E 01	4.014E-02	-6.740E 01	2.656E-01	-6.740E 01
1.000E 01	6.283E 01	7.981E-02	3.015E 02	4.460E-02	-9.000E 01	4.460E-02	-6.891E 01	2.855E-01	-6.891E 01
1.200E 01	7.540E 01	9.450E-02	2.916E 02	5.353E-02	-9.000E 01	5.353E-02	-7.288E 01	3.481E-01	-7.288E 01

TABLE 7.3 PROGRAMME "VECTAN" PRINTOUT FOR TEST 86 - OUTPUT (Cont.)

PR DICTED AND MEASURED OVERALL TRANSMISSION RESPONSE

FREQUENCY		W2/XP-EXP		W2/XP-VEC	
HZ	RAD/SEC	RPM/DEG	DEG LAG	RPM/DEG	DEG LAG
1.00(E-0'	6.283E- 1	1.348E 02	1.00(E-01	1.473E 02	7.870E-(1
6.00 E-01	3.770E 00	1.371E 02	2.90(E 0'	1.487E 02	4.490E (0
1.00)E 00	6.283E 00	1.380E 02	6.20)E 00	1.515E 02	7.993E (0
2.00)E 00	1.257E 01	1.534E 02	1.60)E 01	1.640E 02	1.710E (1
3.00)E 00	1.885E 01	1.688E 02	3.14)E 01	1.891E 02	3.093E (1
4.00)E 00	2.513E 01	1.727E 02	4.95)E 01	2.099E 02	5.675E (1
4.50)E 00	2.827E 01	1.981E 02	6.0!)E 01	2.123E 02	6.118E (1
5.00)E 00	3.142E 01	1.95)E 02	7.3)E 01	2.060E 02	7.549E (1
5.50)E 00	3.456E 01	1.7 6E 02	8.4)E 01	1.842E 02	8.758E (1
6.00)E 00	3.77(E 0'	1.6 3E 02	9.5)E 01	1.572E 02	9.842E (1
6.50)E 00	4.084E 0	1.3 4E 02	1.0)5E 02	1.357E 02	1.078E (2
7.00 E 00	4.398E 0'	1.2 0E 02	1.1 8E 02	1.168E 02	1.131E (2
8.00)E 00	5.027E 01	9.4)5E 01	1.2)9E 02	8.897E 0'	1.255E (2
9.00)E 00	5.655E 01	7.(57E 01	1.323E 02	7.278E 0'	1.338E 02
1.00)E 01	6.283E 01	6.161E 01	1.360E 02	5.845E 01	1.373E 02
1.20(E 01	7.540E 01	4.107E 01	1.474E 02	3.(56E 01	1.482E 02

TABLE 7.3 PROGRAMME "VECTAN" PRINTOUT FOR TEST 86 - OUTPUT (Cont.)

FREQUENCY		SLIP LOSSES	EFFECTIVE BM
HZ	RAD/SEC	FT3/SEC/LBF/IN2	LBF/IN2
1.000E-01	6.283E-01	1.641E-08	3.154E 05
6.000E-01	3.770E 00	1.486E-08	-6.542E 05
.000E 00	6.283E 0	1.479E-08	-4.1[illegible]2E 05
2.000E 00	1.257E 01	1.158E-08	-2.4[illegible]2E 05
3.000E 00	1.[illegible]85E 01	1.327E-08	-2.1[illegible]5E 05
4.000E 00	2.513E 01	1.483E-08	-2.400E 05
4.500E 00	2.827E 0	1.018E-08	-2.0[illegible]7E 05
5.000E 00	3.142E 01	9.798E-09	-2.118E 05
5.500E 00	3.456E 01	9.34[illegible]E-09	-2.141E 05
6.000E 00	3.770E 01	8.42[illegible]E-09	-2.171E 05
6.500E 00	4.084E 01	8.65[illegible]E-09	-2.174E 05
7.000E 00	4.398E 01	7.564E-09	-2.153E 05
8.000E 00	5.027E 01	7.481E-09	-2.199E 05
9.000E 00	5.655E 01	8.089E-09	-2.180E 05
1.000E 01	6.283E 01	8.113E-09	-2.184E 05
1.200E 01	7.540E 01	7.869E-09	-2.200E 05

TABLE 7.3 PROGRAMME "VECTAN" PRINTOUT FOR TEST 86 - OUTPUT (Cont.)

TEST NO.	Mean Pump Input Torque Nm	Mean Load Torque Nm	Mean Motor Speed Rev/min	Volumetric Efficiency η Vol - %	Overall Efficiency η Ov - %	Reservoir Air Press. & Mean Return Line Pressure bar	Mean Effective Bulk Modulus bar x 10^4	Standard Deviation %
88	23.3	29.4	664	84.7	69.8	0.69	1.488	2.3
89	23.3	28.8	658	83.9	67.7	0.69	1.419	7.9
90	19.8	28.3	665	84.9	79.1	1.38	1.546	2.2
91	19.1	29.4	651	83.0	83.5	1.38	1.553	6.0
92	19.5	28.8	654	83.5	80.6	2.76	1.540	2.2
93	18.5	29.5	656	83.7	86.9	2.76	1.554	3.4
94	28.7	29.4	664	84.7	56.7	5.52	1.582	2.5
95	28.4	29.1	666	85.0	56.9	5.52	1.641	2.6

All Tests Carried Out At:

Mean Pump Swash	=	4.90 Deg.	Pump Speed	=	1200 rev/min
Mean Motor Swash	=	7.50 Deg.	Oil Temp	=	$50^oC \pm 2C^o$
Load Inertia	=	.0167 Kg m^2	Amplitude of Pump Input Swash Angle	=	3.76 Deg. Peak to Peak
System Volume	=	1.27 Litres			

TABLE 7.4 TESTS CARRIED OUT TO INVESTIGATE THE EFFECT OF PRESSURISING OIL IN RESERVOIR WITH AIR ON TRANSMISSION DYNAMIC RESPONSE

TEST NO.	Mean Pump Input Torque Nm	Mean Load Torque Nm	Mean Motor Speed Rev/min	Volumetric Efficiency Vol - %	Overall Efficiency Ov - %	Mean Return Line Pressure bar	Mean Effective Bulk Modulus bar x 10^4	Standard Deviation %
96	18.3	28.6	657	83.8	85.6	.69	1.623	4.1
97	17.6	29.1	634	80.8	87.3	.69	1.736	3.1
98	17.4	28.6	633	80.7	86.7	1.38	1.732	2.3
99	17.4	29.0	636	81.1	88.1	1.38	1.775	3.6
100	18.9	29.4	649	82.7	83.9	2.76	1.605	2.8
101	19.2	29.1	646	82.4	81.5	2.76	1.637	4.6
102	19.8	28.7	636	81.1	77.0	4.14	1.677	2.7
103	-	-	-	-	-	4.14	1.717	4.5

All Tests Carried Out At:

Mean Pump Swash	=	4.90 Deg.	Pump Speed	=	1200 rev/min.
Mean Motor Swash	=	7.50 Deg.	Oil Temp	=	$50^{o}C \pm 2C^{o}$
Load Inertia	=	.0167 Kg m^2	Amplitude of Pump Input Swash Angle	=	3.76 Deg. Peak to Peak
System Volume	=	1.27 Litres			

TABLE 7.5 TESTS CARRIED OUT TO INVESTIGATE THE EFFECT OF PRESSURISING OIL IN RESERVOIR WITH CARBON DIOXIDE UPON TRANSMISSION DYNAMIC RESPONSE

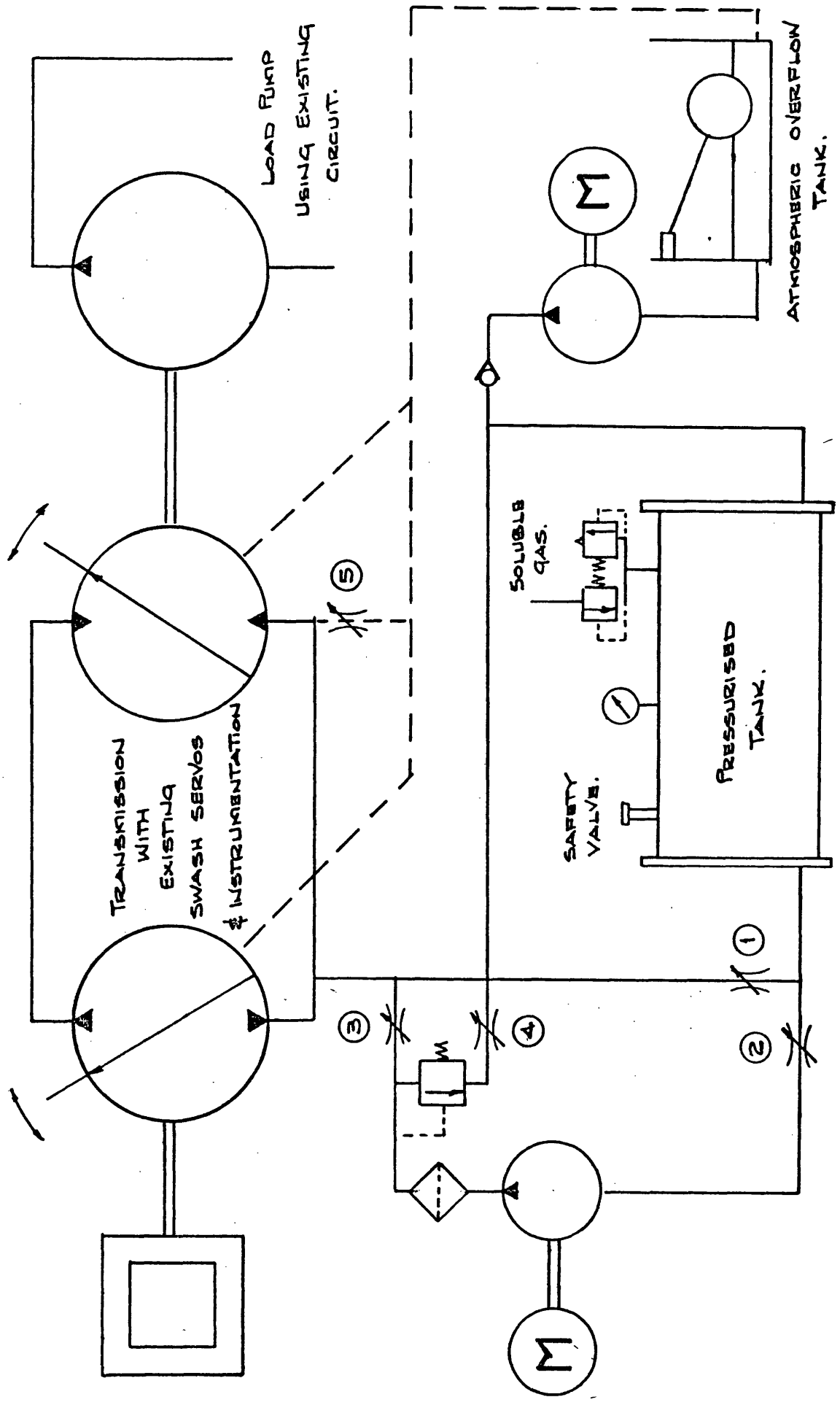

Fig 7.1 Modified Hydrostatic Transmission Circuit For Work On Aeration.

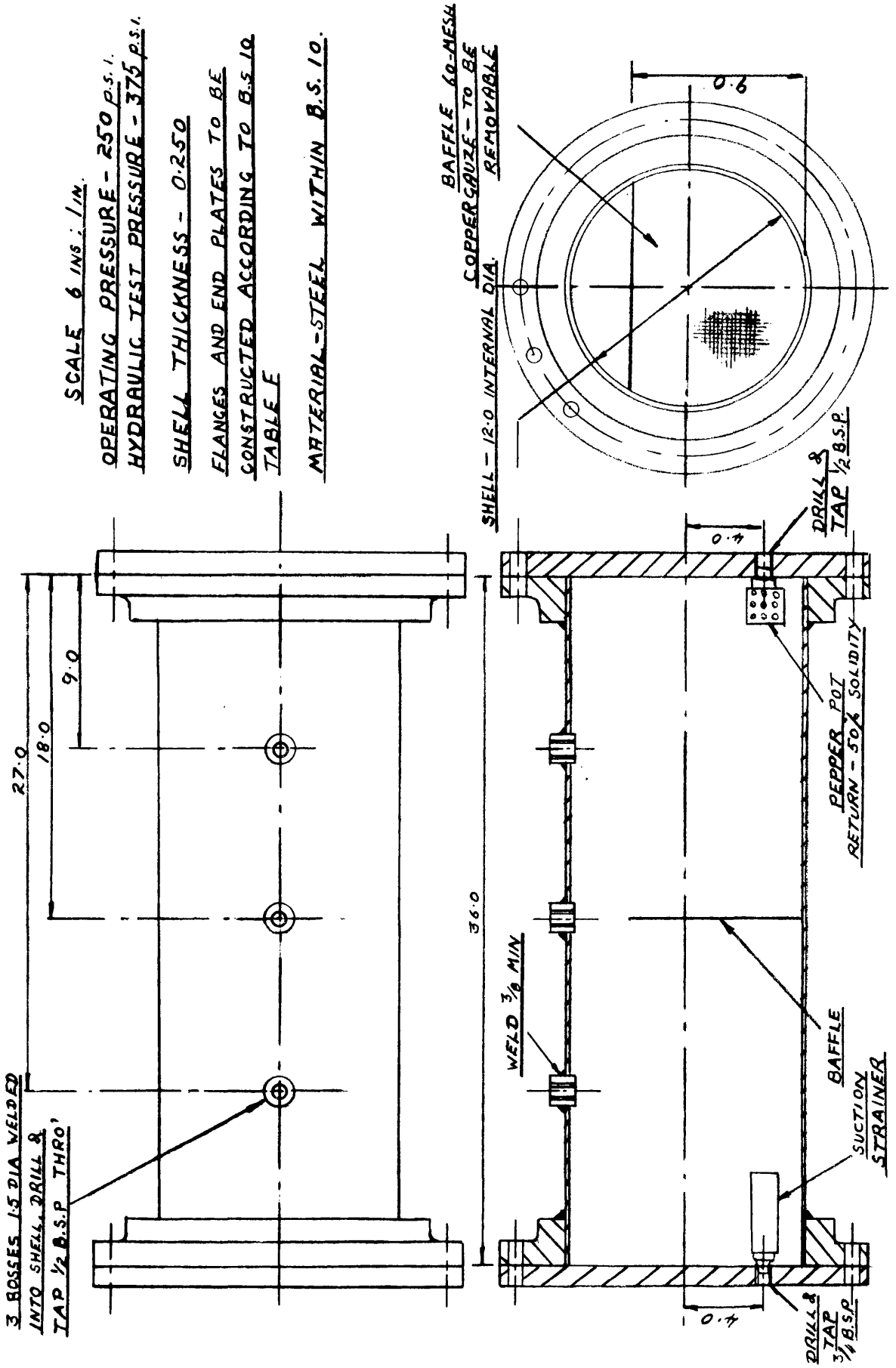

Fig. 7.13 Layout of 15 Gallon Pressurised Tank.

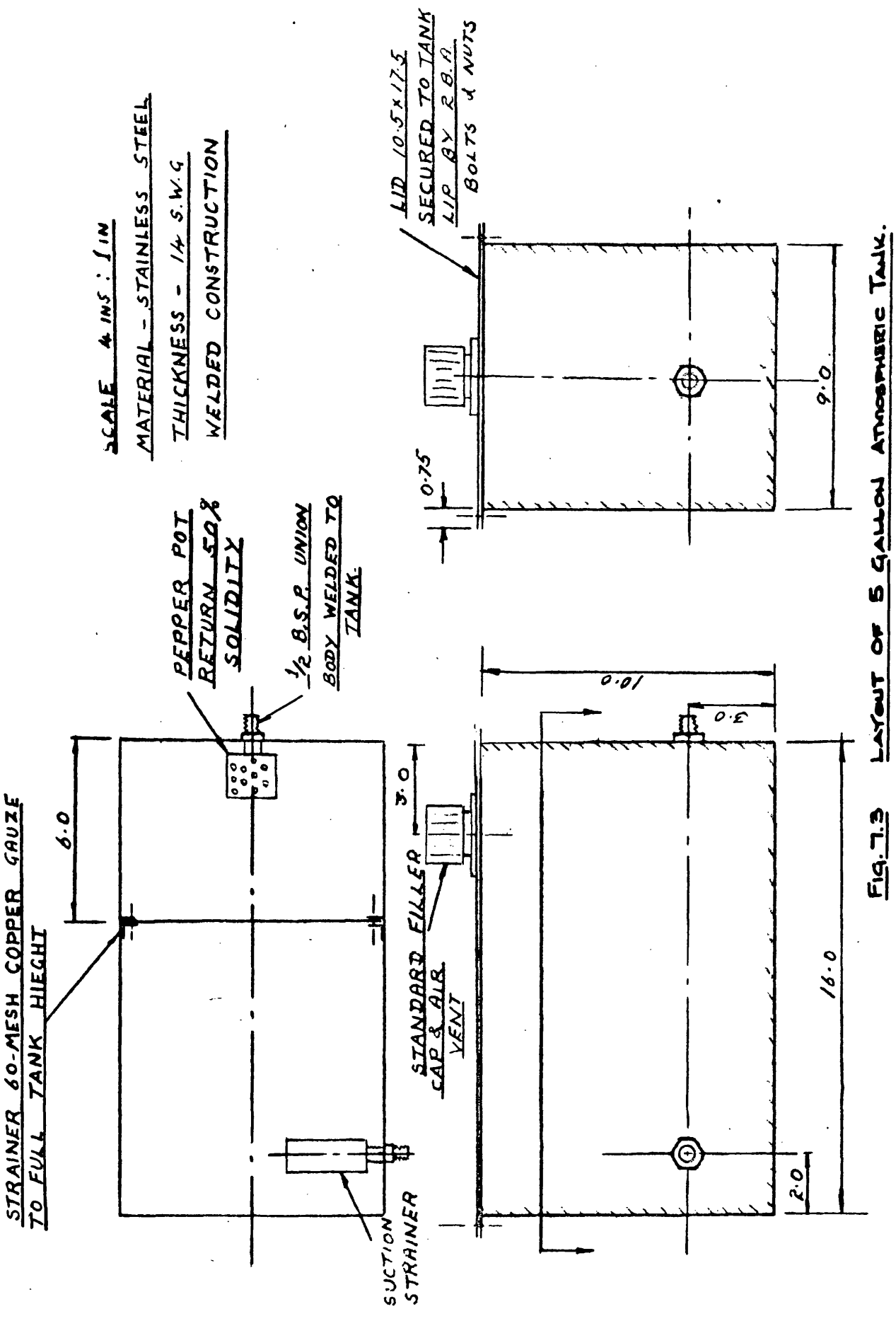

Fig. 7.3 Layout of 5 Gallon Atmospheric Tank.

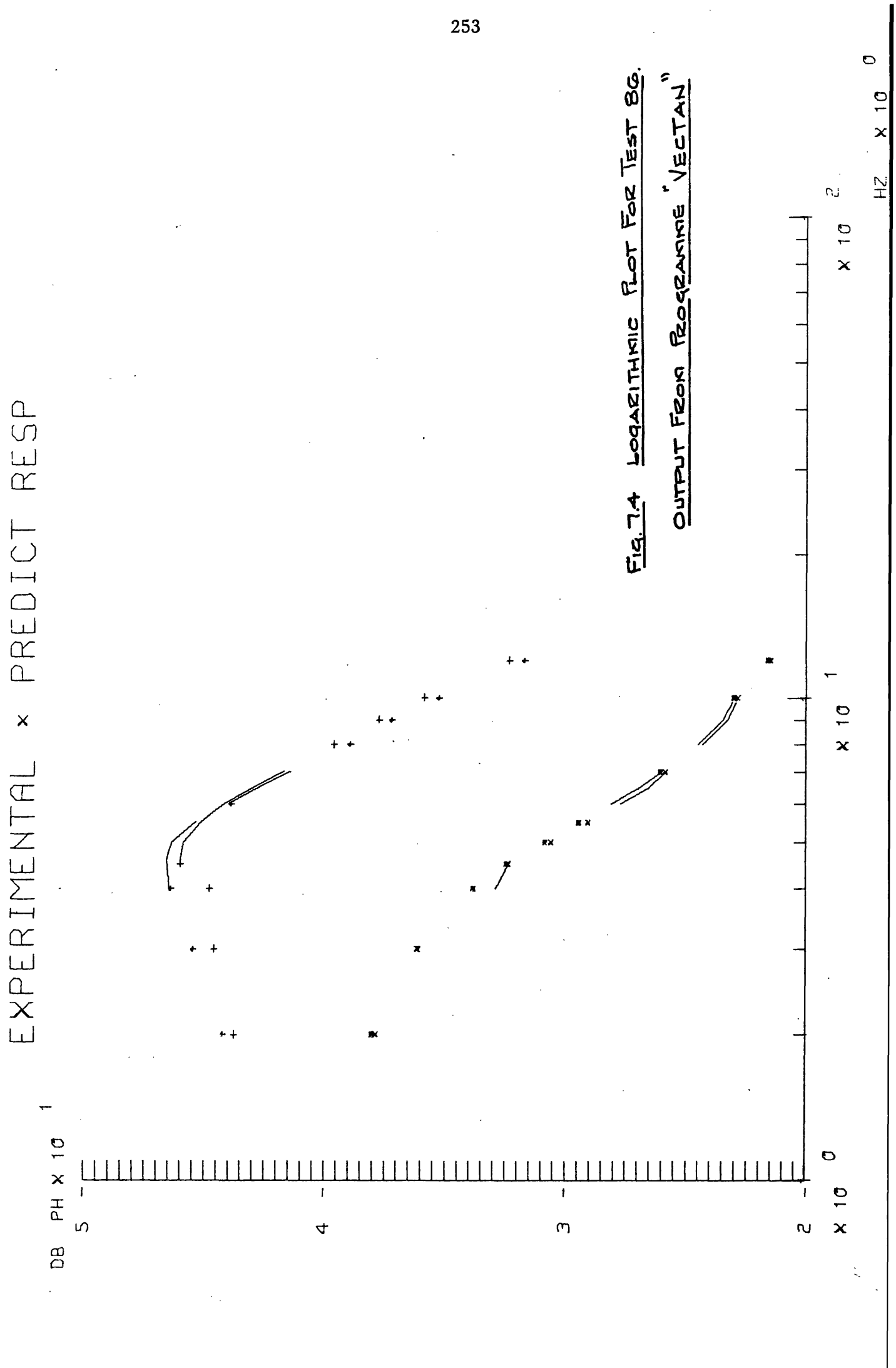

Fig. 7.4 Logarithmic Plot For Test 86.
Output From Programme "Vectan"

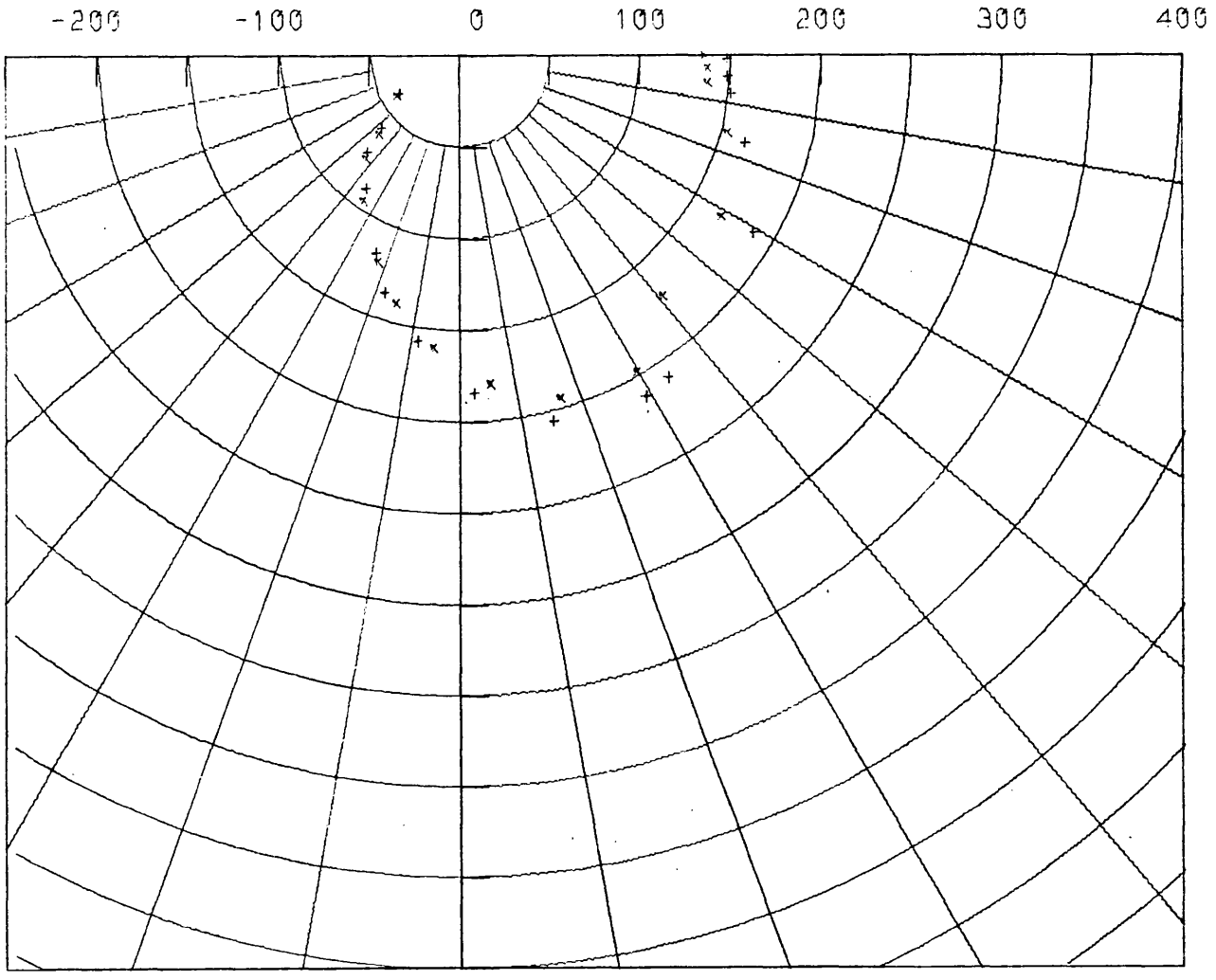

OVERALL RESPONSE VECTOR LOCI

Fig. 7.5 Loci For Test 86 - Output From Programme "VECTAN"

BENA35VAF

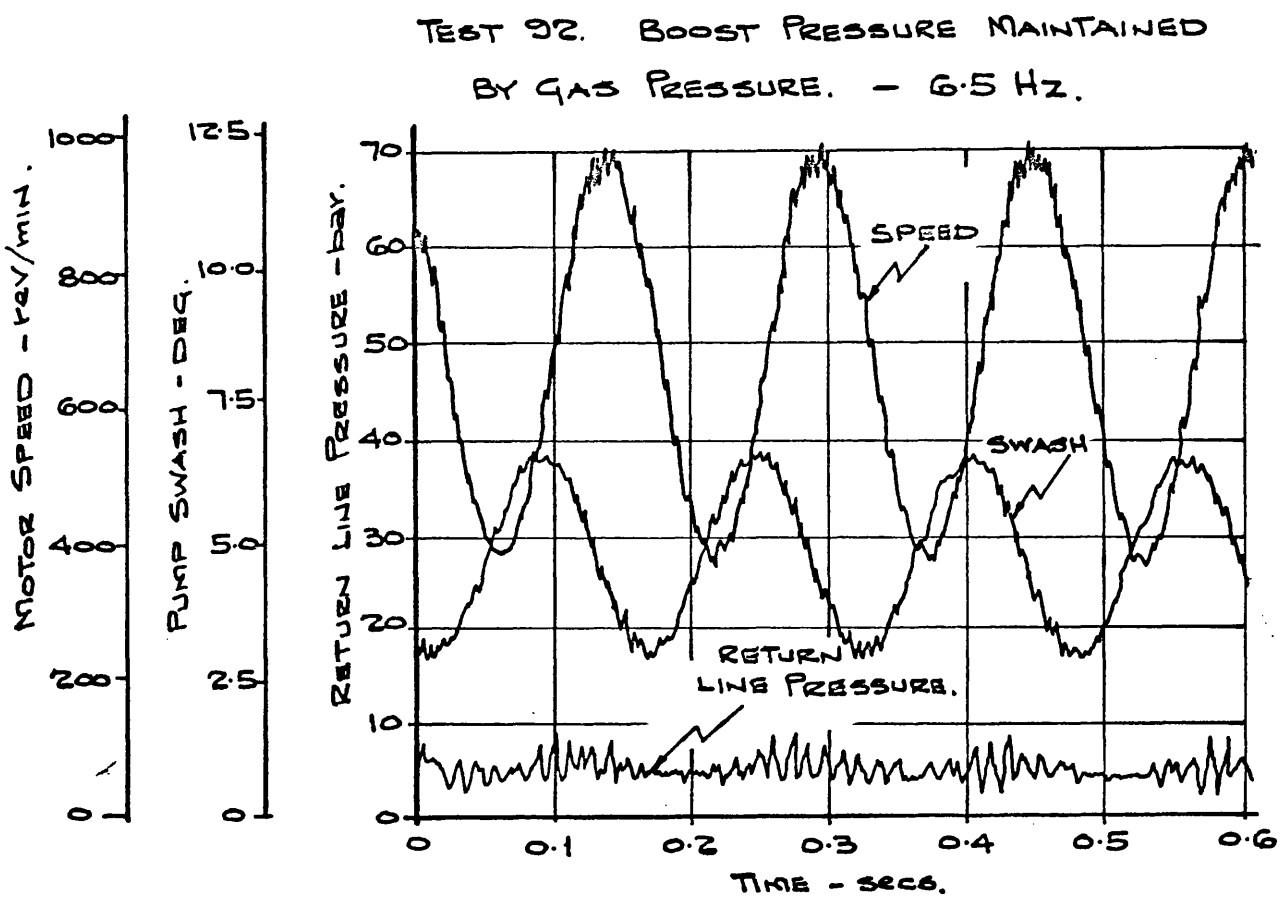

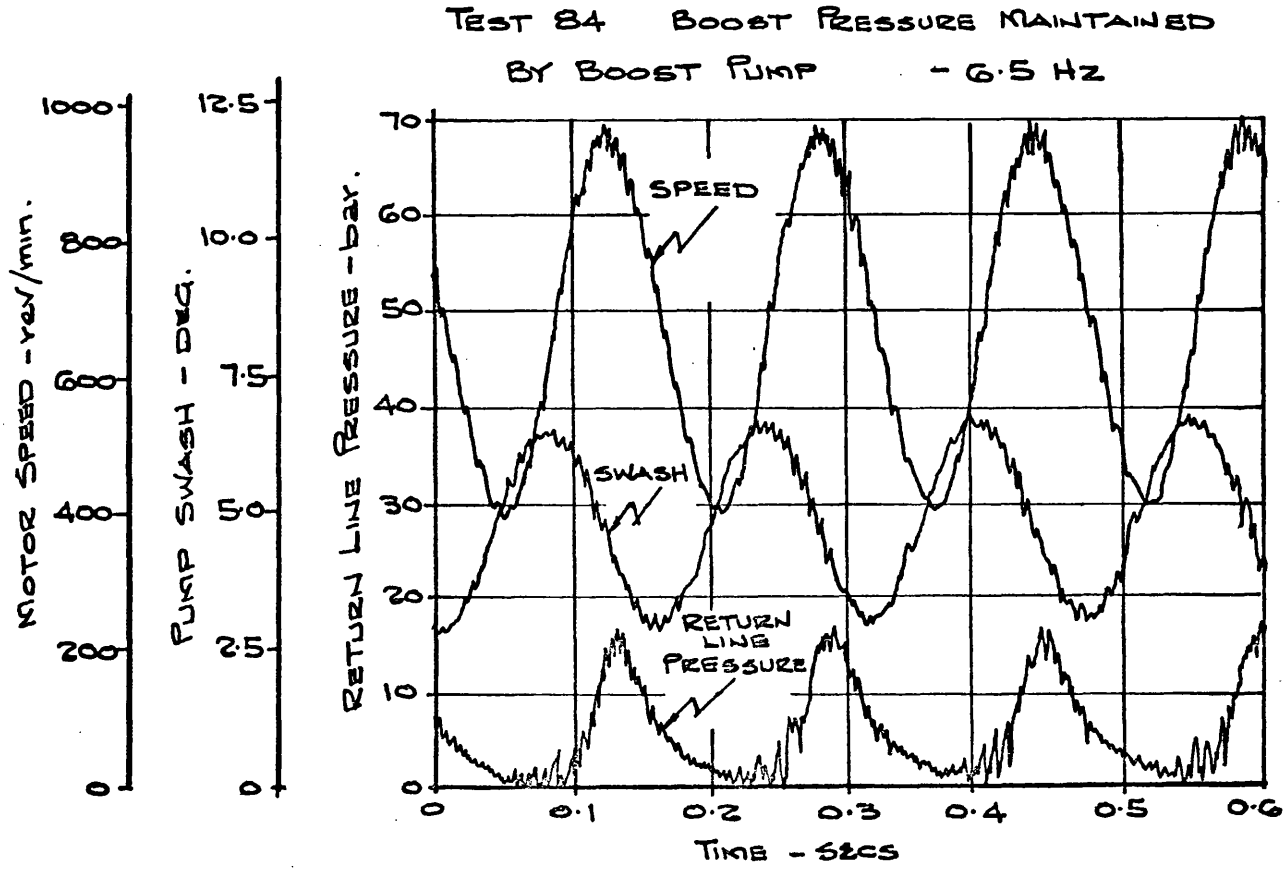

FIG. 7.6 PRESSURE SPEED AND SWASH TRACES FOR SYSTEM WITH BOOST PRESSURE MAINTAINED BY GAS PRESSURE AND BOOST PUMP.

CHAPTER 8 : CONCLUSIONS

The work of this thesis provides a theoretical and experimental base for future mathematical models and computer simulations of hydrostatic transmissions. Starting from the simple text book analysis of the dynamic performance of a hydrostatic transmission and moving forward into the experimental verification of more complex but representative models has served to demonstrate clearly the limitations and validity of the various models considered.

Before carrying out the dynamic analysis of the hydrostatic transmission a detailed study of the characteristics of the pump and motor was carried out to enable them to be represented satisfactorily in the dynamic model for the complete transmission.

8.1 The Positive Displacement Pump and Motor

The analysis of the theoretical discharge of a multi-cylinder reciprocating pump carried out in Chapter 2.2 showed that if the fluctuating delivery was represented as a Fourier Series all odd harmonics were equal to zero.

For a pump with n pistons all the even harmonics were zero up to the n^{th} harmonics when n is even and $2n^{th}$ when n is odd. This expressed mathematically why piston pumps are designed with odd numbers of pistons to reduce flow ripple to a minimum.

The theoretical discharge of a swash plate type piston pump whose swash plate was being oscillated about the zero delivery point reduces towards zero as the ratio of the frequency of oscillation of the swash plate to the frequency of rotation increases. It was not found possible to extend this analysis to the case where the swash plate was oscillated about some mean non zero value. A computerised solution of this case obtained by superimposing curves showed that a proportional relationship between flow and swash plate angle was valid, the only discrepancy being a typical piston flow ripple.

The actual discharge from a reciprocating machine must differ from the theoretical discharge determined from purely geometrical considerations due to the physical limitations of a machine subjected to the high acceleration forces of sinusoidal motions at high frequencies. During the experimental work described in Chapter 6.5.3 an investigation into the leakage losses of swash plate pump showed that no increase in leakage occurred when the swash plate was oscillated at frequencies up to 12 Hz.

At the end of the test programme it was found that the pump components did not show any signs of excessive wear resulting from the programme of frequency response tests.

A study of the mathematical models describing the steady state performance characteristics of positive displacement pumps and motors carried out in Chapter 2.3 revealed two principal schools of thought. The fundamental model developed by Wilson, and a more refined extension of this treatment including the density effect of the working fluid developed by Schlosser. Despite the acceptance of the existance of the density term it was decided that when working with experimental results over only a limited working range their effects could be ignored.

By applying Wilson's model to a pump or motor using an oil at constant temperature and running at constant speeds in its operating range the slip flow losses can be assumed to be proportional to pressure. Experimental measurements of the output of the pump under test described in Chapter 6.1.2 were evaluated in this way. If pump flow is measured at suction line conditions (at boost pressure in this case) the volumetric efficiency will be over-estimated as compressibility flow losses will have been recovered. These must be taken into account as described in Chapter 2.3.1, before expressing the slip losses as a slip loss co-efficient.

The slip losses were found to increase at high speeds as working clearances open up due to centrifugal force.

Wilson's model was again used when evaluating the pump and motor torque losses and no density effects were evaluated. Experimental determination of the pump and motor torque losses described in Chapter 6.1.2 revealed that although a significant viscous torque loss coud be determined, no significant pressure dependent torque loss could be identified. The viscous torque losses were expressed as viscous torque co-efficients evaluated over the pressure range of the unit. The torque co-efficient was found to fall off at higher pressures due to increase in clearances of bearing surfaces.

8.2 Predicting Dynamic Response

Extensive testing of a hydrostatic transmission has been carried out using frequency response and step response techniques. The dynamic response of a transmission is influenced to a large extent by the dynamic characteristics of the load. The scatter of results of much of the earlier work and the inability to attain meaningful correlation with theoretical predictions made using the simple block diagram or the more complex signal flow analysis of Chapter 3.2 and Chapter 3.3 can be attributed to the neglect of this important factor.

If the load cannot readily be represented mathematically as in the case of the loads described in Chapter 6.4.2.5 the prediction of transmission dynamic response cannot be carried out using block diagram or signal flow techniques. The alternative is to use the vector analysis presented in Chapter 3.4 in conjunction with the experimentally measured load characteristic. However, during the dynamic testing described in Chapter 6.6.1 where a transmission with a load that was predominently inertia was tested it was found that an accurate prediction of transmission response could be made using the mathematical methods. For all other loads the vector analysis technique had to be used, but from the good correlation obtained it was then possible to move forward and investigate in more depth the effects of other system parameters.

In the work on mathematical models described in Chapter 3.3 the signal flow analysis was extended to include the effects of prime mover droop and transmission loss co-efficients. As borne out during the early testing described in Chapter 6.3 the effects of prime mover droop are relatively insignificant except in extreme cases where attenuation of the low frequency response of the transmission occurred.

The insertion of the transmission loss co-efficients in the signal flow analysis had the effect of improving the accuracy of dynamic performance predictions particularly where the system volume was small. At these low volumes the simplified analysis underestimated both natural frequency and damping ratio.

The early experimental work described in Chapter 6.2 and Chapter 6.3 showed that the boost system, typical of most conventional closed loop hydrostatic drives, was incapable of maintaining a constant return line pressure during frequency response tests. The pressure variations in the return line contribute to the stiffness of the transmission and must be taken into account. The vector analysis technique developed in Chapter 3.4 enables the effect of return line pressure variations to be included when predicting natural frequency and damping ratio. However, to facilitate correlation the majority of the remaining test work described in Chapter 6 used an artificially large boost system capable of maintaining a near constant return line pressure.

For the transmission considered the hydraulic pipeline was relatively short, 1.80 m (6 ft.) which is approximately 1/50 of the wavelength of pressure waves at 15 Hz and under these conditions a lumped parameter approach is perfectly satisfactory. For longer pipelines it could be necessary to take into account the wave nature of the pressure signals. The inertia of the oil column between the pump and motor was evaluated for the system considered, but was found to add only 1% to the motor inertia when related to the output shaft.

Both frequency response and step response testing were undertaken, but as described in Chapter 6.4.2.4 it was found that the step response technique did not permit detailed studies of system parameters during transients. The availability of digital transfer function analysers has considerably facilatated frequency response testing and enabled techniques to be refined.

As described in Chapter 6.5 after careful evaluation of experimental results it was found that by use of the isentropic tangent bulk modulus of the oil in conjunction with the vector locus technique the natural frequency of the transmission could be predicted to within 5%. This was borne out by subsequent test work where these parameters were applied.

No detectable change in transmission natural frequency could be determined during the testing described in Chapter 6.6.2 and Chapter 7.3.1 when the mean return line pressure was reduced in stages to a level of 1.4 bar (20 lbf/in^2).

During theoretical predictions the effects of pipeline dilation were taken into account and by using the frequency response techniques in reverse the compliance of flexible hose was determined.

As described in Chapter 6.6.4 the value obtained was not in agreement with results obtained using static tests. The effective bulk modulus for oil in flexible hose found by frequency response tests was 4,350 bar (64,000 lbf/in^2) against 6,600 bar (97,000 lbf/in^2) obtained from static tests. The reason for this discrepancy was not determined, and should be subject to further work.

8.3 Aeration Effects Upon Transmission Performance

The vector locus technique was used in conjunction with frequency response testing to measure the bulk modulus of oil in the transmission loop subjected to conditions aimed at promoting aeration. No significant change in oil bulk modulus could be determined when the oil in the return line was saturated with air dissolved in it at pressures up to 5.5 bar (80 lbf/in^2) as described in Chapter 7.4.2.

Attempts to further accentuate aeration effects by saturating the return line with carbon dioxide (five times more soluble than air) at pressures up to 4.1 bar (60 lbf/in^2) resulted in a 7% increase in the measured effective bulk modulus. Further testing will be required to investigate this increase.

The use of oil with no defoamed additives for the aeration investigation did not change the effective bulk modulus of oil measured. Aeration and frothing of the oil in drain line was slow to disperse.

The use of a pressurised reservoir coupled directly to the return line of the transmission proved highly successful as a method of maintaining a boost pressure. Further work will require the use of a device to step down the pressure between the reservoir full of oil saturated with gas and the transmission return line if more excessive aeration conditions are to be artificially introduced.

REFERENCES

1. Ellington, E.B. — "Hydraulic Power Supplies in Towns" Proc. I. Mech. E., 1895. p.353

2. Beacham, T.E. — "Historical Development of Oil Hydraulic Power Transmission and Control". Conf. on Oil Hydraulic Power Transmission and Control. I. Mech. E., 1961. Paper 1

3. Hall, J.W. — British Patent No. 7479. 1896

4. Anon — "The Pittler Rotary Pump and Motor at the Olympia Exhibition", Engineering, London, 1907. Vol. 84, p.421.

5. Barrus, G.H. and Manly, C.M. — "Variable Speed Power Transmission" Trans. A.S.M.E. Vol. 33, p.851. 1911.

6. Heller, Von A. — "Hydraulischer Antrieb für Motorwagen" Zeitschrift Des Vereines Deutscher Ingenieure, April 1912. p.577.

7. Anon — "The Williams-Janney Variable Speed Gear". Engineering, London, Jan. 1913. p.156.

8. Anon — "The Hele-Shaw Rotary Pump and Motor" Engineering, London, June 1912. p.834

9. Edgehill, C.M. — "Some Factors Determining the Choice of a Particular Hydrostatic Transmission Unit". Fluid Power Symposium, B.H.R.A. Jan. 1969.

10. Newton, G.C. Jr. — "Hydraulic Variable Speed Transmissions as Servomotors". Journal of the Franklin Institute, Vol. 243, No. 6. June 1947.

11. Shearer, J.L. — "Fluid Power Control". M.I.T. Press, Cambridge, Mass. 1960.

12. Lewis, E. and Stern, H. — "Design of Hydraulic Control Systems" McGraw-Hill, New York. 1962.

13. Thoma, J. — "Hydrostatic Power Transmission" Trade and Technical Press, London. 1964

14. Gille, J.C. — "Feedback Control Systems". McGraw-Hill, New York. 1956.

15. Emmerson — "Analysis of the Output from a Swash Plate Pump when the Swash Plate is Subjected to an Oscillatory Motion about the point of Zero Tilt". Internal Report, Vickers Ltd. to McKissack. April, 1963.

16. Wilson, W.E. "Methods of Evaluating Test Data Aids Design of Rotary Pumps". Product Engineering. Oct. 1945. p.653-6.

17. Wilson, W.E. "Rotary Pump Theory". Transactions of A.S.M.E. Vol.68. May, 1946.

18. Wilson, W.E. "Positive Displacement Pump and Fluid Motors". Pitman Publishing Corporation. 1950.

19. Wilson, W.E. "How to Calculate Hydrostatic Transmission Co-efficients". Hydraulics and Pneumatics. Sept. 1964. p. 104-6.

20. Wilson, W.E. and Lemme, C.D. "Hydrostatic Transmissions, Hydraulics and Pneumatics". March-December 1970. Parts 1 - 7.

21. Schlosser, Dr.Ir.W.M.J. "Mathematical Model for Displacement Pumps and Motors". Hydraulic Power Transmission. Part 1, April 1961. Part 2, May, 1961.

22. Schlosser, Dr.Ir.W.M.J. and Hilbrands, J.W. "The Volumetric Efficiency of Displacement Pumps". Hydraulic and Pneumatic Power and Controls. July, 1963. p. 486-96.

23. Schlosser, Dr.Ir.W.M.J. and Hilbrands J.W. "The Hydraulic - Mechanical Efficiency of Displacement Pumps". Hydraulic and Pneumatic Power. Part 1, Sept. 1965. Part 2, Oct. 1965.

24. All "Can Mathematical Models Predict Performance - A Panel Discussion".
Panel Members: Wilson, W.E., Schlosser, Dr.I.R.W.M.J., Firth, D., Thoma, J., and Holzbock, W.G.
Hydraulics and Pneumatics. Feb.1971.

25. Toet, G. "The Determination of the Theoretical Stroke Volume of Hydrostatic Pumps and Motors from Volumetric Measurements". Hydraulic and Pneumatic Power. June, 1970.

26. Korn "Hydrostatic Transmission Systems" Chapter 3. Intertext. London. 1969.

27. Unruh. D.R., Fitch, E.C. and Sebosta, H.R. "How Computers Aid Analysis of Fluid Power Systems". Hydraulics and Pneumatics. March, 1971.

28. Alpay, S.A. and Mitchell, T. "Digital Simulation of a Hydraulic Control System". Hydraulics and Pneumatics. March, 1971.

29. Healey, A.J. "The Effect of Oil Inertia on the Resonant Frequency of Hydraulic Drives" Control. April, 1966.

30. Knight, G.C., McCollion, H, and Dudley, B.R. "Connection Capacitance Effects in Hydrostatic Transmission Systems and their Prediction by Mathematical Model" Draft of Proposed Paper to be submitted to the Institution of Mechanical Engineers.

31. Mason, S.J. "Feedback Theory, Further Properties of Signal Flow Graphs". Proc. I.R.E. Vol. 44. 1956.

32. Bowns, D.E. "Signal Flow Diagrams as an Aid to the Analysis of Hydraulic Systems" University of Bath, School of Engineering. Report No. 126. June 1968.

33. Hayward, A.T.J. "Research on Lubricants and Hydraulic Fluids at the National Engineering Laboratory". N.E.L. Report No. 75. Jan. 1963.

34. Hayward, A.T.J. "Compressibility Measurements on Hydraulic Fluids". N.E.L. Report No. 173, Part 1. Dec. 1964.

35. Hayward, A.T.J. "Generalisations for the Isentropic and Isothermal Compressibility of Hydraulic Mineral Oils". Journal of the Institute of Petroleum. Vol. 56, No. 547. Jan. 1970.

36. Anon "Technical Data on Shell Tellus Oils" Shell International Petroleum Company Ltd. Second Edition. 1967.

37. Anon — "Technical Data on Shell Tellus Oils" Shell International Petroleum Company Ltd. First Edition. 1963.

38. Hansen, J.T. — "How to Use Readily Available Specification Data to Predict Dynamic Properties of Hydraulic Motors". Machine Design. Vol. 33, No. 2. Jan. 1961.

39 Lambert, T.H. and Davies, R.M. — "Investigation of the Response of Hydraulic Servo-Mechanism with Inertial Load". Journal of Mechanical Engineering Science. Vol. 5, No. 3. 1963.

40. Renner, H. — "Fluid Motors". Design Engineering Conf. 1965. A.S.M.E. Paper 65-MD-28. March 1966.

41. Healey, A.J. and Stringer, J.D. — "Dynamic Characteristics of an Oil Hydraulic Constant Speed Drive". I. Mech. E. (Automobile Control Group) Vol. 183, Part 1. 1968.

42. Green, W.L. and Crossley, T.R. — "Analysis of the Control Mechanism Used in Variable Delivery Hydraulic Pumps". Proc. I. Mech. E. Vol.185, No. 6. 1971.

43. Keating, T. and Martin, H.R. — "Response Testing of a Hydraulic Servo-Mechanism with Mechanical Feedback". 2nd Fluid Power Synposium, B.H.R.A. Jan.1971. Guildford.

44. Walters, R. "Hydraulic Servo Systems Analysis and Synthesis". Sperry Industrial Group. Pub. IG 100/A. 1964.

45. Streeter "Handbook of Fluid Power Dynamics" McGraw-Hill. Section 12.1.1, 12.1.2 and 12.1.6.

46. McCloy, D. "Cavitation and Aeration - The Effect On Valves and Systems". Hydraulic and Pneumatic Power. Part I and Part II. Jan. and Feb. 1966.

47. Anon "Solubility of Gases in Lubrication Fluids" Confidential Internal Report. Mobil Oil.

48. Smith, L.H. Peeler, R.I. and Bernd, L.H. "Hydraulic Fluid Bulk Modulus: Its Effect on System Performance and Techniques for Physical Measurement". Proceedings of the National Conference on Industrial Hydraulics, U.S.A. Oct. 1960.

49. Hayward, A.T.J. "How Air Bubbles Affect the Compressibility of Oil". Hydraulic Power Transmission. June, 1962.

50. Magorien, V.G. "How Hydraulic Fluids Generate Air". Hydraulics and Pneumatics. June, 1968.

51. Magorien, V.G. "Effects of Air on Hydraulic Systems" Hydraulics and Pneumatics. Oct. 1967.

52. Rendel, B. and Allen, G.R. "Air in Hydraulic Transmission Systems" Aircraft Engineering. 1951 - 23(273).

53. Hayward, A.T.J. "Air Entrainment and Compressibility of Hydraulic Fluids". Letter to the Editor, Mechanical World. Oct. 1961.

54. Tourret, R. and White, N. "Aeration and Foaming in Lubricating Oil Systems". Aircraft Engineering. May, 1952.

55. Livesay, R.M. and Ettinger, M.H. "Separator De-areates Oil, Stops Shimmy on F104 Nose Wheel". Hydraulics and Pneumatics. Oct. 1967.

56. Bowns, D.E. "The Dynamic Transfer Characteristics of Reciprocating Engines". Proc. I. Mech. E. Vol. 185, 16/71. 1970-71.

57. Kemp, J.D. and Barrett, M.T.L. "Compressibility Effects of Fluids in Pipes". University of Bath, School of Engineering. Report No. 136. June, 1969.

58. Bernd "Air - Oil Cavitation Effects in the L.G.C. Drive". Internal Report of General Electric Company. No. R57 APS-34.

APPENDIX I

COMPUTER PROGRAMMES

A.1.1 The Flow from a Hydrostatic Pump with Swash Plate Oscillating about a Mean Non Zero Swash Angle

PROGRAMME 1 : 'DELIV'

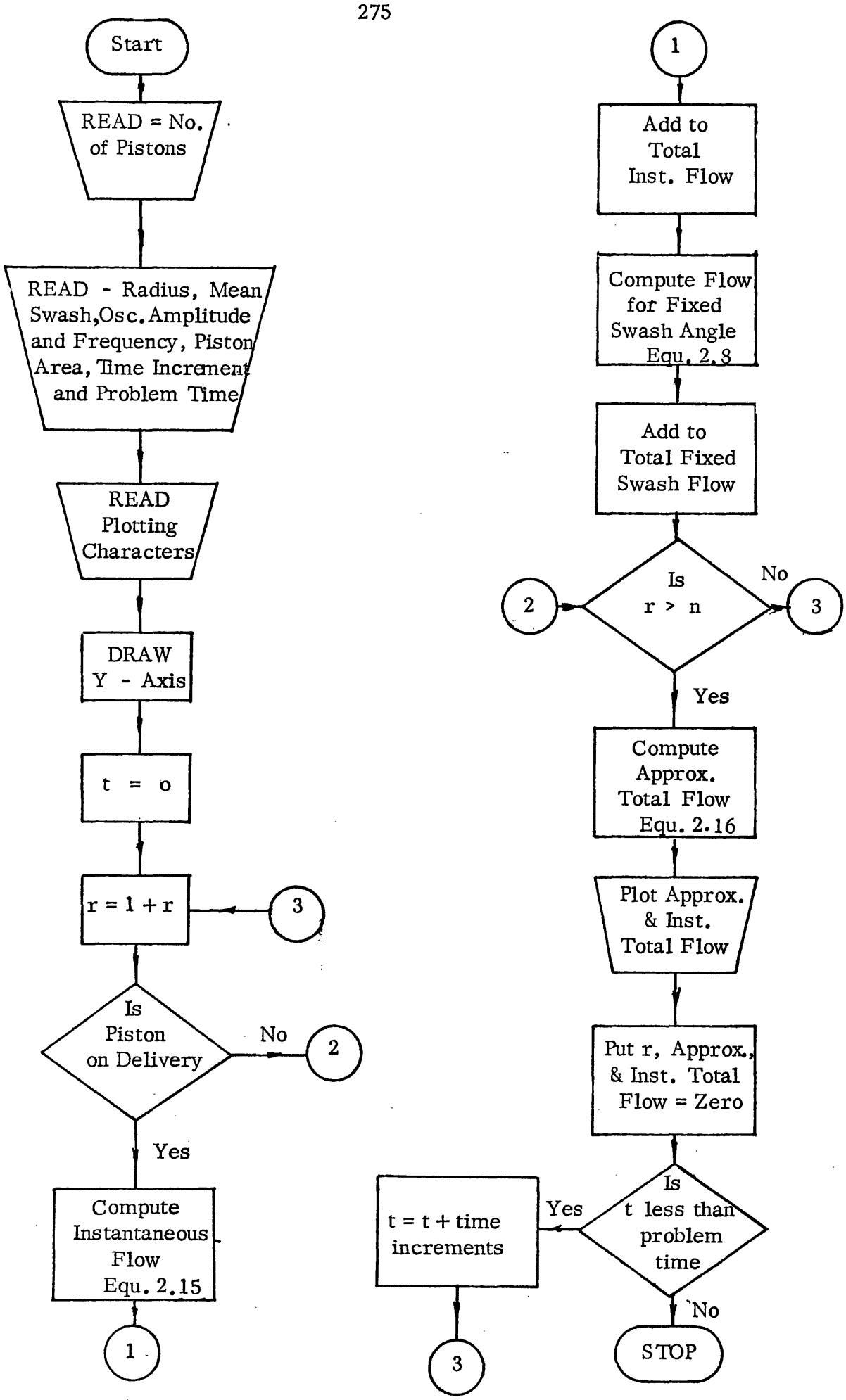

FIG. A.1.1.1 FLOW CHART for 'DELIV'

```
      PROGRAM DELIV
C     DISPLACEMENT OF PUMP WITH SWASH PLATE OSCILLATING SINUSOIDALLY
C     ABOUT A MEAN
      DIMENSION X(20),Y(20),Z(20),LINE(120),Q(20)
      READ (5,9) N
    9 FORMAT(I2)
      READ(5,10)  RAD,BOMG ,ALP,OMG,AMP,AREA,TINC,TLST
   10 FORMAT(8F10.4)
      TIME=0
      READ(5,15) JBLANK,JDOT,JSTAR,JPLUS
   15 FORMAT(4A1)
      DO 16 J=1,120
   16 LINE (J)=JDOT
      WRITE(6,17) LINE
   17 FORMAT (1H1,120A1)
      DO 18 J=1,120
   18 LINE (J)=JBLANK
   21 TOTAL=0
      QTOTAL=0
      DO 14 I=1,N
      IF (SIN(BOMG*TIME+2*3.1416*I/N)) 11,12,12
   11 X(I)=0
      Y(I)=0
      Q(I)= 0
      GO TO 13
   12 X(I)= AREA*AMP*OMG*RAD*COS(BOMG*TIME+2*3.1416*I/N)*COS(OMG*TIME)/
     1COS(ALP-AMP*SIN(OMG*TIME))**2
      Y(I)=AREA*BOMG*RAD*SIN(BOMG*TIME+2*3.1416*I/N)*SIN(ALP-AMP*SIN(OMG
     1*TIME))/COS(ALP-AMP*SIN(OMG*TIME))
      Q(I)=AREA*RAD*BOMG*SIN(ALP)*SIN(BOMG*TIME+2*3.1416*I/N)/COS(ALP)
   13 Z(I)=X(I)+Y(I)
      QTOTAL= Q(I)+QTOTAL
   14 TOTAL=Z(I)+TOTAL
      QINST=QTOTAL*(1.0-SIN(AMP)*COS(ALP)/SIN(ALP)*COS(AMP)*SIN(OMG*
     1TIME))
      LINE(20)=JDOT
      J=TOTAL/20*100+0.5+20
      K=QINST*5.0+20.5
      LINE (J)=JSTAR
      LINE(K)= JPLUS
      WRITE (6,19) LINE
   19 FORMAT(1H ,120A1)
      LINE(J)=JBLANK
      LINE(K)=JBLANK
      LINE(20)=JDOT
      TIME=TIME+TINC
      IF (TLST-TIME) 20,21,21
   20 STOP
      END
```

FIG. A.1.1.2 PROGRAMME LISTING for 'DELIV'

A.1.2 The Evaluation of the Overall Transfer Function of a Hydrostatic Transmission using Signal Flow Analysis

PROGRAMME 2 : 'TRDRES'

A.1.2.1 Main Programme

The transfer function relating output speed to pump swash, Equ. 3.37 is

$$\frac{\omega_2}{x_P} = \frac{D_1 \Omega_1}{D_2 X_M} \frac{1 - (J_1 s + f_P) K_E + D_1 P_D K_E \frac{X_P}{\Omega_1}}{1 - (J_1 s + f_P) K_E - \frac{(f_L + f_M + J_2 s)}{D_2 X_M (D_2 X_M - K_{FM})} X}$$

$$\left\{ (K_P - \frac{V s}{B_e} + K_M)(1 - J_1 K_E s - f_P K_E) + K_E D_1 X_P (D_1 X_P + K_{fP}) \right\}$$

- A.1.2.1

If the terms in s are collected together a general expression can be written

$$\frac{\omega_2}{x_P} = \frac{K (H + As)}{Bs^3 + Cs^2 + Es + G} \qquad \text{- A.1.2.2}$$

The main Programme 'TRDRES' evaluates the co-efficients K, H, A, B, C, E, & G, having read in the transmission parameters. In order to determine the significance of the resulting transfer function two subroutines were written to the main Programme.

A.1.2.2 Subroutine 'RESP'

By substituting $j\omega$ for s in the transfer function and splitting into real and imiginary parts, the amplitude ratio and phase angle of $\frac{\omega_2}{x_P}$ were calculated.

$$\frac{\omega_2}{x_P}(j\omega) = K\left\{\frac{H(G - C\omega^2) + A\omega(E\omega - B\omega^3)}{(G - C\omega^2)^2 + (E\omega - B\omega^3)^2} + j\left\{\frac{A\omega(G - C\omega^2) - H(E\omega - B\omega^3)}{(G - C\omega^2)^2 + (E\omega - B\omega^3)^2}\right\}\right\}$$

- A.1.2.3

The amplitude ratio was also calculated in decibels so that bodes plots from the transfer function could be plotted.

A.1.2.3 Subroutine 'SOLVE'

In order to rewrite the transfer function, the general expression for which is given in Equ. A.1.2 in a standard form, it is necessary to reduce the denominator to a first and second order equation of the form

$$\frac{\omega_2}{x_P} = \frac{K(1 + \tau_2 s)\ \omega_n^2}{(1 + \tau_2 s)\ (s^2 + 2\xi\ \omega_n s + \omega_n^2)} \qquad \text{- A.1.2.4}$$

by evaluating one real root.

The Newton-Raphson technique was used to solve for the real root and the remaining quadratic separated from the denominator. The resulting equation was then rearranged into the form given by Equ. A.1.4 and K, τ_1, τ_2, ω_n, & ξ printed out.

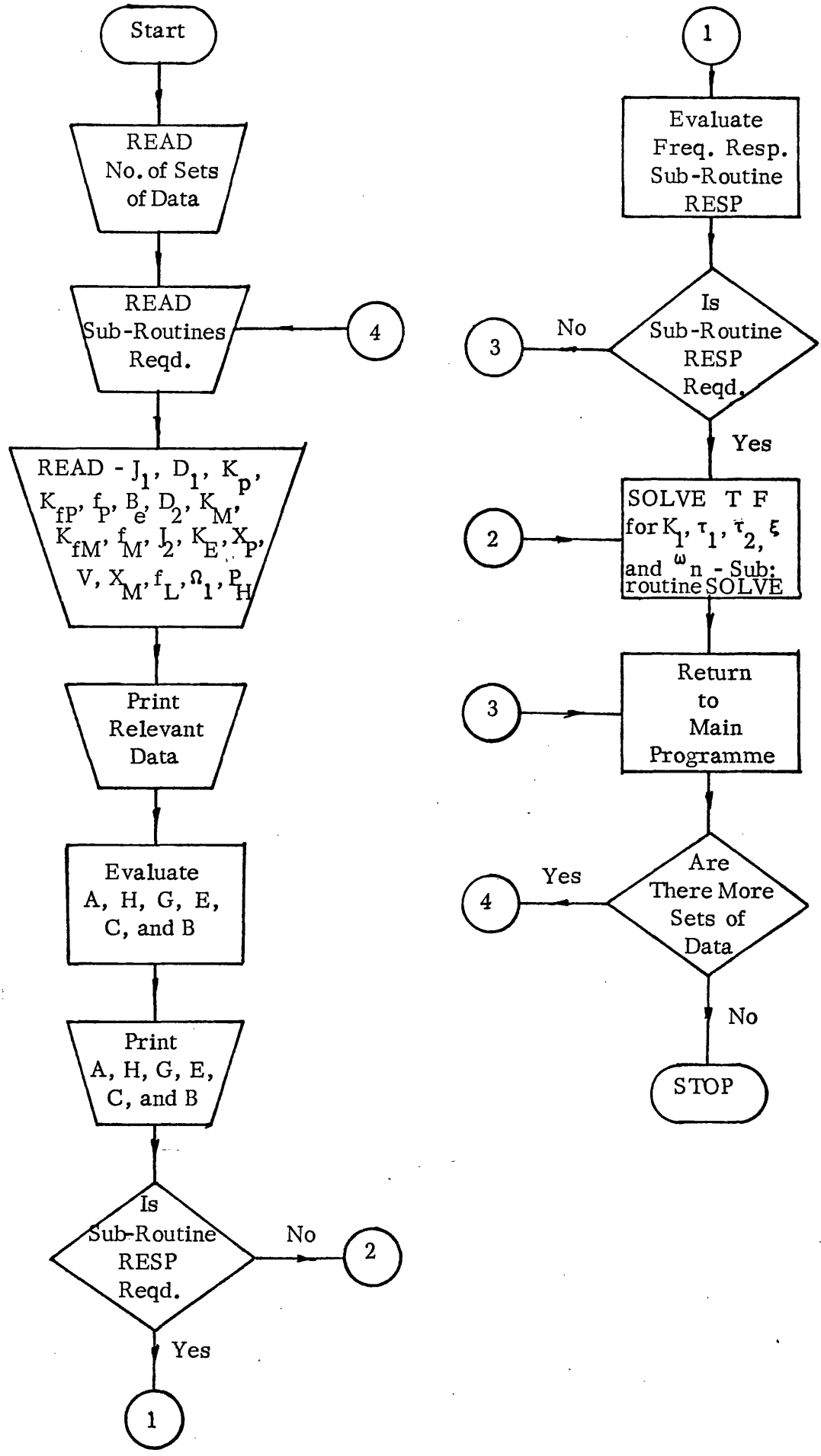

FIG. A 1.2.1 FLOW CHART for 'TRDRES'

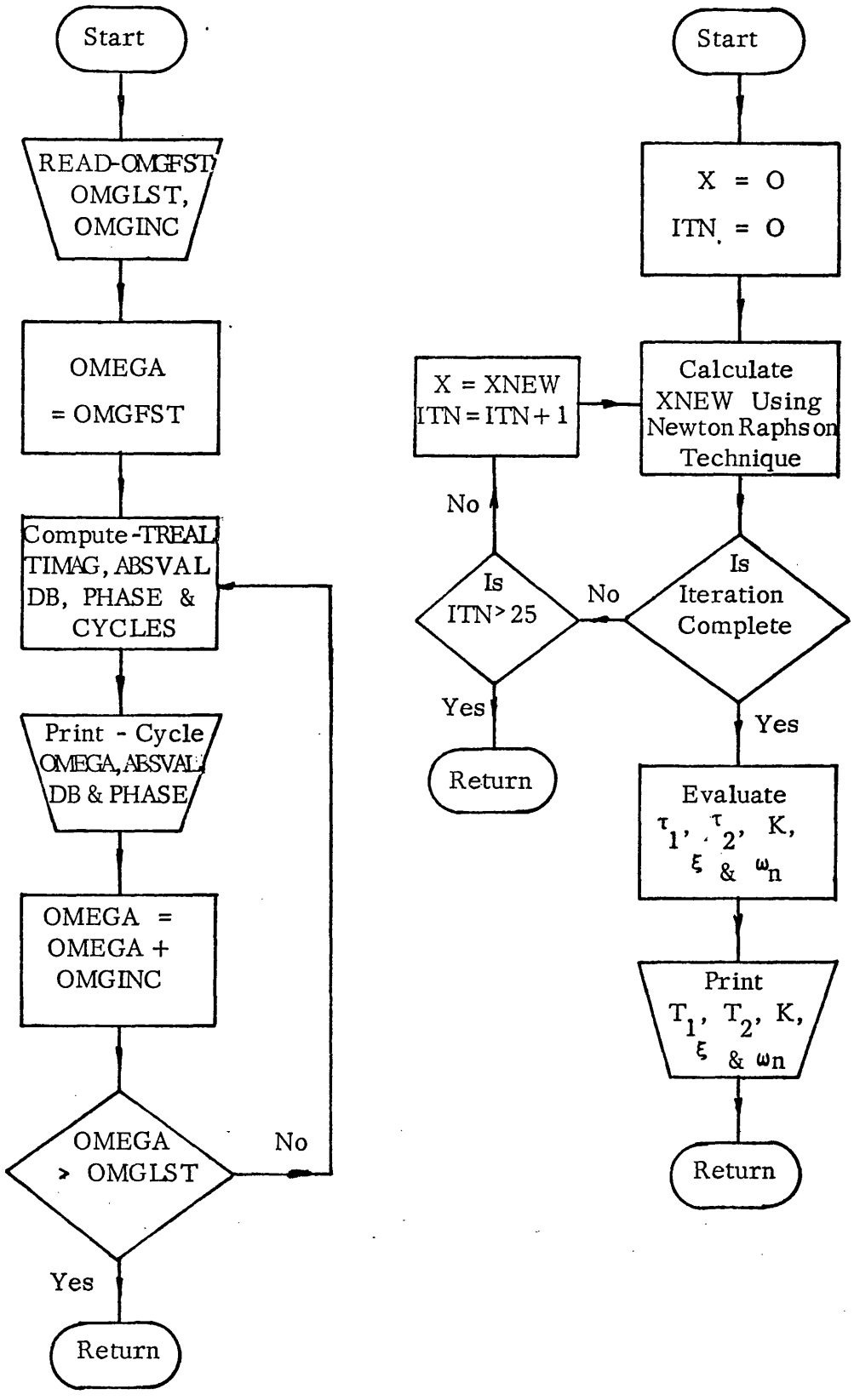

FIG. A1.2.2 FLOW CHARTS for SUBROUTINES 'RESP' and 'SOLVE'

```
      PROGRAM TRDRES
C TRANSMISSION DYNAMIC RESPONSE
      COMMON A, B, C, E, G, H, AMP
   77 FORMAT(I3)
      READ(5,77)NUMBER
      ITEM=0
      DO 99 KOUNT=1,NUMBER
      READ(5,200)KODE
  200 FORMAT(I1)
      READ (5, 3) AINT1, DP, SP, PDTCP, VTCP, B, DM, SM, PDTCM, VTCM,
     1     AINT2,  ESLD, THETAP, VOL, THETAM, DFL, BOMGP, SPRESS
    3 FORMAT  (8E10.3)
      SP=-SP
      SM=-SM
      ESLD=-ESLD
      WRITE (6, 5) ESLD, THETAP, VOL,THETAM, DFL, BOMGP,SPRESS
    5 FORMAT(1H1,10X,4HESLD,13X,6HTHETAP,14X,3HVOL,13X,6HTHETAM,14X,
     -       3HDFL,14X,5HBOMGP,12X,6HSPRESS// 1H0,1P7E18.5////)
      AMP = DP*BOMGP/(DM*THETAM)
      A =-AINT1*ESLD
      H=1-VTCP*ESLD+DP*SPRESS*ESLD*THETAP/BOMGP
      DENOM1 = DM*THETAM*(DM*THETAM-PDTCM)
      G = 1-VTCP*ESLD-(DFL+VTCM)*((SP+SM)*(1-VTCP*ESLD)+ESLD*DP*THETAP*
     1(DP*THETAP+PDTCP))/DENOM1
      E =-AINT1*ESLD-(DFL+VTCM)*(-VOL*(1-VTCP*ESLD))/(DENOM1*B)-AINT2*((
     1    SP+SM)*(1-VTCP*ESLD)+ESLD*DP*THETAP*(DP*THETAP+PDTCP))/DENOM1
     1+(DFL+VTCM)*(SP+SM)*AINT1*ESLD/DENOM1
      C =-(DFL+VTCM)*VOL*AINT1*ESLD/(B*DENOM1)+AINT2*VOL*(1-VTCP*ESLD)/
     1   (DENOM1*B)+AINT1*AINT2*ESLD*(SP+SM)/DENOM1
      B =-AINT1*AINT2*ESLD*VOL/(DENOM1*B)
      WRITE(6,15)AMP,A,G,E,C,B,H
   15 FORMAT(1H0,11X,3HAMP,16X,1HA,17X,1HG,17X,1HE,17X,1HC,17X,1HB,17X,
     -       1HH// 1H0,1P7E18.5////)
      IF(KODE-3)10,20,10
   10 CALL RESP(KODE,&99,&20)
   20 CALL SOLVE(ITEM)
   99 CONTINUE
      WRITE(6,222)NUMBER,ITEM
  222 FORMAT('1 ***',I4,' SETS OF DATA ARE PROCESSED :',I3,' ARE TERMINA
     -TED AFTER 25 ITERATIONS ***')
      STOP
      END
```

FIG. A.1.2.3 PROGRAMME LISTING for 'TRDRES'

```
      SUBROUTINE RESP(KODE,*,*)
      COMMON A, B, C, E, G, H, AMP
      WRITE(6,1)
    1 FORMAT(1H0,19X,9HFREQUENCY,31X,9HAMPLITUDE,23X,5HPHASE//9X,10HCYCL
     1ES/SEC,11X,8HRADS/SEC,12X,6HABSVAL,17X,2HDB,15X,7HDEGREES // )
      READ (5,24) OMGFST, OMGLST, OMGINC
   24 FORMAT (3E10.3)
      OMEGA = OMGFST
   26 OMGSQ = OMEGA*OMEGA
      DENOM2= (G-C*OMGSQ)**2+(E*OMEGA-B*OMEGA*OMGSQ)**2
      TREAL = AMP*(H*(G-C*OMGSQ)+A*(E*OMGSQ-B*(OMGSQ**2)))/DENOM2
      TIMAG = AMP*(A*OMEGA*(G-C*OMGSQ)-H*OMEGA*(E-B*OMGSQ))/DENOM2
      ABSVAL = SQRT(TREAL**2+TIMAGE**2)
      DB = 20*ALOG10(ABSVAL)
      PHASE = ATAN2(TIMAG,TREAL)*57.29578
      CYCLES = OMEGA/(3.142*2)
      WRITE (6,35)  CYCLES, OMEGA, ABSVAL, DB, PHASE
   35 FORMAT(5E20.5)
      OMEGA = OMEGA + OMGINC
      IF (OMEGA-OMGLST) 26,26,38
   38 RETURN KODE
      END



      SUBROUTINE SOLVE(ITEM)
      COMMON A,B,C,E,G,H,AMP
      X = 0
      ITN = 0
      WRITE(6,50)
   50 FORMAT(1H0,//,4X,4HXNEW/)
   35 W = B*X**3+C*X**2+E*X+G
      Y = 3*B*X**2+2*C*X+E
      XNEW = X-W/Y
      WRITE (6, 45) XNEW
   45 FORMAT(' ',1P1E11.4)
      IF ( ABS((X-XNEW)/XNEW)-1.0E-03) 48, 39, 39
   39 ITN = ITN+1
      IF (ITN-25) 41, 47, 47
   41 X = XNEW
      GO TO 35
   47 WRITE(6,222)
  222 FORMAT(//' *** TERMINATED AFTER 25 ITERATIONS ***')
      ITEM=ITEM+1
      RETURN
   48 XNEW = -XNEW
      B1 = C-B*XNEW
      B2 = E-(C-B*XNEW)*XNEW
      WNSQ=B2/B
      GAIN = AMP*H/(B*WNSQ*XNEW)
      T1 = A/H
      T2 =1/XNEW
      DAMP = B1/B
      WN = SQRT(WNSQ)
      ZETA= DAMP/(2*WN)
      WRITE (6, 58)  GAIN, T1, T2, ZETA, WN
   58 FORMAT (1H0, //, 12X , 4HGAIN , 17X , 2HT1 , 18X , 2HT2 , 18X ,
     1   4HZETA , 17X , 2HWN , // , 1P5E20.4 // )
      RETURN
      END
```

FIG. A.1.2.4 PROGRAMME LISTING for SUBROUTINES 'RESP' and 'SOLVE'

A.1.3 The Dynamic Analysis of a Hydrostatic Transmission Using Vectors

PROGRAMME 3 : 'VECTAN'

This Programme was written after a large proportion of the experimental work on the hydrostatic transmission had already been completed. The failure of the block diagram and signal flow analysis to provide correlation between predicted and experimental values of hydrostatic transmission natural frequency due to the problem of load representation lead to the use of vector analysis.

Vector analysis provided a good correlation between experimental and predicted results, and in order to extend the work and investigate the effect of various system parameters, it was decided to write a computer programme that would both evaluate experimental results and carry out a vector analysis to predict the dynamic response of the hydrostatic transmission under the conditions of operation fed into the programme.

During this period it was felt that the programme should be brought into line with the pending change to metric units. All output is listed in both imperial and S.I. units under correct titles and dual systems of units given.

A.1.3.1 Main Programme Elements

Transmission Component Data:

The basic physical dimensions of the transmission such as pump and motor displacement were listed.

Pump and Motor Loss Co-efficients:

The pump and motor loss co-efficients obtained from experimental curves for the conditions of the test being carried out were introduced.

Rig Calibration Constants:

The rig calibration constants, the constants obtained for the various rig transducers, were inserted here.

Steady State Test Conditions:

The steady state voltages enabling the steady state conditions of the transmission to be calculated using the rig calibration constants were inserted here. Where gauge pressures have been measured these were introduced and were used in place of the value obtained from the electronic transducer. The transmission volumetric, mechanical, and overall efficiences were calculated and printed.

Additional Information for Dynamic Analysis

Information on the pipes connecting the pump and motor units, and the dead volumes of the units themselves was introduced. The bulk modulus of the oil could either be fed in at this point or calculated using the generalised equation developed by Hayward described in Section 4.2.1. The isentropic and isothermal tangent bulk moduli were calculated and a mean value determined. An effective value for the oil in the pipeline was also calculated.

Read in Frequency Response Data in Arrays and Print Out Ratios

The measured output obtained during frequency response tests as r.m.s. voltages and phase lags in degrees resulting from sinusoidal driving voltage fed to the pump swash servo were read in. The output was built up into arrays and then formed into ratios and the appropriate calibration constants applied.

The ratios formed were /

The ratios formed were:

$$\frac{\text{Motor Output Speed}}{\text{Pump Swash}} - \frac{\omega_2}{x_P} - \frac{\text{Rev/min.}}{\text{deg.}}$$

$$\frac{\text{Load Torque}}{\text{Motor Output Speed}} - \frac{f_L}{\omega_2} - \text{Nm/}_{\text{rev/min.}}$$

$$\frac{\text{Supply Line Pressure}}{\text{Motor Output Speed}} - \frac{P_H}{\omega_2} - \text{bar/}_{\text{rev/min.}}$$

$$\frac{\text{Return Line Pressure}}{\text{Motor Output Torque}} - \frac{P_L}{\omega_2} - \text{bar/}_{\text{rev/min.}}$$

The amplitude ratio and phase relationship for the ratios were calculated at each frequency under consideration.

Calculate Effective Load Torque and Pressure Difference

The Vector Analysis described in Section 3.4 was commenced by adding the torque required to accelerate the hydraulic motor (Equ. 3.44), to the measured load torque.

The effective load torque was used to determine the pressure difference across the hydraulic motor.

Vector Prediction of Overall Transmission Response

The remainder of the vector analysis described in Section 3.4 was carried out using the data previously fed in and the effective load calculated in the previous element. The calculated response was printed out in tabular form alongside the experimental results to provide a direct comparison.

Using Vector Analysis to Determine Effective Compressibility of Oil

In order to determine the effective compressibility of the oil in the pipeline it is possible to work backwards from the measured response of the transmission to the compressible flow vector $\overline{q_c}$. Using Equ. 3.50 it is then possible to calculate the $\overline{\omega_2}$ effective bulk modulus for the oil in the pipe.

What type of Plotted Output is Required?

On the basis of a control constant it is determined whether to plot the nyquist diagram, bode plot, or both for the transmission response. A standard plotting subroutine GR4( ) was available for the bode plot, but it was necessary to prepare the data.

A typical output from the programme is given in Chapter 7 when the programme was being used for studying the effects of aeration upon transmission dynamic response.

A.1.3.2 Subroutine Loci

This subroutine utilised the standard graph plotter package available under system I.C.L. 450 to construct the polar axes for a Nyquist Diagram, provide axes and title the axes with parameters and units. The size of the framework set up resulted from experience of diagrams prepared for earlier test work.

The overall transmission response obtained by the vector analysis technique and by direct measurement were plotted as points on the polar framework. No attempt was made to join the points as their proximity would depend entirely upon the shape of the transmission response curves obtained.

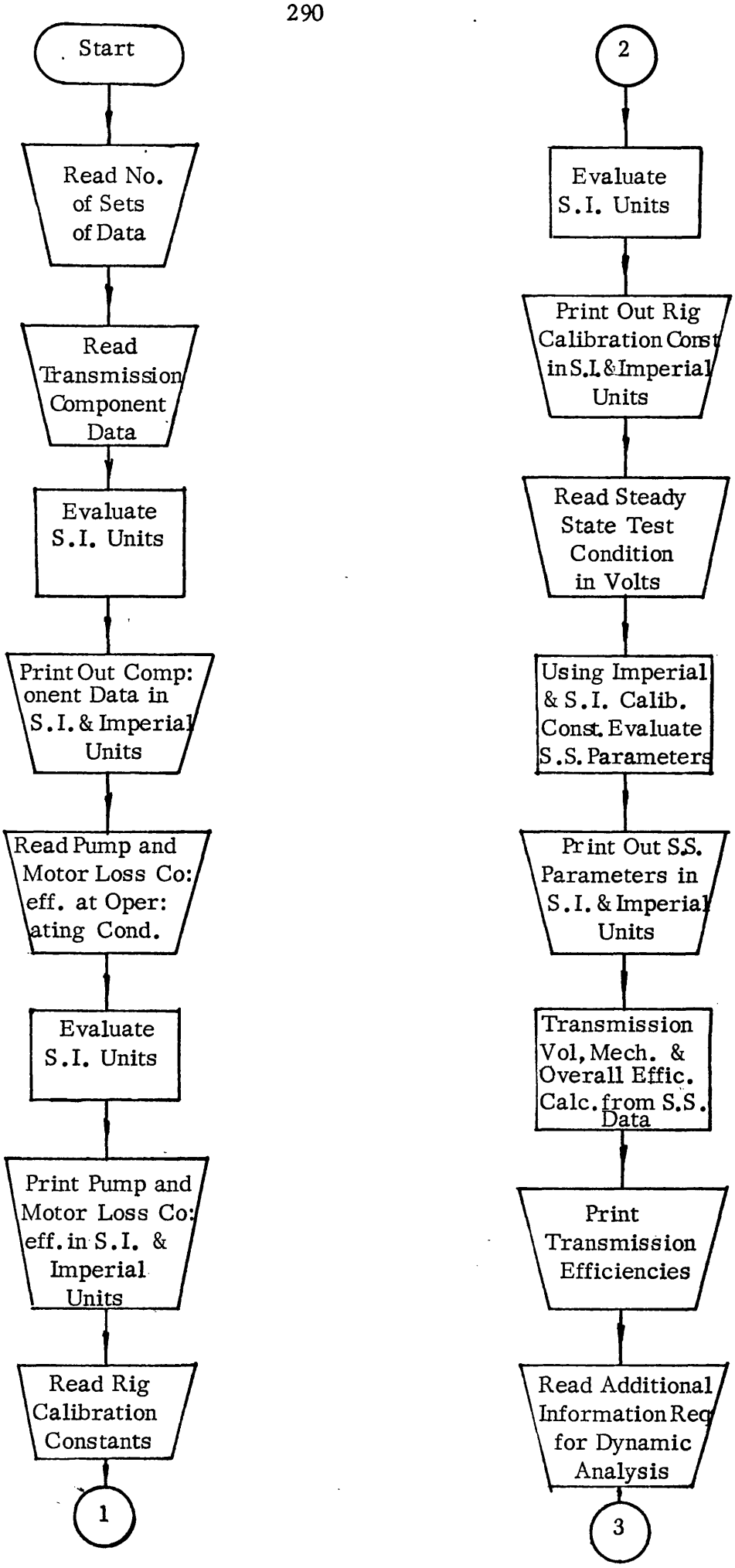

A 1.3.1 FLOW CHART for 'VECTAN'

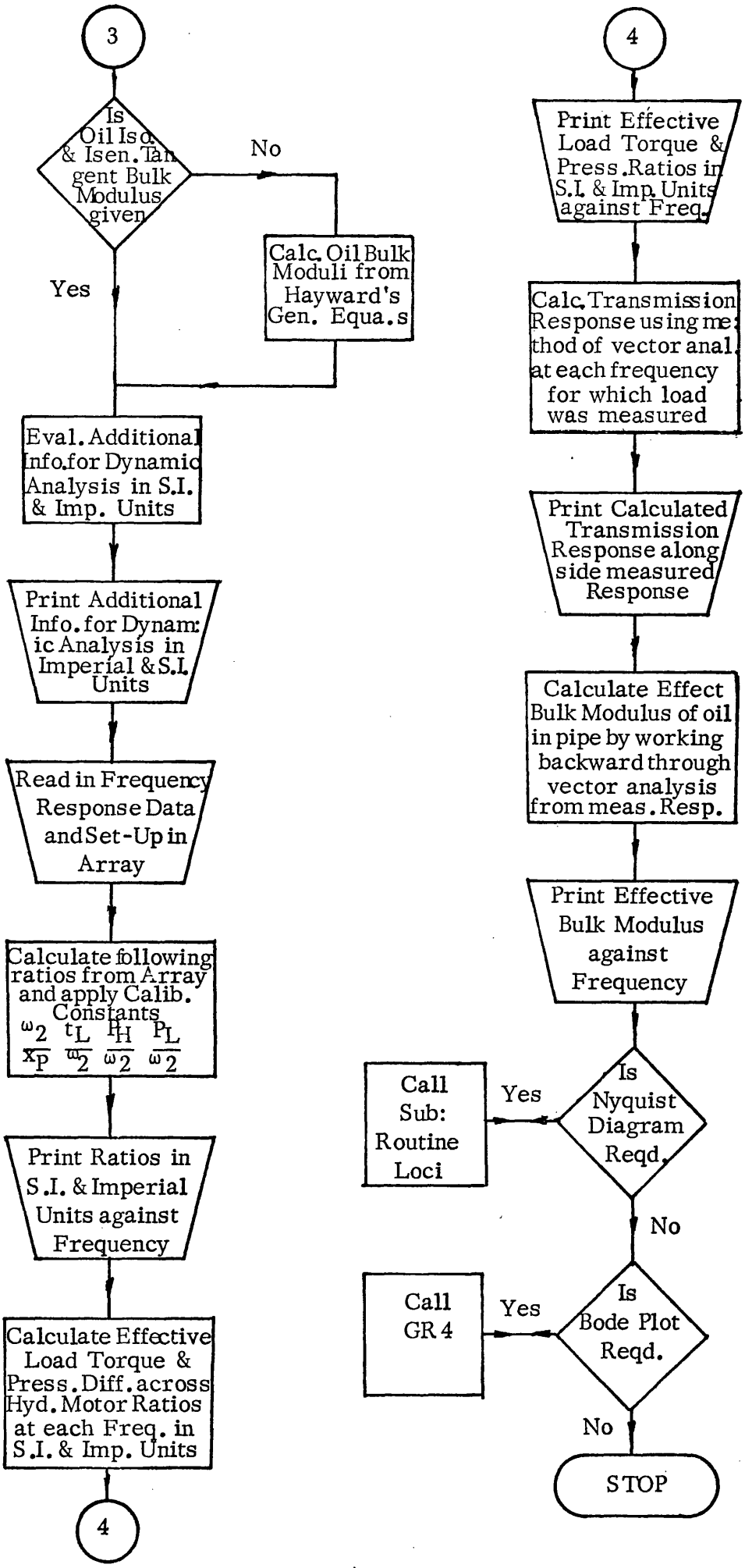

FIG. A 1.3.1 FLOW CHART for 'VECTAN' (Cont.)

```
      PROGRAM VECTAN
C
C     THE DYNAMIC ANALYSIS OF A HYDPOSTATIC TRANSMISSION USING VECTORS
C
      DIMENSION DTFA(50,13),RAD(50),W2XPA(50),W2XPP(50),TLW2A(50),TLW2P
     +(50),PHW2A(50),PHW2P(50),PLW2A(50),PLW2P(50),PDW2A(50),PDW2P(50),T
     +LW2AM(50),PHW2AM(50),PLW2AM(50),PDW2AM(50),TMW2A(50),TMW2P(50),TEM
     +A(50),TEMP(50),T2W2A(50),T2W2P(50),CPDWA(50),CPDWP(50),TMW2AM(50),
     +T2W2AM(50),CPDWAM(50),SFW2A(50),SFW2P(50),CFW2A(50),CFW2P(50),FLW2
     +A(50),FLW2P(50),PFW2A(50),PFW2P(50),OVRSA(50),OVRSP(50),APFW2A(50)
     +,APFW2P(50),AFLW2A(50),AFLW2P(50),ANGLE(50),ASFW2A(50),ACFW2A(50),
     +SPSM(50),EBMIP2(50),X(4,50),Y(4,50)
      ARCTAN(ARG)=ATAN(ARG)
      REAL MOT2,MOT2M,MDVOL,MDVOLM,MBM,MBMM
      READ(5,100) NUMBER
  100 FORMAT (I2)
      DO 24 KOUNT=1,NUMBER
C
C     TRANSMISSION COMPONENT DATA
C
      READ(5,101) BOMGP,DP,DM,XPMAX,XMMAX,MOT2
  101 FORMAT(6E10.3)
      BOMGPR=BOMGP/60*2*3.1416
      DPM=DP*28.3168
      DMM=DM*28.3168
      XPMAXR=XPMAX/57.296
      XMMAXR=XMMAX/57.296
      MOT2M=MOT2*1.3558
      WRITE(6,200) BOMGP,BOMGPR,DP,DPM,DM,DMM,XPMAX,XPMAXR,XMMAX,XMMAXR,
     +MOT2,MOT2M
  200 FORMAT(1H1,'TRANSMISSION COMPONENT DATA',///,
     +20X,'PRIME MOVER SPEED',22X,'=',1PE15.3,5X,'RPM',/,59X,'=',1PE15.3
     +,5X,'RAD/SEC',///,20X,'PUMP DISPLACEMENT/RADIAN SWASH/RADIAN',2X,
     +'=',
     +1PE15.3,5X,     'FT3/RAD SWASH/RAD',/,59X,'=',1PE15.3,5X,'LITRE/'
     +'RAD SWASH/RAD',//,20X,'MOTOR DISPLACEMENT/RADIAN SWASH/RADIAN',1X
     +,'=',1PE15.3,5X,'FT3/RAD SWASH/RAD',/,59X,'=',1PE15.3,5X,'LITRE/'
     +'RAD SWASH/RAD',//,20X,'MAXIMUM PUMP SWASH',21X,'='1PE15.3,5X,
     +'DEGREES',/,59X,'=',1PE15.3,5X,'RADIANS',//,20X,'MAXIMUM MOTOR SWA
     +SH',20X,'=',1PE15.3,5X,'DEGREES',/,59X,'=',1PE15.3,5X,'RADIANS',//
     +/,20X,'HYDRAULIC MOTOR INERTIA',16X,'=',1PE15.3, 5X ,'SLUG FT2',/,
     +59X,'=',1PE15.3,5X,'KG M2')
C
C     PUMP AND MOTOR LOSS COEFFICIENTS
C
      READ(5,103) SP,SM,VTCP,VTCM
  103 FORMAT(4E10.3)
      SPM=SP*28.3168*144/0.068948
      SMM=SM*28.3168*144/0.068948
      VTCPM=VTCP*1.35582
      VTCMM=VTCM*1.35582
      WRITE(6,202) SP,SPM,SM,SMM,VTCP,VTCPM ,VTCM,VTCMM
  202 FORMAT(/////,'PUMP AND MOTOR LOSS COEFFICIENTS',///,20X,'PUMP SLIP
     + LOSS'   ,25X,'=',1PE15.3,5X,'FT3/SEC/LBF/FT2',/,59X,'=',1PE15.3,5X
```

FIG. A.1.3.2 PROGRAMME LISTING for 'VECTAN'

```
     +,'LITRE/SEC/BAR',//,20X,'MOTOR SLIP LOSS',24X,'=',1PE15.3,5X,
     +'FT3/SEC/LBF/FT2',/,59X,'=',1PE15.3,5X,'LITRE/SEC/BAR',//,20X,
     +'PUMP VISCOUS TORQUE LOSS COEFFICIENT',3X,'=',1PE15.3,5X,
     +'LBF FT/RAD/SEC',/,59X,'=',1PE15.3,5X,'NM/RAD/SEC',//,20X,
     +'MOTOR VISCOUS TORQUE LOSS COEFFICIENT',2X,'=',1PE15.3,5X,
     +'LBF FT/RAD/SEC',/,59X,'=',1PE15.3,5X,'NM/RAD/SEC')
C
C      RIG CALIBRATION CONSTANTS
C
      READ(5,104) SWPCC,SWMCC,TPCC,TMCC,SPPCC,SPMCC,SPRCC,RPRCC,DPRCC
  104 FORMAT(8E10.3)
      TPCCM=TPCC*0.737562
      TMCCM=TMCC*0.737562
      SPRCCM=SPRCC/0.0689476
      RPRCCM=RPRCC/0.0689476
      DPRCCM=DPRCC/0.0689476
      WRITE(6,203) SWPCC,SWMCC,TPCC,TPCCM,TMCC,TMCCM,SPPCC,SPMCC,SPRCC,
     +SPRCCM,RPRCC,RPRCCM,DPRCC,DPRCCM
  203 FORMAT(/////,'RIG CALIBRATION CONSTANTS',///,20X,'PUMP SWASH',29X,
     +'=',1PE15.3,5X,'VOLT/DEGREE',//,20X,'MOTOR SWASH',28X,'=',1PE15.3,
     +5X,'VOLT/DEGREE',//,20X,'PUMP TORQUE',28X,'=',1PE15.3,5X,'VOLT/LBF
     + FT',/,59X,'=',1PE15.3,5X,'VOLT/NM',//,20X,'MOTOR TORQUE',27X,'=',
     +1PE15.3,5X,'VOLT/LBF FT',/,59X,'=',1PE15.3,5X,'VOLT/NM',
     +//,20X,'PUMP SPEED',29X,'=',1PE15.3,5X,'VOLT/RPM',
     +//,20X,'MOTOR SPEED',28X,'=',1PE15.3,5X,'VOLT/RPM',
     +//,20X,'SUPPLY LINE PRESSURE',19X,'=',1PE15.3,5X,'VOLT/LBF/IN2',/,
     +59X,'=',1PE15.3,5X,'VOLT/BAR',//,20X,'RETURN LINE PRESSURE',19X,
     +'=',1PE15.3,5X,'VOLT/LBF/IN2',/,59X,'=',1PE15.3,5X,'VOLT/BAR',
     +//,20X,'DIFFERENTIAL LINE PRESSURE',13X,'=',1PE15.3,5X,
     +'VOLT/LBF/IN2',/,59X,'=',1PE15.3,5X,'VOLT/BAR')
C
C      STEADY STATE TEST CONDITIONS
C
      READ(5,105) SPT,SPSP,SMT,SMSP,SSLP,SRLP,SDLP,SPSW,SMSW
     +,PSSLP,PSRLP,VISCD,DEGC,DSPSW,DSMSW
  105 FORMAT (8E10.3)
      SPT=SPT/TPCC
      SPTM=SPT/0.737562
      SPSP=SPSP/SPPCC
      SMT=SMT/TMCC
      SMTM=SMT/0.737562
      SMSP=SMSP/SPMCC
      SSLP=SSLP/SPRCC
      SSLPM=SSLP/SPRCCM
      SRLP=SRLP/RPRCC
      SRLPM=SRLP/RPRCCM
      SDLP=SDLP/DPRCC
      SDLPM=SDLP/DPRCCM
      SPSW=SPSW/SWPCC
      SMSW=SMSW/SWMCC
      IF(SSLP.NE.0) GO TO 27
      IF (SRLP.NE.0) GO TO 27
      PSDLP=PSSLP-PSRLP
      SSLP=PSSLP
      SRLP=PSRLP
      SDLP=PSDLP
```

FIG. A.1.3.2 PROGRAMME LISTING FOR 'VECTAN' (Cont.)

```
      SRLPM=SRLP*0.0689476
      SSLPM=SSLP*0.0689476
      SDLPM=SDLP*0.0689476
   27 IF (SPSW.NE.0) GO TO 28
      IF (SMSW.NE.0) GO TO 28
      SPSW = DSPSW
      SMSW = DSMSW
   28 EFVOL=SMSP*SMSW*DM/(SPSP*SPSW*DP)*100
      EFOV=SMSP*SMT/(SPSP*SPT)*100
      EFMECH=EFOV/EFVOL*100
      WRITE(6,204) SPT,SPTM,SPSP,SMT,SMTM,SMSP,SSLP,SSLPM,SRLP,SRLPM,
     +SDLP,SDLPM,SPSW,SMSW,EFVOL,EFMECH,EFOV
  204 FORMAT(/////,'STEADY STATE TEST CONDITIONS',
     +//,20X,'PUMP TORQUE',28X,'=',1PE15.3,5X,'LBF FT',/,59X,'=',1PE15.3
     +,5X,'NM',//,20X,'PUMP SPEED',29X,'=',1PE15.3,5X,'PPM',//,20X,
     +'MOTOR TORQUE',27X,'=',1PE15.3,5X,'LBF FT',/,59X,'=',1PE15.3,5X,'N
     +M',//,20X,'MOTOR SPEED',28X,'=',1PE15.3,5X,'RPM',///,20X,
     +'SUPPLY LINE PRESSURE',19X,'=',1PE15.3,5X,'LBF/IN2',/,59X,'=',1PE1
     +5.3,5X,'NM',//,20X,'RETURN LINE PRESSURE',19X,'=',1PE15.3,5X,'LBF/
     +IN2',/,59X,'=',1PE15.3,5X,'NM',//,20X,'DIFFERENTIAL LINE PRESSURE'
     +,13X,'=',1PE15.3,5X,'LBF/IN2',/,59X,'=',1PE15.3,5X,'NM',///,20X,'P
     +UMP SWASH',29X,'=',1PE15.3,5X,'DEGREE',//,20X,'MOTOR SWASH',28X,'=
     +',1PE15.3,5X,'DEGREE',///,'TRANSMISSION EFFICIENCIES',///,20X,'VOL
     +UMETRIC EFFICIENCY'  ,18X,'=',1PE15.3,5X,'%',//,20X,'MECHANICAL EF
     +FICIENCY',18X,'=',1PE15.3,5X,'%',//,20X,'OVERALL EFFICIENCY',21X,'
     +=',1PE15.3,5X,'%')
C
C     ADDITIONAL INFORMATION FOR DYNAMIC ANALYSIS
C
      READ(5,102) PDVOL,MDVOL,SPL,SPID,SPWT,SVOL,YM,BMISO,BMISE
  102 FORMAT(8E10.3)
C     HAS A VALUE FOR ISENTROPIC AND ISOTHERMAL BULK MODULUS BEEN INC.
      IF (BMISO.NE.0) GO TO 25
      IF (BMISE.NE.0) GO TO 25
      STBMM =(1.69+0.15*ALOG10(VISCD))*(10.0**(0.0018*(20-DEGC)))*
     +10000.0-5.6*(690.0-SSLPM)
      SSBMM=(1.96+0.15*ALOG10(VISCD))*(10.0**(0.0019*(20-DEGC)))*
     +10000.0-5.6*(690.0-SSLPM)
      TTBMM=STBMM*(STBMM-SSLPM)/STBMM
      TSBMM=SSBMM*(SSBMM-SSLPM)/SSBMM
      BMISO=TTBMM/0.068948
      BMISE=TSBMM/0.068948
   25 TSLV=(PDVOL+MDVOL+SPL*SPID**2/4*12*3.14159)/1728
      TSVOL=(PDVOL+MDVOL+SVOL)/1728
      MBM=(BMISO+BMISE)/2
      BMP=SPWT*YM/SPID
      EBMIP=BMP*MBM/(BMP+MBM)
      PDVOLM=PDVOL*16.3871
      MDVOLM=MDVOL*16.3871
      SPLM=SPL*0.3048
      SPIDM=SPID*2.54
      SPWTM=SPWT*2.54
      YMM=YM*0.068948
      BMISOM=BMISO*0.068948
      BMISEM=BMISE*0.068948
      TSLVM=TSLV*28.3168
```

FIG. A.1.3.2 PROGRAMME LISTING for 'VECTAN' (Cont.)

```
      TSVOLM=TSVOL*28.3168
      MBMM=MBM*0.068948
      BMPM=BMP*0.068948
      EBMIPM=EBMIP*0.068948
      WRITE(6,201)PDVOL,PDVOLM,MDVOL,MDVOLM,SPL,SPLM,SPID,SPIDM,SPWT,SPW
     +TM,TSLV,TSLVM,TSVOL,TSVOLM,VISCD,DEGC,YM,YMM,BMISE
  201 FORMAT(/////' ADDITIONAL SYSTEM INFORMATION FOR DYNAMIC ANALYSIS',
     +///,20X,'PUMP DEAD VOLUME',23X,'=',1PE15.3,5X,'IN3',/,59X,'=',1PE1
     +5.3,5X,'CCS',//,20X,'MOTOR DEAD VOLUME',22X,'=',1PE15.3,5X,'IN3',/
     +,59X,'=',1PE15.3,5X,'CCS',//,20X,'SUPPLY PIPE LENGTH',21X,'=',1PE1
     +5.3,5X,'FT',/,59X,'=',1PE15.3,5X,'METRES',//,20X,'SUPPLY PIPE INTE
     +RNAL',' DIAMETER',10X,'=',1PE15.3,5X,'IN',/,59X,'=',1PE15.3,5X,'CM
     +',//,20X,'SUPPLY PIPE WALL THICKNESS',13X,'=',1PE15.3,5X,
     +                                                'IN',/,59X,'=',1P
     +E15.3,5X,'CM',//,20X,'TOTAL SUPPLY LINE VOLUME(CALCULATED)',3X,'='
     +,1PE15.3,5X,'FT3',/,59X,'=',1PE15.3,5X,'LITRE',//,20X,'TOTAL SUPPL
     +Y LINE VOLUME(MEASURED)'    ,5X,'=',1PE15.3,5X,'FT3',/ ,59X,
     +'=',1PE15.3,5X,'LITRE',///,20X,'KINEMATIC VISCOSITY',20X,'=',
     +1PE15.3,5X,'CENTISTOKES AT 20DEG CENTIGRADE',//,20X,'OIL TEMPERATU
     +RE',24X,'=',1PE15.3,5X,'DEG CENTIGRADE',///,
     +          ///,20X,'PIPE MATERIAL YOUNGS MODULUS',11X,'=',1PE15.3,5X
     +,'LBF/IN2',/,59X,'=',1PE15.3,5X,'BAR',//,20X,'OIL ISENTROPIC BULK
     +MODULUS'   ,12X,'=',1PE15.3,5X,'LBF/IN2')
      WRITE(6,301)BMISEM,BMISO,BMISOM,MPM,MBMM,BMP,BMPM,EBMIP,EBMIPM
  301 FORMAT(  59X,'=',1PE15.3,5X,'BAR',//,20X,
     +    'OIL ISOTHERMAL BULK MODULUS',12X,'=',1PE15.3,5X,'LBF/IN2',/,59
     +X,'=',1PE15.3,5X,'BAR',//,20X,'MEAN OIL BULK MODULUS',18X,'=',1PE1
     +5.3,5X,'LBF/IN2',/,59X,'=',1PE15.3,5X,'BAR',//,20X,'PIPE BULK MODU
     +LUS',22X,'=',1PE15.3,5X,'LBF/IN2',/,59X,'=',1PE15.3,5X,'BAR',//,20
     +X,'MEAN BULK MODULUS OF OIL IN PIPE',7X,'=',1PE15.3,5X,'LBF/IN2',/
     +,59X,'=',1PE15.3,5X,'BAR')
C
C     READ IN FREQUENCY RESPONSE DATA AS ARRAYS AND PRINT OUT RATIOS
C
      READ(5,106) KNO
  106 FORMAT(I3)
      READ(5,107) ((DTFA(I,J),J=1,13),I=1,KNO)
  107 FORMAT(13F6.3)
      WRITE(6,205)
  205 FORMAT(1H1,'EXPERIMENTAL RESULTS - ENGLISH UNITS',////
     +          ,6X ,'FREQUENCY',15X,'W2/XP',17X,'TL/W2',17X,'PH/W2',17X
     +,'PL/W2',17X,'PD/W2',//,5X ,'HZ',6X,'RAD/SEC',5X,'RPM/DEG',4X,
     +'DEG LAG',3X,'LBF FT/RPM',3X,'DEG LAG',2X,'LBF/IN2/RPM',2X,'DEG LA
     +G',2X,'LBF/IN2/RPM',2X,'DEG LAG',2X,'LBF/IN2/RPM',2X,'DEG LAG')
      DO 10 I=1,KNO
      RAD(I)=DTFA(I,1)*2*3.14159
      W2XPA(I)=DTFA(I,4)*SWPCC/(DTFA(I,2)*SPMCC)
      W2XPP(I)=DTFA(I,5)-DTFA(I,3)
      TLW2A(I)=DTFA(I,6)*SPMCC/(DTFA(I,4)*TMCC)
      TLW2P(I)=DTFA(I,7)-DTFA(I,5)+180.0
      PHW2A(I)=DTFA(I,8)*SPMCC/(DTFA(I,4)*SPRCC)
      PHW2P(I)=DTFA(I,9)-DTFA(I,5)
      PLW2A(I)=DTFA(I,10)*SPMCC/(DTFA(I,4)*RPRCC)
      PLW2P(I)=DTFA(I,11)-DTFA(I,5)
      IF (DTFA(1,11).NE.0) GO TO 26
      PLW2P(I)=0.0
```

FIG. A.1.3.2 PROGRAMME LISTING for 'VECTAN' (Cont.)

```
   26 PDW2A(I)=DTFA(I,12)*SPMCC/(DTFA(I,4)*DPRCC)
      PDW2P(I)=DTFA(I,13)-DTFA(I,5)
      TLW2AM(I)=TLW2A(I)/0.737562
      PHW2AM(I)=PHW2A(I)*0.0689476
      PLW2AM(I)=PLW2A(I)*0.0689476
      PDW2AM(I)=PDW2A(I)*0.0689476
   10 WRITE(6,206) DTFA(I,1),RAD(I),W2XPA(I),W2XPP(I),TLW2A(I),TLW2P(I),
     +PHW2A(I),PHW2P(I),PLW2A(I),PLW2P(I),PDW2A(I),PDW2P(I)
  206 FORMAT(//,   1P12E11.3)
      WRITE(6,207)
  207 FORMAT(1H1,'EXPERIMENTAL RESULTS - S.I. UNITS',////
     +          ,6X ,'FREQUENCY',15X,'W2/XP',17X,'TL/W2',17X,'PH/W2',17X
     +,'PL/W2',17X,'PD/W2',//,5X ,'HZ',6X,'RAD/SEC',5X,'RPM/DEG',4X,'DEG
     +LAG',5X,'NM/RPM',4X,'DEG LAG',4X,'BAR/RPM',5X,'DEG LAG',3X,'BAR/RP
     +M',5X,'DEG LAG',3X,'BAR/RPM',5X,'DEG LAG')
      DO 11 I=1,KNO
   11 WRITE(6,208) DTFA(I,1),RAD(I),W2XPA(I),W2XPP(I),TLW2AM(I),TLW2P(I)
     +,PHW2AM(I),PHW2P(I),PLW2AM(I),PLW2P(I),PDW2AM(I),PDW2P(I)
  208 FORMAT(//,1P12E11.3)
C
C     CALCULATE EFFECTIVE LOAD TORQUE AND PRESSURE DIFFERENCE - TO BE
C                              EXTENDED TO ITERATE FOR PL
C
      WRITE(6,209)
  209 FORMAT(1H1,'EFFECTIVE LOAD TORQUE & PRESSURE DIFFERENCE CALCULATED
     +FROM EXPERIMENTAL RESULTS',/,70X,'ENGLISH UNITS',////,
     +            6X,'FREQUENCY',15X,'TL/W2',17X,'TM/W2',17X,'T2/W2',17X
     +,'CAL-PD/W2',//, 5X,'HZ',5X,'RAD/SEC', 4X,'LBF FT/RPM',2X,'DEG LAG
     +',3X,'LBF FT/RPM',2X,'DEG LAG',3X,'LBF FT/RPM',2X,'DEG LAG',2X,  '
     +LBF/IN2/RPM',1X,'DEG LAG',/)
      DO 12 I=1,KNO
      TMW2A(I)=MOT2*RAD(I)*2*3.14159/60
      TMW2P(I)=-90.0
      TEMA(I)=SQRT(TLW2A(I)**2+TMW2A(I)**2-2*TLW2A(I)*TMW2A(I)*COS((90-
     +TLW2P(I))/57.296))
      TEMP(I)=ARCTAN((+TLW2A(I)*SIN(TLW2P(I)/57.296)-TMW2A(I))/(TLW2A(I)
     ++*COS(TLW2P(I)/57.296)))*57.296
      T2W2A(I)=SQRT(TEMA(I)**2+(VTCM*2*3.14159/60)**2-2*TEMA(I)*VTCM*2*
     +3.14159/60*COS((180.0+TEMP(I))/57.296))
      T2W2P(I)=ARCTAN( TEMA(I)*SIN(TEMP(I)/57.296)
     +                                    /(TEMA(I)*COS(TEMP(I)/57.296)
     ++VTCM*2*3.14159/60))*57.296
      CPDWA(I)=T2W2A(I)/(DM*SMSW)*57.296/144
      CPDWP(I)=T2W2P(I)
      TMW2AM(I)=TMW2A(I)/0.737562
      T2W2AM(I)=TMW2A(I)/0.737562
      CPDWAM(I)=CPDWA(I)*0.0689476
   12 WRITE(6,210) DTFA(I,1),RAD(I),TLW2A(I),TLW2P(I),TMW2A(I),TMW2P(I),
     +T2W2A(I),T2W2P(I),CPDWA(I),CPDWP(I),TEMA(I),TEMP(I)
  210 FORMAT(//,1P12E11.3)
      WRITE(6,211)
  211 FORMAT(1H1,'EFFECTIVE LOAD TORQUE & PRESSURE DIFFERENCE CALCULATED
     +FROM EXPERIMENTAL RESULTS',/,70X,'S.I. UNITS',////,
     +            6X,'FREQUENCY',15X,'TL/W2',17X,'TM/W2',17X,'T2/W2',15X
     +,'CAL-PD/W2',//, 6X,'HZ',5X,'RAD/SEC', 6X,'NM/RPM',3X,'DEG LAG',6X
     +,'NM/RPM',3X,'DEG LAG',7X,'NM/RPM',3X,'DEG LAG',5X,'BAR/RPM',4X,
```

FIG. A.1.3.2 PROGRAMME LISTING for 'VECTAN' (Cont.)

```
     +'DEG LAG',/)
      DO 13  I=1,KNO
   13 WRITE(6,212) DTFA(I,1),RAD(I),TLW2AM(I),TLW2P(I),TMW2AM(I),TMW2P(I
     +),T2W2AM(I),T2W2P(I),CPDWAM(I),CPDWP(I)
  212 FORMAT(//,1P10E11.3)
C
C     VECTOR PREDICTION OF OVERALL TRANSMISSION RESPONSE
C
      WRITE(6,213)
  213 FORMAT(1H1,'PREDICTED AND MEASURED OVERALL TRANSMISSION RESPONSE',
     + ////,6X      ,'FREQUENCY',15X,'W2/XP-EXP',13X,'W2/XP-VEC',//, 5X,
     +'HZ',5X,'RAD/SEC',6X,'RPM/DEG',3X,'DEG LAG',5X,'RPM/DEG',3X,'DEG L
     +AG')
      DO 16  I=1,KNO
      SFW2A(I)=(SP+SM)*144*PHW2A(I)
      SFW2P(I)=PHW2P(I)
      CFW2A(I)=TSVOL/EBMIP*RAD(I)*PHW2A(I)
      CFW2P(I)=PHW2P(I)-90.0
      FLW2A(I)=SQRT(CFW2A(I)**2+SFW2A(I)**2)
      FLW2P(I)=-ARCTAN(CFW2A(I)/SFW2A(I))*57.296+PHW2P(I)
      PFW2A(I)=SQRT(FLW2A(I)**2+(DM*SMSW*2*3.14159/(57.296*60))**2
     +-2*FLW2A(I)*DM*SMSW*2*3.14159/(57.296*60)*COS(3.14159+FLW2P(I)
     +/57.296))
      PFW2P(I)= ARCTAN(FLW2A(I)*SIN(FLW2P(I)/57.296)/(DM*SMSW*2*3.14159
     +/(60*57.296)+
     +FLW2A(I)* COS(FLW2P(I)/57.296)))*57.296
      IF (PFW2P(I))15,14,14
   14 PFW2P(I)=-180+PFW2P(I)
   15 CONTINUE
      OVRSA(I)= DP*BOMGP*2*3.14159/(57.296*PFW2A(I)*60)
      OVRSP(I)= -PFW2P(I)
   16 WRITE(6,214)DTFA(I,1),RAD(I),W2XPA(I),W2XPP(I),OVRSA(I),OVRSP(I),
     +FLW2A(I),FLW2P(I),PFW2A(I),PFW2P(I)
  214 FORMAT(//,   1P10E11.3)
C
C     USING VECTOR ANALYSIS TO DETERMINE EFFECTIVE COMPRESSIBILITY OF
C                                                              OIL
C
      WRITE(6,215)
  215 FORMAT(1H1,11X,'FREQUENCY',11X,'SLIP LOSSES',10X,'EFFECTIVE BM',//
     +,10X,'HZ',5X,'RAD/SEC',6X,'FT3/SEC/LBF/IN2',10X,'LBF/IN2')
      DO 19  I=1,KNO
      APFW2A(I)=DP*BOMGP*2*3.14159/(57.296*W2XPA(I)*60)
      APFW2P(I)=-W2XPP(I)
      AFLW2A(I)= SQRT((DM*SMSW*2*3.14159/(57.296*60))**2+APFW2A(I)**2
     +-2*DM*SMSW*2*3.14159/(57.296*60)*
     +APFW2A(I)*COS(APFW2P(I)/57.296))
      AFLW2P(I)= APFW2P(I)+(ARCTAN(DM*SMSW*2*3.14159/(57.296*60)*SIN(
     +APFW2P(I)/57.296) /(APFW2A(I)-DM*SMSW*2*3.14159/(57.296*60) *COS
     +(APFW2P(I)/57.296))))*57.296
      ANGLE(I)=-AFLW2P(I)+PHW2P(I)
      ASFW2A(I)=AFLW2A(I)*COS(ANGLE(I)/57.296)
      ACFW2A(I)=AFLW2A(I)*SIN(ANGLE(I)/57.296)
      SPSM(I)= ASFW2A(I)/(144*PHW2A(I))
      EBMIP2(I)=- TSVOL*RAD(I)*PHW2A(I)/ACFW2A(I)
   19 WRITE(6,216) DTFA(I,1),RAD(I),SPSM(I),EBMIP2(I)
```

FIG. A.1.3.2 PROGRAMME LISTING for 'VECTAN' (Cont.)

```
     +,APFW2A(I),APFW2P(I),AFLW2A(I),AFLW2P(I)
  216 FORMAT(//,6X,1P2E10.3,6X,1PE10.3,10X,    1PE10.3,6X,4E10.3   )
C
C      WHAT TYPE OF PLOTTED OUTPUT IS REQUIRED
C                                1    PLOT LOCUS
C                                2    PLOT BODE PLOT
C                                3    PLOT BOTH
C
       READ (5,108) JUNCK
  108  FORMAT(I1)
       IF(JUNCK-2)20,21,20
   20  CALL LOCI(W2XPA,W2XPP,OVRSA,OVRSP,KNO)
       IF(JUNCK-2)24,21,21
   21  DO 23 I=1,KNO
C      CALCULATE AMPLITUDE AND PHASE ON DB AXIS
       DO 22 J=1,4
   22  X(J,I)=DTFA(I,1)
       Y(1,I)=20*ALOG10(W2XPA(I))
       Y(2,I)=40-W2XPP(I)/8
       Y(3,I)=20*ALOG10(OVRSA(I))
   23  Y(4,I)=40-OVRSP(I)/8
C      THE ARRAYS READY FOR PLOTTING
C          X(I,KNO),Y(1,KNO) - AMP RATIO-EXPERIMENTAL
C          X(2,KNO),Y(2,KNO) - PHASE-EXPERIMENTAL
C          X(3,KNO),Y(3,KNO) - AMP RATIO-PREDICTED
C          X(4,KNO),Y(4,KNO) - PHASE-EXPERIMENTAL
       CALL GR4 (X,Y,4,KNO,1,0,'  HZ  ','DB  PH',' EXPERIMENTAL & PREDICT
     + RESP    ','BENA35VAF')
   24  CONTINUE
       STOP
       END
```

FIG. A.1.3.2 PROGRAMME LISTING for 'VECTAN' (Cont.)

```
      SUBROUTINE LOCI (W2XPA,W2XPP,OVRSA,OVRSP,KNO)
C
C     PLOT OUT VECTOR LOCI OF PREDICTED (+) AND EXPERIMENTAL (X) OVERALL
C                          TRANSMISSION RESPONSE
C
      DIMENSION W2XPA(50),W2XPP(50),OVRSA(50),OVRSP(50)
      TAN(X)=SIN(X)/COS(X)
      CALL GRAFOR (1,0.0,0.0,0,0,'BENA35VAF')
      CALL GRAFOR (3,0.01,0.01,40,0,'OVERALL RESPONSE VECTOR LOCI')
      CALL GRAFOR (4,50.0,50.0,805,10)
      DO 30 K=100,700,100
      CALL GRAFOR (5,K-320.0,20.0)
   30 CALL GRAFOR (10,1.0,3.0,K-300,0)
      CALL GRAFOR (7,100.0,80.0,1,0,'AMPLITUDE RATIO W2/XP-RPM/DEG    ')
      DO 35  LAY=10,180,10
      X1=50*COS(LAY/57.296)
      Y1=-50*SIN(LAY/57.296)
      IF (LAY.NE.90) GO TO 42
      X2=0.0
      Y2=-500.0
      GO TO 34
   42 X2=400.0
      Y2=-400*TAN(LAY/57.296)
   31 IF (LAY.GT.90.0) GO TO 43
      IF (Y2+500.GT.0) GO TO 32
      Y2 = -500.0
      X2 = 500/TAN(LAY/57.296)
   43 Y2=-500.0
      X2=500/TAN(LAY/57.296)
   32 IF(LAY-116.567) 34,33,33
   33 X2=-250.0
      Y2= 250*TAN(LAY/57.296)
   34 CONTINUE
      CALL GRAFOR(5,X1,Y1)
   35 CALL GRAFOR(6,X2,Y2)
      DO 40 LIR=50,600,50
      CALL GRAFOR(5,LIR+0.0 ,0.0)
      J=LIR*2+10
      DO 36 NIR= 10,J,5
      X3= LIR-NIR+10
      Y3=-SQRT(LIR**2-X3**2)
      IF (X3.LT.400.0) GO TO 37
      CALL GRAFOR (5,X3,Y3)
      GO TO 36
   37 IF (250+X3) 40,40,38
   38 IF (Y3+500.0) 36,36,39
   39 CALL GRAFOR (6,X3,Y3)
   36 CONTINUE
      CALL GRAFOR (6,X3,Y3)
   40 CONTINUE
      CALL GRAFOR (5,400.0,0.0)
      CALL GRAFOR (6,400.0,-500.0)
      CALL GRAFOR (6,-250.0,-500.0)
      CALL GRAFOR(6,-250.0,0.0)
```

FIG. A.1.3.3 PROGRAMME LISTING for SUBROUTINE 'LOCI'

```
      DO 41   I=1,KNO
      X4= W2XPA(I)*COS(W2XPP(I)/57.296)
      Y4=-W2XPA(I)*SIN(W2XPP(I)/57.296)
      CALL GRAFOR(7,X4,Y4,1,0,'&')
      X5= OVRSA(I)*COS(OVRSP(I)/57.296)
      Y5=-OVRSA(I)*SIN(OVRSP(I)/57.296)
   41 CALL GRAFOR(7,X5,Y5,1,0,'+')
      CALL GRAFOR (5,0.0,-1000.0)
      CALL GRAFOR(2)
      RETURN
      END
```

FIG. A.1.3.3 PROGRAMME LISTING for SUBROUTINE 'LOCI' (Cont.)

APPENDIX II

THE DESIGN, DEVELOPMENT, and CONSTRUCTION, of the DOWNEL PUMP and MOTOR ELECTRO-HYDRAULIC SWASH SERVOS

A.2.1 General Description

The pump and motor swash servos were identical, the layout and block diagram being shown on Fig. A 2.1 (a). They comprised a valve and jack the motion of which was converted into rotation by a swash arm. The electro-hydraulic servo valves were Dowty Moog Valves, Series 21, driven by a differential amplifier in the current drive arrangement shown in Fig. A 2.1 (b). This was necessary to prevent the output from the valves being frequency sensitive as the driving coils were inductive and their impedence would increase with frequency. It can be shown by applying Kirchoffs Law that for the current drive arrangement

$$I = -E \frac{R_o}{R_1 R_3} \qquad \text{- A 2.1}$$

The Moog valve produced a flow proportional to differential current, but attenuated at very high frequencies due to the response time of the valve.

The oil supply for the servos was obtained from the laboratory supply set at 1,500 lbf/in^2 and filtered to 2.5 microns. The flow from the jack was converted into a linear motion by a Dowty trunion mounted jack of stroke 4.0 in. and area 1.8 in^2 coupled to the swash arm.

Feedback was obtained by a linear inductive transducer in conjunction to an oscillator-demodulator coupled to the jack shaft. Fig. 5.2 shows a close up photograph of the set up and Table A.2.1 the specification of the servo element.

A.2.2 Servo Development

Assuming the elements of the servo to be linear and the oil to be incompressible, the block diagram of Fig. A 2.1 (a) gives the overall transfer functions for the servos to be

$$\frac{x_{po}}{x_{pi}} = \frac{\frac{1}{K_g}\,\frac{K_a K_u K_J}{A_J \tau_M}}{s^2 + \frac{s}{\tau_M} + \frac{K_a K_u K_J}{A_J \tau_M}} \qquad \text{- A 2.2}$$

However only approximate values were available for the time constant of the Moog valve and after calibration of the feedback transducers the differential amplifiers were set to give gains of -10 mA/volt using the resistors shown in Fig. A 2.1 (b).

As both servos were very nearly identical it was decided to evaluate the performance of the motor swash servo and use the results to improve the performance of both the pump and motor servos.

The bode plot of the closed loop frequency response test carried out on the motor servo is shown in Fig. A2.2 (a). It was immediately apparent that the response was highly damped with no resonance occurring. It was realised therefore that the servo response could be increased considerably without using any of the system compensation techniques by an increase of the forward gain. The increase in gain could be most readily achieved by increasing the gain of the differential amplifier. To determine the extent of the gain increase it was decided to open the servo loop with the aid of the Nichols Diagram.

Fig. A2.2(b) shows the open loop response of the motor swash servo and it was apparent that the time constant for the Moog valve τ_m was such as to be just on the limit of the frequency response test carried out. However, an approximate value of 0.0042 sec. was obtained compared to a value obtained from the manufacturer's data given for a valve supplied with oil at 3,000 lbf/in^2 of 0.0046 sec. To achieve a phase margin of 35^o, a typical value for an optimised servo, the gain of the forward path must be increased by 25 dB.

The gain of the operational amplifier was increased to -100 mA/volt by reducing R_3 by a factor of 10 from 100 to 10 Ω. This gave a forward path gain increase of 20 dB, see Fig. A 2.1 (b). Another frequency response test was carried out on the motor servo and the results presented on the bode plot given on Fig. A 2.3 (a). It was apparent that one of the elements of the servo must be saturating and at lower input amplitudes the frequency response looked more like that of a second order system, Fig. A 2.3 (b).

A flow test carried out on the Moog valve showed a saturation flow of 3.0 galls/min. at a supply pressure of 1,500 lbf/in^2. This corresponds to the maximum flow required to drive the servo at an input voltage of 0.15 volts and a frequency of 13.0 Hz.

It was decided that with the improved performance resulting from an increase in the forward path gain the servos would now be uprated sufficiently to cope with the proposed frequency response testing.

Element	Specification
Differential Amplifiers	Fenlow AD.2006 in Current Drive Arrangement Fenlow $\pm$ 15V Stabilised Power Supply $\frac{I}{E}$ = 10 mA/Volt
Electro: Hydraulic Servo Valves	Dowty Moog Valves - Series 21 Max. Rated Flow - 20 $in^3/sec.$ @ 1,000 lbf/in^2 Supply Pressure - 500 - 4,000 lbf/in^2 Proof Pressure - 4,500 lbf/in^2 Max. Rated Current - 15 mA Coil Resistance - 675 Ω Kv = 1.38 $in^3/sec/mA$ @ 1,500 lbf/in^2
Actuators	Dowty Trunion Mounted Two-Way Jack Stroke - 4 in. Area - 1.8 in^2 Internal Diameter - 1.75 in. Shaft Diameter - 0.875 in.
Feedback Displacement Transducers	Pye Split Coil Inductive Displacement Transducers Linear Travel 2.0 ins. Fenlow Oscillator Demodulator Units K_G = 2.38 volt/in. K_G = 2.28 volt/in.

TABLE A.2.1 SWASH SERVOS COMPONENT SPECIFICATION

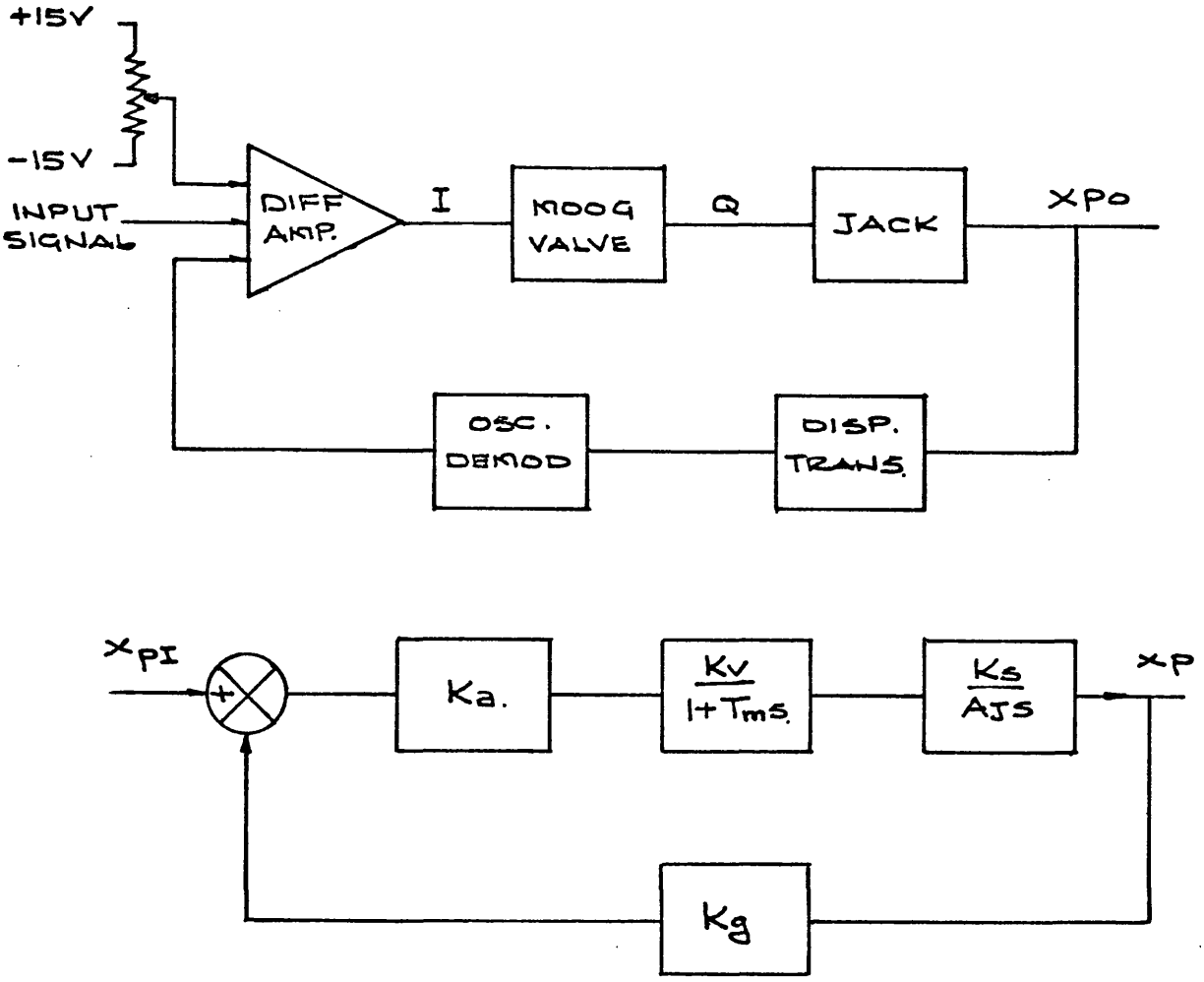

FIG A2.1 (a.) SWASH SERVO LAYOUT & BLOCK DIAGRAM.

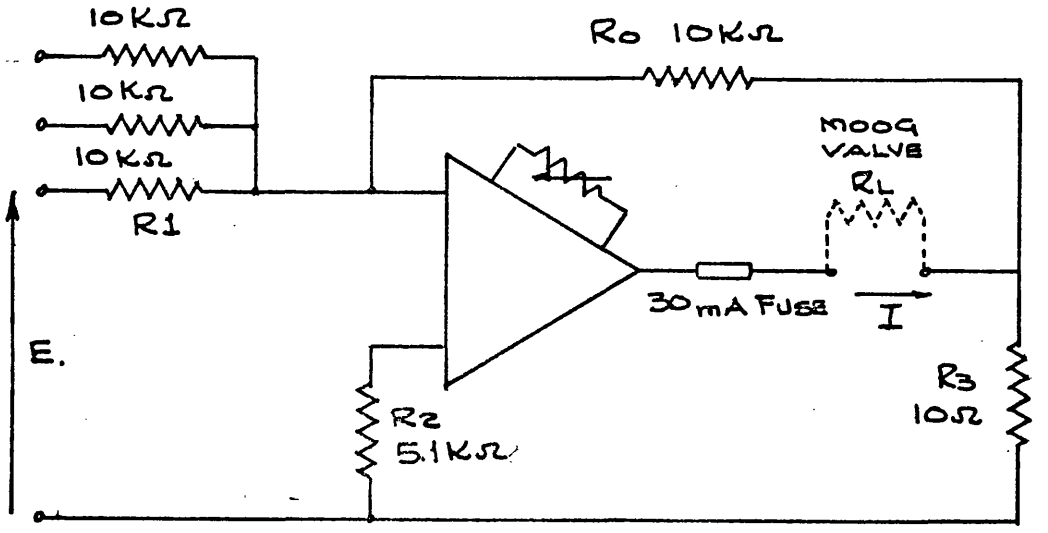

FIG A2.1 (b.) DIFFERENTIAL AMPLIFIED USED FOR CURRENT DRIVE.

FIG A2.1 ELEMENTS OF SWASH SERVOS.

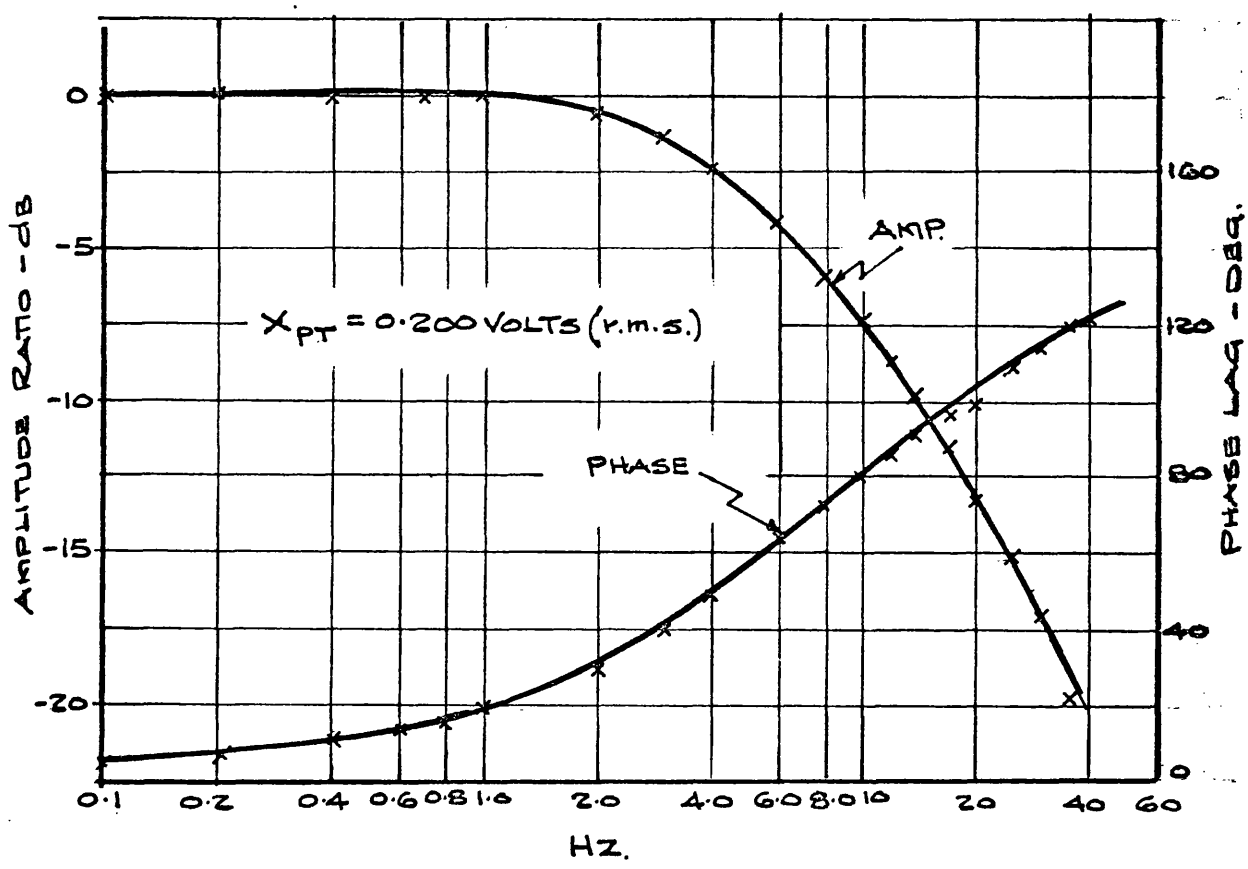

FIG A2.2(a) CLOSED LOOP FREQUENCY RESPONSE TEST OF MOTOR SWASH SERVO.

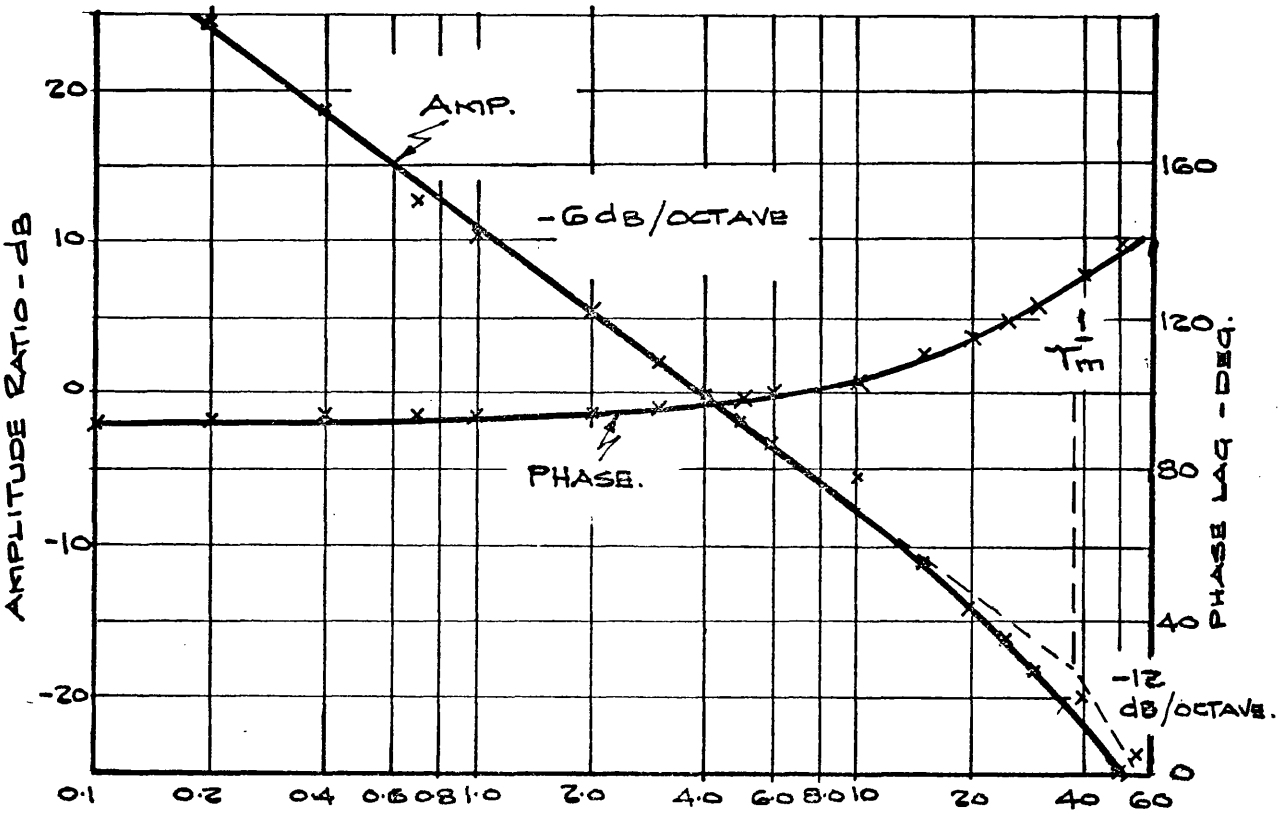

FIG A2.2 (b) OPEN LOOP FREQUENCY RESPONSE OBTAINED USING NICHOLS DIAGRAM FROM FIG. A2.2(a.)

FIG. A2.2. FREQUENCY RESPONSE TEST OF MOTOR SWASH SERVO.

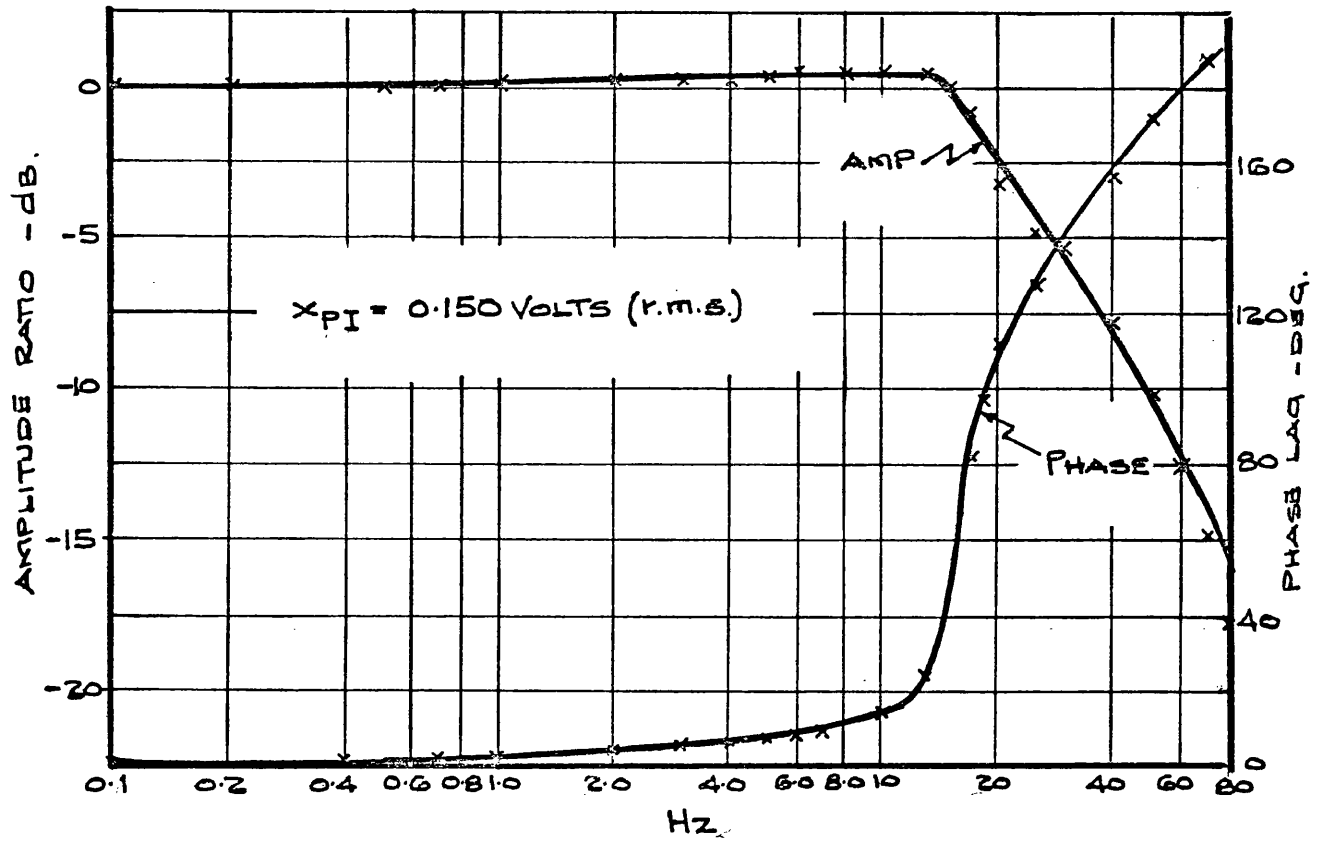

FIG A2.3 (a) LARGE INPUT AMPLITUDE.

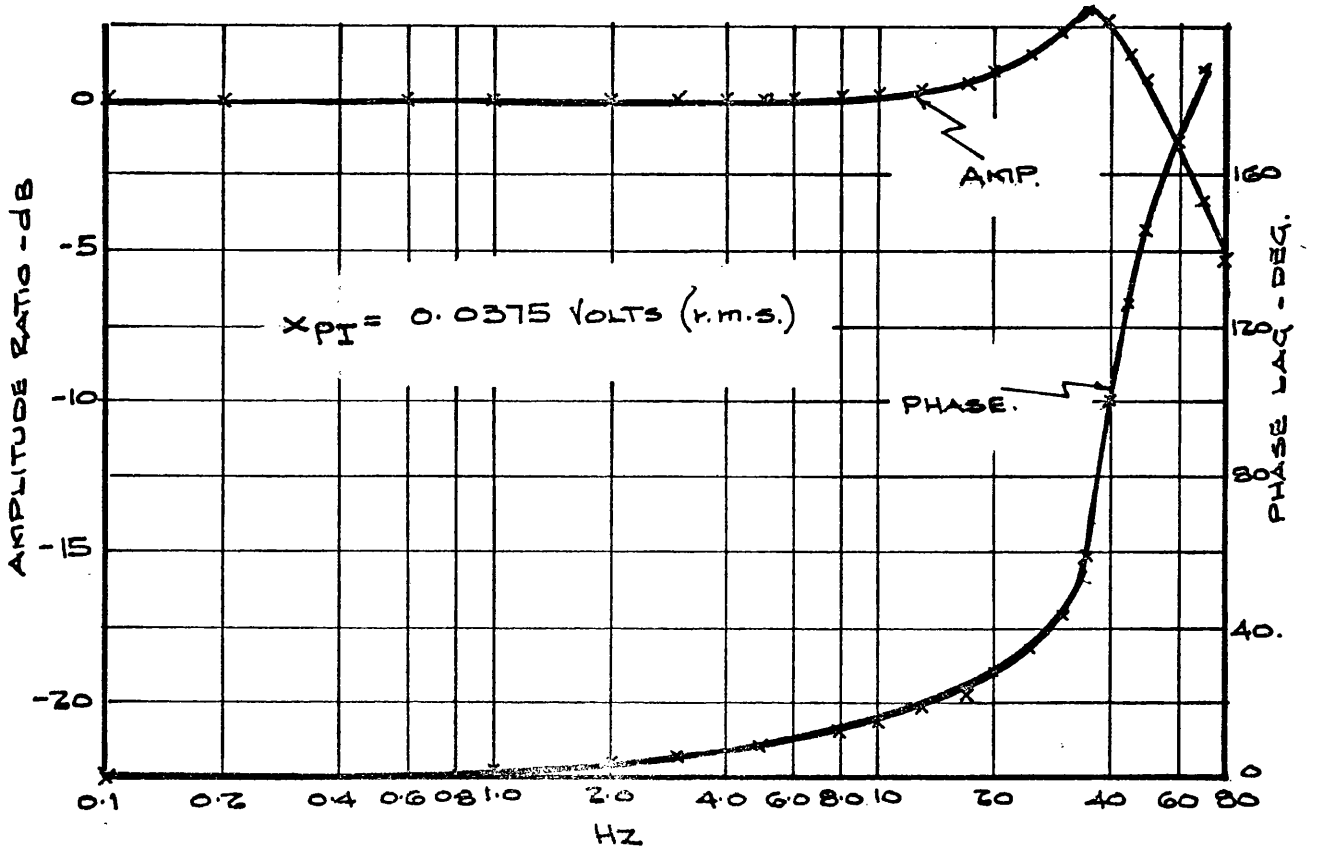

FIG A2.3 (b.) SMALL INPUT AMPLITUDE.

FIG. A 2.3. CLOSED LOOP FREQUENCY RESPONSE TESTS OF MOTOR SWASH SERVO WITH INCREASED FORWARD PATH GAIN.

APPENDIX III

DESIGN PROCEDURE

It may be useful to the reader to outline a suggested analytical procedure to determine the dynamic characteristics of any transmission. A block diagram has been drawn up to outline the design scheme and is shown in Fig. A 3.1. The exact criteria for the design decisions have not been specified as to a large extent these will depend upon the application.

The typical case of Test 31 in the main text is presented in detail to illustrate the design procedure.

Basic Information

Prime Mover Speed, Ω_1 = 125.5 rad/sec.

Maximum Pump Capacity, D_p = 5.34×10^{-2} litres/rev. ($3.25\ in^3$/rev)

Pump Swash Plate or Tilt Movement

X_p (zero to full stroke) = 15.0 deg.

Maximum Motor Capacity, D_M = 5.34×10^{-2} litres/rev. ($3.25\ in^3$/rev)

Motor Swash Plate or Tilt Movement X_M if variable (zero to full stroke) = 15.0 deg.

Steady State Conditions of Test 31:

Load Torque, T_2 = 33.4 Nm (24.6 lbf ft.)

Load Speed, Ω_2 = 61.0 rad/sec.

Pump Swash, X_P = 4.42 deg.

Motor Swash, X_M = 7.42 deg.

Supply Line Pressure, P_H = 87.0 bar ($1,280\ lbf/in^2$)

Return Line Pressure, P_L = 13.6 bar ($200\ lbf/in^2$)

Additional Information Required to Evaluate System Dynamic Performance

Dead Volume in Pump (Exposed to Supply Line) = $86.2\ cm^3$ ($5.27\ in^3$)

Dead Volume in Motor (Exposed to Supply Line) = $86.2\ cm^3$ ($5.27\ in^3$)

Supply Pipe Length = 1.76 m (5.75 ft.)

Supply Pipe Internal Diameter = 2.54 cm (1.00 in.)

Supply Pipe Volume = 924.0 cm^3 (56.5 in^3)

Total Supply Line Volume, V = 1096.4 cm^3 (67.04 in^3)

Pump & Motor Loss Co-efficients at Operating Conditions:

Pump Slip, K_P = 2.23×10^{-4} litre/sec/bar
(3.72×10^{-9} ft^3/sec/lbf/ft^2)

Motor Slip, K_M = 2.33×10^{-4} litre/sec/bar
(3.90×10^{-9} ft^3/sec/lbf/ft^2)

Pump Viscous Torque Loss Co-eff. f_P = 1.53×10^{-2} Nm/rad/sec.
(1.13×10^{-2} lbf ft/rad/sec.)

Motor Viscous Torque Loss Co-eff. f_M = 1.53×10^{-2} Nm/rad/sec.
(1.13×10^{-2} lbf ft/rad/sec.)

Pump Pressure Dependent Torque Co-efficient, K_{fP}

Motor Pressure Dependent Torque Co-efficient, K_{fM}

Very small for units considered and therefore ignored.

Effective /

Effective Compressibility of Oil at Operating Conditions:

At 87.0 bar (1,280 lbf/in^2) and 50^{o}C. for Shell Tellus 27 (36)

Isentropic Tangent Bulk Modulus = 16.5 x 10^3 bar (240,000 lbf/in^2)

Using Equ. 4.15

$$\frac{1}{B_e} = \frac{1}{B_o} + \frac{1}{B_p}$$

gives for steel pipes of wall thickness 0.413 cm (0.1625 in) an effective bulk modulus for oil in the pipe B_e of 15.85 x 10^3 bar (233,000 lbf/in^2).

Design Decisions

Before commencing the design process as laid out in Fig. A 3.1 it is necessary to ensure the validity of lumped parameter analyses by considering the delay time for pressure signals to travel down the pipeline. Also the significance of oil inertia effects in the pipeline should be checked.

1. Is the Prime Mover Droop Significant?

Prime Mover Droop, K_E = 14% No Load to Full Load
= 0.160 rad/sec/Nm
(0.217 rad/sec/lbf ft.)

If the load were removed completely this would only give a prime mover speed increase of 4% so it can be considered as constant speed.

In order to have carried out the signal flow analysis it would be ncessary to determine the driving inertia of the prime mover plus pump, J_1.

2. Can the Load be Represented by a Viscous and Inertial Load?

Type of Load - Positive Displacement Pump and Associated Loading Valves.

It was considered prudent to use the load locus in this case $\frac{\vec{t_L}}{\omega_2}(j\omega)$, see Fig. 6.14.

To represent the load by a first order lead it would be necessary to evaluate the driven inertia, J_2, and the load damping co-efficient, f_L.

3. Is the Return Line Pressure Constant?

A large boost pump and flat characteristic relief valve had been used and the return line pressure was therefore considered constant.

To carry out the suggested iteration it would be necessary to determine the boost pump and relief valve characteristics as shown in Fig. 3.8 (a).

4. As the load has been represented by a locus, the overall response is to be evaluated using the vector analysis technique.

Calculations

Sample calculations are shown for two frequencies, 2.0 Hz and 6.5 Hz, which were evaluated for Test 29.

a) From the Load Locus

		2.0 Hz	6.5 Hz
$\frac{\vec{t_L}}{\omega_2}$ is	AMP:	0.0285	0.0589 Nm/rev/min
	PHASE:	Lead of 40.6^o	Lead of 65.6^o

b) Torque to accelerate Motor

$\frac{\vec{t_m}}{\omega_2}$ is	AMP:	0.0089 0.0289 Nm/rev/min
	PHASE:	Leading speed by 90^o

c) Motor Viscous Torque Co-efficient

$\vec{f_M}$	AMP:	0.0016 Nm/rev/min
	PHASE:	In phase with speed

d) Effective Load Torque

$$\frac{\vec{t_2}}{\omega_2} = \frac{\vec{t_m}}{\omega_2} + \frac{\vec{t_2}}{\omega_2} + f_m$$

	AMP:	0.0350 0.0869 Nm/rev/min
	PHASE:	Lead of 51.8^o Lead of 74.0^o

e) Supply Line Pressure Variation

$$\frac{\overrightarrow{P_h}}{\omega_2} = \frac{\overrightarrow{t_2}}{\omega_2} \cdot \frac{P_h}{\omega_2} = \frac{\overrightarrow{t_2}}{\omega_2} \cdot \frac{1}{D_2 X_M}$$

AMP: 0.099 0.226 bar/rev/min.

PHASE: Lead of 51.8° Lead of 74.0°

f) The Slip Flow Loss

$$\frac{\overrightarrow{q_s}}{\omega_2} = (K_P + K_M) \frac{\overrightarrow{P_h}}{\omega_2}$$

AMP: 0.451×10^{-4} 1.030×10^{-4} litres/sec. / rev/min.

PHASE: In phase with $\frac{P_h}{\omega_2}$

g) The Compressibility Flow Loss

$$\frac{\overrightarrow{q_c}}{\omega_2} = \frac{V}{B_e} j \frac{\overrightarrow{P_h}}{\omega_2}$$

AMP: 0.835×10^{-4} 6.190×10^{-4} litres/sec. / rev/min.

PHASE: Leading $\frac{P_h}{\omega_2}$ by 90°

h) The Total Flow Loss

$$\frac{\overrightarrow{q_L}}{\omega_2} = \frac{\overrightarrow{q_c}}{\omega_2} + \frac{\overrightarrow{q_s}}{\omega_2}$$

AMP: 0.947×10^{-4} 6.270×10^{-4} litres/sec. / rev/min.

PHASE: Lead of 113.4° Lead of 154.6°

i) Flow Continuity in Supply Line

$$\underset{\omega_2}{\overrightarrow{q_p}} = \underset{\omega_2}{\overrightarrow{q_M}} + \underset{\omega_2}{\overrightarrow{q_L}}$$

AMP: 4.07×10^{-4} 6.15×10^{-4} litres/sec. / rev/min.

where $\underset{\omega_2}{\overrightarrow{q_M}} = D_2 X_M$

PHASE: Lead of 12.0^o Lead of 115.5^o

j) Relating Pump Flow to Swash Plate Angle gives:

$$\underset{x_p}{\overrightarrow{\omega_2}} = \underset{x_p}{\overrightarrow{q_p}} \cdot \underset{q_p}{\overrightarrow{\omega_2}}$$

AMP: 174.0 115.0 rev/min/^{o}Swash

PHASE: Lagging by 12.0

Lagging by 115.5^o

This is the Overall Response Vector.

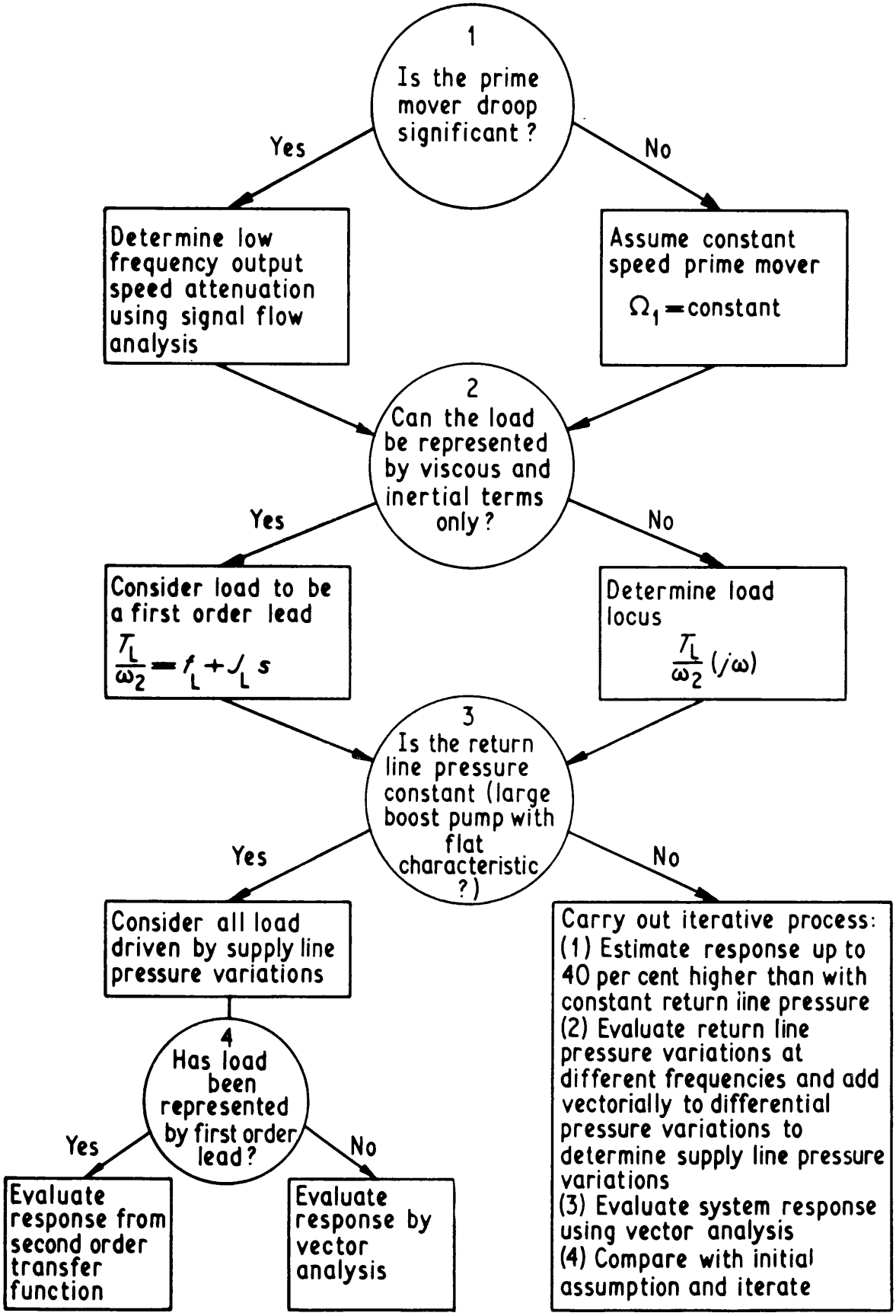

Fig. A 3.1 Design Procedure Block Diagram.

APPENDIX IV

The DYNAMIC CHARACTERISTICS of a HYDROSTATIC TRANSMISSION SYSTEM

Bowns, Dr. D.E., Worton-Griffiths, J.

Proc. Inst. Mech. E. Vol. 186 No. 55, 1972.

THE DYNAMIC CHARACTERISTICS OF A HYDROSTATIC TRANSMISSION SYSTEM

D. E. Bowns, BSc(Eng), PhD, CEng, MIMechE* J. Worton-Griffiths, BSc (*Graduate*)†

The dynamic performance of a hydrostatic transmission with a variable delivery pump used for speed control is predicted using a simple mathematical model. The analysis is then extended to take into account the transmission slip and torque losses, and the prime mover droop by employing signal flow techniques. The results were compared with those from an extensive test programme employing electro-hydraulic test techniques carried out on a typical hydrostatic drive.

The signal flow analysis improved the prediction of the transmission dynamic performance, but it was found that errors of up to 40 per cent were occurring, as many of the loads employed could not be accurately represented by simple mathematical models. A vector approach was adopted, using measured load loci that provided a correlation of within 4 per cent of the experimentally measured response, by using a value of oil bulk modulus midway between the isothermal and isentropic tangent values.

Mean return line pressure, restricted boost system and flexible pipeline effects were investigated.

1 INTRODUCTION

ONE OF THE earliest attempts at the dynamic analysis of hydrostatic transmission systems was carried out in 1947 by Newton (1)‡, but since that time there have been very few reported attempts to verify this analysis and its assumptions. The general method of approach is to consider the pump and motor as continuous linear elements driving a viscous and inertial load, the pump and motor being connected by a compressible oil column. This leads to a simple transfer function, relating changes in output speed with pump swash plate angular position changes, and with changes in load torque.

The analysis gave rise to a second order differential equation, which may have a resonance at a frequency determined by the system compressibility, the motor size and the load characteristic.

Shearer (2), Lewis and Stern (3), Thoma (4), Gille (5) and several other writers have outlined this simple analysis, but more recent work has been concerned with the valve controlled hydraulic servo and much discussion has taken place on the system non-linearities.

The present investigation analyses in detail an engine-driven hydrostatic transmission, and then goes on to check the validity of the assumptions by an extensive experimental programme. The experiments employ electro-hydraulic test techniques both for the control of the load and for providing the necessary inputs to the transmission.

1.1 Notation

B_e Effective bulk modulus of elasticity of oil in pipe.
B_o Bulk modulus of elasticity of oil.
B_P Bulk modulus of elasticity of pipe.
D_M Maximum motor displacement/radian.
D_P Maximum pump displacement/radian.
D_1 Pump displacement/radian of swash/radian.
D_2 Motor displacement/radian of swash/radian.
d Internal diameter of supply line pipe
E Young's modulus for pipe material.
f_L Load torque variations with speed, known as load damping coefficient.
f_M Motor viscous torque loss coefficient.
f_P Pump viscous torque loss coefficient.
J_E Engine inertia.
J_L Load inertia.
J_M Motor inertia.
J_P Pump inertia.
J_1 Driving inertia ($= J_E+J_P$).
J_2 Driven inertia ($= J_M+J_L$).
K Output speed/pump swash steady state gain.
K_E Governed engine speed droop with load.
K_{fM} Motor pressure dependent torque loss coefficient.
K_{fP} Pump pressure dependent torque loss coefficient.
K_G Governor speed control constant.
K_M Motor slip flow loss coefficient.
K_P Pump slip flow loss coefficient.
P_D Pressure difference across lines ($= P_H-P_L$).
P_H Supply line pressure.
P_L Return line pressure.
Q_c Compressed flow.
Q_L Total flow loss.
Q_M Flow to motor.
Q_P Pump output flow.
Q_s Slip flow loss.
s Differential operator ($= \mathrm{d}/\mathrm{d}t$).
T_E Available torque from engine.
T_L Load torque.
T_M Torque to accelerate hydraulic motor.

This paper is published for written discussion. The MS. was received on 22nd July 1971 and accepted for publication on 5th April 1972. 23
* *Fluid Power Centre, School of Engineering, University of Bath, Claverton Down, Bath BA2 7AY.*
† *Project Engineer, Cessna Fluid Power Ltd, Glenrothes, Fife.*
‡ *References are given in Appendix 3.*

T_P Torque available to drive pump.
T_2 Torque required to accelerate motor and load.
t Supply line pipe wall thickness.
V Volume of oil in supply line including the dead volume of pump and motor exposed to supply line.
X_M Fraction of motor displacement.
X_P Fraction of pump displacement.
Y Engine governor setting.
ζ Damping ratio.
τ_1, τ_2 Time constants.
Ω_1 Engine and pump rotational speed.
Ω_2 Motor and load rotational speed.
ω Frequency of sinusoidal swash plate variations.
ω_n Transmission and load natural frequency.

Lower case letters throughout the text refer to small variations about a steady state operating condition, unless otherwise stated.

2 THEORETICAL CONSIDERATIONS

2.1 Bulk modulus

In the reported experimental work on hydraulic systems, there have been many attempts to obtain a reasonable correlation between the experimental and predicted values obtained for system natural frequency. The main unknown has been the effect of the oil compressibility and the pipe resilience, and most experimenters have allowed for this by using an arbitrary value of effective bulk modulus which gave good agreement between predicted and experimentally obtained values.

The determination of the bulk modulus of hydraulic oil has been the subject of papers by Hayward (**6**) (**7**) and other writers, and because of the non-linear change of volume with pressure and the effects of heat interchange, it is necessary to consider, on the one hand, whether to take the secant value or the tangent value and on the other whether to assume that the compression or expansion is isothermal or isentropic. In addition, in practical systems, the effect of wall elasticity has to be taken into account, and the effective bulk modulus is given by the well-known relation

$$\frac{1}{B_e}=\frac{1}{B_o}+\frac{1}{B_p} \quad . \quad . \quad . \quad . \quad (1)$$

where

$$\frac{1}{B_p}=d/tE$$

For example, Hansen (**8**) used an effective bulk modulus B_e of $11{\cdot}6\times10^3$ bar ($1{\cdot}7\times10^5$ lbf/in^2) to predict the dynamic response of a valve-controlled hydraulic motor system. This gave an overestimate of natural frequency. Lambert and Davies (**9**) and Renner (**10**) used values of $7{\cdot}75\times10^3$ bar ($1{\cdot}14\times10^5$ lbf/in^2) and $6{\cdot}8\times10^3$ bar ($1{\cdot}00\times10^5$ lbf/in^2) respectively, and both obtained reasonable

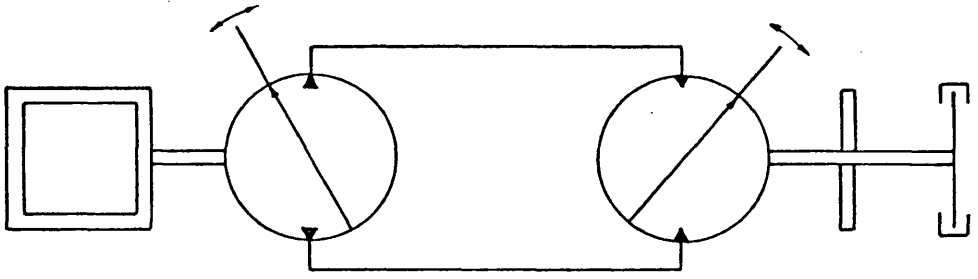

a

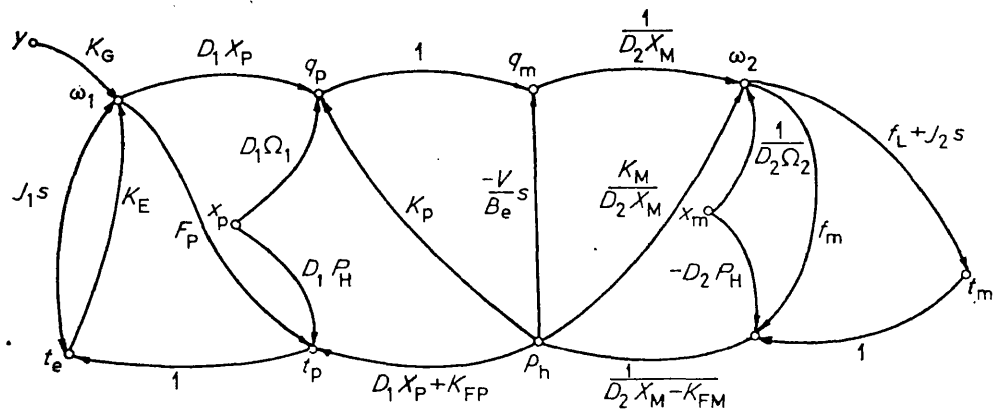

b

$$\frac{\omega_2}{x_p}=\frac{D_1\Omega_1}{D_2X_M}\,\frac{[1-(J_1s+f_p)K_E+D_1P_HK_EX_P/\Omega_1]}{1-(J_1s+f_p)K_E-\dfrac{(f_L+f_m+J_2s)}{(D_2X_M(D_2X_M-K_{FM})}\left[\left(K_P-\dfrac{V}{B_e}s+K_M\right)(1-J_1K_Es-f_pK_E)+K_ED_1X_P(D_1X_P+K_E)\right]}$$

Fig. 1. (*a*) Transmission layout, (*b*) Signal flow diagram and resultant transfer function relating output speed to input swash angle derived from signal flow diagram

agreement between their predicted and experimental values. Aeration and mounting compliances were suggested as possible causes of the low values of bulk modulus.

Healey and Stringer (**11**) used a value of $18{\cdot}4\times10^3$ bar ($2{\cdot}7\times10^5$ lbf/in^2) and obtained good agreement by taking into account the effect of oil inertia in the pipelines.

More recently Keating and Martin (**12**) used a value of $6{\cdot}80\times10^3$ bar ($1{\cdot}00\times10^5$ lbf/in^2) and obtained reasonable agreement between their theoretical approach and their experimentally obtained values for natural frequency.

Many workers in the field including Walters (**13**), Gille (**5**) and Shearer (**2**), suggest a general value for B to be taken as $13{\cdot}6\times10^3$ bar (2×10^5 lbf/in^2), despite the fact that this value is considerably lower than that determined by static tests. Shearer stated 'The logical basis of the practice is open to question, but it seems to work'.

2.2 Transmission transfer function

Simple linearized analysis can be applied to the transmission shown diagrammatically in Fig. 1*a*. Assuming it has a constant speed prime mover, no losses, and constant return line pressure, the following transfer function is obtained:

$$\frac{\omega_2}{x_p}=\frac{\Omega_1 D_1}{D_2 X_M}\cdot\frac{\dfrac{(D_2X_M)^2B_e}{VJ_2}}{s^2+\dfrac{f_L}{J_2}s+\dfrac{(D_2X_M)^2B_e}{VJ_2}} \quad . \quad . \quad (2)$$

a second order equation where

$$\omega_n = D_2X_M\sqrt{\frac{B_e}{VJ_2}}$$

$$\zeta=\frac{f_L}{2D_2X_M}\sqrt{\frac{V}{J_2B_e}}$$

Shearer (**2**) used Newton's linearized analysis (**1**) and carefully discussed the assumptions made. He pointed out that there are lower limits that can occur in line pressures, and that these should be avoided for linearity. Newton's analysis assumed a constant speed prime mover, and took into account the losses within the transmission. The return line pressure was considered to be constant. The natural frequency ω_n and damping ratio ζ obtained is as follows:

$$\omega_n=\sqrt{\frac{\{(K_P+K_M)(f_{LM}+f_L)+(D_2X_M)^2\}B}{J_2V}} \quad (3)$$

$$\zeta=\frac{(K_P+K_M)J_2+\dfrac{V}{B}(f_{LM}+f_L)}{2\sqrt{\dfrac{VJ_2}{B}\{(K_P+K_M)(f_{LM}+f_L)+(D_2X_M)^2\}}} \quad (4)$$

2.3 Analysis using signal flow techniques

A fuller analysis of the basic transmission system shown in Fig. 1 can be obtained with the aid of signal flow theory. This facilitates the use of a more complex model. A change in load, a change in engine speed, or a change in swash plate position of either unit will give a resultant change in the running conditions of each of the units involved. The static and dynamic characteristics of each element are to some extent non-linear, and small perturbation techniques can be used if the changes are not too great.

Fig. 2 shows graphically the static and dynamic characteristics of the various transmission elements. For example, the typical speed–torque characteristics of an engine for various governor settings are shown, together with the linearized equation relating small changes in speed with the engine torque variations and governor settings. The quantity $\delta\Omega_1/\delta T_E$ ($=K_E$), the engine speed droop, shows how the engine speed changes with torque and the quantity $\delta\Omega_1/\delta Y$ ($=K_G$), the governor speed control constant, shows how the engine speed varies with governor setting. Delays in development of engine developed torque after a change in governor setting have been neglected as relatively insignificant.

The hydrostatic pump is dealt with in two parts. First, the linearized relation between flow, speed, swash plate angle, and pressure is obtained. The quantity $\delta Q_P/\delta P_H$ ($=K_P$) is the pump slip coefficient. $\delta Q_P/\delta Y_P$ ($=D_1\Omega_1$) is the change in flow/unit change in swash angle, and $\delta Q_P/\delta\Omega_1$ ($=D_1X_P$) is the flow change/unit change in pump speed. In a similar manner, the change in pump torque for changes in speed, swash plate angle, and pressure are obtained. $\delta T_P/\delta P_H$ ($=D_1X_P+K_{fp}$) is the pump displacement plus the pressure dependent torque coefficient, $\delta T_P/\delta X_P$ ($=D_1P_H$) is the change in pump torque/unit change of swash plate angle. $\delta T_P/\delta\Omega_1$ ($=F_P$) is the pump viscous torque coefficient. A constant return line pressure has been assumed.

An overall transfer function can now be obtained by the use of the signal flow techniques developed by Mason (**14**) and applied to oil hydraulics by Bowns (**15**) and Korn (**16**). The right-hand column on Fig. 2 gives the signal flow graph appropriate to each of the individual equations.

The signal flow graphs can be combined to obtain a complete signal flow graph for the transmission system; using Mason's Rule, the transfer function relating any two system parameters can be readily obtained. The signal flow graph and the transfer function relating output speed to input swash plate position is also shown in Fig. 1. The engine droop increases the order of the equation and is also responsible for the additional terms in the numerator.

A lumping of parameters in the equation of Fig. 1 gives a transfer function of the following form:

$$\frac{\omega_2}{x_p}=\frac{K\omega_n^2(1+\tau_1 s)}{(1+\tau_2 s)(s^2+2\zeta\omega_n s+\omega_n^2)} \quad . \quad . \quad (5)$$

The effect of varying any one system parameter on the overall system response depends on the values of the other relevant parameters, and cannot be expressed in a general form. However, for a particular system, the effect of varying any one parameter can be obtained by substitution of values into the transfer function of Fig. 1. For convenience a digital computer programme has been written to substitute values of system parameter into the above transfer function; it uses the Newton Raphson technique to evaluate τ_1 and hence K, τ_2, ω_n, and ζ (see Appendix 1).

2.4 The effect of a change in system parameters on the natural frequency and damping ratio

The hydrostatic system tested later has been taken as an example and the effect of varying the supply line volume and the slope of the torque speed curve of the load (f_L) has been investigated.

Fig. 3 shows that the natural frequency rises rapidly with the reduction of supply line volume, and is therefore

Element	Steady state characteristic	Transmittance at operating point (lower case letters refer to small changes)	Signal flow graph
ENGINE	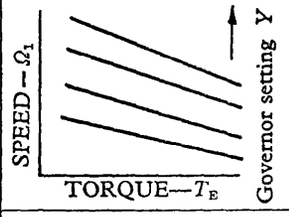	$\Delta\Omega_1 = \frac{\delta\Omega_1}{\delta T_E}\cdot\Delta T_E + \frac{\delta\Omega_1}{\delta Y}\cdot\Delta Y$ OR $\omega_1 = K_E.t_e + K_G.y$	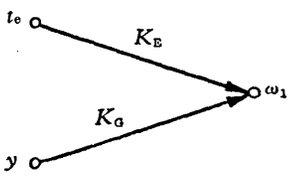
ENGINE & PUMP INERTIA	$T_E = T_P + J_1\frac{d\Omega_1}{dt}$	$\Delta T_e = \Delta T_P + J_1 s\Delta\Omega_1$ OR $t_e = t_p + J_1 s\omega_1$	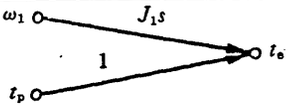
PUMP-FLOW RELATIONSHIP	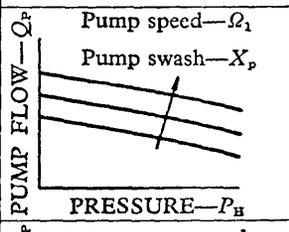	$\Delta Q_P = \frac{\delta P_H}{\delta P_H}\cdot\Delta P_H + \frac{\delta Q_P}{\delta X_P}\cdot\Delta X_P + \frac{\delta Q_P}{\delta\Omega_1}\cdot\Delta\Omega_1$ OR $q_p = K_P.p_h + D_1.\Omega_1.x_p + D_1X_P.\omega_1$	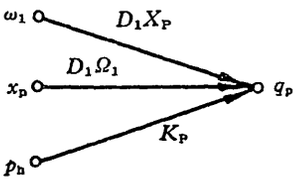
PUMP-TORQUE RELATIONSHIP	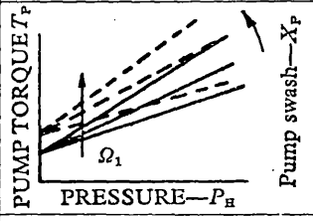	$\Delta T_P = \frac{\delta T_P}{\delta P_H}\cdot\Delta P_H + \frac{\delta T_P}{\delta X_P}\cdot\Delta X_P + \frac{\delta T_P}{\delta\Omega_1}\cdot\Delta\Omega_1$ OR $t_p = (D_1X_P + K_{FP})p_h + D_1P_Hx_p + F_P.\omega_1$	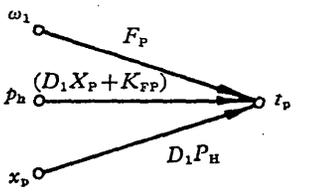
TRANSMISSION LINE COMPRESSIBILITY	$Q_o = Q_P - Q_M = \frac{V}{B_e}\frac{dP_H}{dt}$	$\Delta Q_C = \Delta Q_P - \Delta Q_M = \frac{V}{B_e}\frac{d(\Delta P_H)}{dt}$ OR $q_C = q_p - q_m = \frac{V}{B_e}sp_h$	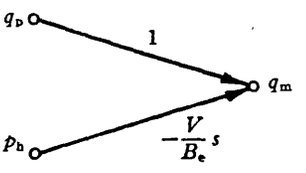
MOTOR-FLOW RELATIONSHIP	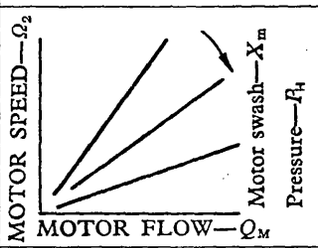	$\Delta\Omega_2 = \frac{\delta\Omega_2}{\delta Q_M}\cdot\Delta Q_M + \frac{\delta\Omega_2}{\delta P_H}\cdot\Delta P_H + \frac{\delta\Omega_2}{\delta X_M}\cdot\Delta X_M$ OR $\omega_2 = \frac{q_m}{D_2X_M} + \frac{K_M}{D_2X_M}\cdot p_h + \frac{x_m}{D_2\Omega_2}$	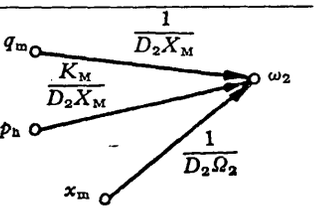
MOTOR-TORQUE RELATIONSHIP	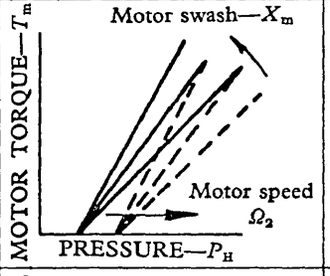	$\Delta T_M = \frac{\delta T_M}{\delta P_H}\cdot\Delta P_H + \frac{\delta T_M}{\delta X_M}\Delta X_M + \frac{\delta T_M}{\delta\Omega_2}\cdot\Delta\Omega_2$ OR $t_m = D_2P_Hx_m - f_m\omega_2 + D_2X_mp_h - K_{FM}p_h$ $p_h = \frac{t_m + f_M\omega_2 - D_2P_Hx_m}{D_2X_M - K_{FM}}$	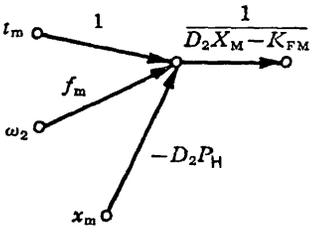
LOAD	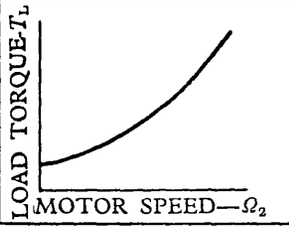	$\Delta T_M = \frac{\delta T_2}{\delta\Omega_2}\Delta\Omega_2 + J_2\frac{\delta\Delta\Omega_2}{dt}$ OR $t_m = f_L\omega_2 + J_2s\omega_2$	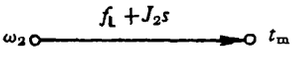

Fig. 2. Signal flow analysis

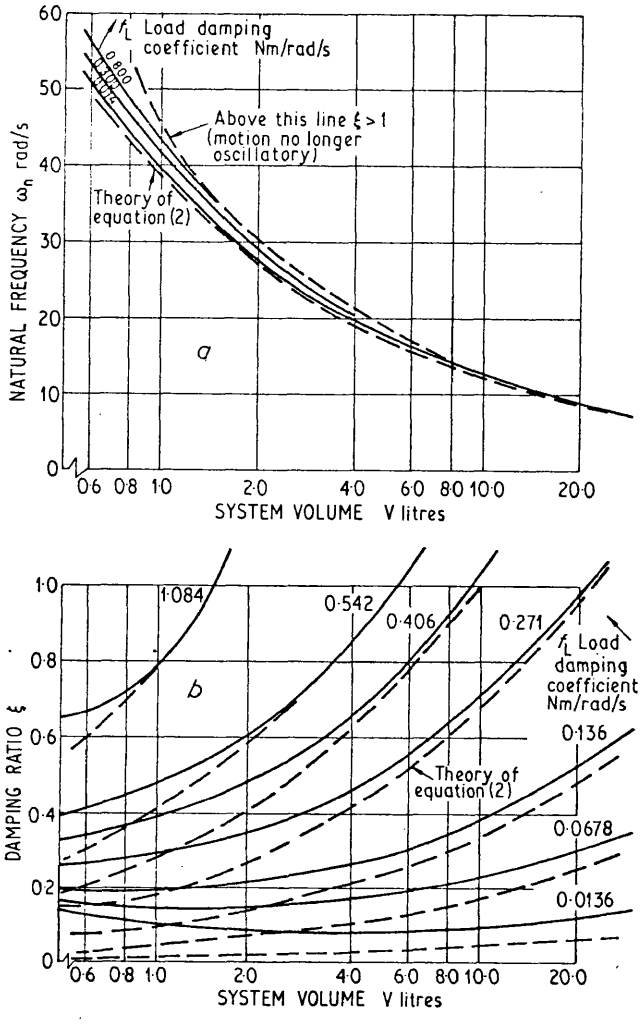

Fig. 3. The effect of system volume on (*a*) transmission natural frequency and (*b*) damping ratio

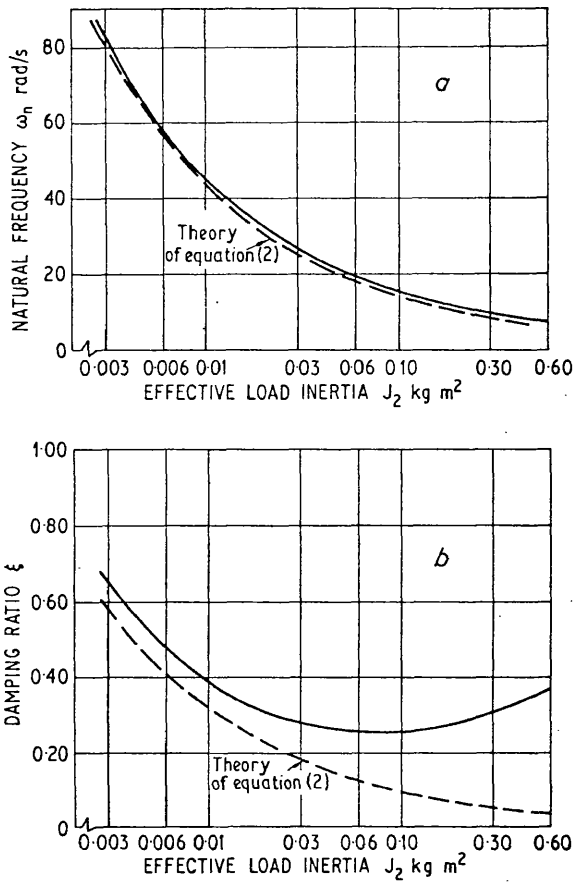

Fig. 4. Effect of load inertia on (*a*) system natural frequency and (*b*) damping ratio

more difficult to determine when the lines are very short. In the case of back to back transmissions, the natural frequency will be determined by the dead volume in the pump and motor units. The figure also shows how a slight increase in natural frequency occurs with increase in the slope of the torque speed curve f_L (termed the load damping coefficient). The results of the simple theoretical treatment of equation (2) is shown dotted on Fig. 3. It can be seen that this gives a lower damping ratio than that predicted by the signal flow analysis.

Fig. 4 examines the effect of load inertia on natural frequency and damping ratio. Again the change in natural frequency is large for changes in load inertia, at low values of load inertia. The damping ratio is again underestimated by the simple theory.

2.5 The effect of prime mover droop

The fall off of speed with load of the prime mover is a secondary effect for systems powered by closely governed engines or electric motors. The natural frequency and damping ratio remain unchanged and the time constants τ_1 and τ_2 in equation (5) are close together, thus making little difference to the overall system response. For example with a 5 per cent droop (no load to full load) the ratio of τ_2/τ_1 is 1·008 giving an attenuation in the output at low frequencies of only 0·05 dB.

In an extreme case the low frequency variation of the output is attenuated considerably. If the governor loop gain was reduced to 1/40 of that in the above example, the ratio of τ_2/τ_1 is 1·718; giving an attenuation of 4·30 dB. The driving inertia J_1 will affect the time constants τ_1 and τ_2, it does not affect the amount of attenuation taking place. However, increases in the load damping coefficient will increase the low frequency attenuation.

2.6 Vector analysis

Many loads which a transmission can be expected to drive cannot be expressed in the form of the first order lag, developed from consideration of an inertial and viscous load, and it may be impossible to obtain simple mathematical models which satisfactorily describe their characteristics. The frequency response of the transmission can, however, be obtained if the frequency response of the load (change of load torque relative to change in load speed) is known, by plotting the vectors of all the relevant quantities.

In Fig. 5 an experimental vector locus YXZ has been plotted for a typical load. Let us assume that at a certain input frequency the load vector is $\overrightarrow{t_L/\omega_2}$ terminating at the point X.

We will now work backwards to the input movement of the swash plate, x_p.

Stage (1) The torque to accelerate the hydraulic motor must be included as the vector $\overrightarrow{t_m/\omega_2}$. This will be 90° in advance of the speed vector ω_2.

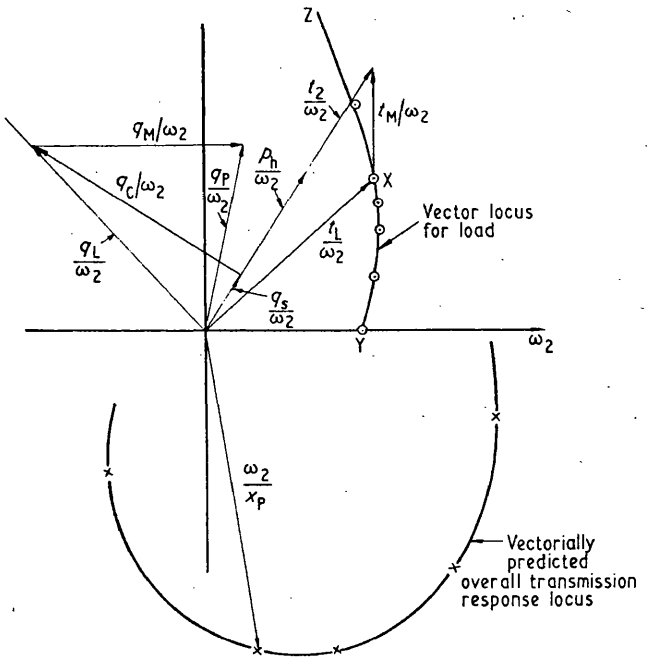

Fig. 5. Vector analysis for determining overall transmission response using measured load locus

Stage (2) By vector addition, the total torque vector $\overrightarrow{t_2/\omega_2}$ is obtained,

$$\frac{\vec{t}_2}{\omega_2} = \frac{\vec{t}_m}{\omega_2} + \frac{\vec{t}_L}{\omega_2}$$

Motor viscous torque losses f_m may be added if significant.

Stage (3) The pressure difference across the motor can be predicted by the relation

$$t_2 = p_d D_2 X_M$$

or

$$\frac{\vec{p}_d}{\omega_2} = \frac{\vec{t}_2}{\omega_2} \cdot \frac{1}{D_2 X_M}$$

It is in phase with $\overrightarrow{t_2/\omega_2}$.

If the return line pressure is considered constant, $p_d = p_h$.

Stage (4) The slip flow loss q_s in the transmission can now be estimated from the steady state characteristics of the pump and motor,

$$q_s = (K_P + K_M) p_h$$

Hence

$$\frac{\vec{q}_s}{\omega_2} = (K_P + K_M) \frac{\vec{p}_h}{\omega_2}$$

and is in phase with $\overrightarrow{p_h/\omega_2}$.

Stage (5) The compressibility flow loss q_c is

$$q_c = \frac{V}{B_e} \frac{dp_h}{dt} = \frac{V}{B_e} j\omega P_h$$

or

$$\frac{\vec{q}_c}{\omega_2} = \frac{V}{B_e} j\omega \frac{\vec{p}_h}{\omega_2}$$

This will be 90° in advance of $\overrightarrow{p_h/\omega_2}$.

Stage (6) By vector addition, the total flow loss $\overrightarrow{q_L/\omega_2}$ may be obtained,

$$\frac{\vec{q}_L}{\omega_2} = \frac{\vec{q}_c}{\omega_2} + \frac{\vec{q}_s}{\omega_2}$$

Stage (7) The motor flow vector $\overrightarrow{q_m/\omega_2}$ can be drawn, since $q_m = D_2 X_m$ in phase with ω_2.

Stage (8) The pump flow vector can now be obtained by vector addition,

$$\frac{\vec{q}_p}{\omega_2} = \frac{\vec{q}_m}{\omega_2} + \frac{\vec{q}_L}{\omega_2}$$

Stage (9) The pump flow variation q_p is

$$q_p = D_1 \Omega_1 x_p$$

Hence

$$\frac{q_p}{x_p} = D_1 \Omega_1$$

Hence

$$\frac{\vec{\omega}_2}{x_p} = \frac{\vec{\omega}_2}{q_p} \cdot \frac{q_p}{x_p}$$

$$= D_1 \Omega_1 \frac{\vec{\omega}_2}{q_p}$$

Thus the overall response of the transmission can be obtained.

2.7 Effect of return line

So far we have ignored the possibility of return line pressure variations; in other words we have considered a system supplied by a large capacity boost pump, or having an efficient accumulator in the return line.

Many systems, however, have a boost pump sufficiently large to make up leakage flows with very little excess capacity, and accumulators are not fitted. In this case a sudden increase in load or swash plate angle can cause suction starvation of the main pump; see McCallion *et al.* (17).

The behaviour of the return line during frequency response tests can be shown by reference to Fig. 6*a*. This shows the return line pressure as a function of system demand from the boost pump. The relief valve shown has a steeply rising characteristic, and when the system demands no flow, the pressure is that which would be given by the relief valve when all the boost pump flow, other than that required to make up leakage, is passing through it (point A).

During low frequency oscillations there is negligible phase difference between pump and motor flows, and the boost pump has only to make up the leakage. Thus there will be a continuous steady flow through the relief valve, and the pressure appropriate to this will be given at point A.

At higher frequencies, the phase difference in flows between the pump and motor will be considerable, and the system demand for flow from the boost system will oscillate at the input frequency from B to B′, with a corresponding change in pressure due to the relief valve characteristic.

If the flow fluctuation in the return line becomes very large, due to large phase differences and/or large swash plate amplitudes, the instantaneous flow requirement may become greater than the boost capacity and the points may move to C and C′, showing that cavitation will occur in the return line. The corresponding pressure time curves for these three conditions are shown on Fig. 6*b*, *c* and *d*. Oil compressibility will modify this simple argument to some extent.

The effect on system dynamic performance can now be deduced. Taking the case of Fig. 6*c*, the return line pressure variations contribute to the motor torque, and hence to the system stiffness. These variations can be included in the signal flow diagram, or can be allowed for in the vector

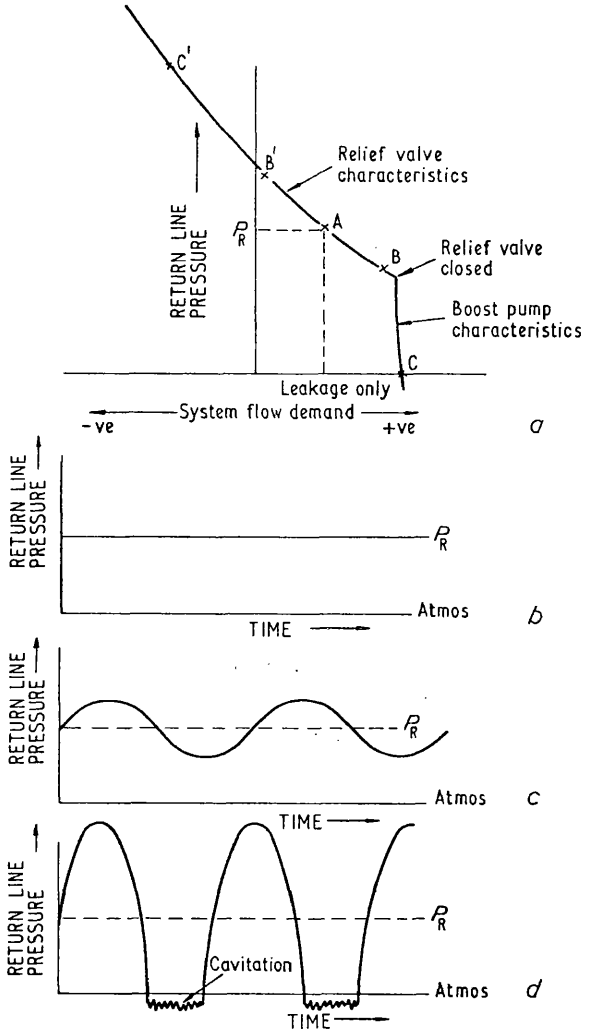

Fig. 6. Behaviour of return line during frequency response tests

locus approach. The effective torque vector $\overrightarrow{t_2/\omega_2}$ can be converted to a differential pressure vector $\overrightarrow{p_d/\omega_2}$. The return line pressure vector $\overrightarrow{p_L/\omega_2}$ can be added to this to obtain the supply pressure $\overrightarrow{p_h/\omega_2}$. The analysis can then be carried forward as above. The case of Fig. 6*d* with cavitation could be analysed in a similar manner using the describing function technique if thought necessary. Extensive cavitation may, however, reduce the pump performance, and the mean motor speed may drop.

The work presented throughout this paper is based upon the use of lumped parameters. The justification for this assumption lies in the fact that all the transmission lines used are very short in relation to the wavelength of the pressure signals being transmitted. However, the assumption must be checked before the analysis presented is applied to any system.

3 EXPERIMENTAL WORK

3.1 Hydrostatic transmission test rig for dynamic analysis

The general layout of the hydrostatic transmission test rig is shown in Figs 7 and 8. Variable delivery axial piston pump and motor units of maximum displacement $53{\cdot}25 \times 10^{-3}$ litre/rev are coupled together in a closed circuit. In order to obtain constant pressure, the return line of the closed circuit was provided with the flow from a large capacity boost pump, 23 litres/min, the excess being returned to tank via a two-stage relief valve specially modified to maintain a constant pressure in the return line. The swash plate angles on the pump and motor units were controlled by electro-hydraulic position servos enabling sinusoidal disturbances to be applied to the swash plates with a bandwidth of 20 Hz at a peak to peak amplitude of 4·3 degrees.

The prime mover was a Perkins three cylinder four stroke diesel of 2·5 litres capacity, modified to provide variable droop governing, using an electro-hydraulic position control servo to actuate the fuel rack with an additional speed feedback loop (17). Hydraulic power for the three electro-hydraulic servos was obtained from a laboratory oil supply.

The output from the transmission motor drives an axial piston load pump with variable delivery and pressure compensation override. The load pump delivers oil to a variable orifice and a pressure relief valve; this enables a variety of load torque–speed curves to be simulated. It should be noted that backlash on the transmission input and output shafts was kept to a minimum, and these shafts were stiff enough to be considered as rigid connections between the engine and pump, and motor and load.

Dynamic measurements required that system variables be measured as electrical signals. The input and output speeds were measured using high quality d.c. tachogenerators, and torques by means of strain gauge torquemeters. The swash plate angles of the pump and motor were measured using rotary inductive position transducers. It was felt desirable to measure and record the supply and return line pressures separately, as well as the differential line pressure and therefore three inductive pressure transducers were employed.

The frequency response testing was carried out with the aid of a digital transfer function analyser.

4 TEST PROGRAMME

Frequency response tests were carried out with a nominally constant engine speed, to determine the effect of pump swash plate angle, motor swash plate angle, mean load torque and the slope of the torque–speed curve, the slope of the engine torque-speed curve, load inertia, system volume, mean pressure in the low pressure line, back up pump capacity, and the low pressure line relief valve characteristic. Effects of flexible pipes and of pressure gauges in the supply line were investigated.

Oil temperature and oil properties were kept as constant as possible. The oil used was Shell Tellus 27, at a temperature of 50°C±2 K.

The input variable for the above tests was pump swash plate angle. Frequency response tests were carried out with different amplitude sinusoidal inputs.

4.1 Test procedure

The main object of the test programme was to correlate the experimental results of the frequency response tests with predictions obtained from measurement of the system parameters.

One method of frequency response testing using

electro-hydraulic inputs is to carry out a closed loop frequency response test of the electro-hydraulic input servo, and subsequently allow for this after obtaining the overall frequency response of the system. This method is time consuming, and it is not always possible to ensure that the servo dynamic performance has not been affected by a change in system variables, such as oil temperature.

However, using the digital transfer function analyser, it is possible to record the response of the electro-hydraulic servo, and the overall transmission, including the servo system, consecutively at any frequency, and then by subtraction immediately obtain the net transmission response. It is also a simple matter to continuously monitor the servo response, to ensure a constant amplitude of pump

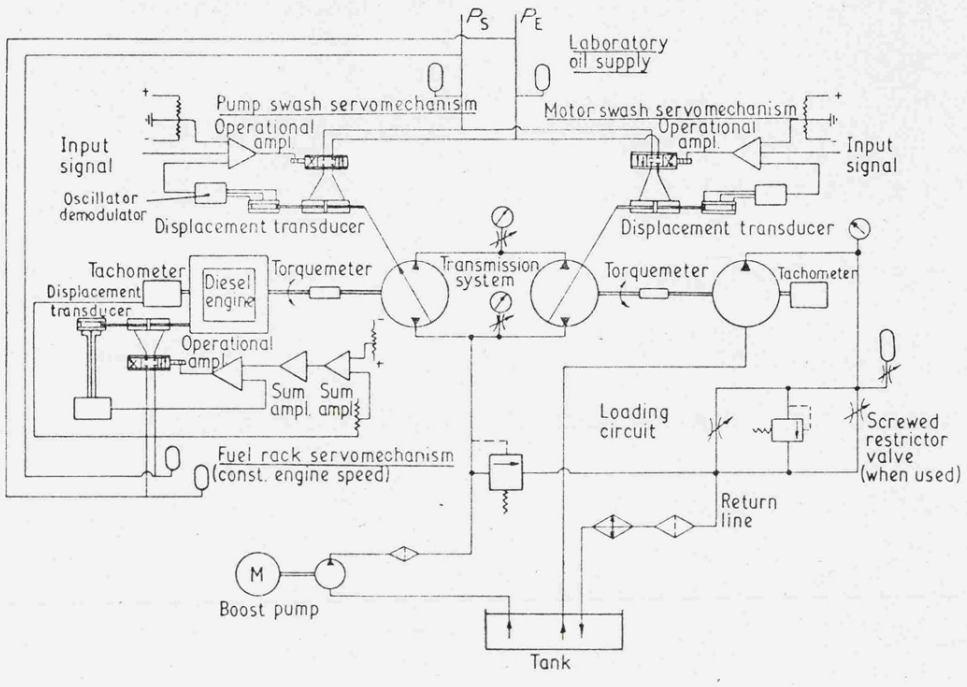

Fig. 7. Line diagram of test rig

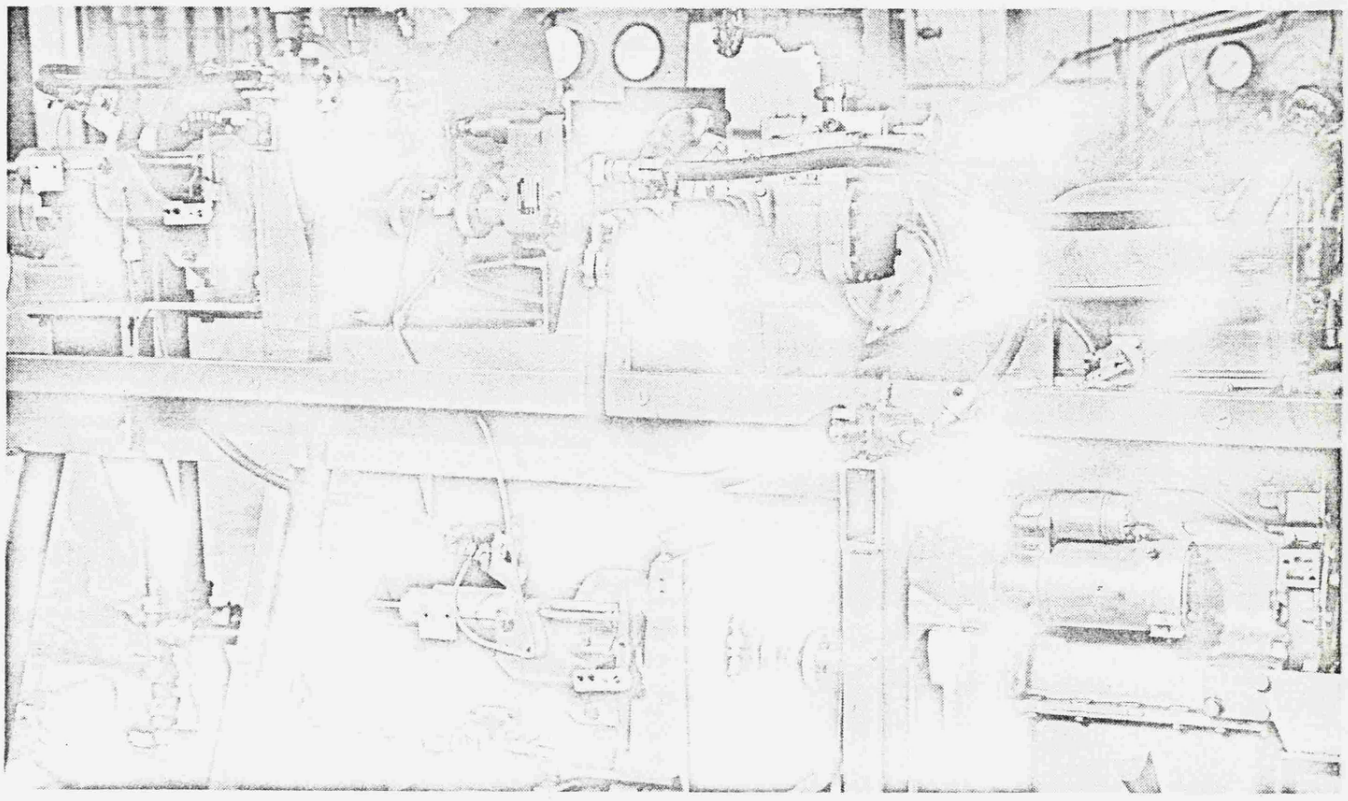

Fig. 8. Layout of engine driven hydrostatic transmission and load pump

swash plate angular movement. In addition to recording the output speed response of the transmission, line pressure variations and torque variations could be recorded simultaneously.

In conjunction with the digital readout from the transfer function analyser, the supply and return line pressures, differential line pressure, transmission output speed, and pump swash plate angle were recorded, using an ultraviolet recorder.

5 DISCUSSION OF RESULTS

5.1 Test with typical load

Consider first tests 1–4 (see Table 1), in which the torque–speed characteristic of the load was set up to represent a typical windage type load. Frequency response tests were carried out at different pump swash plate positions. The load in this case was applied by screwing up a needle valve in the loading pump delivery line. The amplitude of the pump swash plate oscillation was kept constant. The test results are shown on Fig. 9.

However, a short consideration of the set-up shows that many of the system parameters have been altered. For example, the system pressure and the motor speed have both altered, with corresponding change in the slip and torque losses of the units. By increasing the motor speed and moving up the load torque–speed characteristic, the load damping coefficient has been increased. Therefore, the set of results, although valid for the particular engine, transmission and load configuration, lacks generality, and cannot readily be compared with the theoretical work. The remainder of the tests have been carried out in what is apparently a more artificial manner, to allow comparison with the theoretical analysis.

5.2 Investigation of load effects

Variation of load damping coefficient was carried out by altering the loading system characteristics and holding the mean swash plate angles, mean pump and motor speeds and load torque constant (tests 5–8). The rest results are shown on Fig. 9, and the effects are shown on Fig. 10. The apparent natural frequency, as determined from the 90° phase lag point, alters with the load damping coefficient from 4·8 Hz at 0·037 Nm/rad s to 6·5 Hz at 0·587 Nm/rad s. This suggests a considerable increase in natural frequency with increase in load damping coefficient. This is not in agreement with the theoretical predictions, but the reasons for the apparent discrepancy are given below. The damping ratio can be seen to increase rapidly with increase in load damping.

Tests 9–12 were carried out at reduced amplitude. The results are shown on Fig. 11 and are similar in all respects to those shown on Fig. 10, indicating that there were no significant non-linearities present.

Table 1. Frequency response tests carried out on hydrostatic transmission

Test No.	Amplitude of input swash angle, peak to peak, degrees	Mean pump swash, degrees	Mean motor swash, degrees	Load inertia, kg m²	Return line pressure, bar	Load damping coefficient f_L, Nm/rad s	Supply line volume, litres	Test feature
1	2·50	3·40	7·42	0·0167	13·6	0·390	0·957	Windage load simulation
2	2·50	5·20	7·42	0·0167	13·6	0·494	0·957	
3	2·50	7·00	7·42	0·0167	13·6	0·548	0·957	
4	2·50	8·80	7·42	0·0167	13·6	0·637	0·957	
5	3·76	4·75	7·42	0·0167	13·6	0·587	0·957	Load damping coefficient f_L varied, other parameters held constant
6	3·76	4·75	7·42	0·0167	13·6	0·407	0·957	
7	3·76	4·75	7·42	0·0167	13·6	0·194	0·957	
8	3·76	4·75	7·42	0·0167	13·6	0·037	0·957	
9	1·25	4·75	7·42	0·0167	13·6	0·544	0·957	Tests 5–8 repeated with smaller input amplitude
10	1·25	4·75	7·42	0·0167	13·6	0·415	0·957	
11	1·25	4·75	7·42	0·0167	13·6	0·176	0·957	
12	1·25	4·75	7·42	0·0167	13·6	0·035	0·957	
13	1·25	4·75	7·42	0·190	13·6	0·035	0·957	Large load inertia at two input amplitudes
14	3·76	4·75	7·42	0·190	13·6	0·037	0·957	
15	3·76	4·75	7·42	0·0167	6·1	0·415	0·957	Mean return line pressure varied
16	3·76	4·75	7·42	0·0167	20·4	0·419	0·957	
17	3·76	4·75	7·42	0·0167	25·0	0·422	0·957	
18	1·25	4·75	7·42	0·0167	13·6	0·595	0·957	Tests with restricted boost system
19	3·76	4·75	7·42	0·0167	13·6	0·540	0·957	
20	1·25	4·75	7·42	0·0167	13·6	0·230	0·957	
21	3·76	4·75	7·42	0·0167	13·6	0·234	0·957	
22	3·76	4·75	7·42	0·0167	13·6	0·557	0·957	Supply line replaced by flexible hose
23	3·76	4·75	7·42	0·0167	13·6	0·447	0·957	
24	3·76	4·75	7·42	0·0167	13·6	0·204	0·957	
25	3·76	4·75	7·42	0·0167	13·6	0·037	0·957	
26	3·76	4·75	7·42	0·0167	13·6	0·597	0·957	Pressure gauge connected into supply line
27	3·76	4·75	7·42	0·0167	13·6	0·460	0·957	
28	3·76	4·75	7·42	0·0167	13·6	0·324	0·957	
29	3·76	4·75	7·42	0·0167	13·6	0·037	1·096	

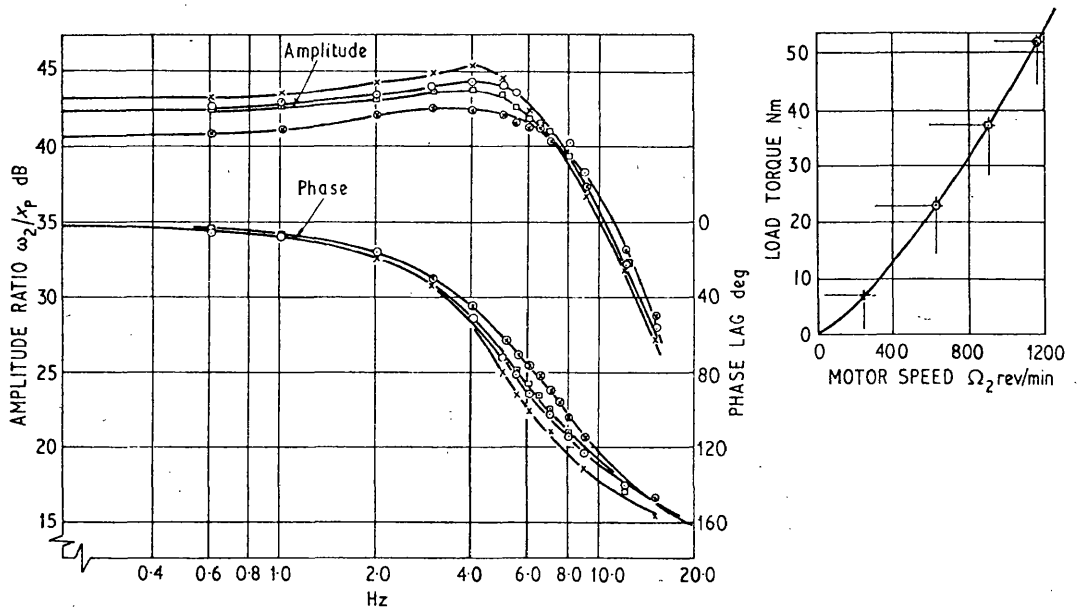

Load characteristics

Test no.	Symbol	Pump swash, degrees	Motor speed Ω_2, rev/min	Load damping coefficient, Nm/rad s
1	×	3·40	245	0·288
2	○	5·20	625	0·365
3	⊡	7·0	910	0·405
4	⊗	8·8	1158	0·471

Fig. 9. Overall frequency response of transmission with windage load. (Pump swash plate oscillated at ±1·25°)

6 CORRELATION OF RESULTS

Four methods have been presented to determine system dynamic response: the simple theory of equation (2), the signal flow graph method, vector analysis, and experiment. In order to obtain values from the first three, the system volume was carefully measured and the isentropic tangent bulk modulus for the oil obtained from the manufacturers' literature (18). The pipe resilience was taken into account in accordance with equation (1).

In comparing numerically the results of the different analyses, the frequency at which the phase lag was 90° was taken as the apparent natural frequency. An apparent damping ratio was also obtained from the phase plot (Table 2).

All the methods give natural frequencies within 30 per cent of each other; if this type of accuracy is all that is required, then any of the methods can be used. However, when it is considered that variations in natural frequency are proportional to the square root of most of the system parameters, it shows that very wide discrepancies have occurred.

6.1 Simple theory

The simple theory of equation (2) gave a value of natural frequency that did not vary with load damping coefficient, and only provided good correlation with the experimental results at the higher load damping coefficients. The damping ratio was very much underestimated.

Table 2. Comparison between theoretically predicted and experimentally measured dynamic response of hydrostatic transmission

Test No.	Natural frequency—ω_n, Hz				Damping ratio—ζ			
	Simple theory of equation (2)	From signal flow analysis	Vector analysis	Experimental	Simple theory of equation (2)	From signal flow analysis	Vector analysis	Experimental
5	6·20	6·63	6·54	6·4	0·44	0·50	0·55	0·60
6	6·20	6·50	6·06	6·0	0·28	0·38	0·48	0·50
7	6·20	6·36	5·45	5·1	0·15	0·24	0·30	0·30
8	6·20	6·24	4·93	4·8	0·03	0·13	0·20	0·20

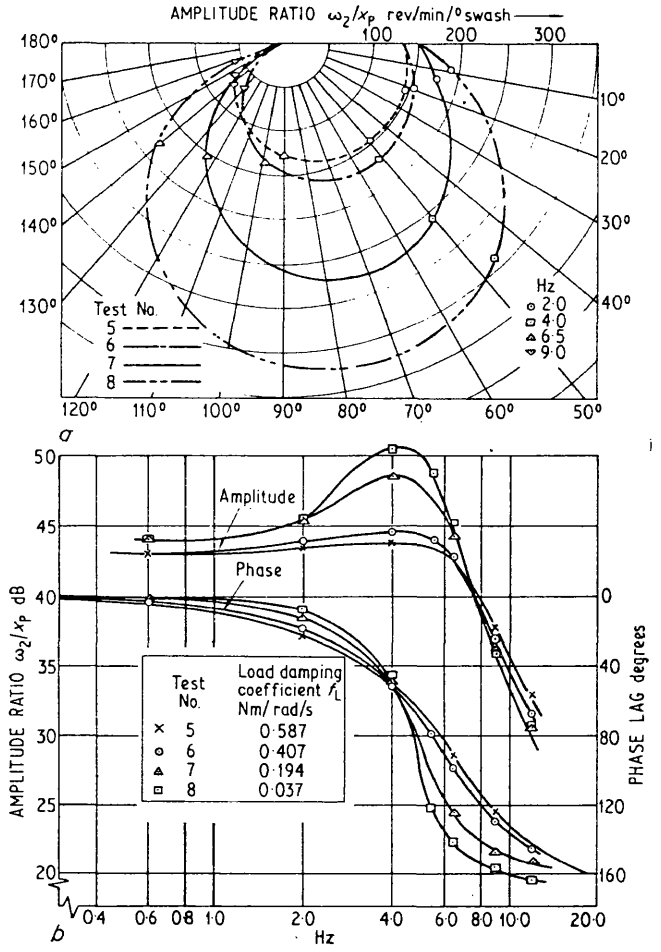

Fig. 10. Effect of load damping coefficent on transmission dynamic response, (*a*) loci, (*b*) logarithmic plot

6.2 Signal flow analysis

The signal flow analysis predicted a small change in natural frequency with load damping coefficient, but not to the extent of the values obtained experimentally (see Table 2). The prediction of damping ratio was very much improved.

6.3 Vector locus technique

While carrying out the frequency response tests, the torque on the load shaft was also measured, and hence the frequency response for the actual load used obtained. In the theoretical analysis, the load was assumed to comprise a viscous and inertial component, the response of the load torque to changes in speed being a first order lead,

i.e. $$t_1 = (f_L + J_L s)\omega_2 \quad . \quad . \quad . \quad . \quad (6)$$

It will be convenient to rearrange this and put it in the form:

$$\frac{t_L}{\omega_2 f_L} = 1 + \frac{J_L}{f_L} s$$

therefore $$\frac{t_L}{\omega_2 f_L}(j\omega) = 1 + \frac{J_L}{f_L} j\omega \quad . \quad . \quad . \quad (7)$$

If this is plotted on a vector locus, it gives the vertical line shown on Fig. 12. The actual values obtained during tests 5–8, which departed significantly from this line, are also shown on Fig. 12. This shows that the load was not by any means the inertial and viscous load first assumed.

As can be seen from Table 2, the vector locus technique is very much more accurate, and would appear to be the most valuable tool for prediction of dynamic performance. It slightly overestimates the natural frequency and slightly underestimates the damping ratio.

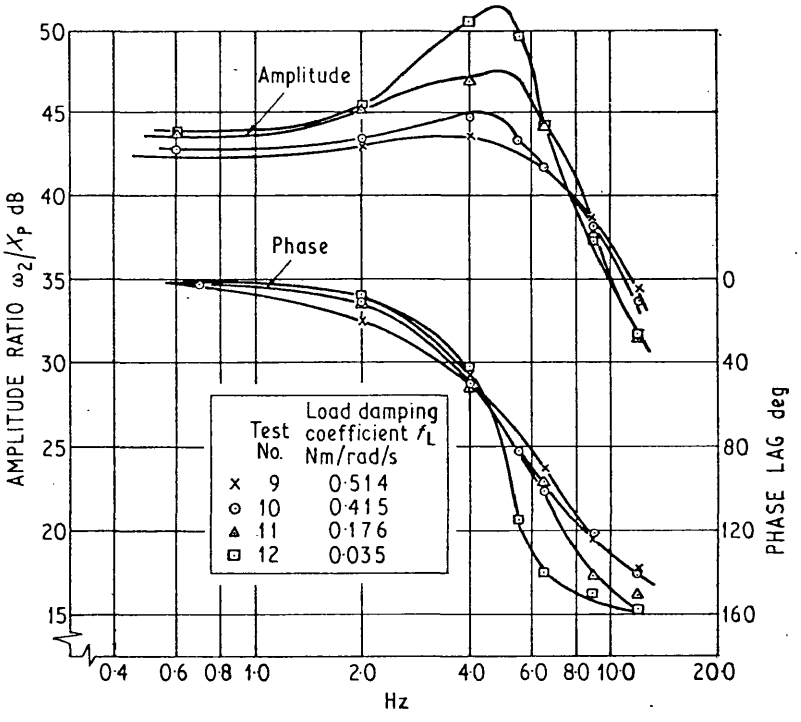

Fig. 11. The effect of load damping on overall transmission response using smaller input amplitude

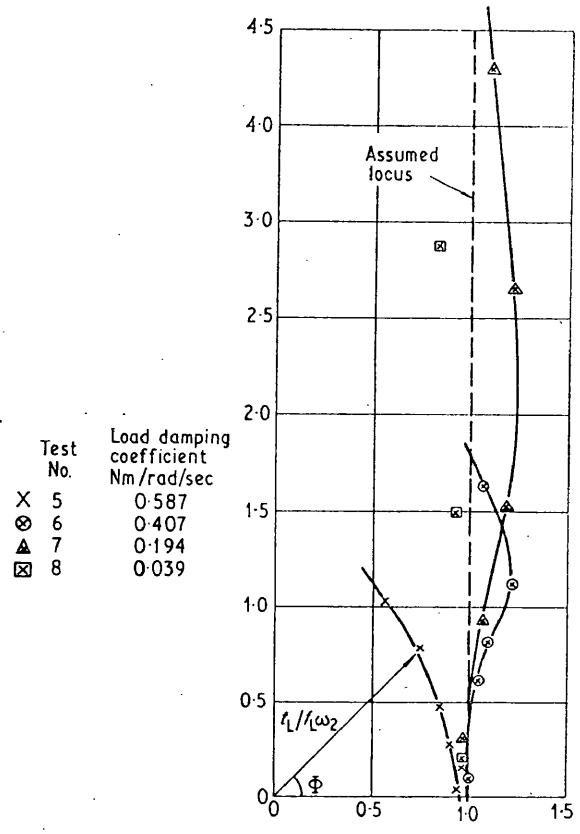

Fig. 12. The locus of the measured hydrostatic load

6.4 Bulk modulus

If we refer to the initial discussion we find that most investigators, when confronted with a discrepancy between their theoretical and experimental results, have worked backwards to determine the effective bulk modulus of the oil in the system. This procedure has also been adopted here for a large number of tests with different load damping coefficients, all using the steel pipe supply line. Over a range of frequencies between 0·1 Hz and 12·0 Hz the load vector has been obtained, and by using the vector diagram of Fig. 5, starting from both ends, the compressible flow vector $\overrightarrow{q_c/\omega_2}$ determined. It is then possible to determine the effective bulk modulus of the oil in the pipe, B_e.

The mean value of the effective bulk modulus of the oil in the pipe was found to be $15{\cdot}5 \times 10^3$ bar ($2{\cdot}28 \times 10^5$ lbf/in^2). A statistical analysis of the results showed a standard error of only 7·3 per cent over the 79 determinations carried out.

If the elasticity of the steel pipe is then allowed for, using equation (1), the bulk modulus for the oil was determined to be $16{\cdot}2 \times 10^3$ bar ($2{\cdot}38 \times 10^5$ lbf/in^2).

This value should be compared with the manufacturers' physical test value at the temperature and pressure of the tests. Secant values of bulk modulus are usually made on the basis of the change in volume which occurs for a change in pressure from atmospheric to working pressure. These are not appropriate in this case as the pressure fluctuations about the mean working pressure are relatively small. Hence tangent values have been used. At 50°C and 82·0 bar:

isentropic tangent bulk modulus of oil

$$= 16{\cdot}5 \times 10^3 \text{ bar } (2{\cdot}40 \times 10^5 \text{ lbf/in}^2)$$

Using the vector locus technique it is therefore possible to predict the natural frequency of the transmission to within 4 per cent.

It should be noted that the analysis had assumed the pump and motor to be continuous linear elements, but from the outset it had been considered possible that the slippers might leave the swash plate under some oscillatory conditions. This would lead to a reduction in flow from the pump, and could cause damage to the unit. The experimental results showed no sign that this had happened, and on stripping the units after the tests no sign of excessive wear of the slipper pad or swash plate surface could be determined.

In order to provide a clear procedure for the designer to adopt when predicting the dynamic performance of a transmission, Appendix 2 has been presented.

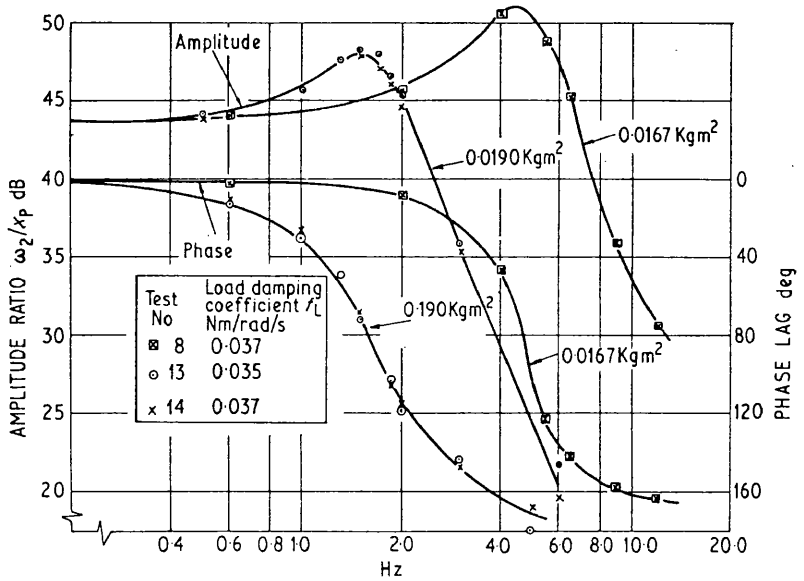

Fig. 13. The effect of an increased inertia load on overall transmission response

6.5 Effect of slip

The leakage past the pump, motor and valves in the system shows as a flow loss which is in phase with the pressure pulsations and 90° out of phase with the compressibility term. Careful tests were carried out on the pump and motor units to determine whether the mean leakage altered with frequency. No change was recorded up to frequency of 12 Hz. This indicates that the pump and motor used were responding well to sinusoidal swash plate movements at the operating conditions of the tests.

At low frequencies, the slip losses cause a reduction in amplitude of response. The amount of this reduction could be predicted by using values of slip obtained by pump and motor calibration.

At higher frequencies, slip losses are insignificant in comparison with compressibility losses.

6.6 Effect of load inertia

The reduction in apparent natural frequency with increased load inertia shown on Fig. 13 was predicted, using the vector locus technique, and good correlation obtained. Since the load was now predominantly inertial, the simple mathematical model for the load was satisfactory. Using a value for the effective bulk modulus of $16{\cdot}2 \times 10^3$ bar ($2{\cdot}38 \times 10^5$ lbf/in^2), the natural frequency of the transmission was predicted to be 1·66 Hz using the simple theory of equation (2) and 1·75 Hz using the signal flow analysis. The experimentally measured value was 1·70 Hz.

6.7 Mean return line pressure

Tests 15–17 were carried out at the conditions of test 6, using the large capacity boost system but varying the mean return line pressure. This was felt desirable, as previous authors had suggested that aeration caused a reduction in natural frequency, and the degree of aeration would be influenced by the mean return line pressure.

No significant changes in frequency response were noted when the return line pressure was varied between 6·0 bar and 25·0 bar.

6.8 Effect of boost system

In the tests so far reported, the return line of the system was supplied by a very large boost pump capable of maintaining a constant return line pressure. A more practical boost system was now fitted, with a boost pump capacity of 6 per cent of the main pump maximum capacity. A single stage pressure relief valve was installed. Tests 18–21 were carried out at the conditions of tests 9, 5, 11, and 7 respectively, but with this new boost system. The mean return line pressure was left constant at 13·6 bar.

Traces of swash plate angle x_p, output speed ω_2, and return line pressure P_R are shown on Fig. 14 for tests 18 and 21. These tests correspond to the smallest and largest pressure variations in the return line obtained in this series with the restricted boost supply. When the amplitude of the flow fluctuations was large, cavitation was marked, and cut off the bottom of the sine wave, for the reasons shown in Fig. 6. There was, however, an intermediate stage which occurred with smaller flow fluctuations in the return line (i.e. correspondingly lower frequencies, see test 21, 2 Hz) where the pressure appears to rise exponentially after cavitation. This could be due to the purging of voids in the return line following local cavitation.

The increase in apparent natural frequency shown in Fig. 15 can be predicted using the vector locus technique. The return line pressure variations $\overrightarrow{P_L/\omega_2}$ may be added vectorially to the differential line pressure variations $\overrightarrow{P_D/\omega_2}$ to give the supply line pressure variations $\overrightarrow{P_H/\omega_2}$. This procedure was carried out for tests 18–21. The vector loci obtained were in very good agreement with the experimental locus for all tests. The previously determined value of oil bulk modulus, $16{\cdot}2 \times 10^3$ bar ($2{\cdot}38 \times 10^5$ lbf/in^2) was used. When considerable cavitation occurred in the return line, there was nevertheless a marked increase in apparent natural frequency, compared with the case where the return line pressure was held constant.

It should be noted that the maximum increase in system stiffness would occur if the relief valve had a very

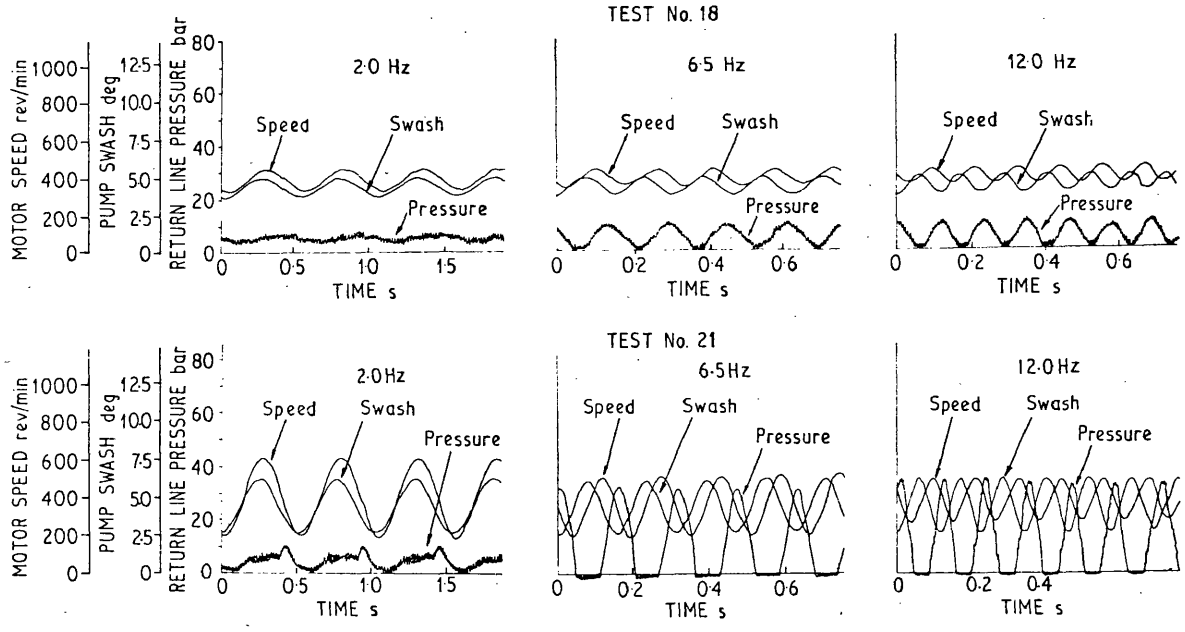

Fig. 14. Pressure, speed, and swash traces for system with restricted boost upply, tests 18 and 21

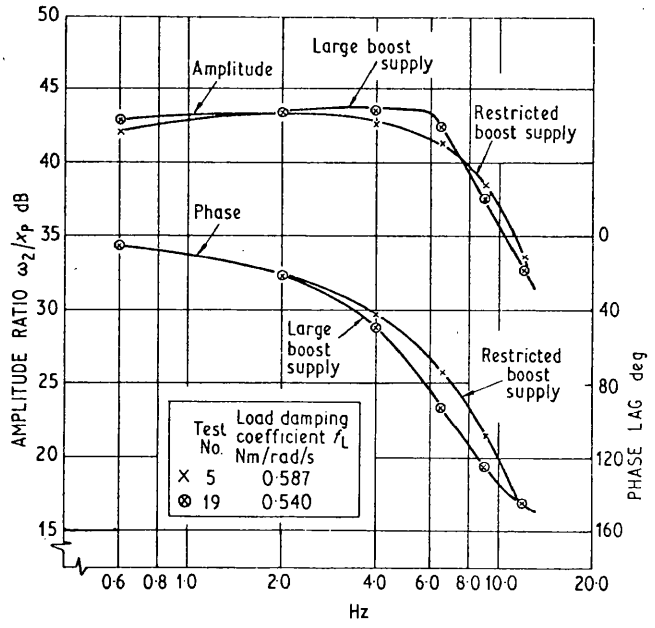

Fig. 15. The effect of restricted boost supply upon overall transmission response

steep pressure–flow characteristic and there was no cavitation in the return line. Both line pressures would then vary equally, and provided the mean return line pressure was high enough to prevent cavitation, the natural frequency would be increased by 40 per cent.

6.9 Effect of flexible hose

One of the many advantages of hydrostatic drives is their ability to transmit power to normally inaccessible places, and very often flexible hose is incorporated. To determine the effect of this, the steel pipes were removed and replaced by a length of 1 in internal bore, two braid flexible hose.

Tests 22–25 were carried out with a hose length of 2·44 m (8 ft) and its overall effect was to reduce the natural frequency to approximately half of the value recorded with steel pipes, as is shown on Fig. 16, where test 24 is compared with test 7.

The vector locus technique was used to determine the effective bulk modulus of the oil in the flexible pipe. A value of $4{\cdot}35 \times 10^3$ bar (64 000 lbf/in^2) was obtained with an 8 per cent scatter. A static test carried out on the same hose full of oil gave an effective isothermal bulk modulus of $6{\cdot}60 \times 10^3$ bar (97 000 lbf/in^2).

This discrepancy between dynamic and static test results was much larger than that when steel pipe was employed.

6.10 Effect of pressure gauges

Most practical hydraulic transmission systems are fitted with Bourdon gauges, with snubbers incorporated if pressure fluctuations are likely to be experienced. Tests 5, 6, 7, and 8 were repeated with a 300 bar Bourdon tube gauge fitted to the high pressure line (tests 26–29). It was connected to the transmission supply line by an 8 m length of $\frac{1}{8}$ in i.d. pipe and snubber, from which the air had been bled.

The average reduction in natural frequency resulting from the inclusion of the pressure gauge and line was $3\frac{1}{2}$ per cent.

7 CONCLUSIONS

An extensive series of frequency response tests has been carried out on a hydrostatic transmission to determine its dynamic characteristics as an aid to system design.

The theoretical base has been extended to include the dynamic characteristics of the load, and the prime mover. The effect of the return line and boost system is also considered.

The test results show that the dynamic response of the transmission is influenced to a large extent by the dynamic characteristics of the load. Much of the scatter obtained in early tests can be attributed to neglect of this important consideration.

The effect of prime mover droop was relatively insignificant and could be ignored except in extreme cases.

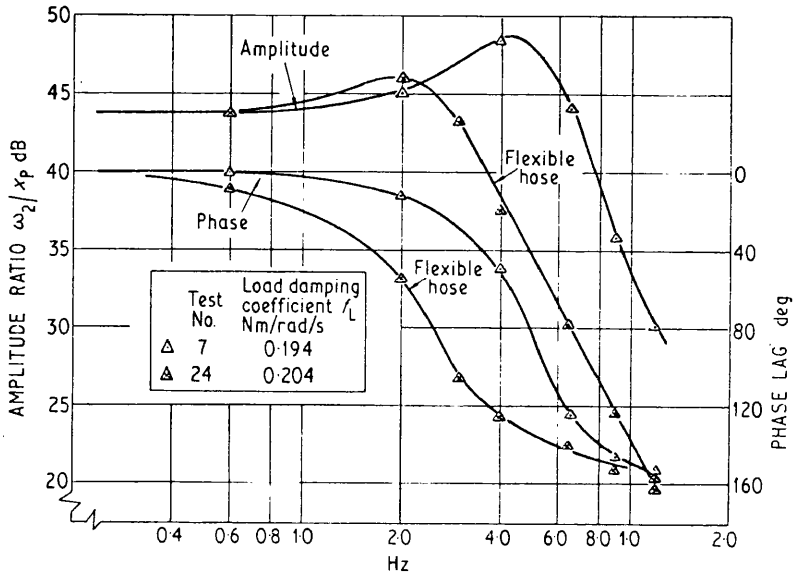

Fig. 16. The effect of using a flexible hose supply line on overall transmission response

The return line in most conventional systems contributes to the stiffness of the transmission.

For the transmission considered the hydraulic pipeline was relatively short, 1·80 m (6 ft), which is approximately $\frac{1}{50}$ of the wavelength of pressure waves at 15 Hz; under these conditions a lumped parameter approach is perfectly satisfactory. For longer pipelines, it may be necessary to take into account the wave nature of the pressure signals.

Oil inertia effects were found to add less than 1 per cent to the effective inertia of the motor.

Use of the isentropic tangent bulk modulus of the oil in conjunction with carefully determined system parameters enables estimates of natural frequency to be made within 4 per cent.

The tests were carried out at relatively low pressure differentials across the pump and motor units, but there is no reason to assume that the method should not apply when the pressure differential is much higher, nor when the oil temperatures are higher.

APPENDIX 1

DIGITAL COMPUTER PROGRAMME FOR EVALUATING OVERALL TRANSFER FUNCTION OF TRANSMISSION FROM SIGNAL FLOW ANALYSIS

Subroutine 'solve'—solves transfer function for τ_1, τ_2, ζ, ω_n and K.

Subroutine 'resp'—evaluates frequency response, amplitude ratio and phase angle.

```
      PROGRAM TRDRES
C TRANSMISSION DYNAMIC RESPONSE
      COMMON A, B, C, E, G, H, AMP
   77 FORMAT(I3)
      READ(5,77)NUMBER
      ITEM=0
      DO 99 KOUNT=1,NUMBER
      READ(5,200)KODE
  200 FORMAT(I1)
      READ (5, 3) AINT1, DP, SP, PDTCP, VTCP, B, DM, SM, PDTCM, VTCM,
     1      AINT2,  ESLD, THETAP, VOL, THETAM, DFL, BOMGP, SPRESS
    3 FORMAT  (8E10.3)
      SP=-SP
      SM=-SM
      ESLD=-ESLD
      WRITE (6, 5) ESLD, THETAP, VOL,THETAM, DFL, BOMGP,SPRESS
    5 FORMAT(1H1,10X,4HESLD,13X,6HTHETAP,14X,3HVOL,13X,6HTHETAM,14X,
     -        3HDFL,14X,5HBOMGP,12X,6HSPRESS// 1H0,1P7E18.5////)
      AMP = DP*BOMGP/(DM*THETAM)
      A =-AINT1*ESLD
      H=1-VTCP*ESLD+DP*SPRESS*ESLD*THETAP/BOMGP
      DENOM1 = DM*THETAM*(DM*THETAM-PDTCM)
      G = 1-VTCP*ESLD-(DFL+VTCM)*((SP+SM)*(1-VTCP*ESLD)+ESLD*DP*THETA
     1(DP*THETAP+PDTCP))/DENOM1
      E =-AINT1*ESLD-(DFL+VTCM)*(-VOL*(1-VTCP*ESLD))/(DENOM1*B)-AINT2
     1     SP+SM)*(1-VTCP*ESLD)+ESLD*DP*THETAP*(DP*THETAP+PDTCP))/DENOI
     1+(DFL+VTCM)*(SP+SM)*AINT1*ESLD/DENOM1
      C =-(DFL+VTCM)*VOL*AINT1*ESLD/(B*DENOM1)+AINT2*VOL*(1-VTCP*ESLD
     1    (DENOM1*B)+AINT1*AINT2*ESLD*(SP+SM)/DENOM1
      B =-AINT1*AINT2*ESLD*VOL/(DENOM1*B)
      WRITE(6,15)AMP,A,G,E,C,B,H
   15 FORMAT(1H0,11X,3HAMP,16X,1HA,17X,1HG,17X,1HE,17X,1HC,17X,1HB,17X
     -        1HH// 1H0,1P7E18.5////)
      IF(KODE-3)10,20,10
   10 CALL RESP(KODE,&99,&20)
   20 CALL SOLVE(ITEM)
   99 CONTINUE
      WRITE(6,222)NUMBER,ITEM
  222 FORMAT('1 ***',I4,' SETS OF DATA ARE PROCESSED :',I3,' ARE TERM
     -TED AFTER 25 ITERATIONS ***')
      STOP
      END
```

```
      SUBROUTINE SOLVE(ITEM)
      COMMON A,B,C,E,G,H,AMP
      X = 0
      ITN = 0
      WRITE(6,50)
   50 FORMAT(1H0,//,4X,4HXNEW/)
   35 W = B*X**3+C*X**2+E*X+G
      Y = 3*B*X**2+2*C*X+E
      XNEW = X-W/Y
      WRITE (6, 45) XNEW
   45 FORMAT(' ',1P1E11.4)
      IF ( ABS((X-XNEW)/XNEW)-1.0E-03) 48, 39, 39
   39 ITN = ITN+1
      IF (ITN-25) 41, 47, 47
   41 X = XNEW
      GO TO 35
   47 WRITE(6,222)
  222 FORMAT(//' *** TERMINATED AFTER 25 ITERATIONS ***')
      ITEM=ITEM+1
      RETURN
   48 XNEW = -XNEW
      B1 = C-B*XNEW
      B2 = E-(C-B*XNEW)*XNEW
      WNSQ=B2/B
      GAIN = AMP*H/(B*WNSQ*XNEW)
      T1 = A/H
      T2 =1/XNEW
      DAMP = B1/B
      WN = SQRT(WNSQ)
      ZETA= DAMP/(2*WN)
      WRITE (6, 58)  GAIN, T1, T2, ZETA, WN
   58 FORMAT (1H0, //, 12X , 4HGAIN , 17X , 2HT1 , 18X , 2HT2 , 18X ,
     1    4HZETA , 17X , 2HWN , // , 1P5E20.4 // )
      RETURN
      END
      SUBROUTINE RESP(KODE,*,*)
      COMMON A, B, C, E, G, H, AMP
      WRITE(6,1)
    1 FORMAT(1H0,19X,9HFREQUENCY,31X,9HAMPLITUDE,23X,5HPHASE//9X,10HCY
     1ES/SEC,11X,8HRADS/SEC,12X,6HABSVAL,17X,2HDB,15X,7HDEGREES // )
      READ (5,24) OMGFST, OMGLST, OMGINC
   24 FORMAT (3E10.3)
      OMEGA = OMGFST
   26 OMGSQ = OMEGA*OMEGA
      DENOM2= (G-C*OMGSQ)**2+(E*OMEGA-B*OMEGA*OMGSQ)**2
      TREAL = AMP*(H*(G-C*OMGSQ)+A*(E*OMGSQ-B*(OMGSQ**2)))/DENOM2
      TIMAG = AMP*(A*OMEGA*(G-C*OMGSQ)-H*OMEGA*(E-B*OMGSQ))/DENOM2
      ABSVAL = SQRT(TREAL**2+TIMAGE**2)
      DB = 20*ALOG10(ABSVAL)
      PHASE = ATAN2(TIMAG,TREAL)*57.29578
      CYCLES = OMEGA/(3.142*2)
      WRITE (6,35)  CYCLES, OMEGA, ABSVAL, DB, PHASE
   35 FORMAT(5E20.5)
      OMEGA = OMEGA + OMGINC
      IF (OMEGA-OMGLST) 26,26,38
   38 RETURN KODE
      END
```

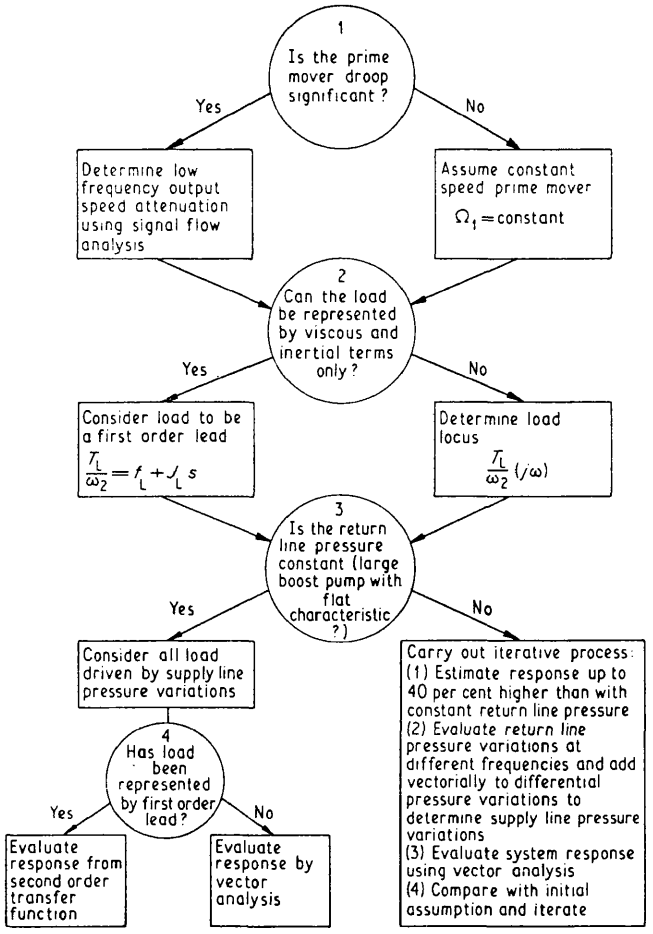

Fig. 17. Design procedure for determining overall transmission response

APPENDIX 2

DESIGN PROCEDURE

It may be useful at this stage to outline a suggested analytical procedure to determine the dynamic characteristics of any transmission. A block diagram has been drawn up to outline the design scheme and is shown in Fig. 17. The exact criteria for the design decisions have not been specified, as to a large extent these will depend upon the application.

The typical case of test 7 is presented in detail to illustrate the design procedure.

Basic information

Prime mover speed, Ω_1 = 125·5 rad/s
Maximum pump capacity, D_P = $5{\cdot}34\times10^{-2}$ l/rev ($3{\cdot}25$ in^3/rev)
Pump swash plate or tilt movement, $X_{P\,max}$ (zero to full stroke) = 15·0°
Maximum motor capacity, D_M = $5{\cdot}34\times10^{-2}$ l/rev ($3{\cdot}25$ in^3/rev)
Motor swash plate or tilt movement, $X_{M\,max}$ if variable (zero to full stroke) = 15·0°

Steady state conditions of test 7:
Load torque, T_2 = 33·4 Nm (24·6 lbf ft)
Load speed, Ω_2 = 61·0 rad/s
Pump swash, X_P = 4·42°
Motor swash, X_M = 7·42°
Supply line pressure, P_H = 87·0 bar (1280 lbf/in^2)
Return line pressure, P_L = 13·6 bar (200 lbf/in^2)

Additional information required to evaluate system dynamic performance

Dead volume in pump (exposed to supply line) = 86·2 cm^3 (5·27 in^3)
Dead volume in motor (exposed to supply line) = 86·2 cm^3 (5·27 in^3)
Supply pipe length = 1·76 m (5·75 ft)
Supply pipe internal diameter = 2·54 cm (1·00 in)
Supply pipe volume = 924·0 cm^3 (56·5 in^3)
Total supply line volume, V = 1096·4 cm^3 (67·04 in^3)

Pump and motor loss coefficients at operating conditions:
Pump slip, K_P = $2{\cdot}23\times10^{-4}$ l/s bar ($3{\cdot}72\times10^{-9}$ ft^3/s lbf/ft^2)
Motor slip, K_M = $2{\cdot}33\times10^{-4}$ l/s bar ($3{\cdot}90\times10^{-9}$ ft^3/s lbf/ft^2)
Pump viscous torque loss coefficient, f_p = $1{\cdot}53\times10^{-2}$ Nm/rad s ($1{\cdot}13\times10^{-2}$ lbf ft/rad s)
Motor viscous torque loss coefficient, f_M = $1{\cdot}53\times10^{-2}$ Nm/rad s ($1{\cdot}13\times10^{-2}$ lbf ft/rad s)
Pump pressure dependent torque coefficient, K_{fp}; Motor pressure dependent coefficient, K_{fM} = Very small for units considered, and therefore ignored

Effective compressibility of oil at operating conditions at 87·0 bar (1280 lbf/in^2) and 50°C for Shell Tellus 27 (**18**):

isentropic tangent bulk modulus = $16{\cdot}5\times10^3$ bar (240 000 lbf/in^2)

Using equation (1),

$$\frac{1}{B_e} = \frac{1}{B_o} + \frac{1}{B_p}$$

gives for steel pipes of wall thickness 0·413 cm (0·1625 in) an effective bulk modulus for the oil in the pipe B_e of $15{\cdot}3\times10^3$ bar (222 000 lbf/in^2).

Design decisions

Before commencing the design process as laid out in Fig. 17, it is necessary to ensure the validity of lumped parameter analyses by considering the delay time for pressure signals to travel down the pipeline. Also, the significance of oil inertia effects in the pipeline should be checked.

(1) Is the prime mover droop significant?

Prime mover droop, K_E = 14 per cent no load to full load
= 0·160 rad/sec/Nm (0·217 rad/sec/lbf ft)

If the load were removed completely, this would only give a prime mover speed increase of 4 per cent, so it can be considered as constant speed.

In order to have carried out the signal flow analysis, it would be necessary to determine the driving inertia of the prime mover plus pump, J_1.

(2) Can the load be represented by a viscous and inertial load?

Type of load: positive displacement pump and associated loading valves.

It was considered prudent to use the load locus, in this case, $t_L/\omega_2(j\omega)$, see Fig. 13.

To represent the load by a first order lead, it would be necessary to evaluate the driven inertia, J_2, and the load damping coefficient, f_L.

(3) Is the return line pressure constant?

A large boost pump and flat characteristic relief valve had been used, and the return line pressure was therefore considered constant.

To carry out the suggested iteration it would be necessary to determine the boost pump and relief valve characteristics as shown in Fig. 6*a*.

(4) As the load has been represented by a locus, the overall response is to be evaluated using the vector analysis technique.

Calculations

Sample calculations are shown for two frequencies, 2·0 Hz and 6·5 Hz, which were evaluated for Fig. 5.

	2·0 Hz	*6·5 Hz*
(*a*) From the load locus		
$\lvert t_L/\omega_2 \rvert$ Nm/(rev/min)	0·0285	0·0589
$\underline{/t_L/\omega_2}$ Degrees	+40·6	+65·6
(*b*) Torque to accelerate motor		
$\lvert t_m/\omega_2 \rvert$ Nm/(rev/min)	0·0089	0·0289
$\underline{/t_m/\omega_2}$ Degrees	+90	+90
(*c*) Motor viscous torque coefficient		
$\lvert f_m \rvert$ Nm/(rev/min)	0·0016	0·0016
$\underline{/f_m}$	IN PHASE	IN PHASE
(*d*) Effective load torque		
$\frac{\vec{t}_2}{\omega_2} = \frac{\vec{t}_m}{\omega_2} + \frac{\vec{t}_2}{\omega_2} + f_m$		
$\lvert t_2/\omega_2 \rvert$ Nm/(rev/min)	0·0350	0·0869
$\underline{/t_2/\omega_2}$ Degrees	+51·8	+74
(*e*) Supply line pressure variation		
$\frac{\vec{p}_h}{\omega_2} = \frac{\vec{t}_2}{\omega_2} \cdot \frac{p_h}{t_2} = \frac{\vec{t}_2}{\omega_2} \cdot \frac{1}{D_2 X_M}$		
$\lvert p_h/\omega_2 \rvert$ bar/(rev/min)	0·099	0·226
$\underline{/p_h/\omega_2}$ Degrees	+51·8	+74
(*f*) Slip flow loss		
$\frac{\vec{q}_s}{\omega_2} = (K_p + K_M)\frac{\vec{p}_h}{\omega_2}$		
$\lvert q_s/\omega_2 \rvert$ (l/s)/(rev/min) $\times 10^4$	0·451	1·030
$\underline{/q_s/\omega_2}$ Degrees	+51·8	+74
(*g*) Compressed flow loss		
$\frac{\vec{q}_c}{\omega_2} = \frac{V}{B_e} j\omega \frac{\vec{p}_h}{\omega_2}$		
$\lvert q_c/\omega_2 \rvert$ (l/s)/(rev/min) $\times 10^4$	0·835	6·19
$\underline{/q_c/\omega_2}$ Degrees	+141·8	+164
(*h*) Total flow loss		
$\frac{\vec{q}_L}{\omega_2} = \frac{\vec{q}_c}{\omega_2} + \frac{\vec{q}_s}{\omega_2}$		
$\lvert q_L/\omega_2 \rvert$ (l/s)/(rev/min) $\times 10^4$	0·947	6·270
$\underline{/q_L/\omega_2}$ Degrees	+113·4	+154·6
(*i*) Flow continuity in supply line		
$\frac{\vec{q}_p}{\omega_2} = \frac{\vec{q}_M}{\omega_2} + \frac{\vec{q}_1}{\omega_2}$		
where $q_m/\omega_2 = D_2 X_M$		
$\lvert q_p/\omega_2 \rvert$ (l/s)/(rev/min) $\times 10^4$	4·07	6·15
$\underline{/q_p/\omega_2}$ Degrees	+12	+115·5
(*j*) Relating pump flow to swash plate angle gives:		
$\frac{\vec{\omega}_2}{x_p} = \frac{\vec{q}_p}{x_p} \cdot \frac{\vec{\omega}_2}{q_p}$		
$\lvert \omega_2/x_p \rvert$ (rev/min)/degrees swash	174·0	115·0
$\underline{/\omega_2/x_p}$ Degrees	−12·0	−115·5

This is the overall response vector.

APPENDIX 3

REFERENCES

(1) NEWTON, GEORGE C., jun. 'Hydraulic variable speed transmissions as servomotors', *J. Franklin Inst.* 1947 (June), **243** (No. 6), 439–469.

(2) SHEARER, J. L. *Fluid power control* 1960 (M.I.T. Press, Cambridge, Mass.).

(3) LEWIS, E. and STERN, H. *Design of hydraulic control systems* 1962 (McGraw-Hill, New York).

(4) THOMA, JEAN. *Hydrostatic power transmission* 1964 (Trade & Technical Press, London).

(5) GILLE, J. C. *Feedback control systems* 1956 (McGraw-Hill, New York).

(6) HAYWARD, A. T. J. 'Research on lubricants and hydraulic fluids at the National Engineering Laboratory', N.E.L. Report No. 75, 1963 (Jan.).

(7) HAYWARD, A. T. J. 'Compressibility measurements on hydraulic fluids', N.E.L. Report No. 173 (Pt I), 1964 (Dec.).

(8) HARSEN, J. T. 'How to use readily available specification data to predict dynamic properties of hydraulic motors', *Machine design*, Jan. 1961 **33** (No. 2), 132–136.

(9) LAMBERT, T. H. and DAVIES, R. M. 'Investigation of the response of hydraulic servomechanisms with inertial load', *J. mech. Engng Sci.* 1963 **5** (No. 3), 281.

(10) RENNER, H. 'Fluid motors', Design Engineering Conf. 1965, A.S.M.E. Paper 65-MD-28, 1966 (March).

(11) HEALEY, A. J. and STRINGER, J. D. 'Dynamic characteristics of an oil hydraulic constant speed drive', *Proc. Instn mech. Engrs* 1968–69 **183** (Pt 1), 683.

(12) KEATING, T. and MARTIN, A. R. 'Response testing of a hydraulic servomechanism with mechanical feedback', 2nd *Fluid Power Symp., Jan. 1971*, A2–25 to 44 (B.H.R.A., Cranfield).

(13) WALTERS, R. 'Hydraulic servo systems analysis and synthesis', Sperry Industrial Group, pub. IG 100/A, 1964.

(14) MASON, S. J. 'Feedback theory. Further properties of signal flow graphs', *Proc. Inst. Radio Engrs* 1956 **44**, 920–926.

(15) BOWNS, D. E. 'Signal flow diagrams as an aid to the analysis of hydraulic systems', University of Bath, School of Engineering Report No. 126, 1968 (June).

(16) KORN, J. *Hydrostatic transmission systems* 1969 (Intertext Books, London).

(17) MCCALLION, H., DUDLEY, B. R. and KNIGHT, G. C. 'Analysis of a dynamically loaded hydrostatic transmission system', *First Fluid Power Symposium*, 1969 (Jan.) (B.H.R.A., Cranfield).

(18) BOWNS, D. E. 'The dynamic transfer characteristics of reciprocating engines', *Proc. Instn mech. Engrs* 1970–71 **185**, 185–201.

(19) ANON. 'Technical data on Shell Tellus oils', Shell International Petroleum Company Limited, 1963.

Discussion

G. A. Broadhurst Wolverhampton

I note that the boost circuit is incorrectly designed for a closed circuit, reversible flow, transmission circuit such as this.

In such a circuit, there is no return line as such, both lines being interchangeable. Accordingly, when the flow is reversed so that the so-called return line is connected to the outlet flow from the pump by operating the swashplate control, the motor attempts to continue rotating in the same direction due to inertia, and the pump flow reverses; thus both pump and motor are discharging into the same line whose pressure is only controlled by the boost relief valve.

Inevitably the pressure rises above the boost setting, in this case 13·6 bar, and oil is discharged from the closed loop. The loop is now deficient of oil, and when next the swashplate is reversed, cavitation must take place, because the boost pump cannot replace the missing oil rapidly enough.

The remedy is to connect the boost to both pressure lines via a pair of check valves. It is also essential to provide cross line relief valves operating in both directions to discharge the high transient pressures which will occur at the moment of reversal. I have had personal experience of such transients of nearly 1000 bar, sufficient to destroy a motor.

Ideally, an industrial closed circuit would also include a purging valve to remove the surplus boost flow, so that the main loop is continually flushed with clean, cool oil.

An experimental circuit such as this, however, could just have a boost entry with a maintaining valve, since it will not normally be run for long periods. Fig. 18 shows what I feel is the correct circuit for this application.

I think that the reduction in bulk modulus due to the cavitation might have had a marked effect on the results obtained from this experiment, although I am not in a position to argue with the mathematics.

C. R. Burrows Member

The vector technique used to determine the overall response (limited in the paper to the case where $x_m = 0$ and $K_{FM} = 0$) is very interesting. Using a measured-load locus rather than a theoretical-load locus would be expected to produce an improved agreement between the theoretical and experimental results, since it amounts to removing one area of uncertainty, that is, a more refined model is used. However, the marked improvement in correlation is significant, in that it shows how useful a linearized analysis is for predicting the performances of a pump–motor combination.

Concerning Fig. 1*b*, the last term in the denominator should be K_{FP} not K_E.

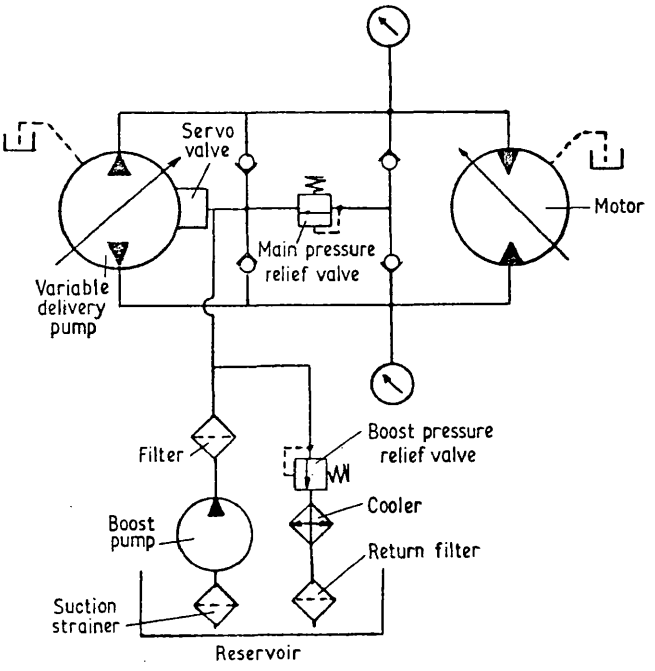

Fig. 18

In Fig. 2, the coefficient of x_p the expression for t_P should be D_1P_D rather than D_1P_H, unless P_L is taken as zero. Similarly, for the motor, the coefficient for x_m in the equation for the change in T_M should be D_2P_D.

The coefficient for x_m in the equation giving the change in Ω_2 should be $-\Omega_2/X_M$, not $1/D_2\Omega_2$. The reason for the negative sign is obvious from physical considerations.

If the normal expression for motor flow is used, then the constant K_M is positive and it becomes necessary to introduce a negative sign for the coefficient p_h in the equation denoting the change in motor speed. This has the advantage of making the equation more easily interpreted from physical reasoning.

These modifications lead to minor changes to the signal flow diagram in Fig. 1*b* and Fig. 2.

There are a number of ways to represent the pump and motor characteristics; I would like the authors to discuss their choice, since alternative representations seem more helpful in determining the operating point under steady-state conditions.

A. B. Goodwin Fellow

I would like to draw the authors' attention to four points of minor detail:

(1) In Fig. 1:

(*a*) The branch J_1s between nodes t_e and w_1 should have one arrow only, pointing towards t_e.

(*b*) The branch $1/(D_2X_m-K_{FM})$ entering node p_h should have an arrow at the node p_h end.

(*c*) A branch of unity should be indicated from node w_2 to the true output node w_2.

(2) In Section 2.3:

$\delta Q_P/\delta Y_P\ (=D_1\Omega_1)$ is the change in flow/unit change in swash angle, it should read $\delta Q_P/\delta X_P$, etc.

(3) In Fig. 2:

Pump–flow relationship should read:

$$\Delta Q_P = \frac{\delta Q_P}{\delta P_H}\cdot\Delta P_H + \text{ etc.}$$

(4) In section 1.1, Notation:

s is the Laplace complex variable.

The various system equations established and the signal flow diagram derived from these appear to be based on the assumption that:

(*a*) $t_p = x_P D_1 P_H + (D_1X_P + K_{FP})P_h$

(*b*) $p_h = \dfrac{1}{D_2X_m - K_{FM}}\cdot t_m + f_m\omega_2 - x_m D_2 P_H$

(*c*) there is no pressure loss in the transmission lines.

I would be inclined to assume that the pressure terms in (*a*) and (*b*) should in fact be the line differential pressure P_D and p_d since with a constant value of P_H any change of P_L, as datum or even incremental change, should influence the torque parameters at both pump and motor.

I would like the authors' comments on (*c*), as I appreciate that establishing an expression for such losses in pipes, fittings and valves might be difficult and wonder if any consideration was given to this.

Referring to equation (4) it may be deduced that there is a minimum value of $\zeta\ (>0)$ at which value

$$\frac{J_2B_e}{V} = \frac{f_{LM}+f_L}{K_P+K_m}$$

and $$\zeta_{min} = \sqrt{\left(\frac{(K_P+K_m)(f_{LM}+f_L)}{(K_P+K_m)(f_{LM}+f_L)+(D_2X_m)^2}\right)}$$

It is to be noticed that this value of ζ corresponds to the values at which:

$$\frac{1}{2}\sqrt{\left(\frac{B_eJ_2}{V}\frac{(K_P+K_m)^2}{(K_P+K_m)(f_{LM}+f_L)+(D_2X_m)^2}\right)} = \frac{1}{2}\sqrt{\left(\frac{V}{B_eJ}\frac{(f_{LM}+f_L)^2}{(K_P+K_m)(f_{LM}+f_L)+(D_2X_m)^2}\right)}$$

i.e. the components of the damping ratio due to leakage and viscous friction are equal. Away from this value of ζ, there can be two values of B_eJ_2/V for each value of ζ, one with increased J_2 (say) and the other with decreased J_2 (say). I would be interested to know if the authors pursued this line of argument at all during their work.

C. Martin Dresden

Determination of the dynamic characteristics of hydrostatic systems can generally be reached from two viewpoints:

(1) from the transmission behaviour due to a disturbing quantity arising from a temporary but exact change in the working conditions as well as random input disturbance when regard is had to the damping characteristic compared with an external disturbing vibration.

(2) from the behaviour due to parametric excitation from the driving chain.

The analysis of parametric hydrostatic control systems, especially hydraulic motors and pumps, involves one of rotor position dependent variables and the authors' case with fluctuations in cell connections. Principal parametric functions are given in the diagram as functions of the displacement volume and leakage oil.

As a result of periodical stepped changes there is irregularity in angular speed at output, in circuit pressure and with it in the return moment M_P, which leads to:

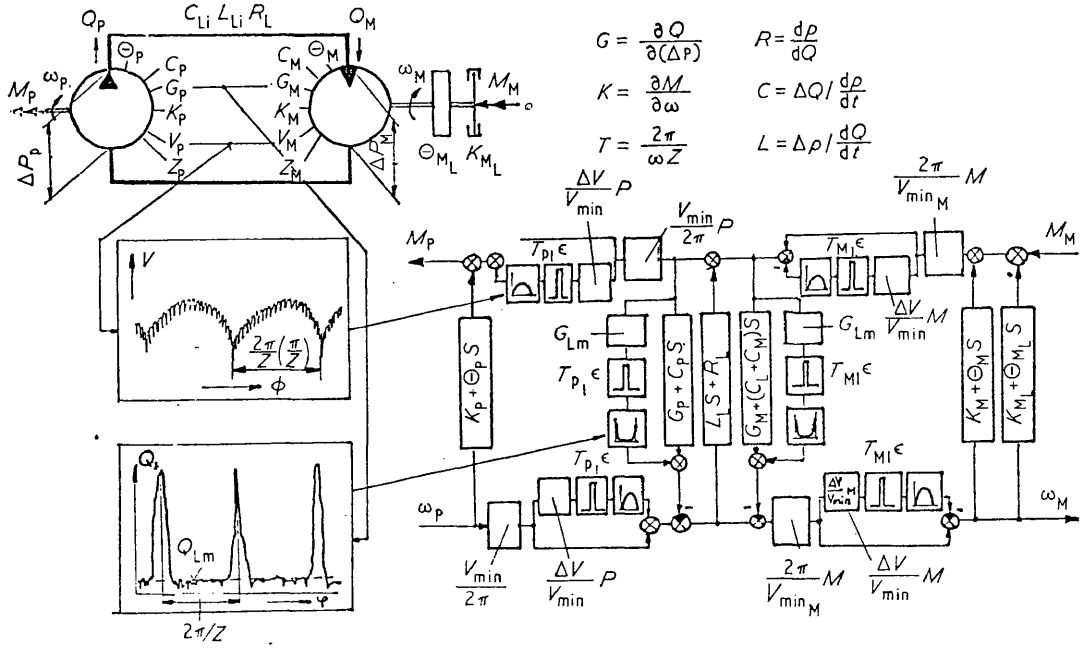

Fig. 19. Significance of the periodic variability parameter by determination of the dynamic characteristics of hydrostatic systems

(1) reduction in performance,
(2) energization in adjoining systems with the driving chain indicated, and thereby,
(3) inherent noise whilst under hydrostatic control.

This appears remarkable when most operating conditions are static.

Considering the periodical parametric variability in connection with the determination of dynamical behaviour we employ the linearized equation of motion—a differential equation with variable coefficients of the Hills type, which are solvable only in special cases. For the dynamic model, in order to describe the parametric vibrations in hydrostatic equipment we borrow control engineering methods in the calculation of a scanning system based on formal impulses and so employ Z-transforms to obtain a good approximate solution. This relates to the diagram, and the necessary modification in the drive of the dynamic model. On this model the magnitude of the noise level can be calculated, the likelihood of achievement of designed displacement seen, and the steps necessary for improvement made.

BIBLIOGRAPHY

MARTIN, C. 'Der Einfluss drehwinkelabhängiger Motorparameter auf das stationäre Betriebs-Verhalten von Hydromotoren', *Maschinenbautechnik* 1972 **21** (Heft 5), 224–232.

MARTIN, C. 'The effect of motor parameter as function of angle of rotation on steady state performance of hydromotors', *Hydraul. Pneum. Pwr* 1972 **18** (No. 212), 356 and (No. 213), 400.

G. Orloff Fellow

Referring to section 6.3, the accuracy requirements of performance prediction can vary in industry, depending on the purpose of the calculations. For tendering, the simple equation (2) leads to rapid results of sufficient accuracy for ω_n and errs in the direction of safety with respect to ζ, and this is usually corrected for from experience—consequently the formula serves a very useful purpose.

In the case of the more detailed design work which may follow, perturbation theory gives adequately good accuracy in most conditions, and even in the absence of computers, an experienced performance analyst will choose perturbed coefficients sufficiently well to give confidence in the hardware manufactured. In the presence of gross load non-linearities it can be more desirable to avail oneself of a digital computer for dealing with a multiplicity of coefficients derived from an empirical load curve, replacing the more simple speed-dependent relationship in Fig. 2—it is not clear to me, however, why changing methods to 'vector locus' should result in greater accuracy.

Signal-flow techniques are understood to be suited particularly for handling the perturbed equations of multivariable systems and others of high complexity—what is the justification for doing so in the present case which is relatively simple?

It would have been interesting to know the contents of the significant parameters in equation (5) and to compare them with equations (3) and (4).

It would have been interesting also to see a set of Bode curves for tests 5–8 permitting a comparison with Fig. 11, particularly since values of f_L taken as tangents to the relevant curve in Fig. 9 lead one to suspect the presence of large-amplitude cyclic non-linearities.

Some non-linear behaviour is already apparent in Fig. 11, where the phase curves intersect at about −50° and consequently result in widely differing lags at the frequency ω_n.

Whereas such behaviour is not unusual in this kind of system, this suggests that there are too many unknowns for making any accurate deductions concerning values of bulk modulus—in this connection the assumption that the stiffness contribution of the fluid is solely provided by one hydraulic line appears to be invalidated by the results shown in Fig. 14, where peak values of return line pressure reach about 600 lb/in^2, which is a high proportion of the transmission line pressure. This leads one to the conclusion that the return line must play a significant part in the stiffness of the system, meaning that the effective value of B_0 is no longer 240 000 lb/in^2, but is somewhere between 120 000 and 240 000 lb/in^2.

The N.E.L. report (7) is really concerned with conditions of pressure in excess of 5000 lb/in^2 and where care has been taken to ensure the total absence of free air. Since it is known that transmissions such as the one used are subjected to cavitation locally at the 'kidney' ports and at other discontinuities, it is very likely that some of the air dissolved comes out of solution: since it takes a finite time for it to be re-dissolved into the liquid, I suggest that one is concerned not only with lower pressures than those of (7), but also with free air being present, and consequently it may be more appropriate to consider the system as being double-acting and to allow for the free air in the manner suggested by Rendel and Allen (20), where they show that with a 10 per cent free-air content at 500 lb/in^2, the combined bulk modulus has a value of 50 per cent of the nominal value of B_0.

This certainly seems to be valid for normal modes of operation of positioning systems, and it would also seem desirable to use similar assumptions in the case of velocity transmissions like the one under discussion, particularly if they are intended to behave normally when occasionally filled with a fluid containing a high proportion of air, as sometimes happens in industry.

REFERENCE

(20) RENDEL, D and ALLEN, G. R. 'Air in hydraulic transmissions', *Aircr. Engng* 1951 **23**, 337–338.

A. H. Richards Member

With regard to the evaluation of bulk modulus, which remains the only unknown in the theoretical treatment, I should like to ask the authors whether they have considered the effect of rate of change of pressure, $\mathrm{d}(\Delta P_H)/\mathrm{d}t$.

As a frequency response test proceeds from low to high frequencies, the acceleration of the load will be directly proportional to the product of signal frequency and half amplitude. The increasing acceleration will entail greater pressure oscillation amplitude, and hence greater rate of change of pressure.

It is usually assumed that the isothermal bulk modulus is associated with slow changes of pressure and the isentropic value with rapid changes. In consequence, I am interested to know if a trend in the bulk modulus could be detected over the test, and was any attempt made to fit equation (5) to the measured results over the whole range of one test?

Alternatively, for a particular system configuration, did the bulk modulus as derived from the vector locus method show any trend as the input amplitude was varied?

J. Thoma Fellow

This paper contains a very clear and detailed small-signal analysis, where Fig. 2 with the derivations of the various gains is a great help to understanding. To put this information together for the transmission system of Fig. 1*a*, a comparatively new technique, the Bondgraph, can make the transition to a signal flow graph much easier, both for original analysis and for communication to outsiders.

Bondgraphs (**21**) (**22**) have been set up from the energy interchanges between various components of a system as for instance Fig. 1*a* or an equivalent circuit such as used frequently in electronics. Energy flux or power is the product of an effort variable (torque, pressure, voltage) and a flow variable (rotational frequency, volume flow, electric current). Simple Bondgraphs are acausal, that is without a definite direction of action between variables. Causality is then added observing a few rules but otherwise at the discretion of the analyst, and indicated by a short cross stroke. Furthermore, the direction of positive power can be assigned at will and is usually represented by a half arrow.

Fig. 20 shows an acausal Bondgraph where engine and load are given in words and the variable displacement pump and motor as modulated transformers, mTF, controlled by X_p and X_m over activated bonds. Both input and output shafts are supplied over a series junction (equal rotational frequency, addition of torque) with inertia, resistive elements and effort sources, the latter showing a torque loss proportional to pressure independent of rotational frequency.

The power line (hydraulic conduit) between pump and motor is connected over a parallel junction (equal pressure, addition of flows) with a capacitance representing fluid compressibility and two resistances showing the leakage of both pump and motor.

Whilst Fig. 20 shows the various effects included in a transparent way, Fig. 21 also shows positive energy flows and selected causalities, and the values of the various elements are given behind double points using the same symbols as in the paper. The engine is replaced by a flow (rotational frequency) source in parallel with a resistance element (alternatively it could be a torque source with a series resistor) and the load by a simple resistor element. Whilst Fig. 21 contains essentially the same information as Fig. 1*b*, it is still more easily interpreted. Furthermore it gives, due to the positive power indication, information on the signs and it is not limited to small signals. The representation of pump and motor as modulated transformers is well in accord with accepted ideas of the action of hydrostatic variable displacement machines.

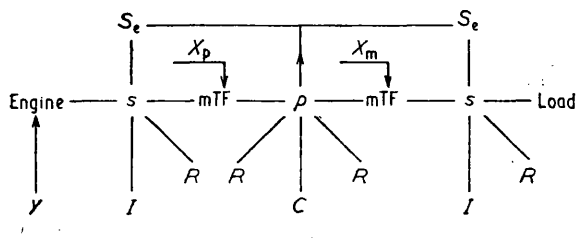

Fig. 20

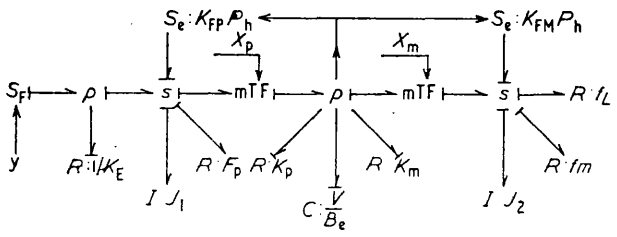

Fig. 21

I do in no way wish to indicate that the Bondgraphs replace the signal flow graph, Fig. 1*b*, or the subsequent analysis. Rather I feel that they are a systematic means of deriving such flow graphs and to select their causality. They would therefore be most suitable for more complex systems, for instance to include pressure drop in the main conduit. This could be done simply by coupling a resistor to the main conduit by an *s*-junction. The various resistance elements do not need to be linear, they only have to indicate a definite (for instance, a quadratic) relation between flow and effort.

Finally it should be pointed out that there exists in the U.S.A. a so-called ENPORT computer programme (**23**) written in FORTRAN, that allows to set up a simulation directly from a simple Bondgraph with indicated positive energy flows. This includes selection of causality in a dialogue between the user and the computer. My own preference, however, is the use of Bondgraphs for representing comparatively complex systems in mechanical engineering, fluid power and electronics on paper. It allows to include causality and signs without losing the engineering feel of what happens in real machines.

REFERENCES

(**21**) KARNOPP, D. and ROSENBERG, R. *Analysis and design of multiport systems* 1968 (MIT Press, Cambridge, Ma.).

(**22**) THOMA, JEAN 'Bondgraphs for flow control valves and other hydrostatic components', *Hydraul. Pneum. Pwr* 1972 **18**, 165.

(**23**) *A users guide to* ENPORT *4* 1972 (Michigan State University, East Lansing, Mich. 48 823, U.S.A.).

I. Watts Whetstone

There is an increasing use of hydrostatic transmissions for both vehicular and non-vehicular applications, not least in the field of servos, where in some instances efficiency can have a higher priority than servo bandwidth and any extension of our knowledge of the subject is to be welcomed.

I would like to ask the authors if they would enlarge upon their reasons for employing the vector analysis technique. Whilst accepting that it is a useful method for obtaining the frequency response, I am not wholly convinced of the need for it. The load can be expressed mathematically in three ways, either in purely linear or non-linear terms or a combination of the two. If the load is so complex as to defy even an approximate analysis, then it is likely that the measured load frequency response would also be difficult to obtain without recourse to such techniques as describing function analysis. It is unlikely in my experience that the load frequency response would be known, and if it is available it is usually only valid for one amplitude of input.

My second enquiry refers to the relief valve characteristic and the possible excursions of replenishment flow. Normally in the type of reversible transmission described in the paper, the replenishment flow source is connected to both of the fluid transmission lines via check valves, since the role of either fluid line is reversed when the direction of rotation of the motor is reversed. This would

prevent negative replenishment flow, as shown in Fig. 6*a*, and, as a consequence, cavitation could exist for larger portions of the pressure oscillation. The high-pressure peaks would normally only be limited by the pressure-limiting valves connected across the motor ports.

It follows, therefore, that the hydraulic stiffness of the return line would be more dependent on the oil characteristics than the impedance of the relief valve, and could result in worthwhile increase in natural frequency. Could the authors comment on this aspect?

Finally, could the authors give their views on employing much higher boost pressures with a view to stiffening the system and preventing cavitation?

D. E. Bowns Member and **J. Worton-Griffiths** (*Graduate*) **(Authors)**

G. Orloff discusses the use of equation (2) and we agree with him that, as a rapid check on natural frequency, it is extremely valuable. However, it gives consistently high results if the correct value of bulk modulus is used and therefore is of dubious value for tendering purposes, particularly as customers become more aware of the necessity for dynamic specification of performance. If the load is frequency dependent, as was the load in the experimental rig, no computerized method is possible which would take this into account, except a completely step-by-step approach such as that adopted by Knight *et al.* (**24**), which is considerably more complex than the methods discussed here. The vector-locus technique is familiar in concept to most control engineers and does give a rapid and accurate check on the dynamic response of this type of mechanical system. It can cope with many non-linearities and does not necessitate the use of a computer. Examples of its use are discussed below.

The signal-flow technique assists greatly in the analysis of systems such as the one under discussion; the block diagram is complex and extremely difficult to disentangle and a straightforward mathematical approach involves the solution in the simplest case of eight simultaneous differential equations. The problem is, in fact, multivariable and one advantage of the signal-flow approach is that with very little additional work the relation between any other input and output (for example, the effect of the change in load torque on motor speed) can be obtained very easily. However, in spite of all the care taken, poor correlation was obtained between the theoretical Bode plot developed from equation (5) and the experimentally determined values. It was for this reason that the vector-analysis technique was adopted.

G. Orloff's request for Bode curves for tests 5–8 is easily fulfilled, as they are all included on Fig. 10, whilst his worry about the intersection of the phase lag curves at about $-50°$ is not relevant as the transfer function of the system is much more complex than the second order form on which he appears to be basing his arguments. Curve 9 was in fact carried out with a load of different torque speed characteristics and when the load static and dynamic characteristics were taken into account the transmission coefficients obtained were in close agreement with those of the other tests.

G. Orloff goes on to state that the stiffness of the return line makes some contribution to the system stiffness—indeed it does, and one of the most important advantages of the vector locus approach is that it can be used to account for this. For several of the tests reported in the paper, an artificially large boost system was used to keep return-line pressure variations to a minimum, but for tests 18–21 a restricted boost system was used and the effective value of bulk modulus which allowed prediction of the experimental dynamic response using the vector locus approach was still 240 000 lbf/in^2 within 4 per cent. Indeed, one of the most important points of the paper is to show that there are not too many unknowns in a hydrostatic transmission system. An accurate assessment of natural frequency and damping ratio can be made without too much difficulty.

It might be opportune to point out that the transmission tested contained a relatively small oil volume and had a load of low inertia. Predictions would be more accurate still with larger volumes and high inertias.

The effect of air on transmission performance has interested the authors and G. Orloff is referred to (**25**). Air in the fluid is not the bogey it has hitherto been thought and work on the transmission dynamics with air present has substantiated the methods of analysis used in the present paper.

In reply to A. H. Richards, the effect of the rate of change of pressure has been taken into account in the overall transmission analysis but not in considering whether to use isentropic or isothermal bulk moduli.

The results obtained by analysing the experimentally determined frequency response using the vector-analysis technique did not indicate any trends in the bulk modulus values as the frequency or input amplitude were varied.

Values obtained for a typical test are given in Table 3.

It should be pointed out that at low frequencies where the flow losses were small and where slip losses made up the significant part of the total loss, this method for determining the effective bulk modulus of the oil was not satisfactory. This made an evaluation of bulk modulus at low rates of change of pressure impossible.

C. R. Burrows's comments on the use of the measured load loci are very pertinent and so are his algebraic corrections. They have been incorporated in the corrigenda.

A. B. Goodwin's points about Fig. 1 and Fig. 2 are both correct, and we are in agreement with both him and C. R.

Table 3. Effective bulk modulus $\times 10^5$ lbf/in^2

Hz	Test No.		
	1·01	1·05	2·03
2·0	2·70	2·33	2·45
3·0	2·28	2·23	2·29
4·0	2·18	2·11	2·18
4·5	2·24	2·10	2·17
5·0	2·30	2·07	2·15
5·5	2·34	2·11	2·18
6·0	2·18	2·14	2·21
6·5	2·20	2·14	2·22
7·0	2·18	2·14	2·21
8·0	2·24	2·18	2·25
9·0	2·20	2·18	2·27
10·0	2·26	2·19	2·27
12·0	2·29	2·22	2·30
Mean	2·24	2·15	2·23
Standard deviation, per cent	2·5	2·3	2·2

(Three tests at different mean return line pressures and load damping coefficients.)

Burrows that the line-differential pressure p_D rather than the high-pressure line variation p_H should be used in the torque equations. Indeed when variations in return-line pressure were significant, the former value was used in the analysis presented in the paper.

With the relatively short lines used it was considered justifiable to neglect pipe losses, but for systems where they are not negligible it might be better to incorporate them as a deduction from the motor torque coefficient. A. B. Goodwin's point about minimum damping has academic interest. However, low damping is to be avoided in hydrostatic transmission systems and unfortunately the designer usually has no means of controlling it.

In reply to I. Watts's point about load frequency response, we do not underestimate the difficulties in obtaining this. Indeed, determination of the load characteristics is a major part of the difficulty in all hydraulic design. However, it seems to us important to pinpoint the difficulties, rather than attribute subsequent inaccuracy to such effects as that of air in the transmission fluid or other unknowns.

We agree with G. A. Broadhurst that a closed-circuit reversible flow transmission system should be designed as in Fig. 18 and indeed the test system was initially arranged in this manner. However, the system was being used as a speed-control circuit and the pump swash-plate angles were never reversed. Hence the large transient pressures mentioned by G. A. Broadhurst were not experienced in the experimental system. The reason for removing the check valves was to remove some of the system unknowns and enable reasonable control of the experiments. There are, however, still transient pressures as can be seen from Fig. 16. These would not be reduced by the inclusion of non-return valves as the line pressure differential is not reversed.

I. Watts is incorrect in assuming that cavitation would occur for longer periods with non-return valves installed in the system. The cavitation described in Fig. 6*d* occurs when the relevant non-return valve is fully open and the boost system has too little capacity to cope with the large demands made on it. He is, however, correct in stating that much higher boost pressures can stiffen up the system and prevent cavitation. Unfortunately higher boost pressures would reduce the maximum pressure differential available for any given design of pump or motor unit and also lead to increased power losses in the boost system. In a design where such considerations are unimportant, high boost pressures would certainly be advantageous.

We thank J. Thoma for his contribution on Bondgraphs and consider that this method should be more widely known.

C. Martin's contribution is also interesting. He suggests the use of sampled data techniques for determining the cyclic flow and pressure fluctuations and corresponding resonances. Such methods have already been used by one of the present authors for analysis of the dynamic behaviour of reciprocating engines (**18**) but during the test work carried out on the transmission there was no experimental evidence of behaviour which could be attributed to sampling phenomena.

REFERENCES

(**24**) KNIGHT, G. C., MCCALLION, H. and DUDLEY, B. R. 'Connection capacitance effects in hydrostatic transmission systems and their prediction by mathematical model', *Proc. Instn mech. Engrs* 1972 **186**, 661–670.

(**25**) BOWNS, D. E., EDGE, K. and WORTON-GRIFFITHS, J. 'The effect of air on the operating characteristics of a hydrostatic transmission', *Proc. Third Int. Fluid Pwr Symp.*, Turin, 1973 (to be published).

Corrigenda

P. 756, Fig. 1. Last term in denominator. For 'K_E' read 'K_{FP}'.

P. 757, Section 2.3. For '$\delta Q_p/\delta Y_p$' read '$\delta Q_p/\delta X_p$'.

P. 758, Fig. 2. Pump-flow relationship should read: $\Delta Q_p = \dfrac{\delta Q_p}{\delta P_H}\Delta P_H \ldots$ etc.

P. 758, Fig. 2. Pump-torque relation. If change in low-pressure line is significant substitute P_D for P_H in equations.

P. 758, Fig. 2. Motor-flow relationship should read: $\omega_2 = \dfrac{q_m}{D_2 X_m} + \dfrac{K_m}{D_2 X_m} p_H - \dfrac{\Omega_2}{X_m} x_m$.

W. C. & S. Ltd, England